Synthesis and mechanistic studies on the monoamine oxidase (MAO) catalyzed oxidation of 1,4-disubstituted-1,2,3,6-tetrahydropyridines

Jian Yu

Dissertation submitted to the faculty of the Virginia Polytechnic Institute and State University in partial fulfillment of the requirements for the degree of

DOCTOR OF PHILOSOPHY

IN

CHEMISTRY

APPROVED:

Dr. Neal Castagnoli, Jr. Chair

Dr. Mark R. Anderson

Dr. Michael Calter

Dr. Joseph S. Merola

Dr. James F. Wolfe

August 10, 1998
Blacksburg, Virginia

Keywords: Monoamine oxidase, Tetrahydropyridine, Mechanism, Isotope effect, Deuterium, Rate-determining, Chiral Auxiliary.

Synthesis and mechanistic studies on the monoamine oxidase (MAO) catalyzed oxidation of 1,4-disubstituted-1,2,3,6-tetrahydropyridines

Jian Yu

(ABSTRACT)

The parkinsonian inducing drug 1-methyl-4-phenyl-1,2,3,6-tetrahydropyridine (MPTP) is bioactivated in a reaction catalyzed by the flavoenzyme monoamine oxidase B (MAO-B) to form the corresponding dihydropyridinium ($MPDP^+$) subsequently pyridinium (MPP^+) metabolites.

As part of our ongoing studies to characterize the structural features responsible for this unexpected biotransformation, we have synthesized and examined the MAO-B substrate properties of a variety of MPTP analogs bearing various heteroaryl groups at the 4-position of the tetrahydropyridinyl ring. The results of these SAR studies indicate that electronic features, steric features and polar interactions can contribute to the substrate activities.

Additionally, isotope effects have been examined to investigate the mechanism and stereoselectivity of the MAO-B catalytic pathway. The synthesis and characterization of regio and stereoselectively deuterated MPTP analogs have been achieved. The results indicate that the catalytic step occurs exclusively at the allylic C-6 position and is rate-determining for both good and poor substrates. The two enantiomers of MPTP bearing a deuterium atom at C-6 have been prepared via chiral aminooxazolinyl derivatives and have been characterized by ^2H NMR in a chiral liquid crystal matrix. These enantiomers were used to determine the selectivity of the MAO-B catalyzed α C-H bond cleavage reaction leading to the dihydropyridinium metabolite $MPDP^+$.

Some of the cyclopropyl analogs of MPTP have also been synthesized as the potential inhibitors.

ACKNOWLEDGMENTS

I would like to express my sincere gratitude and appreciation to Professor Neal Castagnoli, Jr. for his guidance, encouragement and patience during my stay at Virginia Polytechnic Institute and State University.

Grateful acknowledgments are also made to Dr. Mark R. Anderson, Dr. Michael Calter, Dr. Joseph S. Merola and Dr. James F. Wolfe for their generous donation of time and critical reviews of my work and progress.

I wish to express my appreciation to the faculty members in the Chemistry Department and the past and present members of Castagnoli research group for their valuable advice and assistance.

Finally, I would like to thank my parents for their encouragement and support. Their love and understanding are invaluable.

A special thanks goes to the NIH and the Harvey W. Peters Research Center for the study of Parkinson's Disease and Disorders of the Central Nervous System for supporting this research project.

TABLE OF CONTENTS

LIST OF SCHEMES

LIST OF FIGURES

LIST OF TABLES

Chapter 1. Historical background

1.1. Enzyme

1.1.1. Enzymes and coenzymes

A. General aspects

Enzymes are proteins that function as catalysts for biological reactions. A catalyst is a substance that accelerates a chemical reaction without itself undergoing any net change. The types of chemical reactions that can be catalyzed by proteins alone are limited by the chemical properties of the functional groups found in the side chains of nine amino acids:[1] the imidazole ring of histidine, the carboxyl groups of glutamate and aspartate, the hydroxyl groups of serine, threonine, and tyrosine, the amino group of lysine, the guanidinium group of arginine, and the sulfhydryl group of cysteine. These groups can act as general acids and bases in catalyzing proton transfers and as nucleophilic catalysts in group transfer reactions.

However, many metabolic reactions involve chemical changes that cannot be brought about by the structures of the amino acid side chain functional groups in enzymes acting by themselves. In catalyzing these reactions, enzymes must act in coorperation with coenzymes which are smaller organic molecules or metallic cations and possess special chemical reactivities or structure properties that are useful for catalyzing reactions. Most coenzymes are derivatives of the water-soluble vitamins, but a few, such as hemes, lipoic acid, and iron-sulfur clusters, are biosynthesized in the body. Each coenzyme plays a unique chemical role in the enzymatic processes of living cells.

The two important characteristics of enzyme catalysis are the selectivity and rate acceleration.

It has been recognized that an enzyme has three levels of selectivity: structural selectivity, regioselectivity, and stereoselectivity. An enzyme must first recognize some common structural features present on a substrate (and coenzyme) to produce catalysis. Second, catalysis must occur at a specific region on the substrate (or the coenzyme) and the stereochemical outcome must be controlled by the enzyme.

The function of a catalyst is to provide a new reaction pathway in which the rate-determining step has a lower energy of activation than the rate-determining step of the

uncatalyzed reaction. An enzyme has many ways to invoke catalysis, for example, by destabilization of the enzyme substrate complex, by stabilization of the transition states and by destabilization of intermediates. Consequently, multiple steps, each having small $\Delta G^{\ddagger}$ values, may be involved. This is responsible for the rate acceleration that results.

B. Flavin coenzymes

Flavin coenzymes act as co-catalysts with enzymes in a large number of redox reactions, many of which involve O_2.[2] Flavin adenine dinucleotide (FAD) and flavin mononucleotide (FMN) are the coenzymatically active forms of vitamine B_2, riboflavin (Figure 1).

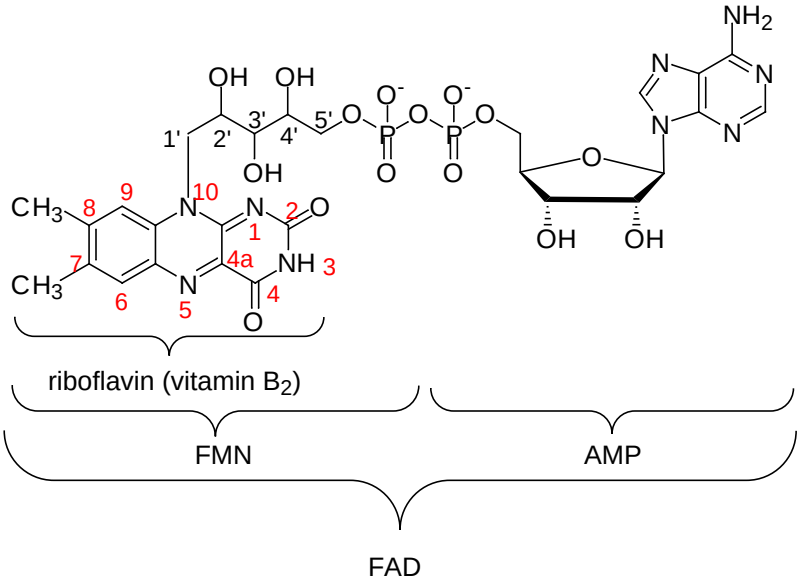

Figure 1. Structures of the Vitamin Riboflavin and the Derived Flavin Coenzymes

Riboflavin is the N^{10}-ribitylisoalloxazine portion of FAD, which is enzymatically converted into its coenzymatic forms first by phosphorylation of the ribityl C-5′ hydroxy group to FMN and then by adenylation to FAD. FMN and FAD are functionally equivalent coenzymes and the one that is involved with a given enzyme appears to be a matter of enzymatic binding specificity.

The catalytically functional portion of the coenzymes is the isoalloxazine ring, specifically the N-5 and C-4a positions, which is thought to be the immediate locus of catalytic function. Even so, the entire chromophoric system extending over N-5, C-4a, C-10a, N-1, and C-2 should be regarded as an indivisible catalytic entity.

The flavin coenzymes exist in four spectrally distinguishable oxidation states that account in part for their catalytic functions (Scheme 1).[1] They are the yellow oxidized form, the red or blue one-electron reduced form, and the colorless two-electron reduced form.

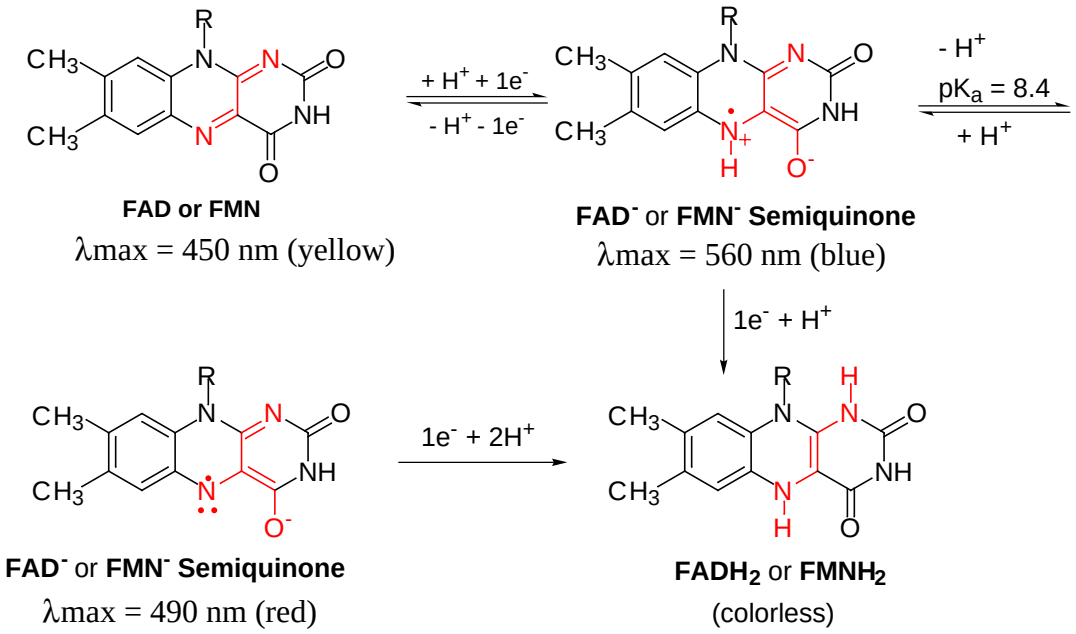

Scheme 1. Oxidation States of Flavin Coenzymes

1.1.2. Kinetics of enzyme-catalyzed reactions

A. Enzyme-catalyzed reactions

Enzymes have localized catalytic sites. The substrate (S) binds at the active site to form an enzyme-substrate complex (ES). Subsequent steps transform the bound substrate into product and regenerate the free enzyme E (Scheme 2).

$$E + S \underset{k_2}{\overset{k_1}{\rightleftharpoons}} ES \underset{k_4}{\overset{k_3}{\rightleftharpoons}} E + P$$

Scheme 2. Enzyme-catalyzed Reaction

The overall speed of the reaction depends on the concentration of ES. Based on the steady-state kinetics analysis assumption, shortly after the enzyme and substrate are mixed, [ES] becomes approximately constant and remains so for a period of time, that is the steady state. The rate (ν) of the reaction in the steady state usually has a hyperbolic dependence on the substrate concentration. It is proportional to [S] at low concentrations but approaches a maximum (V_{max}) when the enzyme is fully occupied with substrate (Figure 2).

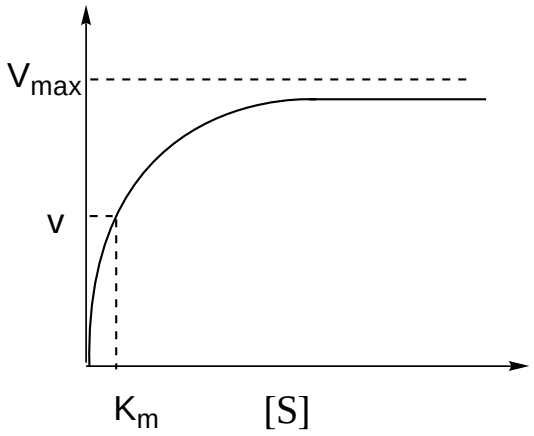

Figure 2. The Reaction Velocity ν as a Function of the Substrate Concentration [S] for an Enzyme-catalyzed Reaction

V_{max}, the maxium velocity, is obtained when all the enzyme is in the form of the enzyme-substrate complex. K_m, the Michaelis constant, is the substrate concentration at which the velocity is half maximal. If ES is in equilibrium with the free enzyme E and substrate S, K_m is equal to the dissociation constant for the complex (K_s). More generally, K_m depends on at least three rate constants and is larger than K_s. k_{cat}, the turn over number,

is the maximum number of molecules of substrate converted to product per active site per unit time and is V_{max} divided by the total enzyme concentration. k_{cat}/K_m, the specificity constant, provides a measure of how rapidly an enzyme can work at low substrate concentration [S]. It is useful for comparing the relative abilities of different compounds to serve as substrates for the same enzyme. The bigger this number, the better the substrate.

B. The measurement of the kinetic parameters

Kinetic parameters are determined by measuring the initial reaction velocity as a function of the substrate concentration. The usual procedure for measuring the rate of an enzymatic reaction is to mix enzyme with substrate and observe the formation of product or disappearance of substrate as soon as possible after mixing, that is when the substrate concentration is still close to its initial value and the product concentration is small. The measurements usually are repeated over a range of substrate concentrations to map out how the initial rate depends on concentration. K_m and V_{max} often can be obtained from a plot of $1/v$ versus $1/[S]$ (Figure 3). Spectrophotometric techniques are commonly used in such experiments to measure the concentration of a substrate or product continuously as a function of time.

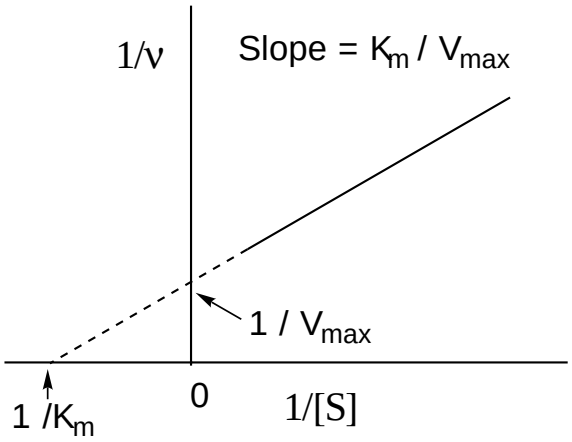

Figure 3. The Lineweaver-Burk Double-reciprocal Plot

1.1.3. The mechanisms of enzyme catalysis

Several factors are considered when attempting to describe the mechanism by which an enzyme catalyzes a particular reaction. Among them, the most common factors are: (1) the proximity effect, (2) electrostatic effect, (3) general-acid and general-base catalysis, (4) nucleophilic or electrophilic catalysis by enzymatic functional groups, and (5) structural flexibility.

The proximity effect is due simply to differences between the entropic changes that accompany the inter- and intramolecular reactions. Enzymes that catalyze intermolecular reactions take advantage of the proximity effect by binding the reactants close together in the active site so the reactive groups are oriented appropriately for the reaction. Once the substrates are fixed in this way, the subsequent reaction behaves kinetically like an intramolecular process. The decrease in entropy associated with the formation of the transition state has been moved to an earlier step, the binding of the substrate to form the enzyme-substrate complex. This step often is driven by a decrease in enthalpy associated with electrostatic interactions between polar or charged groups of the substrates and enzyme.

Electrostatic interactions can promote the formation of the transition state. Charged, polar, or polarizable groups of the enzyme are positioned to favor the redistribution of electrical charges that occur as the substrate evolves into the transition state. The energy difference between the initial state and the transition state thus depends critically on the details of the protein structure.

General-base and general-acid catalysis provide ways of avoiding the need for extremely high or low pH. The task of a catalyst is to make a potentially reactive group more reactive by increasing its intrinsic electrophilic or nucleophilic character. In many cases the simplest way to do this is to add or remove a proton.

Enzymatic functional groups provide nucleophilic and electrophilic catalysis. The basic feature of the nucleophilic and electrophilic catalysis is the formation of an intermediate state in which the substrate is covalently attached to a nucleophilic group on the enzyme.

Structural flexibility can increase the selectivity of enzymes by ensuring that substrates bind or react in an obligatory order and by sequestering bound substrates in pockets that are protected from the solvent.

1.1.4. Enzyme inhibition

A. Forms of enzyme inhibition

Enzymes can be inhibited by agents that interfere with the binding of substrate or with conversion of the ES complex into products. There are two kinds of inhibitors: reversible and irreversible inhibitors.

Reversible inhibition involves no covalent interactions. Reversible inhibitors include competitive, noncompetitive, and uncompetitive inhibitors. A competitive inhibitor competes with substrate for binding at the active site. Consequently, a sufficiently high concentration of substrate can eliminate the effect of a competitive inhibitor. Noncompetitive inhibitors bind at a separate site and block the reaction regardless of whether the active site is occupied by substrate. A noncompetitive inhibitor decreases the maximum velocity of an enzymatic reaction without affecting the K_m. This inhibitor removes a certain fraction of the enzyme from operation, no matter the concentration of the substrate. An uncompetitive inhibitor binds to the ES complex but not to the free enzyme. These three forms of inhibition are distinguishable by measuring the rate as a function of the concentrations of the substrate and inhibitor.

Irreversible inhibitors (inactivators) are compounds that produce irreversible inhibition of the enzyme. They often provide information on the active site by forming covalently linked complexes that can be characterized.

B. Mechanism-based inactivation

(1) The kinetics of mechanism-based inactivation

A mechanism-based inactivator is an inactive compound whose structure resembles that of either the substrate or product of the target enzyme and which undergoes a catalytic transformation by the enzyme to a species that, prior to release from the active site, inactivates the enzyme. [4]

The basic kinetics are described in Scheme 3. A mechanism-based inactivator (I) requires a step to convert the compound to the inactivating species (k_2). This step, which generally is responsible for the observed time dependence of the enzyme inactivation, usually is irreversible and forms a new complex E˘I which can have three fates: (1) if E•I′

is not reactive, but forms a tight complex with the enzyme, then the inactivation may be the result of a noncovalent tight-binding complex E•I′; (2) if the I is a reactive species, then a nucleophilic, electrophilic, or radical reaction with the enzyme may ensure (k_4) to give the covalent complex E•I''; and (3) the species generated could be released from the enzyme as a product (k_3).

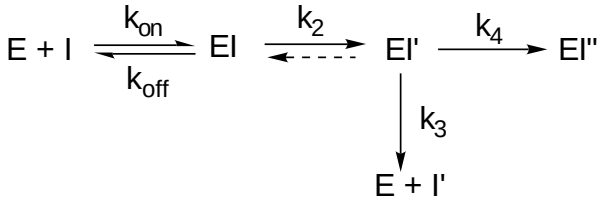

Figure 3. The Lineweaver-Burk Double-reciprocal Plot

Based on this mechanism, the two principal kinetic constants that are useful in describing mechanism-based enzyme inactivators k_{inact} and K_i are obtained. k_{inact} represents the inactivation rate constant at infinite concentrations of inactivator. When k_2 is rate determining and k_3 is 0, $k_{inact} = k_2$. K_i represents the dissociation constants for the breakdown of the EI complex when k_{on} and k_{off} are very large.

$$k_{inact} = k_2k_4 / (k_2 + k_3 + k_4) \qquad (1)$$

$$K_1 = [(k_{off} + k_2) / k_{on}][(k_3 + k_4) / (k_2 + k_3 + k_4)] \qquad (2)$$

The ratio of product release to inactivation is the partition ratio and represents the efficiency of the mechanism-based enzyme inactivator. When inactivation is the result of the formation of a covalent bound adduct, the partition ratio is described by k_3/k_4.

(2) The experimental criteria for mechanism-based inactivation

The major experimental criteria established for the characterization of mechanism-based inactivators are as follows:

(a) There is a time-dependent loss of enzyme activity. Because following a rapid equilibrium of the formation of the EI complex, there is a slower reaction that converts the inactivator to a form that actually inactivates the enzyme (k_2).
(b) Saturation kinetics are observed. The rate of inactivation is proportional to the concentration of the inactivator until sufficient inactivator is added to saturate all of the enzyme molecules.
(3) Addition of a substrate or competitive reversible inhibitor slows down the rate of enzyme inactivation. Because mechanism-based inactivators act as modified substrates, they compete with other substrates for the target enzymes and bind to the active site.
(4) Dialysis or gel filtration does not restore enzyme activity, i.e., mechanism-based inactivators form stable covalent adducts.
(5) A 1:1 stoichiometry of radio-labeled inactivator to active site usually results after inactivation followed by dialysis or gel filtration. Because mechanism-based inactivators require the catalytic machinery at the active site of the enzyme to convert them to the form that inactivates the enzyme, at most one inactivator molecule should be attached per enzyme active site.

(3) The uses of mechanism-based enzyme inactivators

There are two principal areas where mechanism-based enzyme inactivators have been most useful: (1) in the study of enzyme mechanisms and (2) in the design of new potential drugs.

Mechanism-based inactivators are modified substrates for the target enzymes. Once inside the active site of the enzymes, they are converted to products that inactivate the enzyme by the catalytic mechanism for the normal substrates. Therefore, whatever information can be obtained regarding the inactivation mechanism is directly related to the catalytic mechanism of the enzyme.[5]

A mechanism-based inactivator could have the desirable drug properties of specificity and low toxicity if the nonspecific reactions with other biomolecules is limited and the partition ratio is small. Since mechanism-based inactivators are unreactive compounds, there are usually no nonspecific reactions with other biomolecules. Only enzymes that are capable of catalyzing the conversion of these compounds to the form that inactivates the enzyme, and enzymes that have an appropriately positioned active site group to form a covalent bond, would be susceptible to inactivation.[3]

1.2. Monoamine oxidase (MAO)

1.2.1. Compositions and locations

Monoamine oxidase (MAO, EC 1.4.3.4) is a flavin-adnosine-dinucleotide (FAD) containing enzyme located on the outer mitochondrial membrane.[6] It exists in two functional isozymic forms, termed MAO-A and MAO-B, which have 70% sequence identity as deduced from their cDNA clones.[7] These two forms of the enzyme can be distinguished by differences in substrate preference, inhibitor specificity, tissue distribution, immunological properties, and amino acid sequences.[6] The active forms of the enzymes are homodimers with subunit molecular weights, determined from their cDNA structure, of 59,700 and 58,800, respectively. The genes for both MAO-A and MAO-B have very similar structures; both consist of 15 exons and exhibit identical exon-intron organization, suggesting that MAO-A and MAO-B are derived from duplication of a common ancestral gene.[8] By consensus, the selective substrate of the A form is the serotonin (5-HT, **1**) and it can be selectively inhibited by clorgyline (**2**); that of the B form is β-phenylethylamine (PEA, **3**) and it can be inhibited by (*R*)-deprenyl (**4**) (Figure 4).[6] Selective inhibitors of MAO-A exhibit antidepressent activities[9-10] whereas MAO-B inhibitors exibit antiparkinsonian activities.[11-12]

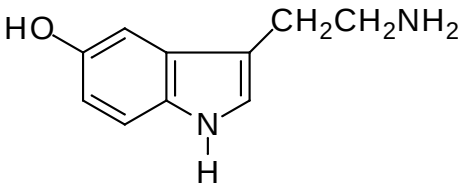

Serotonin (1)

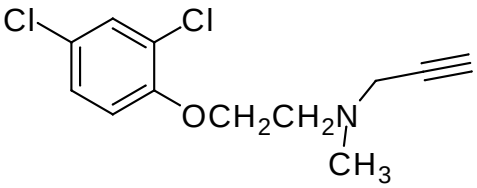

Clorgyline (2)

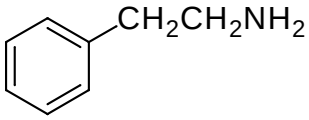

β-Phenylethylamine (3)

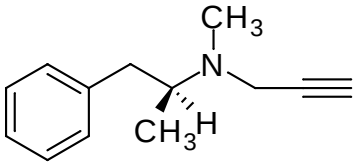

(*R*)-Deprenyl (4)

Figure 4. The Selective Substrates and Inhibitors of MAO

The active site of MAO consists of the FAD residue that is covalently bound to an identical cysteinyl-pentapeptide fragment [Ser-Gly-Gly-(cys-FAD)-Tyr] via a C-8a linkage in both forms of the enzymes (Figure 5).[13-14] Nine cysteines were found in the deduced amino acid sequences of both human liver MAO-A and MAO-B. Each cysteine residue of MAO-A and MAO-B was mutated to a serine residue, and it was found that, in addition to the FAD binding site (Cys-406 in MAO-A and Cys-397 in MAO-B), Cys-374 plays an important role in the catalytic activity of MAO-A, whereas Cys-156 and Cys-365 are important for MAO-B activity.[15]

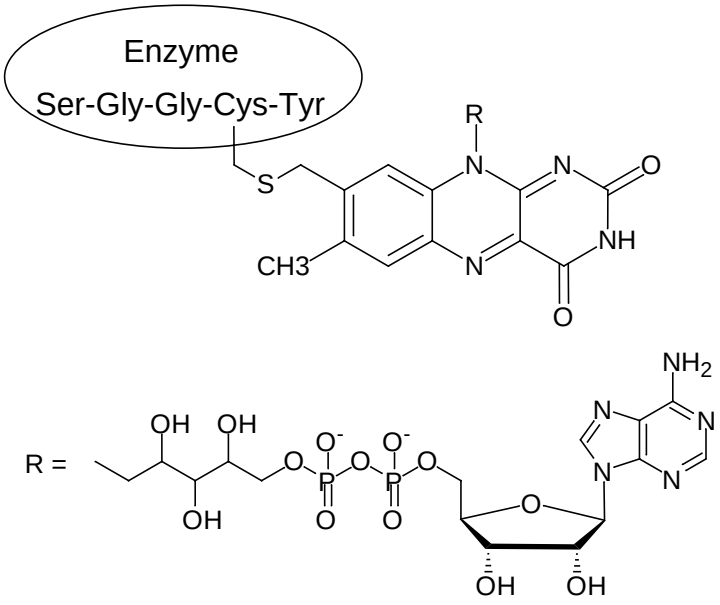

Figure 5. Monoamine Oxidase

1.2.2. Functions

The monoamine oxidases catalyze the oxidative deamination of various biogenic amines, such as neurotransmitters, to the corresponding imines which are nonenzymatically hydrolyzed to aldehydes.[6] The cofactor FAD actively participates in the enzyme reaction. The process involves three steps that are the same for both enzymes (Scheme 4):

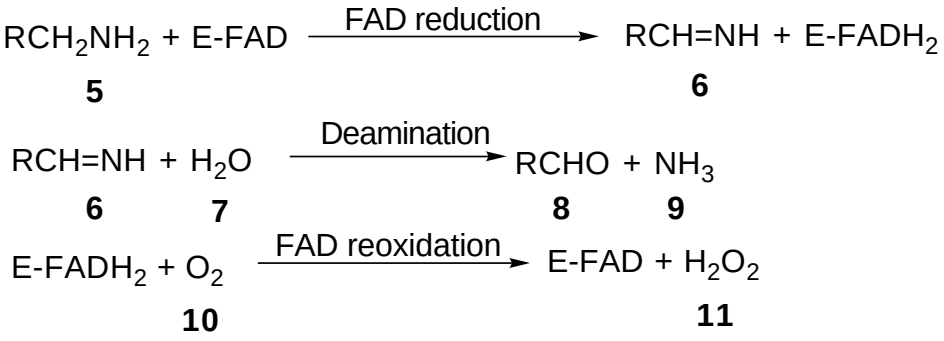

Scheme 4. The Oxidative Deamination of Amines Catalyzed by MAO

The enzymatic reaction requires molecular oxygen and produces aldehyde and hydrogen peroxide. The consequences are that, under hypoxic conditions, the activity of the enzyme will decrease or, conversely, increased enzyme activity may cause higher oxygen consumption or local hypoxia. The aldehyde product will be rapidly reduced either to an alcohol or oxidized to a carboxylic acid by aldehyde reductase or dehydrogenase, respectively. For example, it has been hypothesized that in different pathological stages under particular circumstances, dopamine turnover in the basal ganglia of the brain will be increased resulting in an excessive formation of hydrogen peroxide. This might lead to the production of a cytotoxic hydroxyl radical (·OH) and could impose oxidative stress on neurons, causing local cell death.[6]

MAO catalyzes the oxidative deamination of biogenic amines and, in this way, has a role in their biological inactivation in vivo. The inhibition of MAO-A results in increased brain levels of the biogenic amines including noradrenaline (**12**) and serotonin (**1)** which may be pathologically low in depression. The selective inhibition of the B form preferentially decreases the deamination of dopamine (**13**). This makes it a useful drug in the treatment of Parkinson's disease because the dopamine level of the parkinsonian human brain basal ganglia is dramatically decreased.[3]

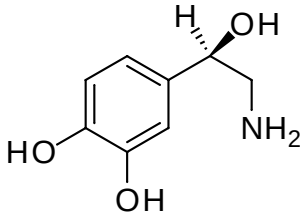

Noradrenaline (12)

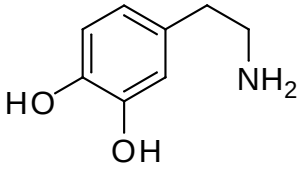

Dopamine (13)

1.2.3. The detailed mechanisms of the enzyme-catalyzed oxidation

The precise mechanism of this biotransformation has been described by three pathways: (1) single electron transfer (SET) pathway, (2) hydrogen atom transfer (HAT) pathway, and (3) nucleophilic (polar) pathway.

A. The SET pathway

(1) The proposed SET pathway

The generally accepted mechanism for the MAO catalyzed α-carbon oxidation of amines according to Silverman[5] proceed via an initial single electron transfer step (Scheme 5) from the nitrogen lone pair of the substrate **14** to the oxidized flavin FAD to generate an aminyl radical cation, **15**, and the flavin semiquinone $FAD^{\cdot -}$. α-Carbon deprotonation of **15** yields the α-amino radical **16** (pathway **a**) which can either transfer the second electron to the semiquinone to give the reduced flavin $FADH^-$ or undergo radical combination with an active site radical (pathway **c**) to give a covalent adduct **17**, which should decompose by β-elemiantion to give the iminium ion **18**. An alternative pathway to proton transfer (pathway **a**) followed by electron transfer (pathway **b**), is hydrogen atom transfer (pathway **d**), which bypasses the α-amino radical intermediate **16**.

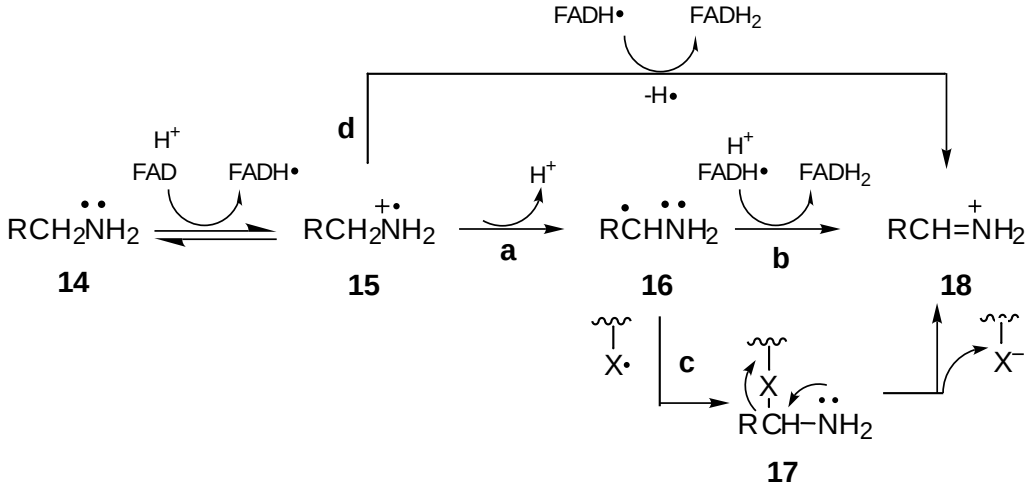

Scheme 5. The Proposed SET Oxidation Pathways for MAO Catalysis

The proposed fate of FAD during the catalytic reaction is indicated in Scheme 6. The oxidized form FAD accepts an electron from the amine substrate to form the semi-reduced radical anion $FAD^{\cdot -}$. A second electron transfer and protonation converts the FAD^- to the reduced flavin ion $FADH^-$. Finally protonation of $FADH^-$ yields $FADH_2$

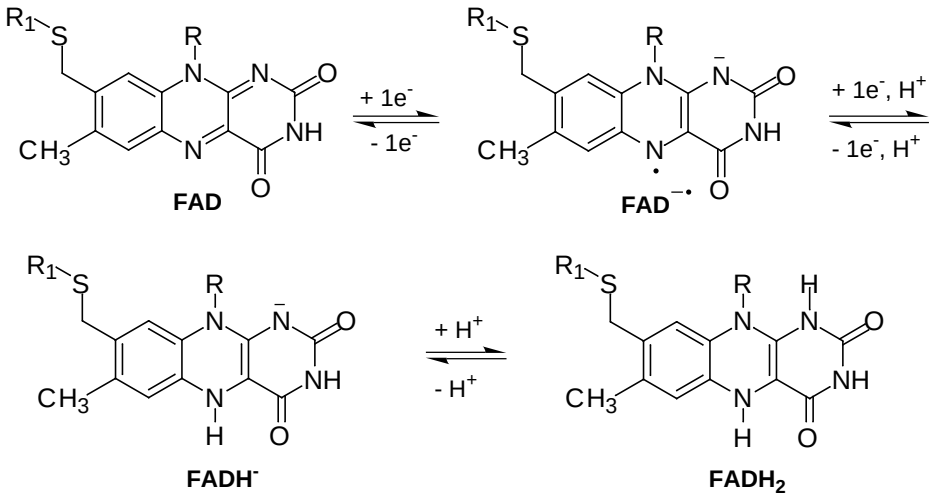

Scheme 6. The Reduction of the Flavin

Silverman and coworkers have provided evidence for the initial electron transfer step, the proton/electron and hydrogen atom transfer step and covalent pathway.

(2) Evidence for the initial electron transfer

Because no evidence for radical intermediates were found by EPR spectroscopy during substrate turnover[16] and stopped-flow kinetics experiments failed to provide evidence for a flavin semiquinone intermediate,[71] it is assumed that the potential radical intermediates are very short-lived, at low concentration, or spin paried with another radical.[18-19] In support of the MAO-B SET pathway is a series of chemical studies using mechanism-based inactivators, such as cyclopropylamine and cyclobutylamine derivatives.

The selection of cyclopropyl mechanism-based inactivator analogs was based on the laser flash photolysis work of Maeda and Ingold.[20] In their studies, it was found that secondary aminyl radicals could be generated and observed by low-temperature EPR spectroscopy. When the corresponding cyclopropylaminyl radical **20** was generated from **19** by the same method, it could not be observed. Instead, the ring-cleaved primary radical product **21** was detected (Scheme 7). The rate of cyclopropyl ring opening was too fast to measure and was estimated at $> 5 \times 10^8$ s^{-1}. This diversion of the normal chemistry provides a potential way for the molecules to form the attachement to the enzyme.

Therefore, the isolation and structure identification of the reaction products are expected to shed light on the mechanism of this reaction.

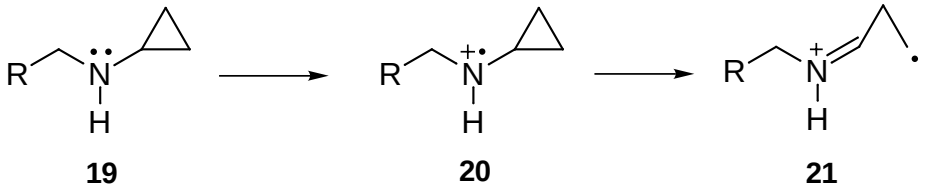

19 **20** **21**

Scheme 7. The Ring Opening of the Cyclopropylamines

Many cyclopropylamine-containing substrate analogs were synthesized as potential mechanism-based inactivators and were studied as substrates for MAO.[21-27] With the use of [phenyl-^{14}C]-**22** it was shown that this compound becomes attached to MAO in a 1:1 stoichiometry either at the flavin or at an active site cysteine residue (Scheme 8).[26] The product of attachment at the flavin was stable, but the cysteinyl residue adduct was not.

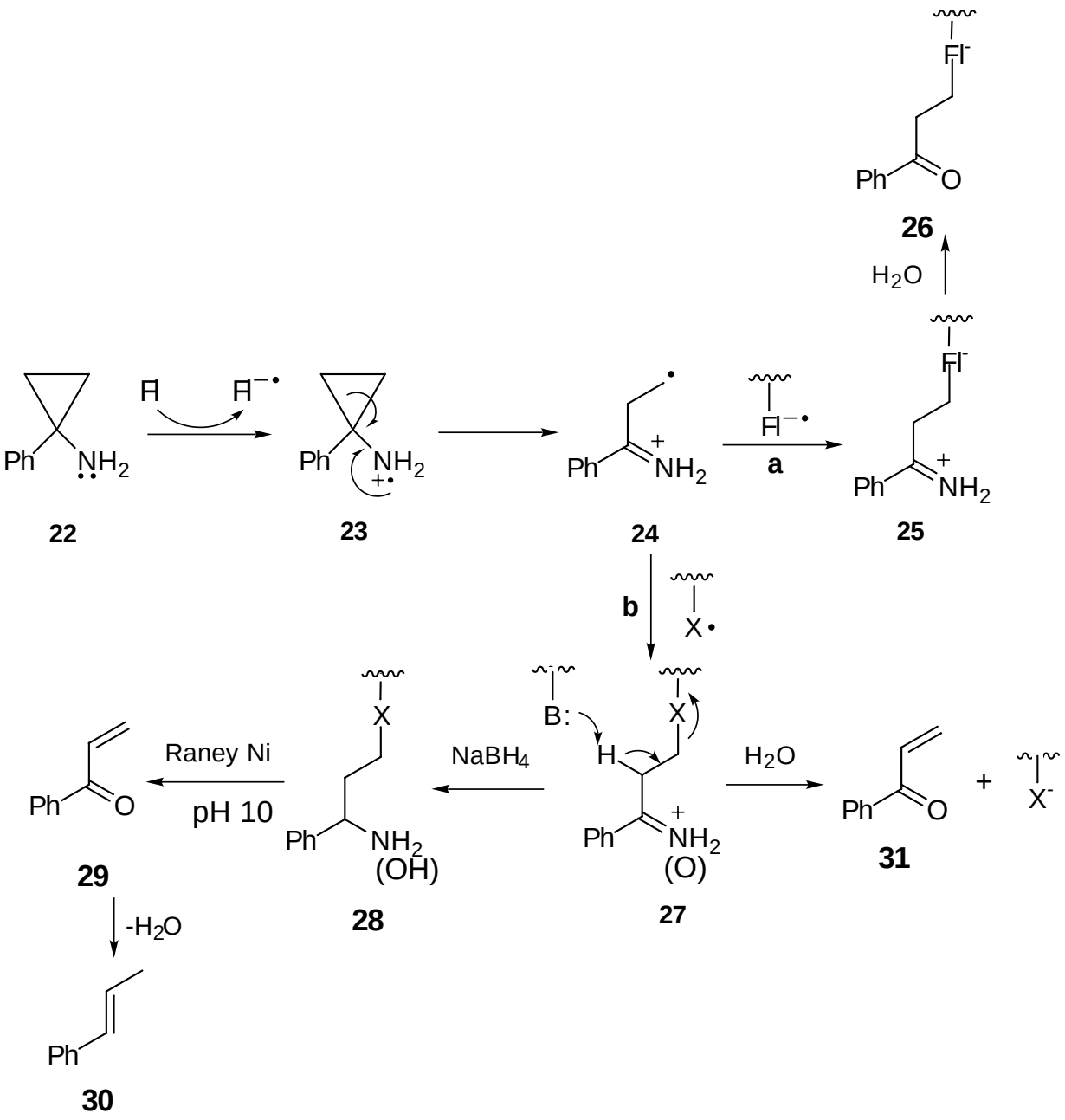

Scheme 8. Proposed MAO Inactivation Pathways for **22**

Based on the proposed mechanism shown in Scheme 5, inactivation could arise from the activation of the cyclopropyl ring **22** by the proposed normal catalytic mechanism to give a reactive primary radical **23**, which could react either with the flavin semiquinone (pathway **a**), leading to adduct **26**, or with an amino acid radical (pathway **b**) to give **27**.

A Retro-Michael reaction would cleave the inactivator from the enzyme to yield acrylophenone (**31)** and active enzyme. The structure of **26** was determined by carrying out three aqueous-based organic reactions. Treatment of **26** with sodium [^{3}H]borohydride led to the incorporation of 1 equivalent of tritium into the inactivated enzyme that did not go into native enzyme, indicating the presence of a ketone (or imine) moiety. Baeyer-Villiger oxidation with trifluoroperoxyacetic acid (to give phenyl ether) followed by saponification with sodium hydroxide released all of the radioactivity from the enzyme as [^{14}C]phenol, indicating a phenyl ketone moiety. Finally, incubation of labeled enzyme with 0.5 M sodium hydroxide released the radioactivity as acrylophenone, indicating enolization of **26** followed by β-elimination of the flavin. Attatchment to the flavin was demonstrated by first showing spectrophotometrically that the flavin was in a reduced state and then carrying out a proteolytic digestion of the labeled enzyme and showing by gel filtration chromatography that the radioactivity release paralled the change in the flavin absorption.

The flavin spectrum indicated that it was oxidized in adduct **28**, suggesting that this adduct was not attached to the flavin. When the treatment of the radioactively-labelled and sodium borohydride reduced amino acid adduct **28** with Raney nickel, a reagent known to reduce C-S bonds exclusively,[28-29] the only radioactive product isolated was *trans*-β -methylstyrene (**30**). This was confirmed by the 5, 5'-dithiobis(2-nitrobenzoic acid) titration that showed only five cysteine residues whereas the native enzyme titrated for six. Therefore, one cysteine is lost upon amino acid labeling.

From previous studies it was not possible to determine if the cysteinyl residues of MAO were in the active site or were important for the appropriate conformation of the enzymes. Recent research[30] has found that racemic N-cyclopropyl-N-α-methylbenzylamine (**32**), a mechanism-based inactivator of bovine liver MAO-B, labels Cys-365, which corresponds to Cys-374 and Cys-365 in human MAO-A and MAO-B, respectively (Scheme 9), and identifies these cysteinyl residues to be in the active site of the respective isozymes. The active site S-3-hydroxypropylcysteinyl residue **36** in which the propyl carbon atoms were shown to be derived from the cyclopropyl group of racemic N-cyclopropyl-N-α-methylbenzylamine (**32**), provides definitive evidence for the SET pathway.

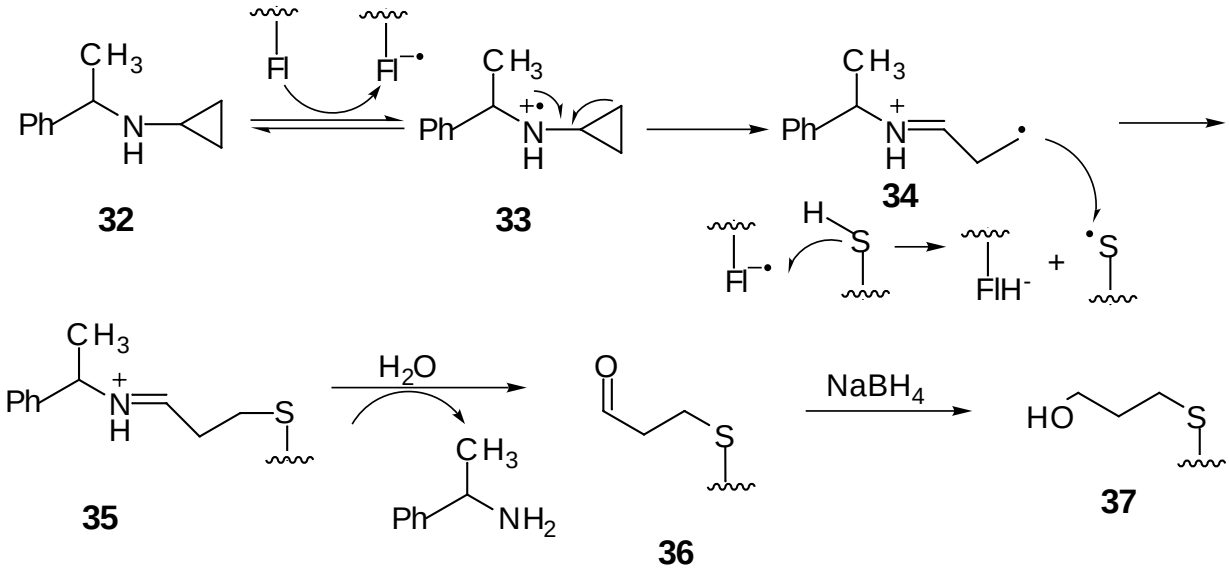

Scheme 9. The Inactivation of MAO-B by N-Cyclopropyl-N-α-methylbenzylamine (**32**)

Another strategy to detect the initial electron transfer is to use the built-in radical trap (the imine double bond), an intermediate of the cyclobutylamine analogs. Incubation of MAO with 1-phenylcyclobutylamine (**38**) led to the time-dependent inactivation (Scheme 10), presumably by the trapping of **40** by the flavin semiquinone.[31] 1-Phenylcyclobutylamine (**38**) undergos one-electron rearrangement upon one-electron oxidation catalyzed by MAO and leads to **39**, which would trigger cyclobutyl ring cleavage, leading to **40**. There is a lot of examples that intermediates related to **40**, regardless of whether they contain a carbon-carbon, carbon-oxygen, or carbon-nitrogen double bond, undergo endo-cyclization to cyclopentyl, tetrahydrofuranyl, or pyrrolidinyl radicals, respectively.[32-34] Second-electron transfer would give the corresponding cyclopentene, dihydrofuran, or pyrroline, respectively. A time-dependent decrease in the concentration of 1-phenylcyclobutylamine (**38**) was observed with a concomitant increase in the formation of 2-phenyl-1-pyrroline (**42**) (Scheme 10, pathway **a**). These results are consistent with the initial formation of the 1-phenyl-1-cyclobutylaminyl radical cation (**39**). It is assumed that if the intermediate **41** is stable enough to leak out of the active site, it could be trapped by a radical spin trap. Incubation of MAO with 1-phenylcyclobutylamine (**38**) in the presence of the radical spin trap α-phenyl *N-tert*-butylnitrone (**45**) resulted in a

time-dependent formation and increase in an EPR triplet of doublets centered at a g value of 2.006, suggesting of the formation of a stable nitroxyl radical.[35]

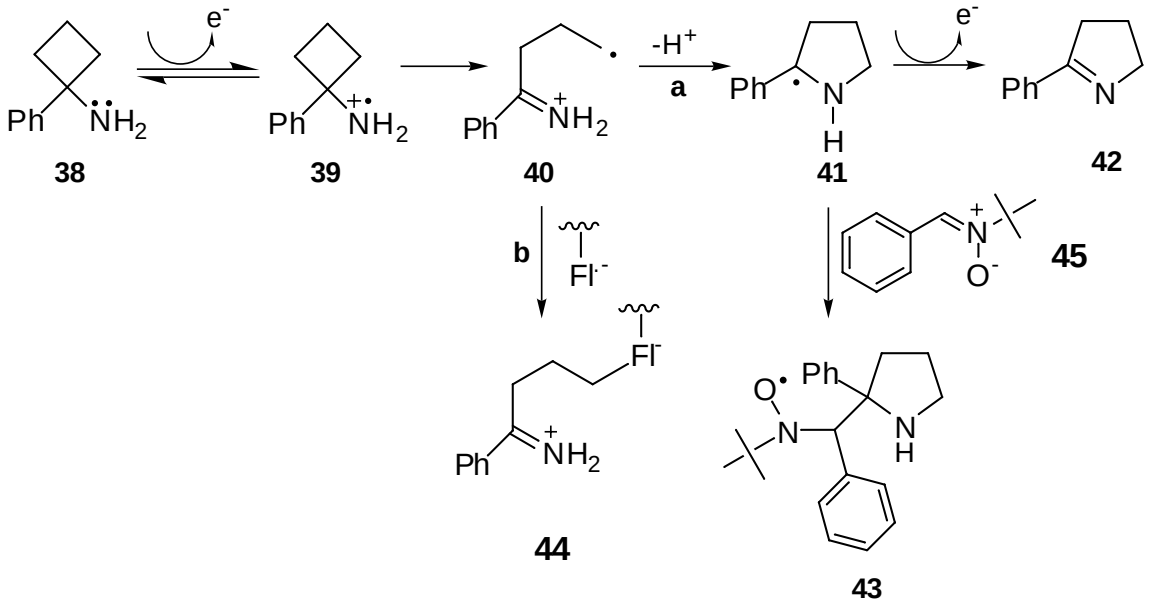

Scheme 10. Evidence for Initial Electron Transfer Using Spin Traps

(3) Differention between proton/electron and hydrogen atom transfer mechanisms

Since the spectroscopic methods failed to provide evidence of the radical intermediate, the strategy to differentiate the principal difference in the proton/electron (Scheme 5, pathway **a**) and hydrogen atom transfer (Scheme 5, pathway **d**) pathways is to use compound *trans*-1-(aminomethyl)-2-phenylcyclopropane (**46**) as a probe to check the fate of the *trans*-(2-phenylcyclopropyl)carbinyl radical (**47**) (Scheme 11).[36] The key point here is the presence or absence of intermediate carbon-centered radical **48**.

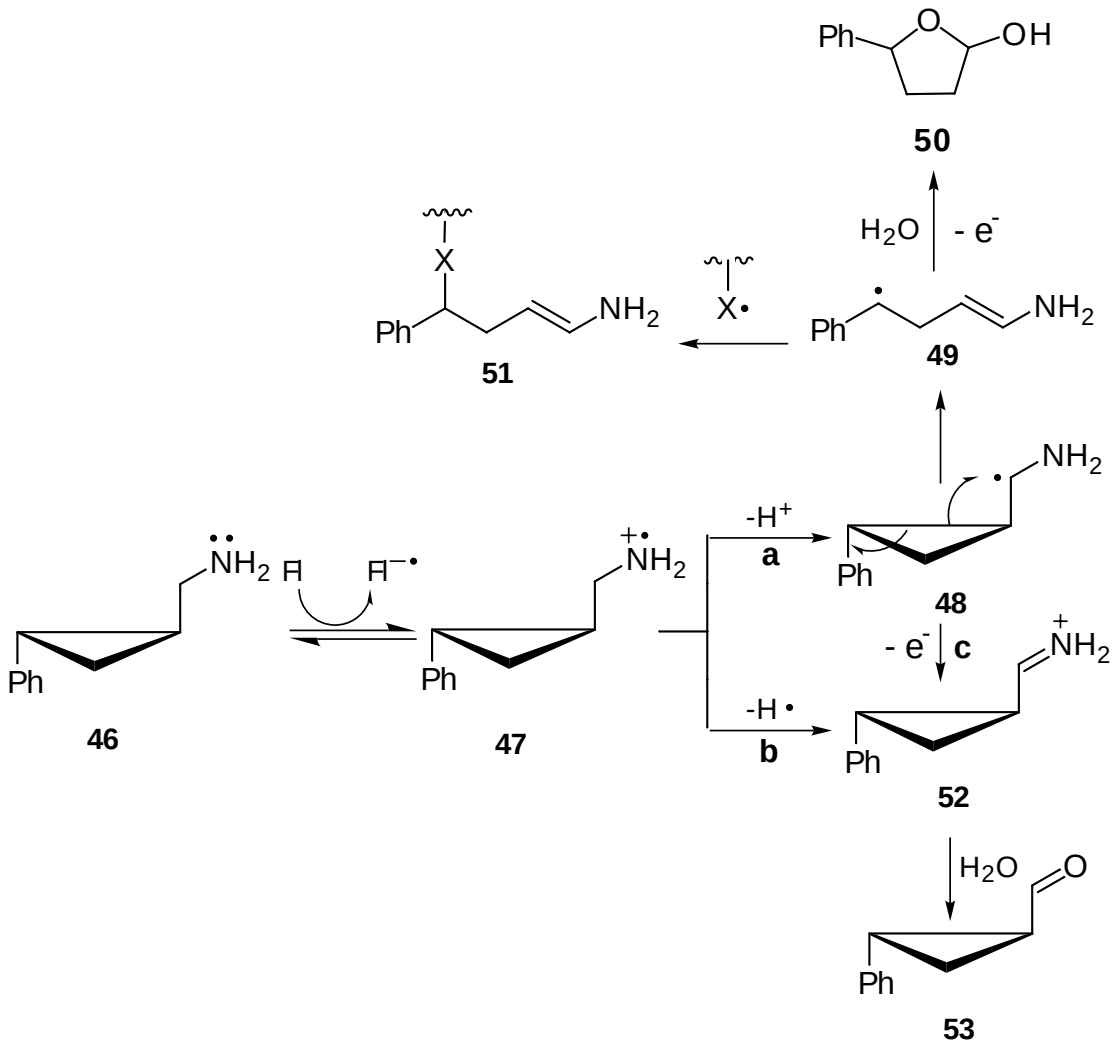

Scheme 11. The Differentiation of Proton/Electron and Hydrogen Atom Transfer Mechanism

The *trans*-2-(phenyl-1-methylcyclopropyl)carbinyl radical is an unstable radicals, decomposing, with cleavage of the cyclopropyl ring, at a rate of 3×10^{11} s^{-1}.[37] If proton removal occurred following initial electron transfer (pathway **a**), the intermediate cyclopropylcarbinyl radical **48** would result. Ring cleavage would then give **49**. If hydrogen atom transfer occurred (pathway **b**), however, the cyclopropylcarbinyl radical would be bypassed and the corresponding cyclopropylimine **53** would form. A chemical

model study revealed that the intermediate **48** will produce the product **50**. Incubation of MAO with **46** produced *trans*-2-phenylcyclopropanecarboxaldehyde (**53** exclusively; no inactivation occured, and no **50** was produced. This meant that either the exclusive pathway for the MAO-catalyzed oxidation of amines was pathway **b** or second-electron transfer (pathway **c**) occurs faster than cyclopropyl ring cleavage.

Two rationalizations for why second-electron transfer could be faster than ring cleavage are (1) the amino group stabilizes the radical, thereby slowing down the rate of ring cleavage, and (2) free rotation is frozen during enzyme binding so that overlap between the α-carbon radical orbital and the orbitals of the cyclopropyl ring is poor.

Aminomethylcubane (**54**) was used to test the orbital overlap hypothesis (Scheme 12).[38] If an α-radical **56** is generated during turnover, then there are three symmetrical bonds in three different orientations that could overlap with the orbital containing the radical, any one of which would lead to cubane ring cleavage at a rate of 3×10^{10} s^{-1}.[39]

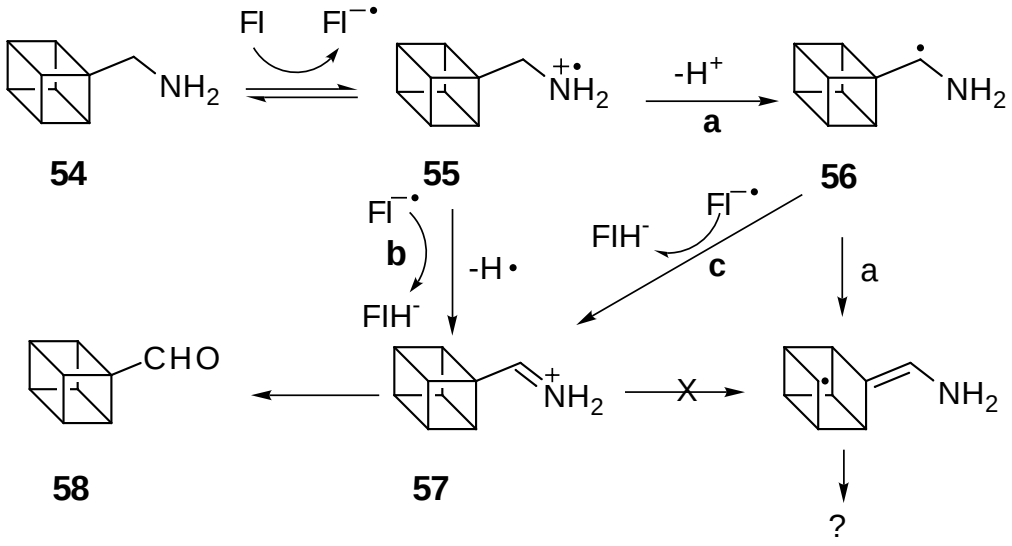

Scheme 12. Evidence for the Proton/Electron Transfer Mechanism

Treatment of MAO with aminomethylcubane (**54**) led to time-dependent irreversible inactivation of the enzyme. Two metabolites were isolated; one was identified as cubanecarboxaldehyde (**58**), and the other was shown by GC-MS to be missing an intact cubane structure and to contain a resonance in the NMR spectrum in the aromatic region.

The important finding is that the cubane structure is destroyed, indicative of the generation of an α-radical. The ring cleavage product could not have come from the corresponding cation (iminium ion) **57**, because cubylcarbinyl cations are well-known to undergo exclusive rearrangement to homocubanes without ring cleavage.[40-42] No evidence for a homocubane was found. Therefore, the decomposition of the cubane nucleus must result from generation of an α-radical or possibly from an α-carbanion.[43-44] Formation of cubanecarboxaldehyde **58** could arise by second-electron transfer from the α-radical **56** prior to cubane ring cleavage (pathway **c**). These results strongly argue against a transfer of a hydrogen atom from the amine radical (cation) (pathway **b**) and support the proton/electron transfer mechanism (pathway **a**).

Experiments designed to differentiate the radical and carbanion pathways have been achieved via the MAO-catalyzed reaction of cinnamylamine 2,3-oxide.[45] The results support the formation of an α-radical rather than a carbanion during the MAO-catalyzed reactions. These results add support for the formation of an α-radical during the MAO processing of primary amines.

(4) Evidence for a covalent pathway

From an α-radical intermediate **16** (Scheme 5), the radical combination to **17** followed by β-elimination is also reasonable. It was found that inactivation of MAO-B by either (*R*)- or (*S*)-[^{3}H]-3-aryl-5-((methylamino)methyl)-2-oxazolidinone (**59**) (Scheme 13) led to the incorporation of 1 equiv of tritium per enzyme after denaturation, suggesting that a covalent adduct was formed.[46] (*R*)- and (*S*)-[carbonyl-^{14}C]-3-aryl-5-((methylamino)methyl)-2-oxazolidinone (**59**) also inactivated MAO-B with the incorporation of 1 equivalent of radioactivity after denaturation. The fact that both the tritium in the side chain and the ^{14}C in the oxazolidinone ring become attached stoichiometrically to the enzyme suggests that the entire molecule is part of the enzyme adduct **62**. This adduct has two heteroatoms (the methylamino group nitrogen and the X group of the enzyme) attached to an sp^3 carbon atom of the inactivator. These types of systems (e.g., acetals, aminals, thioaminals, etc.) are stabilized by electron-withdrawing groups attached to the α-position. In this case, the electron-withdrawing atoms of the oxazolidinone could act to stabilize the adduct relative groups such as alkyl and arylalkyl that are part of normal substrates for enzyme. Therefore, it is believed that this adduct, an analog of **17**, is stable and will not decompose by β-elimination to give the imine product.

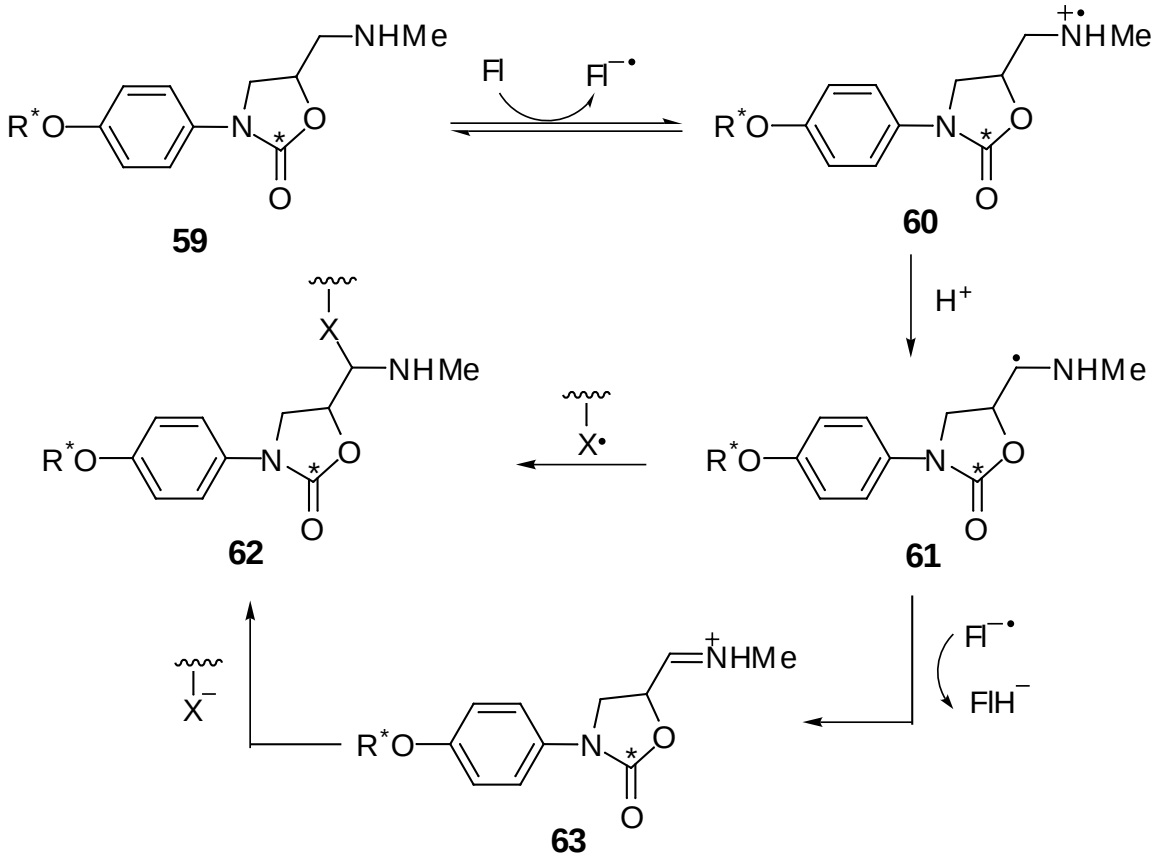

Scheme 13. The Inactivation of MAO by 3-Aryl-5-((methylamino)methyl)-2-oxazolidinones (**59**)

B. HAT pathway

(1) Evidence against the SET pathway

Even though the SET mechanism has been supported by a series of inactivation studies, some experiments also provided evidence against this mechnaism. The major issues are: (1) spectral data failed to find any observable intermediates such as a flavin semiquinone or an amine substrate 4a-flavin adduct during the time course of MAO-B flavin reduction under anaerobic reductive half-reduction stopped-flow experiments with a

variety of α,α-diprotio- or α,α-dideuteriobenzylamine and phenylethylamine analogs.[47-48] Additionally, a magnetic field in the range 10-6500 G has no influence on the rate of flavin reduction, thereby precluding the formation of any stable radical pair intermediates with a lifetime longer than 10^{-6} s;[47] (2) energy calculations indicate that the the single-electron transfer from the amine to the flavin is thermodynamically improbable.[48] In order for the SET mechanism to be thermodynamically permitted, the free energy of activation rate-limiting reduction of MAO by amine substrates under anaerobic conditions ($G^{\ddagger}$), must be lower than the free energy of electron transfer from the substrate to flavin (G_{et}°).[49] The calculated $G^{\ddagger}$ for the *meta*-substituted benzylamine analog (using the stopped flow kinetic data and Eyering equation) is 12.3 kcal/mol and the calculated G_{et}° is in the range of 20-30 kcal/mol;[48] (3) some 1-cyclopropyl-4-substituted-1,2,3,6-tetrahydropyridines exibit excellent substrate properties rather than the expected mechanism-based inactivation. The two principal metabolites are the dihydropyridinium and N-decyclopropyl species.[50a]

(2) The proposed HAT mechanism

Based on these observations, it was suggested that the aminyl radical cation may not be obligatory intermediates in the MAO-catalyzed oxidation. It was therefore proposed that a mechanism involving direct hydrogen atom abstraction from the substrate **14** to give the α-radical **16** followed by rapid electron transfer from the aminyl substrate radical to form the flavin hydroquinone and the protonated imine product **14**, may be an alternative catalytic pathway for these biotransformations.[50b]

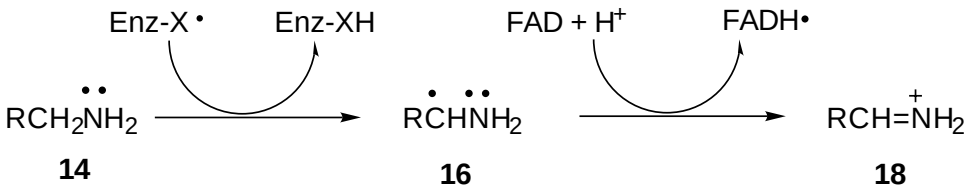

Scheme 13. The Inactivation of MAO by 3-Aryl-5-((methylamino)methyl)-2-oxazolidinones (**59**)

C. Polar pathway

A nucleophilic (polar) mechanism has also been proposed based on chemical model studies of primary and secondary amines (Scheme 15).[51-53] These experiments demonstrated that, under certain conditions (wet acetonitrile containing 10 mM HCl heated to 80 °C for 7 days to give a 30% yield of oxidized primary amine), benzylamine could be oxidized to benzaldehyde in the presence of the model flavin 3-methyllumiflavin.[52] Mariano et al. also demonstrated[53] that with the use of 3-methyl-5-ethyllumiflavinium perchlorate it is possible to show that primary amines, and hydrazines, can undergo oxidation by nucleophilic mechanisms. According to this pathway, the amine substrate **64** forms an adduct **65** with FAD. Subsequent cleavage of **65** yields the iminium metabolite **66** and $FADH_2$.

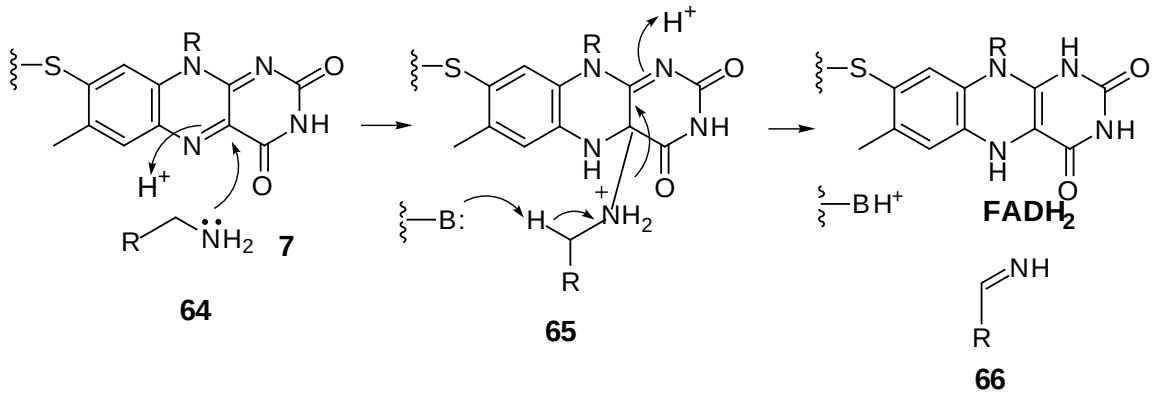

Scheme 15. The Proposed Polar Mechanism for the MAO-Catalyzed Oxidation

1.3. 1-Methyl-4-phenyl-1,2,3,6-tetrahydropyridine (MPTP)

1.3.1. Neurotoxin and Parkinson's disease

1-Methyl-4-phenyl-1,2,3,6-tetrahydropyridine (MPTP, **67**) is a good MAO-B and to a lesser extent, MAO-A substrate.[54] Researchers' interest in this compound is due to its neurotoxicity. MPTP causes a permanent form of Parkinsonism that closely resembles

Parkinson's disease. Investigators discovered this effect in the 1980s[55-56] when heroin addicts in California who had taken an illicit street drug contaminated with MPTP began to develop severe Parkinsonism. This discovery, which demonstrated that a toxic substance could damage the brain and produce parkinsonian symptoms, caused a dramatic breakthrough in Parkinson's research. For the first time scientists were able to simulate Parkinson's disease in animals and conduct studies to increase understanding of the disease.[57-58]

Parkinson's disease is both a chronic and progressive neurological disorder which is characterized clinically by a decrease in spontaneous movements, gait difficulty, postural instability and rigidity and tremor. Parkinson's disease occurs when about 80% of the dopaminergic neurons of the substantia nigra die or become impaired.[59] Dopamine is the neurotransmitter of nigrostriatal neurons. The signal stimulated by the activation of receptors on the postsynaptic neurons produces smooth, purposeful muscle activity. Loss of dopamine causes the nerve cell of the striatum to fire out of control, leaving patients unable to direct or control their momvements in a normal manner.[59] The cause of this cell death or impairment remains unknown but a combination of oxidative damage, exposure to environmental toxins, genetic predisposition and accelerated aging may be involved in neurodegeneration.

1.3.2. The biotransformation of MPTP

A considerable amount of work has been done toward elucidation of the mechanism of MPTP-induced neurotoxicity. The toxication of MPTP is mediated by MAO-B.[60] MPTP has been shown to be oxidized by MAO-B to the 2,3-dihydropyridinium species ($MPDP^+$, **68**) (Scheme 16).[61-63] This metabolite is not stable and undergoes a further two electron-oxidation that may be enzyme mediated or by a disproportionation mechanism to yield the 1-methyl-4-phenylpyridinium ion (MPP^+, **69**).[64-66]

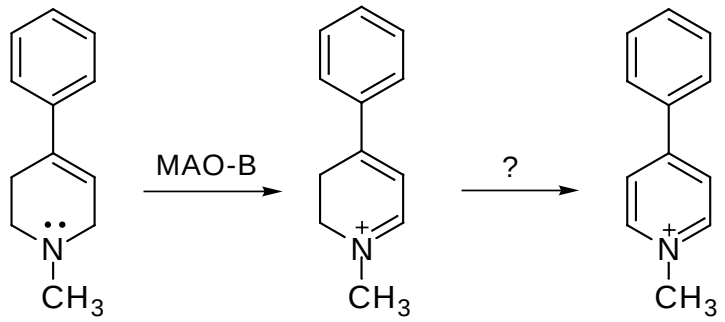

67 **68** **69**

Scheme 16. MAO Catalyzed Oxidation of MPTP

This pyridinium metabolite is actively accumulated in nigrostriatal nerve terminals by the DA transport system[67-68] where it inhibits Complex 1 of the mitochondrial respiratory chain within the dopaminergic neurons, thereby causing their death.[69-71] This MAO-dependent formation of MPP^+ appears to be a necessary event in the neutrotoxic process because pretreatment of mice and monkeys with MAO-B inhibitors prevents the MAO-B-catalyzed oxidation of MPTP and MPTP-induced neurotoxicity.[72-73] The metabolite MPP^+, but neither MPTP nor $MPDP^+$, has high affinity for the DA uptake system and administration of a DA uptake blocker prevents the neurotoxicity of the subsequent administration of MPTP.[67-68,74-75] MPP^+, but neither MPTP nor $MPDP^+$, inhibits the oxidation of NADH-linked substrates such as pyruvate and melate by mitochondria [67,70,71,76] following the localization of MPP^+ by the mitochondria.[71] The resulting depletion of ATP within the neurons may be the primary mechanism by which MPTP ultimately destroys the neurons.[71]

Researchers also found that MPTP, $MPDP^+$, and MPP^+ are reversible, competitive inhibitors of both MAO-A and MAO-B.[77] MPTP and $MPDP^+$, but not MPP^+, are mechanism-based inhibitors of MAO-A and MAO-B. Under the experimental conditions used, the decay of activity on incubation of either enzyme with MPTP is exponential and is not reversed by gel exclusion or brief dialysis. After a prolonged dialysis of MAO-B previously inactivated by MPTP, a part of the activity returns.[77] The partition coefficients for the inactivation are large since the rate of oxidation of MPTP by either enzyme greatly exceeded the rate of inactivation.[77] When [^{3}H]MPTP was used for inactivation of the

MAO-B, about 5 mol of product was incorporated/mol protein, suggesting dissociation of the product(s) from the enzyme and suprious recombination with nucleophiles in the enzyme.

1.3.3. SAR studies of MPTP analogs

Many MPTP analogs have been synthesized and examined for their MAO activities. The purpose of this research is to use these compounds to probe the structural requirements of the active site of the enzyme. Since there are no reports of the three-dimensional structure of MAO, all of the information available on the structure of the active sites are based on their structure activity relationship (SAR) studies. Based on these structural insights, mechanism-based inhibitors of the enzyme may be designed and synthesized.

A. MPTP analogs as MAO substrates:

Some common findings of the structural features which are associated with MAO substrate properties of MPTP analogs include the following:

1. The 4,5- double bond of the tetrahydropyridinyl ring is essential for compounds to be MAO substrates.[80]

2. Substituents at the C-4 and N-1 positions of the heterocyclic moiety are allowed. Placement of a substituent anywhere else in the tetrahydropyridinyl ring diminishes MAO substrate activity.[81]

3. Substitution at the N-1 position is limited to small substituents. The N-methyl group is better than hydrogen, ethyl and the α-hydroxyethyl groups.[82]

4. Substitution at the C-4 position of the tetrahydropyridine is necessary. But the phenyl group is not necessary for compounds to be MAO substrates. Replacement of the phenyl group by a 1-methyl-2-pyrrolyl,[83] a benzyl,[82] a phenoxyl,[84] a thiophenoxyl,[85] or a cyclohexyl group[82] enhances or maintains the MAO activity.

5. *Para*-substituents on the phenyl ring produce steric hindrance unfavorable to reactivity, while some *ortho*- or *meta*-substituents may increase the reactivity.[54, 82, 86, 87-90]

6. Substitution of an electron-withdrawing group, such as pyridinyl group at the C-4 position of the tetrahydropyridine causes a decrease in MAO activity.[91]

In addition to the above findings, quantitative SAR (QSAR) studies[86,91] also indentified that lipophilicity, sterics and electronics play important roles in determining MAO activity.

B. MPTP analogs as MAO inhibitors

An early effort focused on the modification of MPTP to form a mechanism based inactivator.[4] MPTP is a good MAO-B substrate. The substitution of a small group such as cyclopropyl at N-1 produces a structural analog with overall similar geometry. We already know that cyclopropyl groups attached to a radical bearing atom undergo very rapid ring opening. According to the SET mechanism, when this compound is incubated with MAO-B, an initial one-electron transfer from **70** to FAD would generate the aminium radical **72** (Scheme 17). This intermediate would have the option to ring open to the reactive primary radical **74** (pathway **a**) leading to enzyme inactivation, or subsequently undergo a second one-electron loss to generate the dihydropyridinium intermediate **78** (pathway **b**).

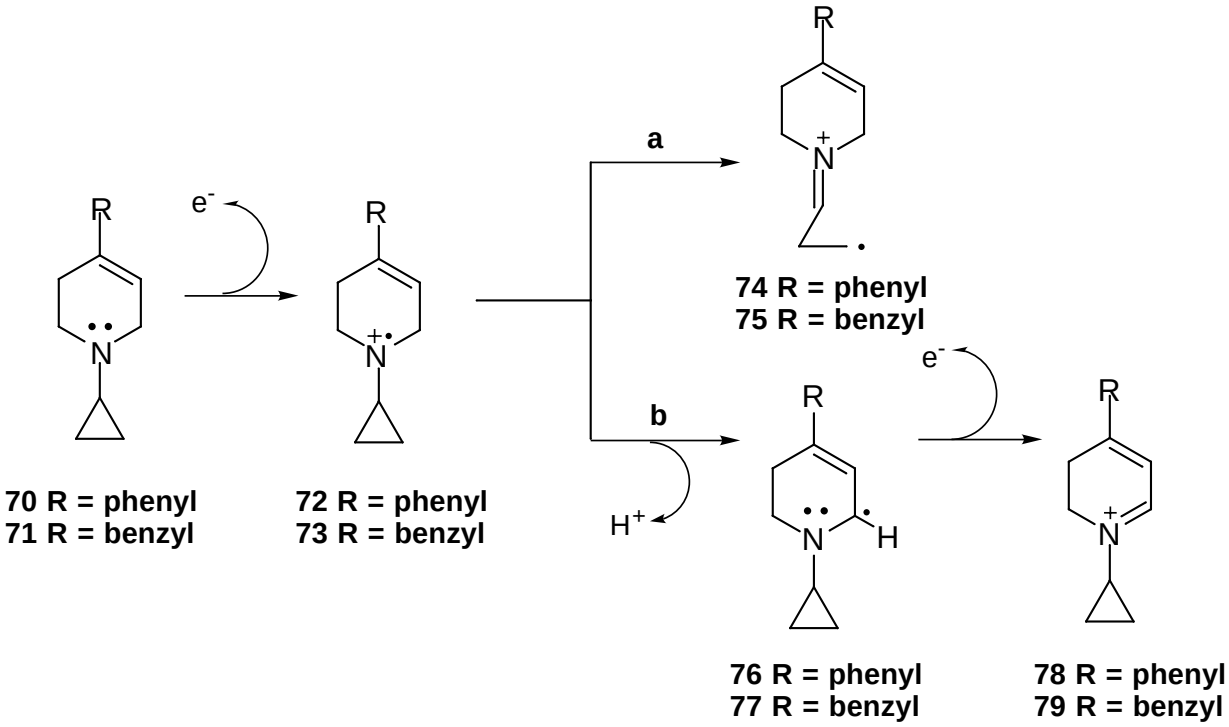

Scheme 17. Proposed SET Pathway for the MAO-B Catalyzed Oxidation of 1-Cyclopropyl-4-substituted-1,2,3,6-tetrahydropyridines

Experiments established that 1-cyclopropyl-4-phenyl-1,2,3,6-tetrahydropyridine (**70**) is a good time and concentration dependent inhibitor of MAO-B (k_{inact}/K_i=1.0 min^{-}

$^{1}mM^{-1}$).[92] The absence of detectable levels of the dihydropyridinium metabolite **78** implies that the enzyme processes the compound as a substrate but the intermediate formed in the catalytic process inactivates (forms a covalent bond with) the enzyme prior to escaping from the active site and that the deprotonation of **72** to form **76** (pathway **b**) does not compete effectively with the ring opening (pathway **a**).

Similarly, another MPTP analog 4-benzyl-1-cyclopropyl-1,2,3,6-tetrahydropyridine (**71**) is also reported to be a good time and concentration dependent inhibitor of MAO-B,[93] although the k_{inact} and K_i could not be obtained because of the nonlinear inactivation behavior of this compound. However, what is surprising, it is also an excellent MAO-B substrate, with k_{cat}/K_m=1500 $min^{-1}mM^{-1}$ at 37 ˚C, and the partition ratio greater than 1000. These data clearly suggest that dihydropyridinium formation is the preferred pathway over enzyme inactivation. This finding leads us to reconsider this biotransformation. If the SET is an obligatory pathway, the intermediate cyclopropylaminyl radical cation **73** must partition between pathway **a**, leading to the primary carbon-centered radical **75** and enzyme inactivation, and pathway **b**, leading to the allylic radical intermediate **77** and product formation. Because the rate of ring opening of cyclopropylaminyl radical cations is believed to be very fast, it was anticipated that the ring opening pathway **a** would be the major one. The obvious contradiction between the experimental results and the assumptions argue that the dihydropyridinium formation does not proceed via the SET pathway or that the rate of cyclopropyl ring opening does not compete with the rate of proton loss at C-6. Another interpretation of these results is that this transformation proceeds via an HAT mechanism. This pathway relies on homolytic cleavage of the relatively week allylic carbon-hydrogen bond which might be affected by an enzyme bound radical proposed to be present in MAO-B purified from beef liver. Another tentative explanation is that the conformational constraints lead to poor overlap of the half-filled p-orbital on the nitrogen radical cation and the p-type orbitals of the cyclopropyl group. This restriction prevents the cyclopropyl from opening and, therefore, restricts the ring opening reaction leading to product formation.

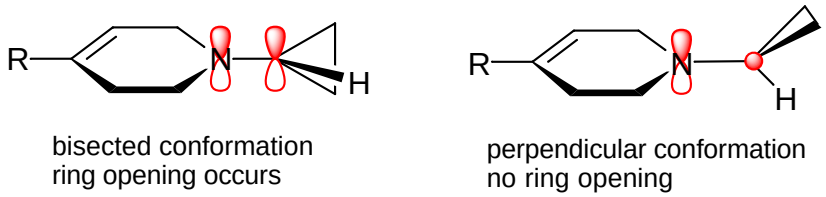

Figure 6. The Conformational Constrains of the Cyclopropyl Group

1.4. Research proposal

As part of our ongoing studies to characterize the structural features responsible for this unexpected biotransformation, we have synthesized and examined the MAO-B substrate properties of a variety of MPTP analogs bearing various heteroaryl groups at the 4-position of the tetrahydropyridinyl ring. The SAR studies focus on electronic features, steric features and polar interactions which may contribute to the substrate activities.

Additionally, isotope effects have been examined to investigate the mechanism and stereoselectivity of the MAO-B catalytic pathway. The synthesis and characterization of regio and stereoselectively deuterated MPTP analogs have been achieved. The results indicate that the catalytic step occurs exclusively at the allylic C-6 position and is rate-determining for both good and poor substrates. The two enantiomers of MPTP bearing a deuterium atom at C-6 have been prepared via chiral aminooxazolinyl derivatives and have been characterized by ^{2}H NMR in a chiral liquid crystal matrix. These enantiomers were used to determine the selectivity of the MAO-B catalyzed α C-H bond cleavage reaction leading to the dihydropyridinium metabolite $MPDP^{+}$. Some of the cyclopropyl analogs have also been synthesized as the potential inhibitors.

Chapter 2. The SAR Study on the MAO-Catalyzed Oxidation of 1-Methyl-4-heteroaryl-1,2,3,6-tetrahydropyridines

2.1. Introduction

Many MPTP analogs have been synthesized in order to investigate MAO-catalyzed oxidation reaction mechanisms and to explore the topology of the active site of the enzyme.[80-92] It has been found that many factors, including electronic and steric features, may contribute to the substrate properties.

As part of our previous studies on the MAO-B catalytic pathway related to this series of compounds, we have examined the effects of varying the C-4 substituent on the k_{cat}/K_m values of various 1-methyl-4-substituted-1,2,3,6-tetrahydropyridinyl derivatives. The results indicate that stabilization of the proposed radical intermediates (analogs of **16**) by the C-4 electron rich group may be related to the efficiency of MAO-B catalysis.[82-85] For example, the transformations of substrates bearing C-4 substituents (**80**-**89**) that should stabilize the putative allylic radicals (Figure 7) occur more readily (k_{cat}/K_m = 155 to 4151 $min^{-1}mM^{-1}$) [82-85, 92] than the transformations of compounds bearing more electronegative C-4 substituents [**87**-**89**] (k_{cat}/K_m = 6 to 60 $min^{-1}mM^{-1}$).[92]

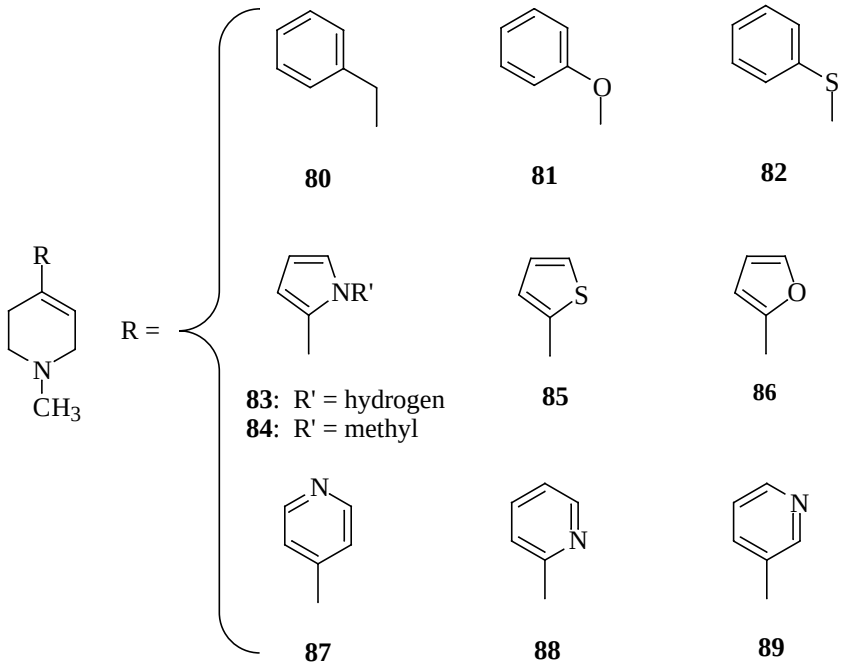

Figure 7. MPTP Analogs Exhibiting Different Substrate Activities

The idea of substituting the five-membered heteroarenes for the phenyl group at the C-4 position of MPTP is based on the knowledge of the electronic properties of the five-membered heteroarenes such as furan, thiophene, pyrrole and imidazole.[95-98] To illustrate, it is assumed that all ring atoms of furan are sp^2-hybridized (Figure 8). The overlap of the five 2Pz atomic orbitals yields delocalized π-MOs , three of which are bonding and two antibonding. MOs π_2 and π_3, as well as π_4* and π_5*, are energetically nonequivalent (Figure 8, a, b, c), in contrast to the carbocycle benzene which is iso-π-electronic with furan. Because the nodal plane of π_3 passes through the heteroatom, in contrast to that of π_2, the degeneracy is lost. Every C-atom contributes one electron and the O-atom two electrons to the cyclic conjugated structure. The six electrons occupy the three bonding π-MOs in pairs. As there are six electrons distributed over five atoms, the π-electron density on each ring atom is greater than one. Furan is thus a π-electron excessive heterocycle. Because electron density on each ring atom of thiophene, pyrrole and imidazole (except its 2-position) is greater than one, they all belong to the π-electron excessive heterocycles.

The substrate properties of compounds with different kinds of 5-membered heteroarenes substituted at the 4-position of 1,2,3,6-tetrahydropyridine may reflect the electronic properties of the heteroarens. The differences of these heteroarenes are displayed in several ways. The dipole moment of furan is 0.71D, with the negative end situated on the O-atom. Because of the lower electronegativity of sulfur compared with oxygen, the dipole moment of thiophene is 0.52D and is even smaller than that of furan. The dipole moment of pyrrole is 1.58D. In contrast to furan and thiophene, the heteroatom represents the positive end of the dipole. This could be due to the fact that the heteroatom in pyrrole possesses only one nonbonding electron pair, whereas in furan and thiophene, there are two. The dipole moment of imidazole is 3.7D in the gas phase. In solution, the values for imidazole depend on the concentration because of strong intermolecular hydrogen bonds.

Based on several criteria of aromaticity in heterocycles, such as bond length, ring current effects, empirical resonance energies and molecular orbitals and declocalization energy, it is concluded that the grading of aromaticity is furan < pyrrole < thiophene < benzene.

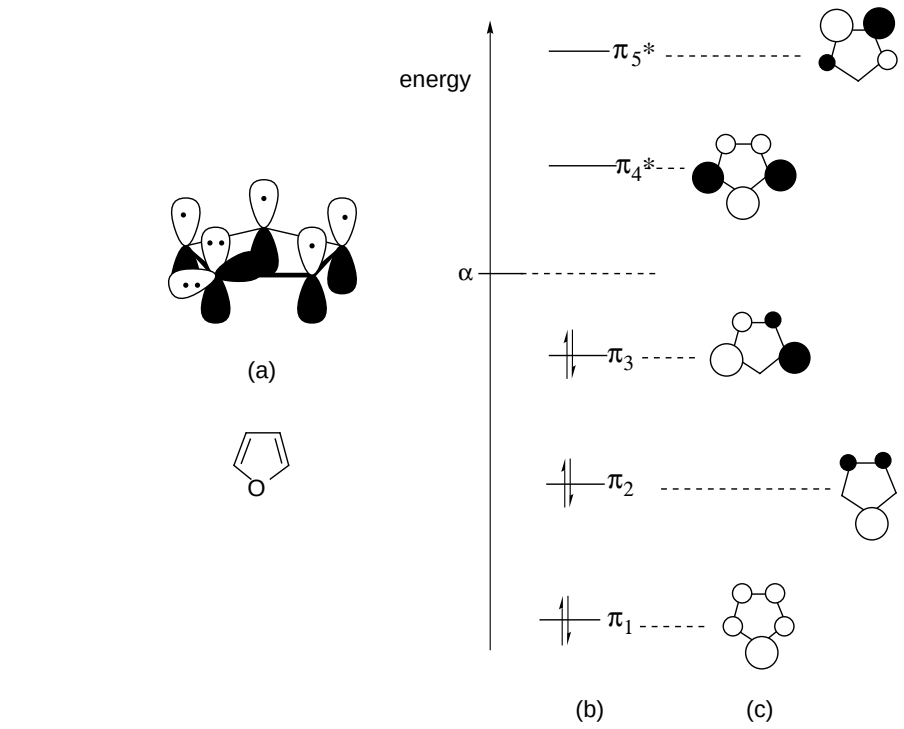

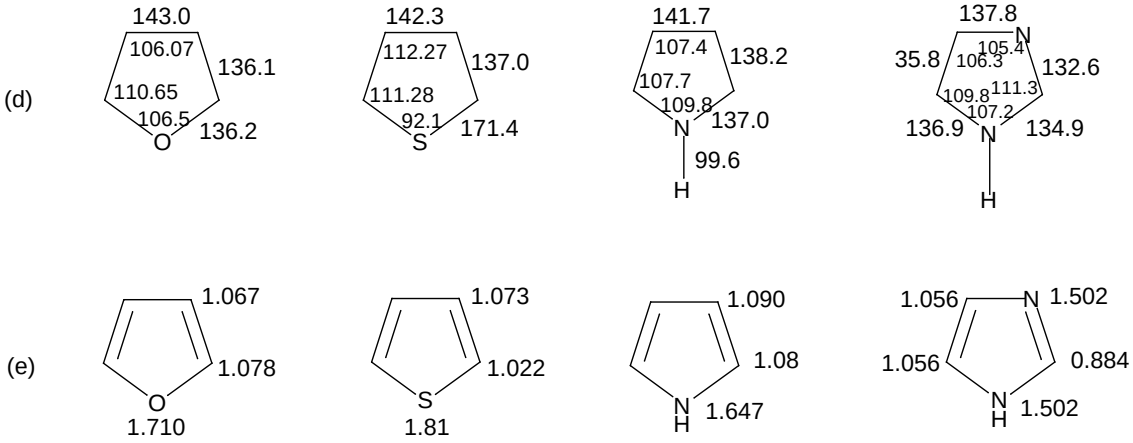

(a) sp^2-hybridization of the ring atoms

(b) energy level scheme of the π-MO (qualitative) and occupation of electron

(c) π-MO (the O-atom is situated at the lower most corner of the pentagon)

(d) Bond lengths in pm, bond angle in degrees

(e) π-electron densities calculated by ab initio MO methods

Figure 8. The Five-membered Heteroarenes *vs* . Phenyl Group

Steric effects, however, also may contribute to the substrate properties of these types of compounds. Youngster reported the effects of altering the substituents on the phenyl ring of MPTP on the ability of the compounds to be oxidized by MAO-B and to produce nigrostriatal dopaminergic toxicity in mice.[54,82,89,100] It was found that alkyl groups substituted at the 2'-position of the MPTP have significant effects on their rates of the MAO-B catalyzed oxidation (Figure 9). For example, the 2'-methyl-MPTP analog **90** has a higher k_{cat} and somewhat lower K_m value than does MPTP. Further lengthening the side chain leads to a progressive decline in the k_{cat}/K_m values. This is due both to a decrease in k_{cat} and increase in K_m with increasing alkyl chain length in the 2'-position. Thus the k_{cat}/K_m at 30 °C (all in $min^{-1}mM^{-1}$) follows the order 2'-methyl-MPTP (**90**, k_{cat}/K_m =1275) > MPTP (**69**, k_{cat}/K_m =523) > 2'-ethyl-MPTP (**91**, k_{cat}/K_m =295) > 2'-n-propyl-MPTP (**92**, k_{cat}/K_m =86) > 2'-isopropyl-MPTP (**93**, k_{cat}/K_m =51)[54] The finding that k_{cat}/K_m values for 2'-chloro-MPTP (**94**, k_{cat}/K_m =1353) and 2'-methoxy-MPTP (**95**, k_{cat}/K_m =233) are similar to the values for 2'-methyl-MPTP **90** and 2'-ethyl-MPTP **91**, respectively, is consistent with the importance of the size of the 2'-substituent in determining the MAO-B substrate properties with their series.[54] Metabolic studies also indicate that high brain levels of the pyridinium metabolite persist for a much longer time after the peripheral administration of 2'-methyl-MPTP than they do following the equivalent administration of MPTP. Therefore, 2'-methyl- and 2'-chloro-MPTP are more potent neurotoxins than MPTP.[82,89,100]

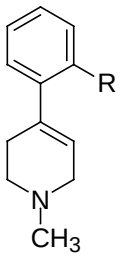

	k_{cat}/K_m ($min^{-1}mM^{-1}$)
69: R = hydrogen	523
90: R = methyl	1275
91: R = ethyl	295
92: R = propyl	86
93: R = isopropyl	51
94: R = chloro	1353
95: R = methoxyl	233

Figure 9. The 2′-Substituted MPTP Analogous

In our recent studies on the MAO-B-catalyzed oxidation reaction of 1-methyl-4-(5-membered heteroarene)-1,2,3,6-tetrahydropyridinyl analogs,[91,101] we also observed the effect of structural alterations on the substrate activities of these molecules. For example, comparison of the substrate properties of analogs **83** vs **84** (Figure 7) involving the introduction of a methyl group at the 1'-position of pyrrole increases the k_{cat} and decreases the K_m values such that the overall substrate activities, as measured by k_{cat}/K_m, increase by a factor of 39 for N-methylpyrrolyl analog. The reason of this phenomenon remains unclear. It may be caused by steric effect or some kind of polar interaction between the molecule and the enzyme.

The present study was undertaken in an attempt to provide additional information on the stereoelectronic features that contribute to the unexpected substrate properties of 1,4-disubstituted-1,2,3,6-tetrahydropyridinyl derivatives and in particular to assess the influence of steric and electronic effects of the C-4 substituent by comparing the substrate properties of a series 1-methyltetrahydropyridinyl derivatives bearing substituted and unsubstituted five-membered heteroaryl groups. The structures of the compounds examined in this study (**96**-**107**) are shown in Figure 10. The newly synthesized analogs are 1-methyl-4-(3,4-dimethylpyrrol-2-yl)-1,2,3,6-tetrahydropyridine (**96**), 1-methyl-4-(1-ethylpyrrol-2-yl)-1,2,3,6-tetrahydropyridine (**97**), 1-methyl-4-(1-n-propylpyrrol-2-yl)-

1,2,3,6-tetrahydropyridine (**98**), 1-methyl-4-(1-isopropylpyrrol-2-yl)-1,2,3,6-tetrahydropyridine (**99**), 1-methyl-4-(1-cyclopropylpyrrol-2-yl)-1,2,3,6-tetrahydropyridine (**100**), 1-methyl-4-(3-methylpyrrol-2-yl)-1,2,3,6-tetrahydropyridine (**101**) and 1-methyl-4-(1,3-dimethylpyrrol-2-yl)-1,2,3,6-tetrahydropyridine (**102**), 1-methyl-4-(2-methylfuran-2-yl)-1,2,3,6-tetrahydropyridine (**103**), 1-methyl-4-(1-ethylfuran-2-yl)-1,2,3,6-tetrahydropyridine (**104**), 1-methyl-4-(3-methylthien-2-yl)-1,2,3,6-tetrahydropyridine (**105**), 1-methyl-4-(1-ethylthien-2-yl)-1,2,3,6-tetrahydropyridine (**106**), and 1-methyl-4-(1-methylimidazol-2-yl)-1,2,3,6-tetrahydropyridine (**107**).

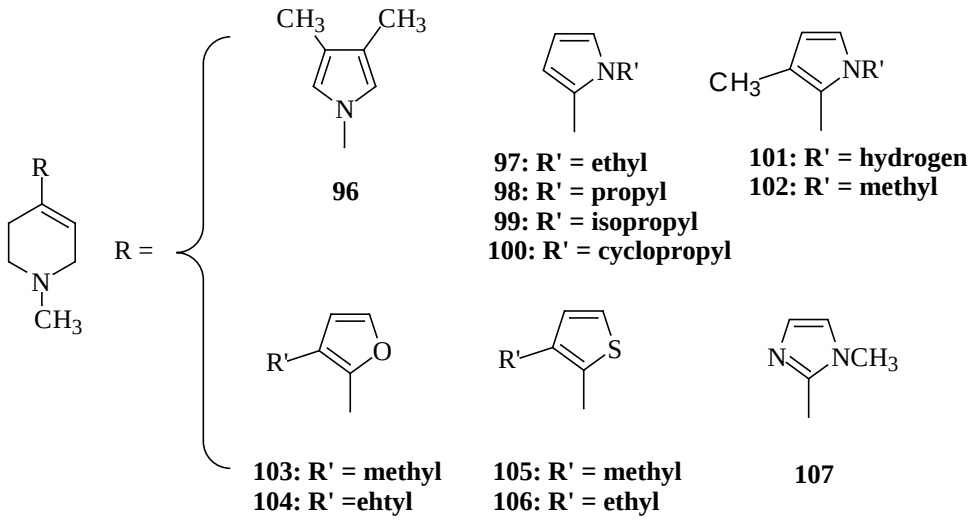

Figure 10. The Newly Synthesized 1-Methyl-4-substituted-1,2,3,6-tetrahydropyridines

2.2. Synthetic approches to 1-methyl-4-substituted-1,2,3,6-tetrahydropyridines

2.2.1. The general strategy for the synthesis of 1,4-disubstituted-1,2,3,6-tetrahydropyridines and the substituted five-membered heteroarens

Based on previous studies, the 1,4-disubstituted-1,2,3,6-tetrahydropyridines often

exhibit MAO substrate properties. This structural unit can be considered as the combination of three parts (Figure 11). The N-1 substituent R', the C-4 substituent R and the tetrahydropyridinyl skeleton.

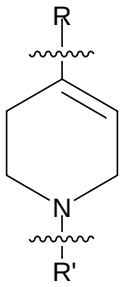

Figure 11. The 1,4-Disubstituted-1,2,3,6-tetrahydropyridines

A. The N-1 groups

As was pointed out in Chapter 1, when the N-1 group is a methyl group, the compound usually exhibts high substrate activity. When the N-1 position is substituted by a cyclopropyl group, the compound is expected to behave as an mechanism-based inhibitor . The incoporation of the methyl group will be discussed in the following part. The synthesis of N-cyclopropyl analogs will be discussed in chapter 4.

B. The 1,4-disubstituted-1,2,3,6-tetrahydropyridinyl skeleton

When 1,4-disubstituted-1,2,3,6-tetrahydropyridine is considered in the light of a retrosynthetic analysis (Scheme 18), it can be visualized as being derived from a 1,4-disubstituted pyridinium salt (route I) or 4-piperidinol (route II), or tetrahydropyridyl triflate or from organometallic precursors (route III). Therefore, it can be constructed retroanalytically in three ways (I, II, III) as shown in Scheme 18.

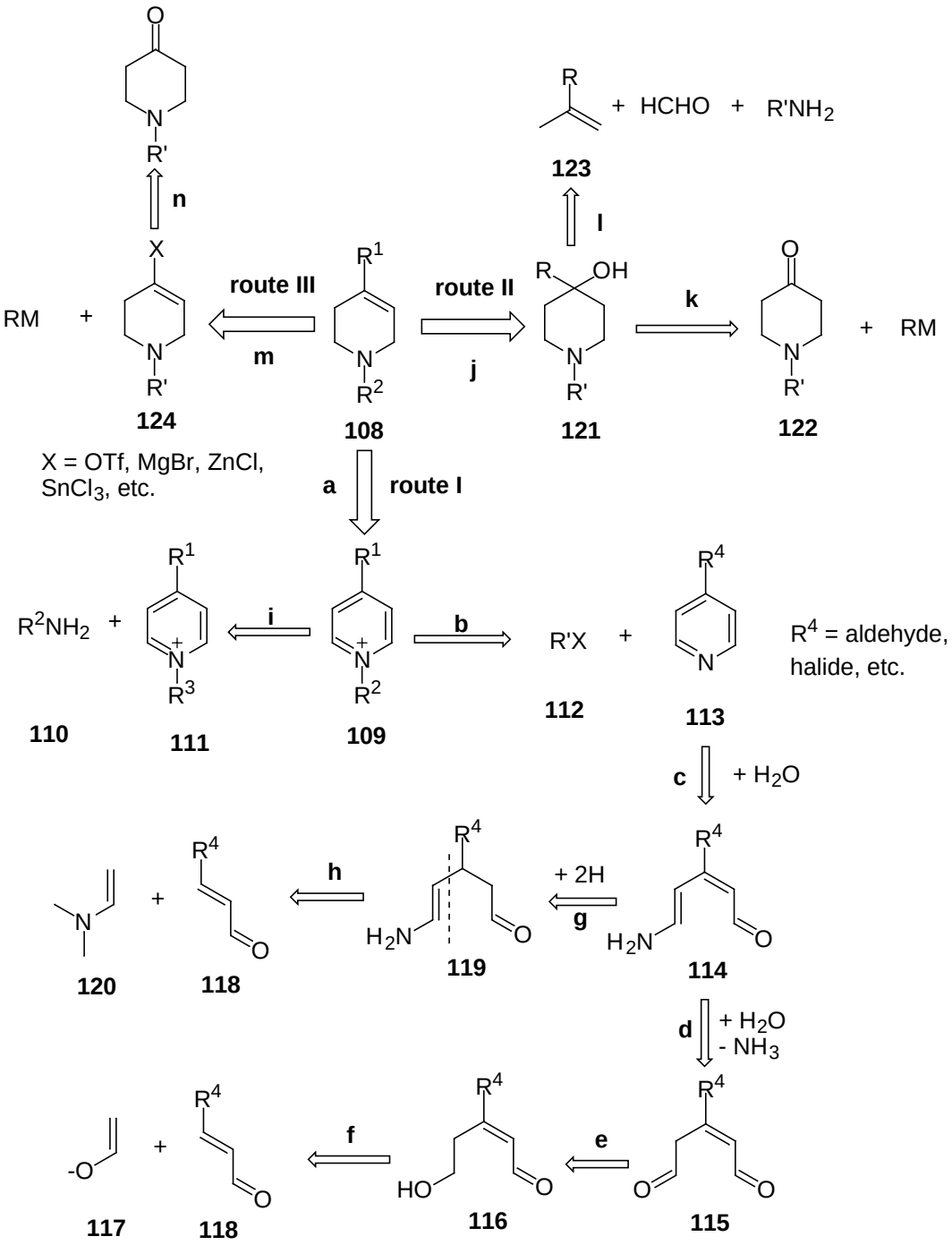

Scheme 18. The Retrosynthesis of 1,4-Disubstituted-1,2,3,6-tetrahydropyridines

If the retrosynthesis follows route I, it can be seen that the oxidation of the tetrahydropyridine leads to the pyridinium salt intermediate **109**. Further retroanalysis of **109** leads via **i** to the primary amine **110** and **111**, a pyridinium salt with different N-substituted group, or via **b** to the alkyl halide **112** and 4-substituted pyridine **113**. Species **113** can be retroanalytically rationalized in several ways.

If the azine structure of the **113** is considered by itself,[95-98] then the retrosynthetic analysis can start at the imine structural element (H_2O addition O→C-2, retrosynthetic pathway **c**). Suggestions for the cyclocondensation of various intermediates arise based on the 5-aminopentadienal or -one system **114**, and further (pathway **d**, NH_3 loss) on glutaconic dialdehyde or its corresponding ketoaldehyde **115**. The ketoaldehyde **115** can be obtained by the oxidation of **116** (pathway **e**) whereas **114** can also be obtained by dehydrogenation of enaminone **119** (pathway **g**). Both **119** and **116** can be obtained by retro-Michael addition involving enamines or enolates with α,β-unsaturated carbonyl systems as starting materials. Of course, the retrosynthetic analysis of pyridinyl unit may also offer the opportunity to prepare this system by the cocycloligomerization of alkynes with nitriles or by [4+2] cycloadditions of azadienes with activated alkynes or alkenes. Cycloaddition between 1,3-dienes and imines also could be explored. But these methods appear to be less practical.

Following route II (addition of water to the tetrahydropyridinyl C-4/C-5 bond), the 4-substituted-4-piperidinol **121** is obtained as the potential starting material. Starting from **122**, the tetrahydropyridinyl system could be formed by addition of an organolithium or Grignard reagent (RM) to the 1-substituted-4-piperidone followed by dehydration of the resulting 4-piperidinol intermediate (pathways **k** and **j**). An alternative way to the 4-piperidinol is the reaction of 2-substituted propenes **123** with formaldehyde and primary amines (pathway **l**).

Route III yields the tetrahydropyridyl organometallic compounds or triflates **124** as potential starting materials, which should produce 1,4-disubstituted tetrahydropyridines by cross coupling reactions with halides or organometallic compounds (pathway **m**). If the starting material is tetrahydropyridyl triflate, further retroanalysis of **124** leads via **n** to the 1-substituted-4-piperidone. It can be converted to the triflate first by enolization and then reaction with phenyltrifluromethanesulfonimide.

Some practical methods for the construction of 1,2,3,6-tetrahydropyridine skeleton have been summarized in the following paragraph.

(1) Addition-dehydration synthesis, in which 1-substituted-4-piperidones are treated with organolithium compound or Grignard reagent followed with water, leads to the 4-substituted-4-piperidinols. Acid catalyzed dehydration of the 4-piperdinols gives the 1,4-disubstituted-1,2,3,6-tetrahydropyridines. For example, the synthesis of 1-methyl-4-(2-furanyl)-1,2,3,6-tetrahydropyridine (**128**) had been achieved by acid catalyzed dehydration of the corresponding 4-(2-furanyl)-4-piperidinol **127** (Scheme 19).[91] The intermediate carbinolamine was prepared by reaction of 1-methyl-4-piperidone with 2-furanyllithium.

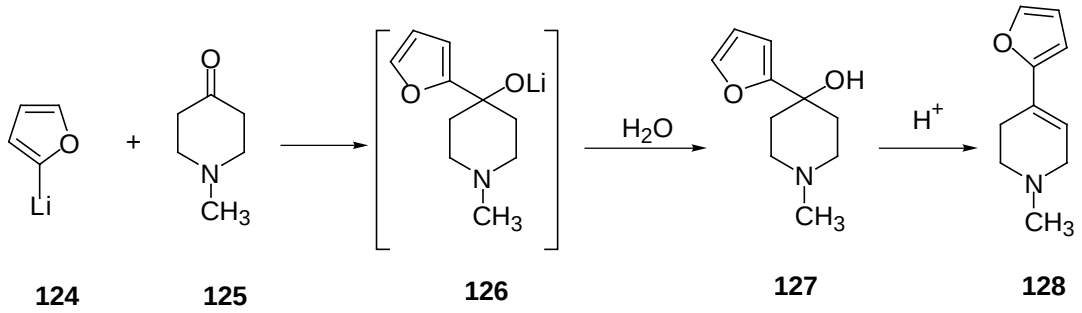

124 **125** **126** **127** **128**

Scheme 19. The Synthesis of 1-Methyl-4-(2-furanyl)-1,2,3,6-tetrahydropyridine

Sometimes, the bulky Grignard regent may increase the extent of enolization resulting in a low yield of the addition product. Difficulties with the dehydration step also have been observed with hindered tertiary piperidinols.[91] When the molecule contains an acid sensitive group, it simply can not be dehydrated under acid conditions.

The 1,4-disubstituted-1,2,3,6-tetrahydropyridine system may also be obtained via intramolecular aminomethylation which yields 4-substituted-4-piperidinols as intermediates. A simplified preparation of 1-cyclobutyl-4-phenyl-1,2,3,6-tetrahydropyridine (**134**) from 2-phenylpropene (**129**), formaldehyde (**130**) and cyclobutylamine (**131**) was achieved by the simultaneous rearrangement of 3-cyclobutyl-6-methyl-6-phenyltetrahydro-1,3-oxazine (**132**) and dehydration of the 4-phenyl-4-piperidinol **133** since the conditions for both these reactions are similar (Scheme 20).[102]

The conversion of **132** to **134** via **133** may be looked upon as cleavage of the oxazine ring followed by intramolecular aminomethylation.[103-104]

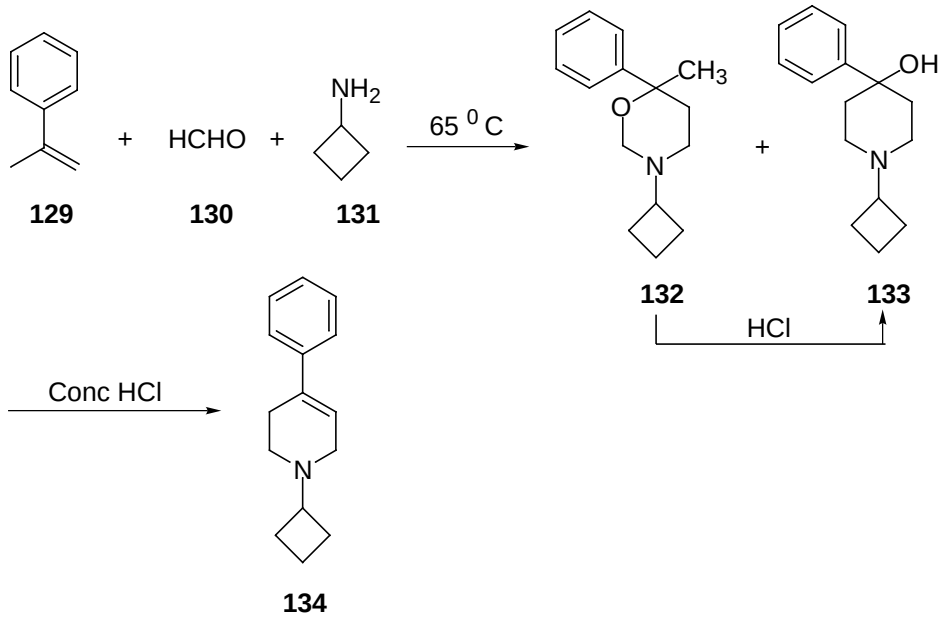

Scheme 20. The Synthesis of 1-Cyclobutyl-4-phenyl-1,2,3,6-tetrahydropyridne

(2) Reduction of pyridinium salts with sodium borohydride in alcohol or aqueous solution yields the corresponding 1,4-disubstituted-1,2,3,6-tetrahydropyridines. This method is universally applicable. For example, methylation of the 4-ethenylpyridine (**135**) (Scheme 21), gave the corresponding 1-methylpyridinium intermediate **136** which yielded **137** when treated with 1 mole of sodium borohydride (excess hydride reagent resulted in further reduction of the exocyclic double bond).[102]

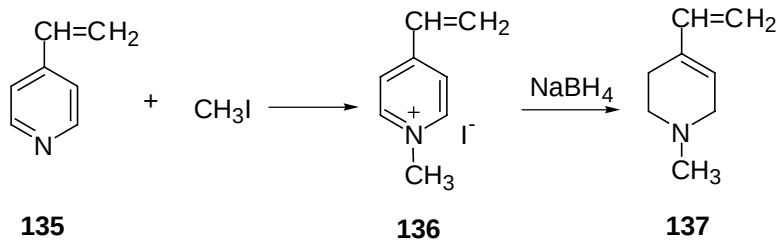

Scheme 21. The Synthesis of 1-Methyl-4-ethenyl-1,2,3,6-tetrahydropyridine

The pyridinium salts can be obtained by several ways. In addition to the alkylation of the pyridine by an alkyl halide, which is described in the above example (Scheme 22), the Zincke reaction can also produce a pyridinium salt from another pyridinium starting material which has a different N-substituent.[105] For example, the treatment of 4-(4-chlorophenyl)pyridine (**138**) with 2,4-dinitrochlorobenzene (**139**) produces 4-(4-chlorophenyl)-1-(2,4-dinitrophenyl)pyridinium chloride (**140**) which, upon coupling with (*R,S*)-4-amino-1-(4-flurophenyl)butanal, yields (*R,S*)-4-(4-chlorophenyl)-1-[4-(4-flurophenyl)-4-hydroxybutyl]pyridinium chloride (**141**) (Scheme 22).[106]

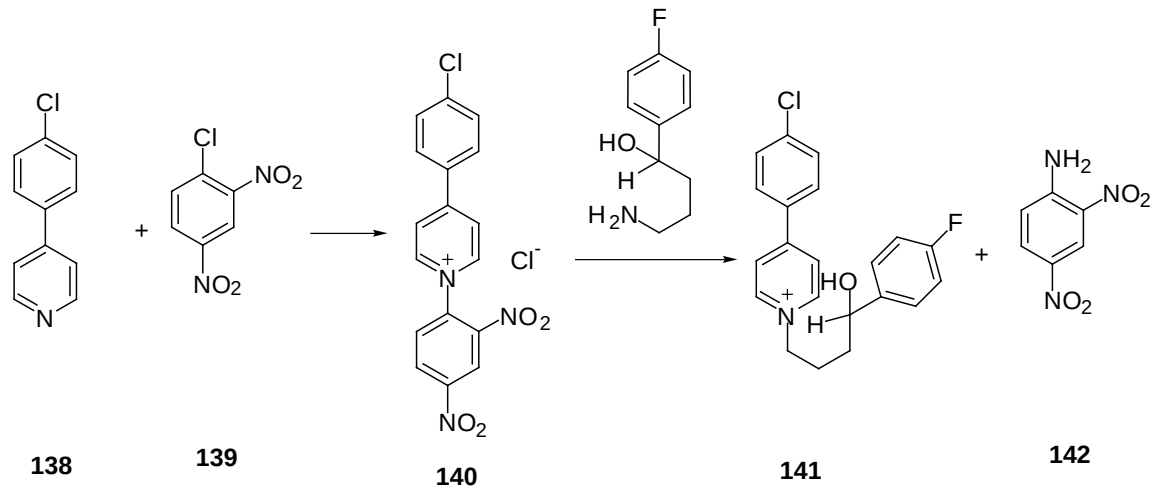

138 **139** **140** **141** **142**

Scheme 22. The Synthesis of 4-(4-Chlorophenyl)-1-(2,4-dinitrophenyl)pyridinium

The precusors of pyridinium salts are the 4-substituted pyridines. Many ways have been employed to synthesize 4-substituted pyridines. Some 4-substituted pyridines have special C-4 substituents such as the bromo, chloro, formyl or methyl group which can be used as a handle to anchor another desired group at C-4 position.

For example, the $Pd(PPh_3)_4$ catalyzed cross-coupling reaction between the pyrrylzinc reagent **144** [prepared from 1-methylpyrrole (**143**) and *sec*-butyllithium] and 4-bromopyrridine gave the 1-methyl-4-(1-methyl-2-pyrryl)-1,2,3,6-tetrahydropyridine (**146**) (Scheme 23).[91]

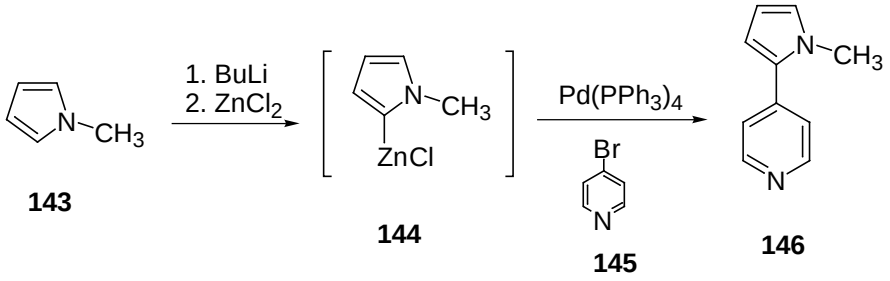

Scheme 23. The Synthesis of 4-(1-Methylpyrrol-2-yl)pyridine

The second example involves the treatment of 4-pyridinecarboxaldehyde with Grignard or organolithium reagent such as phenyl Grignard (**148**) to yield the corresponding secondary alcohol **149** (Scheme 24). Zinc-mediated reduction of the benzylic alcohol, yielded the corresponding 4-benzylpyridine **150**.[107]

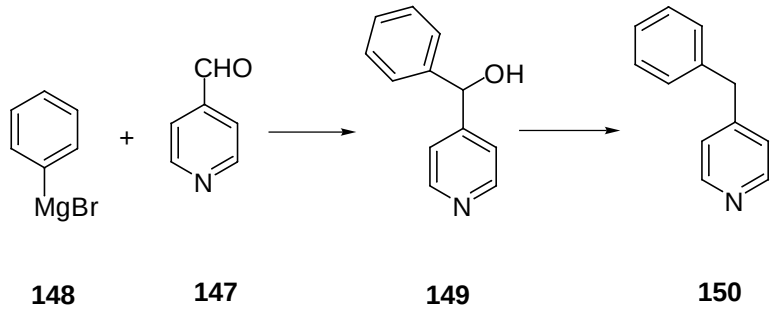

Scheme 24. The Synthesis of 4-Benzylpyridine

In the third example, Baker reaction of 4-methylpyridine (**152**) and benzaldehyde (**151**) produced the *trans*-stilbazole **153** which can be reduced to 4-phenylethylpyridine (**154**) by hydrogenation in the presence of the catalyst of Pd/C.[107]

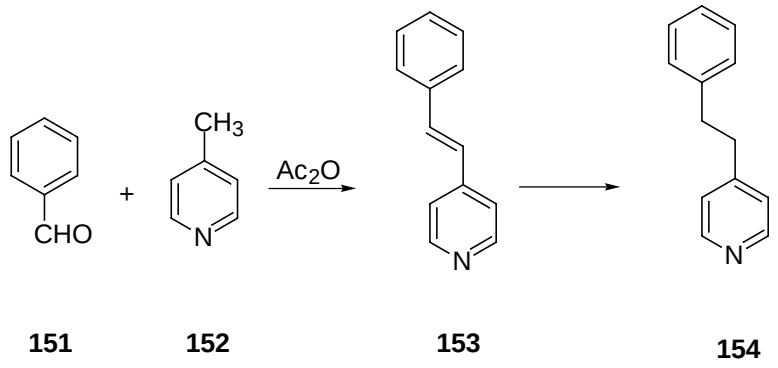

151 **152** **153** **154**

Scheme 25. The Synthesis of 4-Phenylethypyridine

(3) Stille-type cross-coupling reactions, involve the vinyl triflates ($C=C-SO_3CF_3$) which readily react with vinyltin derivatives to generate dienes.[108] This method has been employed in the synthesis of tetrahydropyridines (Scheme 26). Treatment of 1-methyl-4-piperidone (**124**) with lithium diisopropylamide followed by reaction of the resulting lithium enolate with phenyltrifluromethane sulfonimide yields the tetrahydropyridyl triflate **155**. This vinyl triflate reacts with 3-(trimethylstannyl)pyridine in the presence of tetrakis-(triphenylphosphine)palladium (0) to give the 1-methyl-4-(3-pyridyl)-1,2,3,6-tetrahydropyridine (**157**).[91]

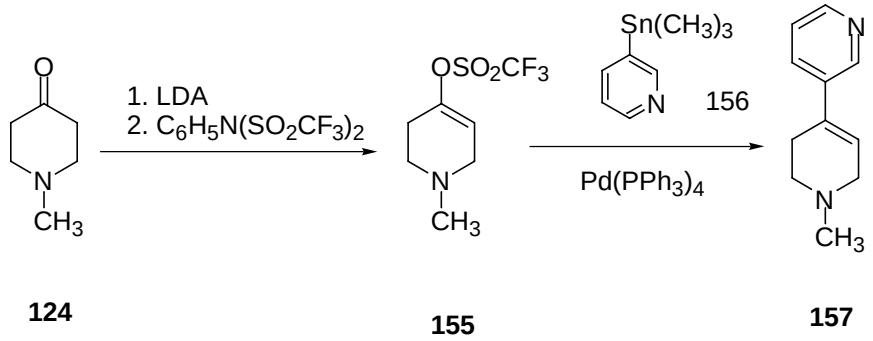

124 **155** **157**

Scheme 26. The Synthesis of 4-(3-Pyridyl)-1,2,3,6-tetrahydropyridine

C. C-4 substituents

In our project, the C-4 substituents are substituted five-memberd heteroarenes, such as substituted furans, pyrroles, thiophenes and imidazoles. A variety of methods and reagents have been developed to synthesize specific five-membered heteroarenes. However, retroanalysis suggests the generally logical starting materials and preparatively important methods for constructing the required structures.

1. The synthesis of pyrroles

(1) The retroanalysis for the synthesis of the pyrrole analogs

The proposed retrosynthesis of pyrroles is given in Scheme 27.[95-99] Route I (steps **a**-**c**) yields the 1,4-dicarbonyl compounds **161**, the potential starting materials, which should produce pyrroles by cyclocondensation with NH_3 or a primary amine. When intermediate **160**, the γ-ketoenamine, follows step **d**, bond cleavage results to form fragments **162** and **163**, rather than **158**, suggesting the α-halocarbonyls **162** and enamines **163** as alternative starting materials. After water addition and enamine hydrolysis (**e**/**f**), route II leads to the γ-aminoadol intermediate **165**. Aldol fission follows (retroanalysis step **g**) resulting in the formation of the α-aminocarbonyl compounds **166** and methylene ketones **167**.

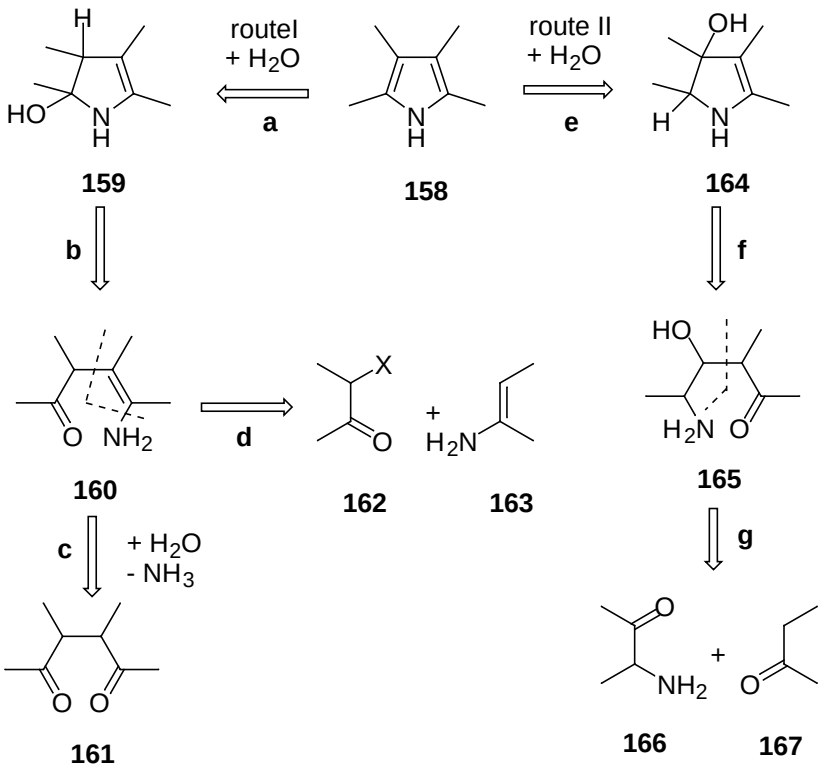

Scheme 27. The Retrosynthesis of Pyrrole

(2) Some practical methods for the synthesis of pyrroles[95-98]

a. The Paar-Knorr synthesis, in which 1,4-dicarbonyl compounds are treated with NH_3, or primary amines in ethanol or acid, leads to substituted pyrroles (Scheme 28) and is broadly applicable. For instance, hexane-2,5-dione (**168**) reacts with NH_3 to yield 2,5-dimethylpyrrole (**171**). The primary step leads to the double hemiaminal **169** which, by stepwise water elimination, furnishes the pyrrole system **171** via the imine **170**.

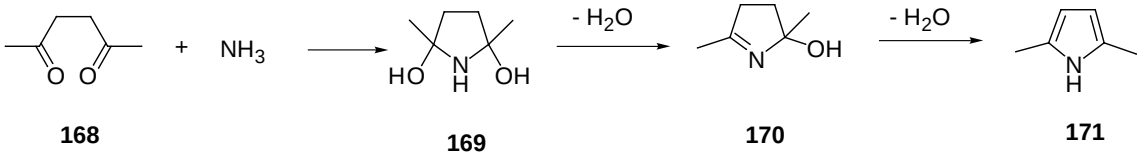

Scheme 28. The Paal-Knorr Synthesis of Pyrroles

b. The Hantzsch synthesis, in which α-halocarbonyl compounds react with β-keto estersor β-diketones and ammonia or primary amines, gives 3-alkoxycarbonyl- or 3-acryl-substituted pyrrole derivatives, respectively (Scheme 29). The regioselectivity depends on the substituents in the starting materials but gives mainly the 1,2,3,5-tetrasubstituted pyrrole. For example, the β-keto esters **172** react with ammonia or amine to give the β-aminoacrylic esters **173** in the primary step. C-Alkylation of the enamine function in **173** by the halo ketone produces the 1,2,3,5-substituted pyrroles **175** while N-alkylation leads to the 1,2,3,4-substituted pyrroles **176**.

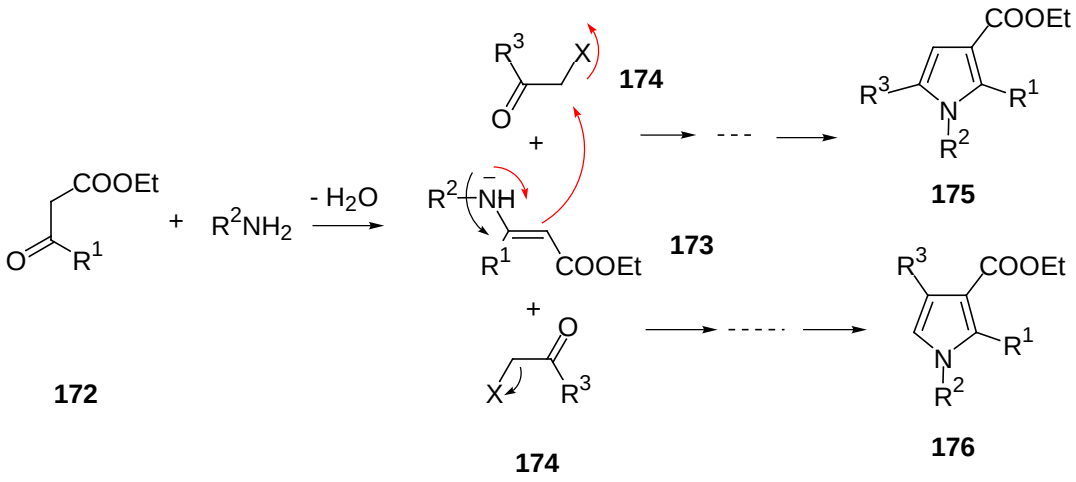

Scheme 29. Hantzsch Synthesis of Pyrroles

c. The Knorr synthesis, in which α-amino ketones **166** undergo cyclocondensation with β-keto esters **172** or β-diketones, gives the 3-alkoxylcarbonyl- or 3-acyl-substituted pyrroles **179** (Scheme 30).

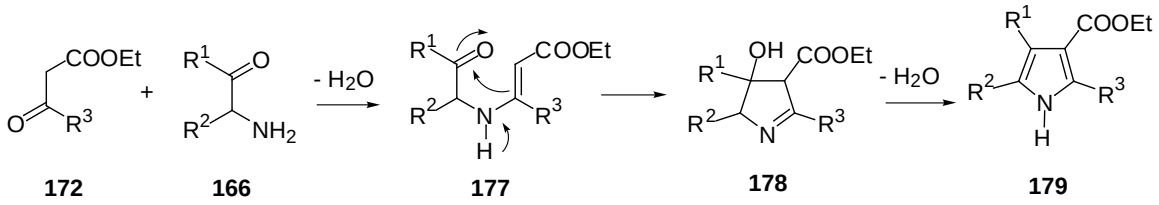

Scheme 30. Knorr Synthesis of Pyrroles

d. Michael addition followed by an intramolecular aldo addition reaction results in the conversion of, N-tolylsulfonyl glycine esters **180** and vinyl ketones **181** to the pyrrolidine-2-carboxylic esters **182**. These are converted into pyrroles by dehydration of cleavage of the N-tosyl protecting group (Scheme 31).

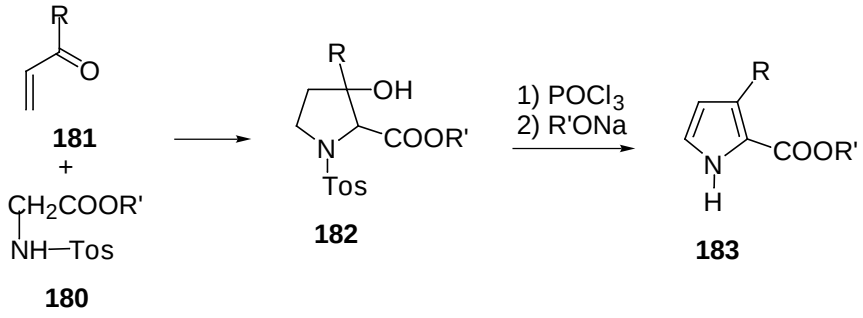

Scheme 31. The Michael Addition and Intramolecular Aldo Addition Pathway to Pyrrole

e. Cyclocondensation of nitroalkenes **184** with isocyanides **185** (Scheme 32) in the presence of base leads to the formation of the trisubstituted pyrroles **186**. The first step in this reaction is a Michael addition of the isocyanide to the nitroalkene. Cyclization and elimination of HNO_2 follow.

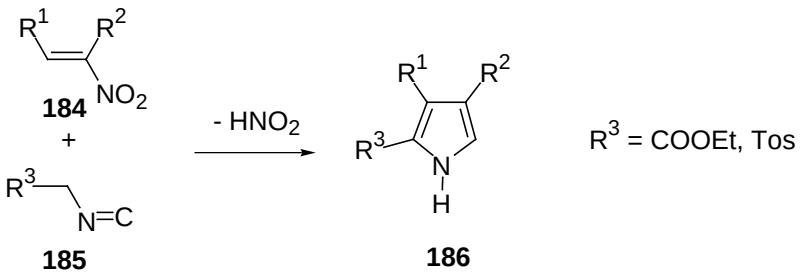

Scheme 32. Cyclocondensation Pathway to Pyrrole of Nitroalkenes with CH-acidic Isocyanide

2. The synthesis of Furans

(1) The retroanalysis for the synthesis of furan analogs[95-99]

The proposed retrosynthesis for furans is given in Scheme 33. Furan can be seen to derive from a double enol ether and be dissected retroanalytically in two ways (I, II). In route I (addition of water to the furan C-2/C-3 bond followed by bond opening O/C-2, i.e. an enol ether hydrolysis according to steps **a**-**c**), the 1,4-dicarbonyl system **161** is obtained as the first adduct. Starting from **161**, the furan system should be formed by cyclic dehydration. Further retroanalysis of **161** leads via **f** to the α-halocarbonyl compound **162** and to the enolate of the carbonyl compound **167**. The latter should be convertible into the 1,4-dicarbonyl system **161** by alkylation with **162**.

Following route II, it can be seen that the primary water addition to the furan C-2/C-3 bond can also occur according to the retrostep **d**. This leads to the intermediate **190** for which the bond cleavage O/C-2 (**e**) is retroanalytically rationalized and leads to the γ-halo-β-hydroxycarbonyl system **191**. A retroaldol operation (pathway **g**) provides the same starting materials **162** and **167** as the retrosynthesis I. Route II, however, suggests as the first step an aldol addition between **162** and **167** to give **191** followed by intramolecular S_N cyclization of the enolate **191** to the dihydrofuran **190** and conversion into furan by dehydration.

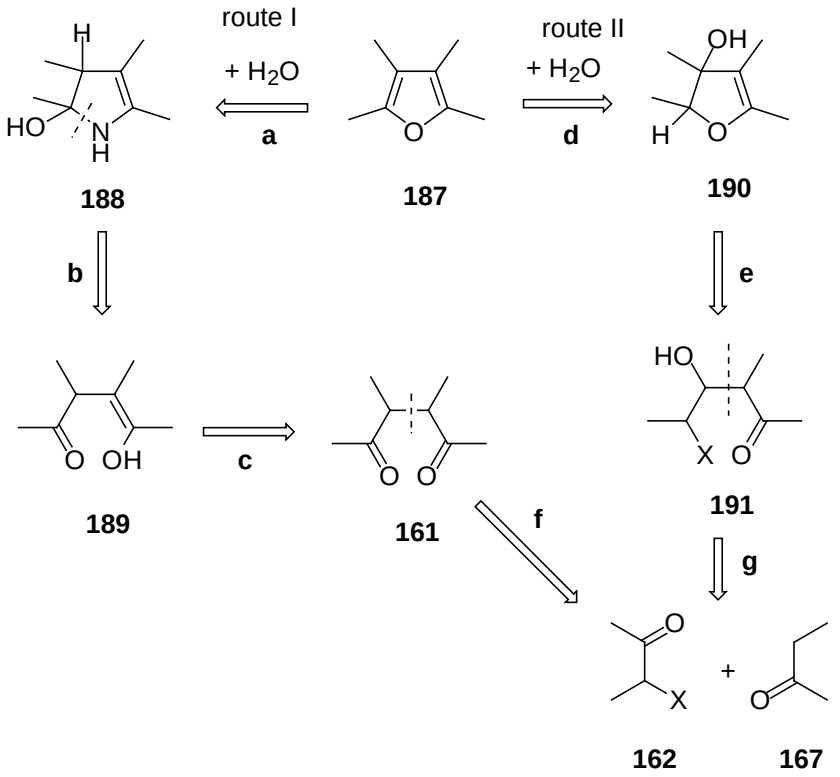

Scheme 33. The Retrosynthesis of Furans

(2) Some practical methods for the synthesis of furans[95-99]

a. In the Paal-Knorr synthesis, the 1,4-dicarbonyl compounds **161** undergo cyclodehydration when treated with concentrated H_2SO_4, polyphosphoric acid, $SnCl_2$ or DMSO, providing 2,5-disubstituted furans **194** (Scheme 34). In an acid-base equilibrium, the acid adds to one of the carbonyl groups in the 1,4-dicarbonyl system **161** enabling a nucleophilic intramolecular attack by the second carbonyl group to form **193**. Finally, the β-elimination step, which is also base-catalyzed, occurs.

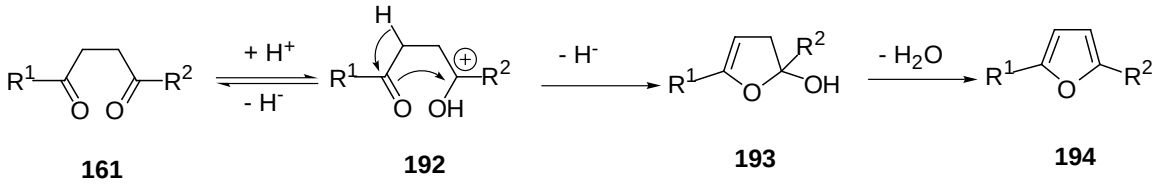

Scheme 34. The Paal-Knorr Synthesis of Furan

b. In the Feist-Benary synthesis, the α-halocarbonyl compounds **195** react with the β-keto carboxylic esters **172** to yield derivatives of 3-furoic acid **198** by cyclocondensation (Scheme 35). The formation of **196** results from an aldol addition and that of **197** from an intramolecular nucleophilic substitution reaction.

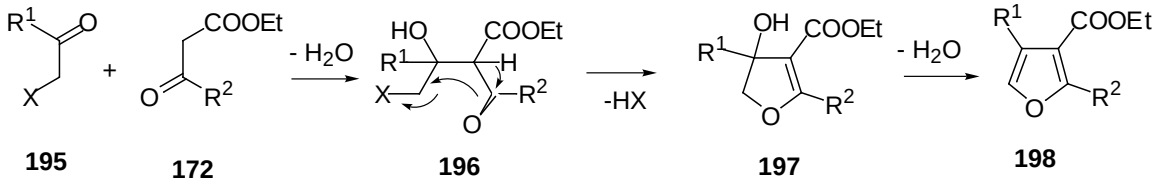

Scheme 35. The Feist-Benary Synthesis of Furans

c. In the Diels-Alder reaction, the ring transformation of oxazoles is achieved with activated alkynes. For example, 4-methyloxazole (**199**) reacts with dimethyl acetylenedicarboxylate (**200**) to provide dimethylfuran-3,4-dicarboxylate (**203**) via the nonisolable adduct **201** (Scheme 36). The first step is a [4+2] cycloaddition reaction and the second a [4+2] cycloreversion reaction. The fact that cycloreversion is not a retroaction of the first step is due to the formation of thermodynamically stable acetonitrile and furan products.

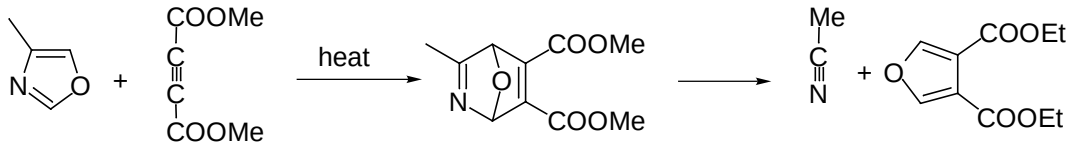

Scheme 36. Diels-Alder Synthesis of Furans

3. The synthesis of thiophenes[95-99]

The proposed retrosynthesis of thiophenes can be worked out in principle by analogy to that of furan. The frequently used methods are given in the following.

(1) The simplest approach is 'sulfurization' followed by cyclization and dehydration of 1,4-dicarbonyl compounds **161** analogous to the Paal-Knorr synthesis of furan (Scheme 37). This cyclocondensation is carried out with P_4S_{10} or H_2S, and furnishes 2,5-disubstituted thiophenes.

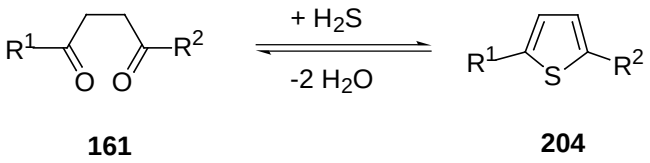

Scheme 37. The Paal-Knorr Synthesis of Thiophenes

(2) Fiesselmann synthesis. 1,3-Dicarbonyl compounds or β-chlorovinyl aldehydes react with thioglycolates or other thiols possessing a reactive methylene group to give the thiophene-2-carboxylic esters **208** in the presence of pyridine (Scheme 38) . Initially, a formal vinyl substitution of the chlorine atom by Michael addition takes place, followed by loss of HCl to give the intermediate **207**. Finally, cyclization occurs by an intramolecular aldol condensation.

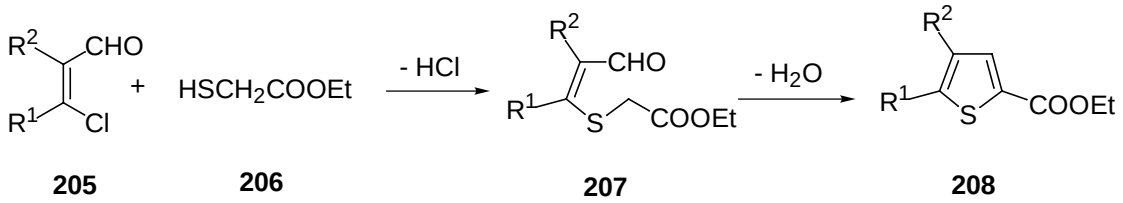

205 **206** **207** **208**

Scheme 38. The Fiesselmann Synthesis of Thiophenes

(3) In the Gewald synthesis, the α-methylene carbonyl containing compounds undergo cyclocondensation with cyanoacetic ester or malononitrile and sulfur in ethanol in the presence of morpholine to give 2-aminothiophenes **212** (Scheme 39). Initially, a Knoevenagel condensation between the carbonyl compound and the reactive methylene group takes place. The α,β-unsaturated nitriles **211** that are formed are cyclized by the sulfur, probably via the sulfanyl derivatives of **211** as intermediates.

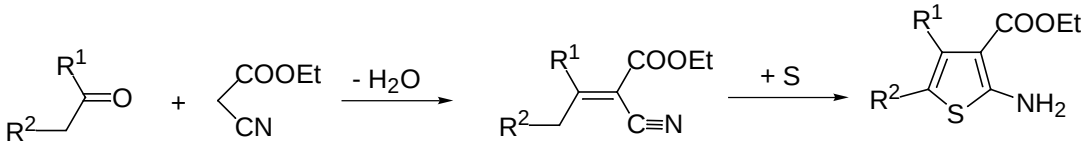

209 **210** **211** **212**

Scheme 39. The Gewald Synthesis of Thiophenes

(4) In the Hinsberg synthesis. the 1,2-dicarbonyl compounds can be made to cyclize with thiodiglycolic acid esters **214** under base catalysis (Scheme 40). This widely applicable and high-yield synthesis leads to β-substituted thiophene dicarboxylic esters **215** via a double aldol condensation with the two CH_2 groups of **214**. Hydrolysis and decarboxylation of the esters yield 3,4-disubstituted thiophenes **216**.

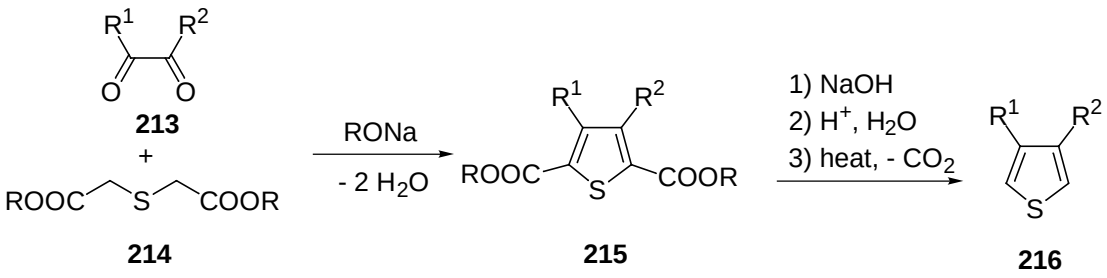

Scheme 40. The Hinsberg Synthesis of Thiophenes

4. The synthesis of imidazoles

(1) The retroanalysis for the synthesis of imidazole analogs[95-99]

The imidazole system possesses the functionality of an amidine on C-2 and that of a 1,2-enediamine on C-4/C-5. Retroanalysis should, therefore, consider two approaches (Scheme 41):

Route I leads via the retrosynthetic operations **a** and **b** to the α-acylaminocarbonyl system **219**. This suggests NH_3 or a primary amine as starting materials. According to route II, addition of H_2O (pathway **c**) leads to intermediate **220** which can be further dissected in line with the retroanalytical scheme. Route **d** points to an α-halo- or α-hydroxycarbonyl compound and amidine, whereas route **e** suggests an α-aminoketone and acid amide or nitrile as starting materials.

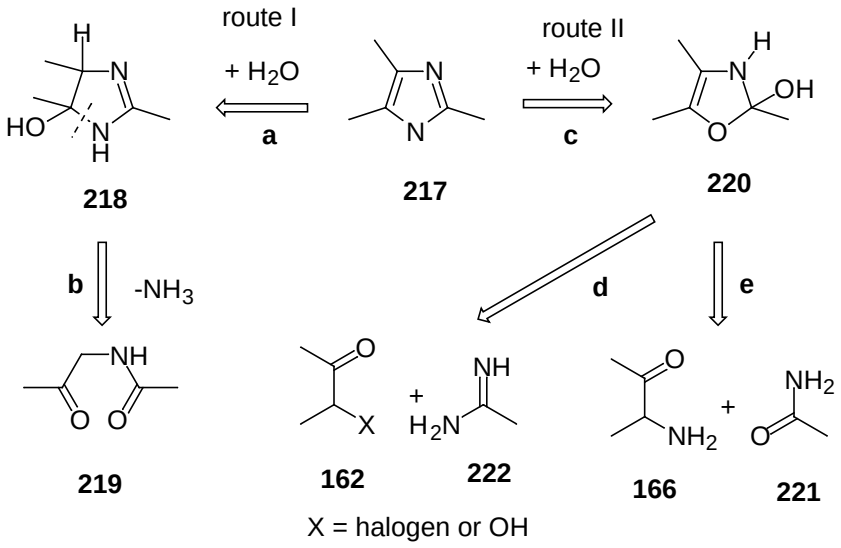

Scheme 41. The Retrosynthesis of Imidazole

(2) Some practical methods for the synthesis of imidazoles

(1) 1,2-Dicarbonyl compounds undergo cyclocondensation with ammonia and aldehydes to form imidazole derivatives **214** (Scheme 42).

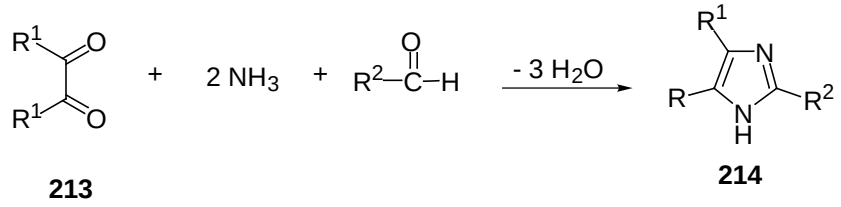

Scheme 42. The Synthesis of Imidazole (1)

(2) Imidazoles **223**, with a variable substitution pattern (Scheme 43), are obtained from α-halo or α-hydroxyketones **215** and amidines **222**.

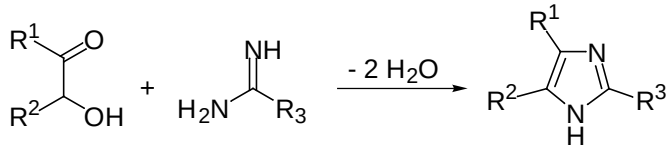

215 **222** **223**

Scheme 43. The Synthesis of Imidazole (2)

Imidazoles **225** unsubstituted in the 2-position are obtained from α-hydroxyketones **215** and formamide (**224**) (Scheme 44).

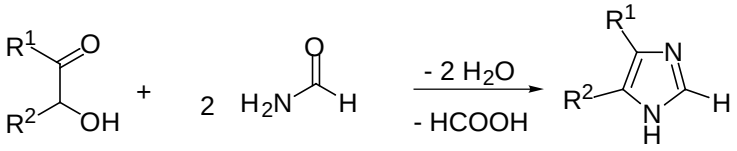

224 **225**

Scheme 44. The Synthesis of Imidazole (3)

(3) α-Aminaoketones can be condensed with cyanamide (**226**) to form 2-aminoimidazoles **227** (Scheme 45).

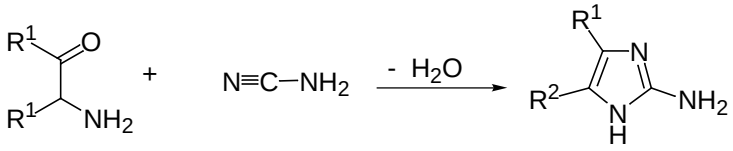

116 **226** **227**

Scheme 45. The Synthesis of Imidazole (4)

(4) Aldimines **228** react in the presence of K_2CO_3 with tosylmethylisocyanide (**229**) to form 1,5-disubstituted imidazoles **230** (Scheme 46). The carbanion formed from tosylmethylisocyanide adds to the aldimine. The addition product cyclizes to give 4,5-dihydroimidazoles **230**, which eliminate p-toluenesulfinic acid to give the imidazoles.

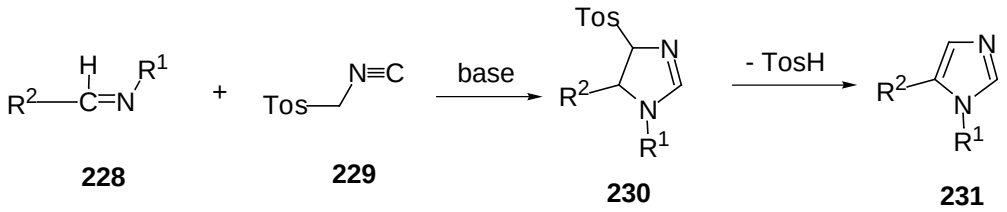

Scheme 46. The Synthesis of Imidazole (5)

2.2.2. The synthesis of 1-methyl-4-substituted-1,2,3,6-tetrahydropyridines

Because the substrate properties of 1-methyl-4-(2-pyrrolyl)-1,2,3,6-tetrahydropyridine (**83**)[91] and 1-methyl-4-(1-methylpyrrol-2-yl)-1,2,3,6-tetrahydropyridine (**84**)[101] are tremendously different, we decided to determine if the methyl group substituted at the 3′-position of the pyrrole would also display this kind of effect and if the result could be extended to other five-membered heteroarene analogs. A series of synthetic strategies has been developed to achieve these molecules.

A. The synthesis of pyrrole analogs of MPTP

The initial effort was to prepare the 4-(3,4-dimethylpyrrol-2-yl) analog **237** (Scheme 47). Treatment 3,4-dimethylpyrrole[109] first with n-butyllithium and then with $ZnCl_2$ yielded the 3,4-dimethylpyrrol-1-yl znic chloride intermediate **234**. Upon reaction with 4-bromopyridine in the presence of $Pd(PPh_3)_4$, the only product isolated from the reaction mixture was 4-(3,4-dimethylpyrrol-1-yl)pyridine analog **235**. None of the 4-(3,4-dimethylpyrrol-2-yl)pyridine isomer **237** was formed. This result suggests that the steric hindrance introduced by the methyl groups at the 3′ or 4′-position of the pyrrole ring controls the regiochemistry of the reaction and prevents reaction at the electronically favored α-position.[97] Methylation of **235** using methyl iodide followed by $NaBH_4$ reduction of the resulting pyridinium species **236** yielded the 1,2,3,6-tetrahydropyridinyl product **96** which was purified as its oxalate salt.

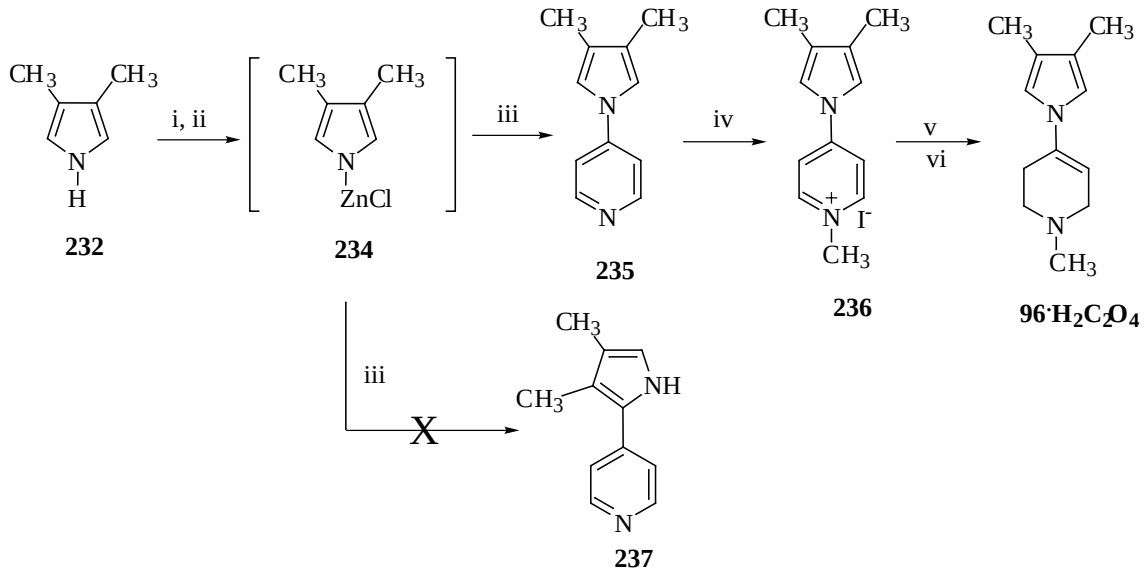

[a] Reagents and conditions: (i) n-BuLi, THF; (ii) $ZnCl_2$, THF; (iii) 4-Bromopyridine, $Pd(PPh_3)_4$; (iv) CH_3I, acetone; (v) $NaBH_4$, MeOH; (vi) $H_2C_2O_4$, Et_2O.

Scheme 47. Synthetic Pathway to 1-Methyl-4-(3,4-dimethylpyrrol-2-yl)-1,2,3,6-tetrahydropyridine (96)

The starting material 3,4-dimethylpyrrole **232** was prepared according to the reported method.[109] Ethyl carbamate (**238**) was treated with thionyl chloride (**239**) in the presence of pyridine at low temperature to produce the N-sulfinyl compound **240** (Scheme 48). Treatment of **240** with 2,3-dimethylbutadiene (**241**) yielded the cycloadduct 2-ethylcarbonyl-3,6-dihydro-4,5-dimethyl-1,2-thiazine-1-oxide (**242**), which afforded 3,4-dimethylpyrrole (**232**) in satisfactory yield upon heating in a concentrated potassium hydroxide methanolic solution.

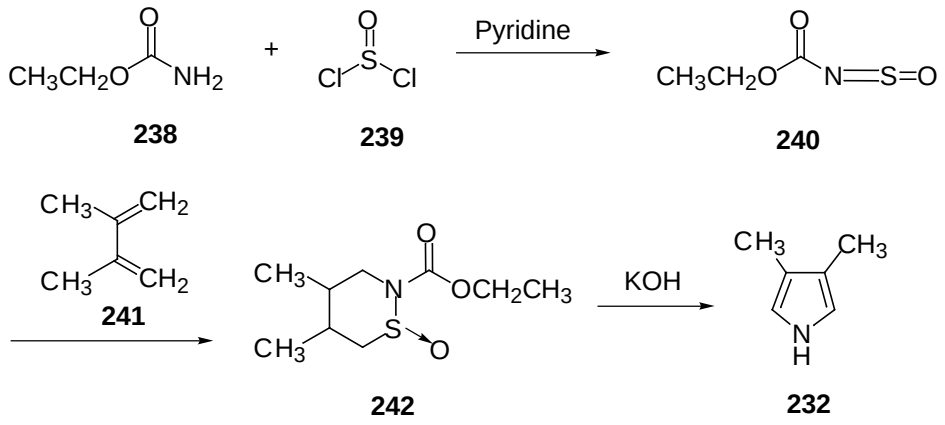

Scheme 48. The Synthesis of 3,4-Dimethylpyrrole

The failure to obtain the 3,4-dimethyl analog **237** led to some caution with respect to the selection of starting materials to synthesize the desired compounds. Having reviewed the retroanalysis of pyrroles, we noticed that the Paar-Knorr synthesis is an attractive approach. Treatment of 1,4-dicarbonyl compounds with primary amines leads to 1,2,5-trisubstituted pyrroles. If 4-oxo-(4-pyridyl)butanal derivatives with appropriate substituents at the 3-position (Figure 12) could be obtained, they could be used to synthesize the desired pyrrolyl analogs of MPTP. Because the Paar-Knorr method is broadly applicable, it also might be used in the synthesis of furan and thiophene analogs.

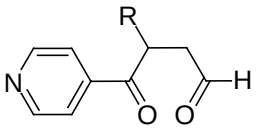

Figure 12. The Ring Precursor of Five-membered Heteroarenes

In general , a large number of synthetic methods for 1,4-dicarbonyl compounds is available.[111-113] Several methods for the synthesis of 4-oxoalkanals and the aryl analogs have been reported.[114-119] But these methods have not been applied to the 3-substituted-4-oxo-(4-pyridyl)butanal analogs.

The first approach to the 4-oxo-(4-pyridyl)butanal system was developed as the cyanide-ion-catalyzed Michael addition[120] of 4-pyridinecarboxaldehyde (**147**) to α,β-

unsaturated aldehydes (Scheme 49). For example, the ring precursor 3-methyl-(4-pyridyl)butanal (**244**) was obtained from the reaction of 4-pyridinecarboxaldehyde with crotonaldehyde (**243**) using potassium cyanide as a catalyst (Scheme 49). This method was originally used to synthesize 1,4-diketones. When it was employed to prepare 3-methyl-4-oxo-(4-pyridyl)butanal in our case, the reaction did not stop at the expected stage. The desired 3-methyl-(4-pyridyl)butanal underwent self condensation or reaction with the starting materials resulting in low yields and difficulities in isolation.

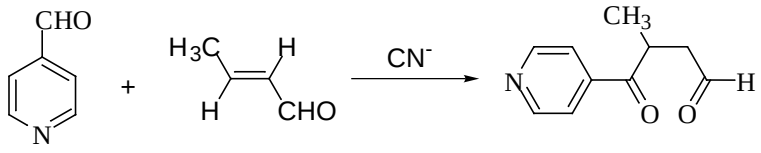

147 **243** **244**

Scheme 49. The Synthesis of 3-Methyl-(4-pyridyl)butanal by Michael Addition

The second approach to the 4-oxo-(4-pyridyl)butanal was developed via the oxidation of the intermediate 4-oxo-(4-pyridyl)-1-butanol, which can be synthesized by the addition of 4-pyridyllithium to γ-butyrolactone. For example, treatment of 4-bromopyridine with n-butyllithium in ether at -78 °C afforded 4-pyridyllithium **245** which upon reaction with γ-butyrolactone **246** yielded the corresponding 4-oxo-4-(4-pyridyl)-1-butanol (**248**) (Scheme 50). Using the same method only starting from the 4-pyridinyllithium and α-methyl-γ-butyrolactone (**247**) gives the 3-methyl-4-oxo-4-(4-pyridyl)-1-butanol (**249**). After oxidation of the corresponding alcohol with chromium trioxide in pyridine, the final product of 3-methyl-4-oxo-4-(4-pyridyl)butanal (**244**) or 4-oxo-4-(4-pyridyl)butanal (**250**) was obtained in reasonable yield and it is easy to purify.

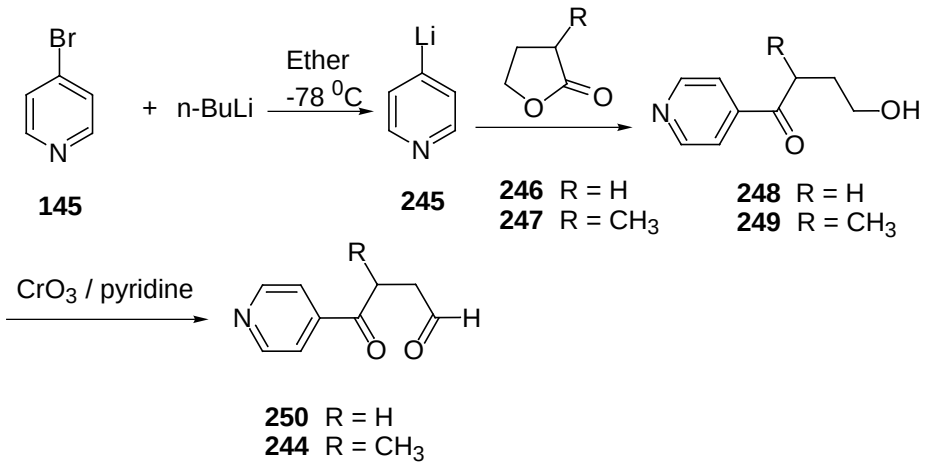

Scheme 50. The Synthesis of 4-Oxo-4-(4-pyridyl)butanals

The Paar-knorr dehydrative cyclization[97,119-120] in which the 3-substituted-4-(4-pyridyl)butanal analogs **244** or **250** underwent reaction with ammonia or primary amines generates the corresponding pyridinylpyrroles **251-256** (Scheme 51). Methylation of the 4-substituted pyridines with methyl iodide followed by $NaBH_4$ reduction of the resulting pyridinium species **257-262** yielded the corresponding 1,2,3,6-tetrahydropyridinyl products **97-102** which were purified as their oxalate salts .

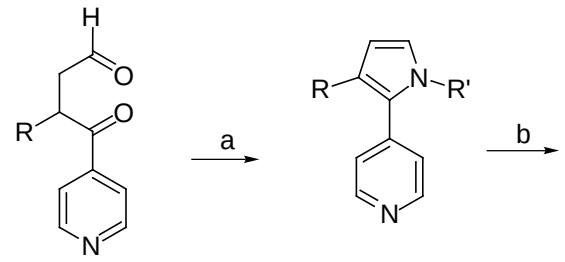

26

250 R = H
244 R = CH_3

251 $H_2C_2O_4$ R = H, R'=CH_2CH_3
252 $H_2C_2O_4$ R = H, R'=$CH_2CH_2CH_3$
253 R = H, R'=$CH(CH_3)_2$
254 $H_2C_2O_4$ R = H, R'=c-C_3H_5
255 R = CH_3, R' = H
256 R = CH_3, R' = CH_3

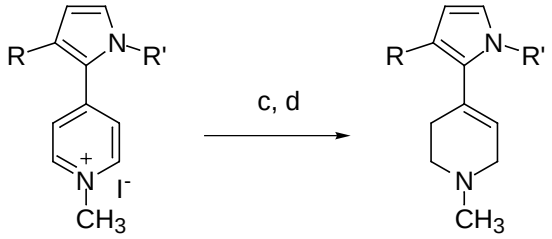

257 R = H, R'=CH_2CH_3
258 R = H, R'=$CH_2CH_2CH_3$
259 R = H, R'=$CH(CH_3)_2$
260 R = H, R'=c-C_3H_5
261 R = CH_3, R' = H
262 R = CH_3, R' = CH_3

97 $H_2C_2O_4$ R = H, R'=CH_2CH_3
98 $H_2C_2O_4$ R = H, R'=$CH_2CH_2CH_3$
99 $H_2C_2O_4$ R = H, R'=$CH(CH_3)_2$
100 $H_2C_2O_4$ R = H, R'=c-C_3H_5
101 $H_2C_2O_4$ R = CH_3, R' = H
102 $H_2C_2O_4$ R = CH_3, R' = CH_3

Reagents and conditions: a) R'NH_2, CH_3OH, room temperature, 12h;
b) CH_3I, room temperature; c) $NaBH_4$, methanol, 0 ^{0}C;
d) $H_2C_2O_4$, Et_2O, room temperature.

Scheme 51. The Synthesis of the Pyrrolyl MPTP Analogs by Paar-Knorr Method **(97-102)**

B. The synthesis of furan analogs of MPTP

The furan analogs of MPTP were synthesized either by the condensation pathway or the Paar-Knorr cyclization reaction.

The route to the 4-(3-methyl-2-furanyl) analog **103** (Scheme 52) was based on the observation reported by Kondo *et al*. that unsaturated 5-membered lactols are converted to

the corresponding furanyl derivatives under acidic conditions.[122] The addition of 4-pyridinyllithium to 3-methyl-(5H)-2-furanone (**263**) followed by the hydrolysis generated the unsaturated lactol intermediate **264** which was very unstable and could not be isolated (Scheme 52). Treatment of intermediate **264** with H_2SO_4 in THF gave the dehydrated compound 4-(3-methylfuran-2-yl)pyridine (**265**) which was purified as its oxalate salt. If the reaction mixture containing **264** was quenched under basic conditions, the ring opened product **267** was formed. Compound **267** was stable and underwent ring closure under acidic conditions to give the **265**. Methylation of **265** followed by $NaBH_4$ reduction of the resulting pyridinium species **266** yielded the 1,2,3,6-tetrahydropyridinyl product **103** which was purified as its oxalate salt.

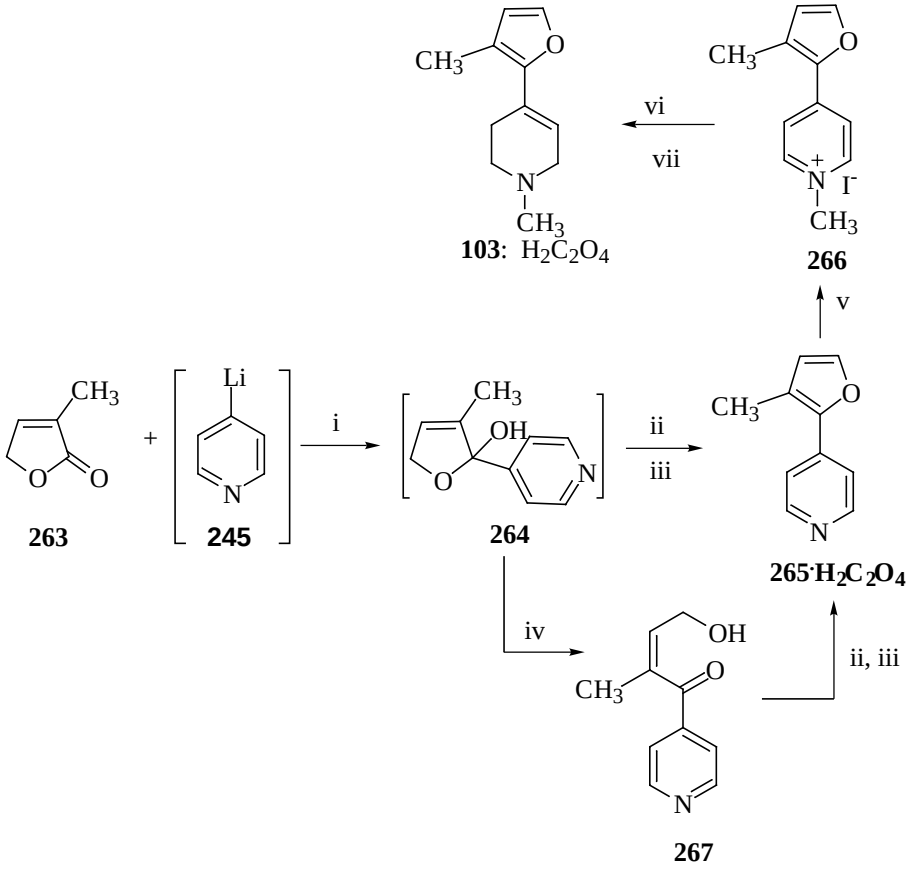

[a] Reagents and conditions: (i) THF, -78 °C, 4h, then room temperature, 24h; (ii) H_2SO_4 in THF, -78 °C; (iii) $H_2C_2O_4$ in Et_2O; (iv) Aq. NaOH; (v) CH_3I, acetone; (vi) $NaBH_4$, CH_3OH; (vii) $H_2C_2O_4$ in Et_2O.

Scheme 52. The Synthesis of 1-Methyl-4-(3-methylfuran-2-yl)-1,2,3,6-tetrahydropyridine **(103)**

The synthetic pathway for the preparation of the 1-methyl-4-(3-ethylfuran-2-yl)-1,2,3,6-tetrahydropyridine (**104**) is given in Scheme 53. Treatment of γ-butyrolactone (**246**) in THF at -78 °C with lithium diisopropylamide and then with an excess of ethyl iodide (**245**) in the presence of hexamethylphosphoramide [123] gave α-ethyl-γ-butyrolactone (**268**) in good yield. The addition of 4-pyridyllithium (**245**) to **268** followed by hydrolysis yielded 3-ethyl-4-oxo-4-(4-pyridyl)butanol (**269**). The hydroxy group in **269**

could be oxidized to the corresponding aldehyde **270** by chromium trioxide in pyridine. This product underwent intramolecular addition and β-elimination under acid conditions to afford the 4-(3-ethylfuran-2-yl)pyridine (**271**). The resulting 4-substituted pyridine **271** was converted to the required tetrahydropyridine **104** by $NaBH_4$ reduction via the corresponding N-methylpyridinium intermediates **272**.

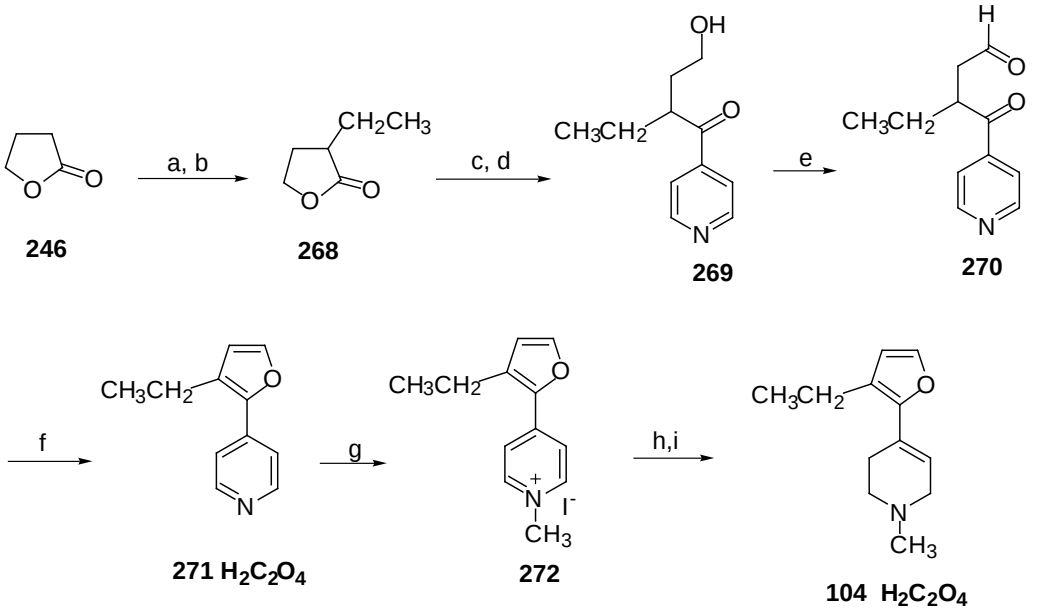

Reagents and conditions: a) LDA; b) HMPA/CH_3CH_2I; c) 4-pyridinyllithium; d)H_2O; e) Cr_3O / pyridine; f)H_2SO_4, H_2O/THF, 55 ^{0}C; g) CH_3I, room temperature; h) $NaBH_4$, methanol, 0 ^{0}C; i) $H_2C_2O_4$, Et_2O, room temperature.

Scheme 53. The Synthesis of 1-Methyl-4-(3-ethylfuran-2-yl)-1,2,3,6-tetrahydropyridine **(104)**

In the same way, 4-(3-methylfuran-2-yl)pyridine (**264**) was synthesized as described in Scheme 53 except that α-methyl-γ-butyrolactone (**247)** was used as the starting material.

C. The synthesis of thiophene analogs of MPTP

Two ways have been developed to prepare the thiophene analogs of MPTP-- the cross-coupling method and the Paar-Knorr cyclization method.

The synthesis of 4-(3-methyl-2-thionyl)pyridine (**275**) was achieved by a cross-coupling reaction between 4-bromopyridine and the zinc salt **274** of 3-methyl-2-thiophene in the presence of $Pd(PPh_3)_4$ (Schemes 54). The formation of 3-methylthiophen-2-yllithium and zinc chloride intermediates must be carried out at low temperature (starting at -78 °C and then the temperature was increased to room temperature slowly). Otherwise, these intermediates underwent polymerization. The resulting 4-substituted pyridine, **275**, was converted to the required tetrahydropyridine by $NaBH_4$ reduction of the corresponding N-methylpyridinium intermediate **276** to give the 1-methyl-4-(3-methylthiophen-2-yl)-1,2,3,6-tetrahydropyridine (**105**).

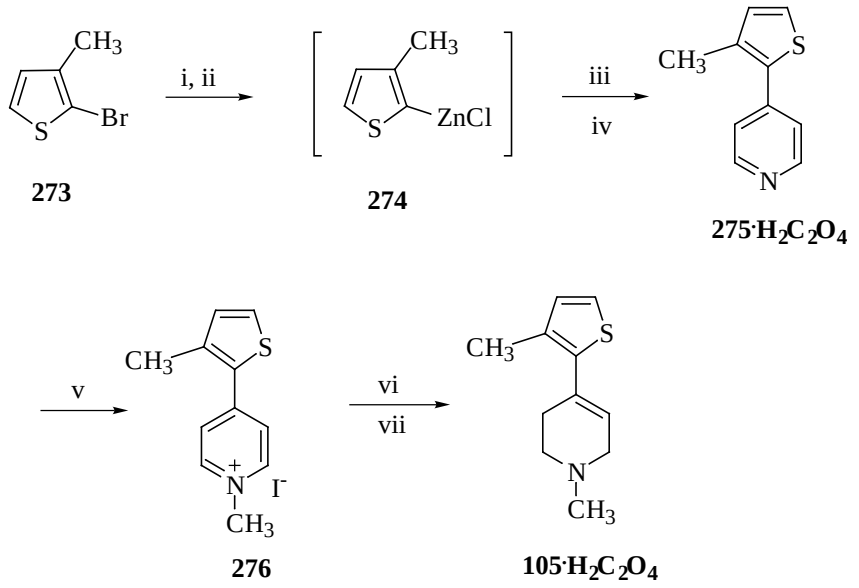

273 **274** **275·$H_2C_2O_4$**

276 **105·$H_2C_2O_4$**

[a] Reagents and conditions: (i) n-BuLi, THF, -78 ^{0}C; (ii) $ZnCl_2$, THF; (iii) 4-bromopyridine, $Pd(PPh_3)_4$, THF; (iv) $H_2C_2O_4$, Et_2O; (v) CH_3I, acetone; (vi) $NaBH_4$, MeOH; (vii) $H_2C_2O_4$, Et_2O.

Scheme 54. Synthetic Pathway to 1-Methyl-4-(3-methylthien-2-yl)-1,2,3,6-tetrahydropyridine **(105)**

The synthesis of 1-methyl-4-(3-ethylthiophen-2-yl)-1,2,3,6-tetrahydropyridine (**106**) was achieved via a similar way Scheme 55). Sulfurization of the 3-ethyl-4-oxo-(4-pyridyl)butanal (**270**) with P_4S_{10}[124] followed by the cyclizing dehydration yielded the 4-(3-

ethylthiophen-2-yl)pyridine (**277**) which was converted first to the N-methylpyridinium salt **278** by methylation with methyl iodide which then was reduced by $NaBH_4$ to the 1-methyl-4-(3-ethylthiophen-2-yl)-1,2,3,6-tetrahydropyridine (**106**).

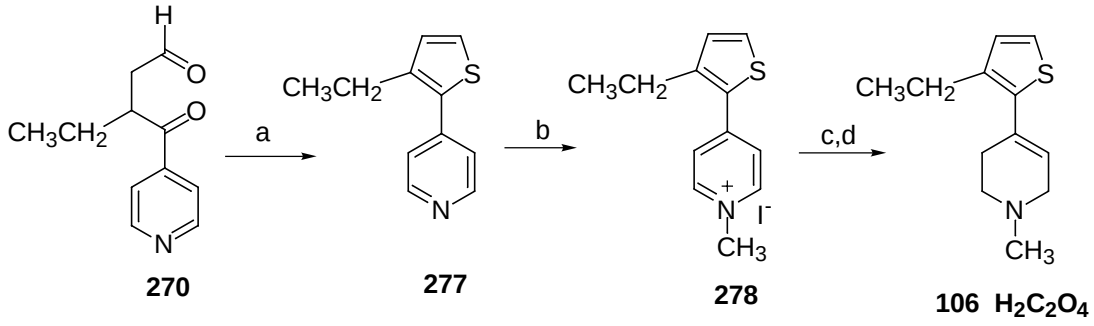

270 **277** **278** **106** $H_2C_2O_4$

Reagents and conditions: a) P_2S_5, toluene, 100 ^{0}C;
b) CH_3I, room temperature; c) $NaBH_4$, methanol, 0 ^{0}C;
d) $H_2C_2O_4$, Et_2O, room temperature.

Scheme 55. The Synthesis of and 1-Methyl-4-(3-ethylthien-2-yl)-1,2,3,6-tetrahydropyridine **(106)**

D. The synthesis of imidazole analogs of MPTP

The reaction of n-butyllithium with commercially available 1-methylimidazole (**279**) afforded 1-methylimidazol-2-yllithium (**280**), which in turn was added to the 1-methyl-4-piperidone (**124**) (Scheme 56). After the hydrolysis of the adduct, 4-(1-methylimidazole-2-yl)-4-piperidinol (**281**) was produced. However, the attempts to bring about the normal acid catalyzed dehydration (HCl/HOAc or dilute H_2SO_4 solution, reflux) of **281** failed. Attempts to functionalize the piperidinol hydroxy group as a tosylate or mesylate also failed. Finally, it was found that this compound can be dehydrated in concentrated phosphoric acid (85% H_3PO_4 : H_2O = 4:1) at 100 °C to give 1-methyl-4-(1-methylimidazol-2-yl)-1,2,3,6-tetrahydropyridine (**107**) which was purified as dihydrochloride salt.

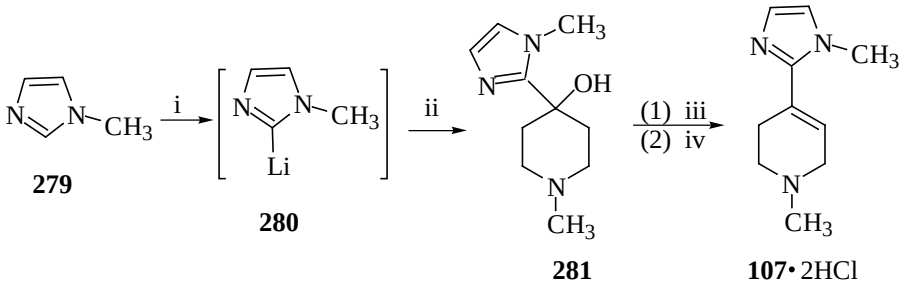

[a] Reagents and conditions: (i) n-BuLi, THF, room temperature; (ii) 1-methyl-4-piperidone, -78 ^{o}C; (iii) H_3PO_4:H_2O=4:1, 100 ^{o}C; (iv) HCl gas, Et_2O, room temperature.

Scheme 56. Synthetic Pathway to the Dihydrochloride Salt of 1-Methyl-4-(1-methylimidazol-2-yl)-1,2,3,6-tetrahydropyridine **(107)**

2.3. Enzymology

The MAO-B (0.09 μM) substrate properties of the newly synthesized terahydropyridines **96** - **107** (100-500 μM) were examined using enzyme purified from beef liver. In each case, the time dependent increase of a chromophore consistent with that expected for the corresponding dihydropyridinium metabolite was observed. The enzyme kinetic parameters of the test compounds then were determined by estimating the initial rates of formation (first 120 seconds) of the dihydropyridinium metabolites at initial substrate concentrations that bracketed the K_m for that substrate. Since not all of the dihydropyridinium metabolites were available as synthetic standards, rates of product formation were approximated using ε values for the structurally related compounds identified in the Table 1 footnotes. The plots of the initial velocities vs substrate concentrations were linear in all cases as were the corresponding double-reciprocal plots (Figure 13-24) from which k_{cat} and K_m were calculated (Table 1). The k_{cat}/K_m values, used to estimate the relative substrate properties of this series of compounds, covered the range of 17 to 11,000 $(minmM)^{-1}$.

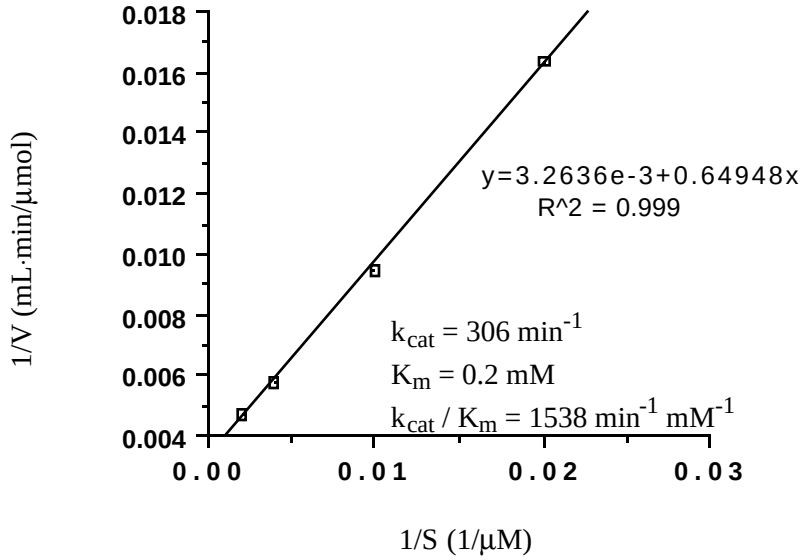

Figure 13. Lineweaver-Burke Plot for the MAO-B Catalyzed Oxidation of 1-Methyl-(3,4-dimethylpyrrol-2-yl)-1,2,3,6-tetrahydropyridine **(96)**

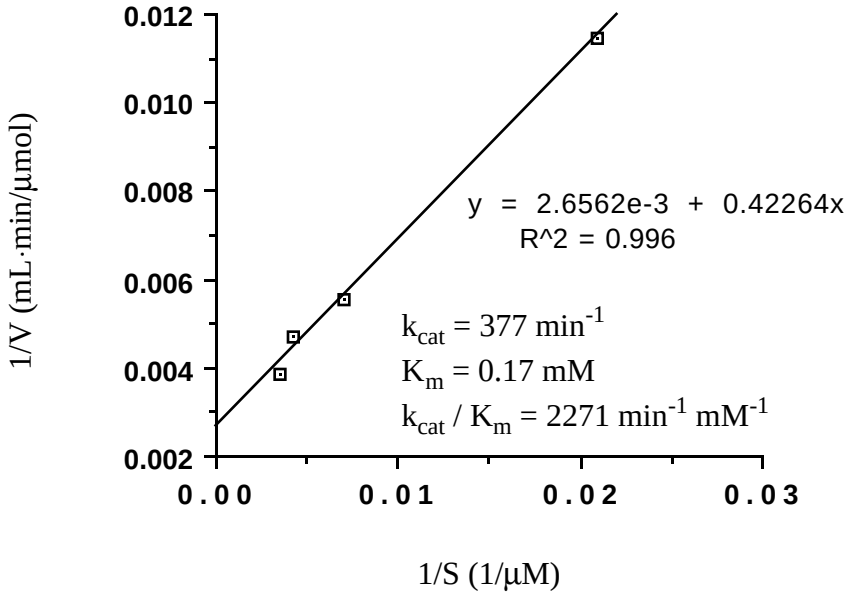

Figure 13. Lineweaver-Burke Plot for the MAO-B Catalyzed Oxidation of 1-Methyl-(3,4-dimethylpyrrol-2-yl)-1,2,3,6-tetrahydropyridine **(96)**

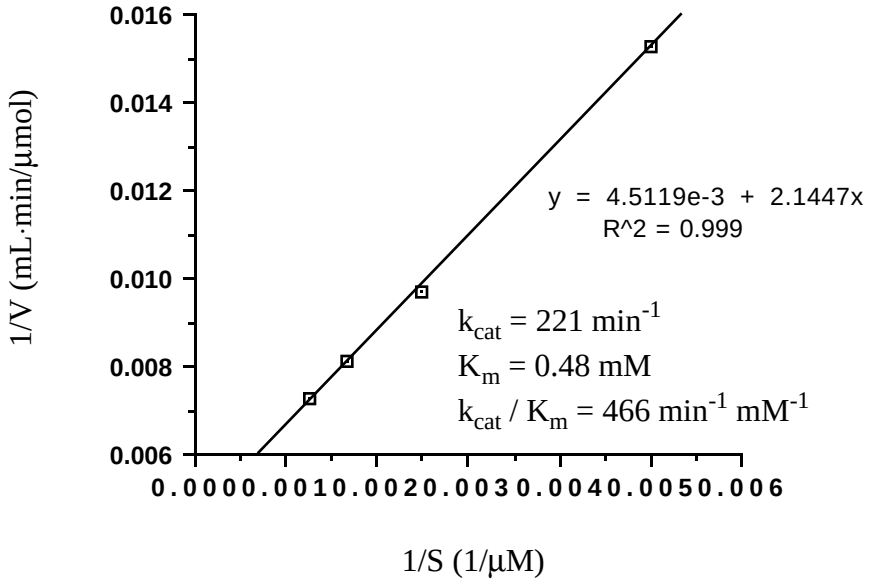

Figure 15. Lineweaver-Burke Plot for the MAO-B Catalyzed Oxidation of 1-Methyl-4-(1-n-propylpyrrol-2-yl)-1,2,3,6-tetrahydropyridine **(98)**

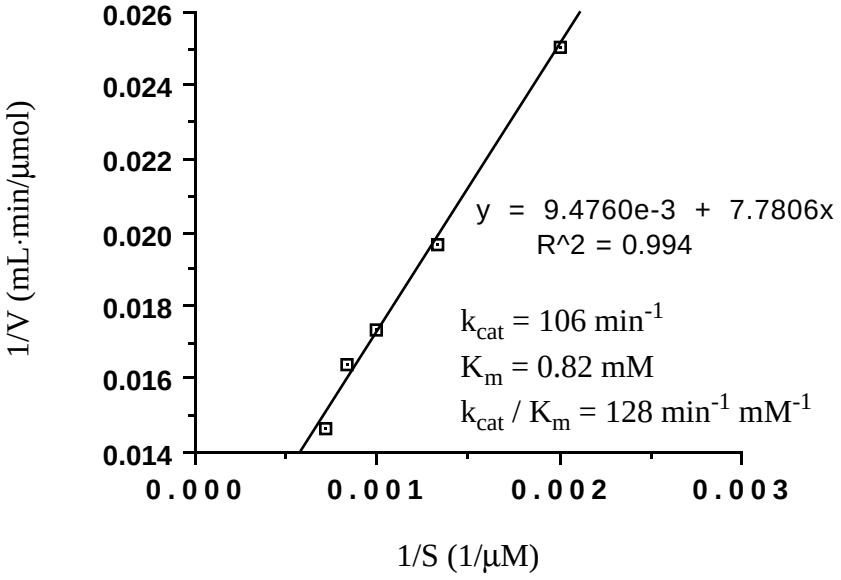

Figure 16. Lineweaver-Burke Plot for the MAO-B Catalyzed Oxidation of 1-Methyl-4-(1-isopropylpyrrol-2-yl)-1,2,3,6-tetrahydropyridine **(99)**

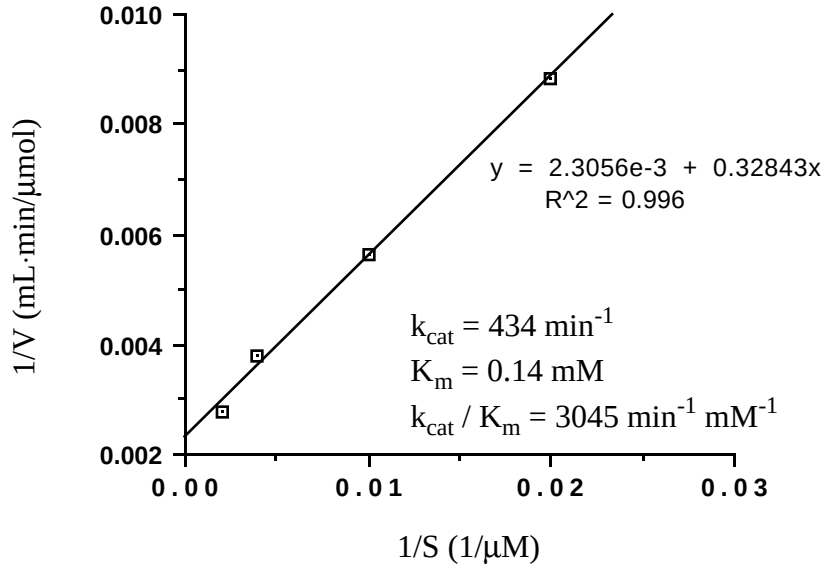

Figure 17. Lineweaver-Burke Plot for the MAO-B Catalyzed Oxidation of 1-Methyl-4-(1-cyclopropylpyrrol-2-yl)-1,2,3,6-tetrahydropyridine **(100)**

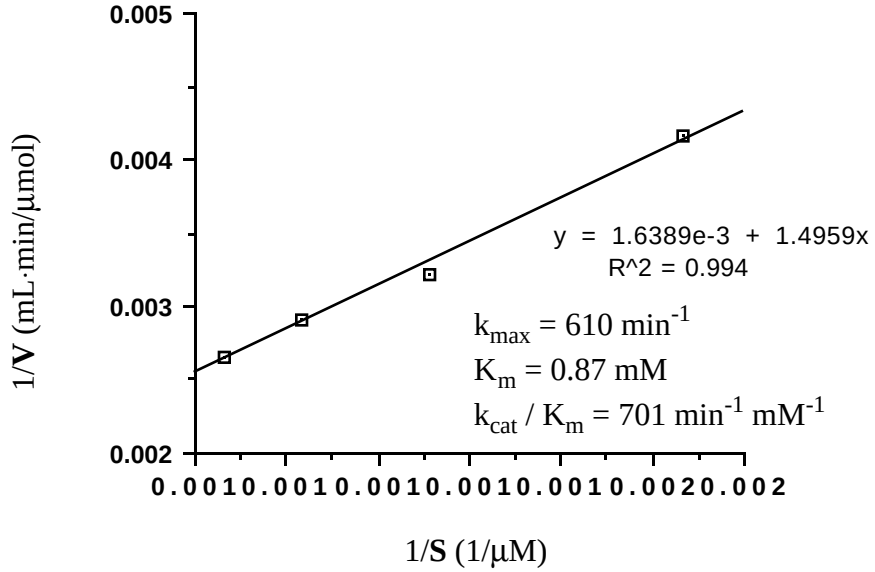

Figure 18. Lineweaver-Burke Plot for the MAO-B Catalyzed Oxidation of 1-Methyl-4-(3-methylpyrrol-2-yl)-1,2,3,6-tetrahydropyridine **(101)**

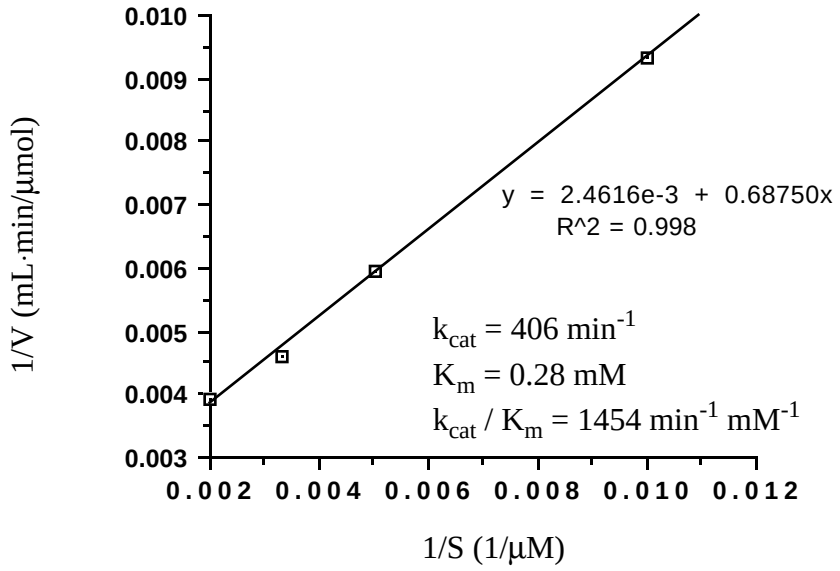

Figure 19. Lineweaver-Burke Plot for the MAO-B Catalyzed Oxidation of 1-Methyl-4-(1,3-dimethylpyrrol-2-yl)-1,2,3,6-tetrahydropyridine **(102)**

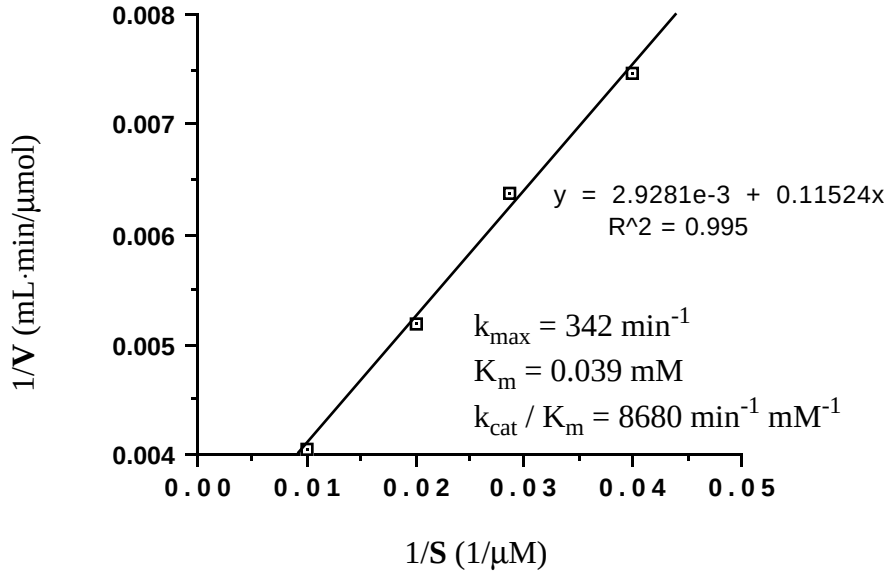

Figure 20. Lineweaver-Burke Plot for the MAO-B Catalyzed Oxidation of 1-Methyl-4-(2-methylfuran-2-yl)-1,2,3,6-tetrahydropyridine **(103)**

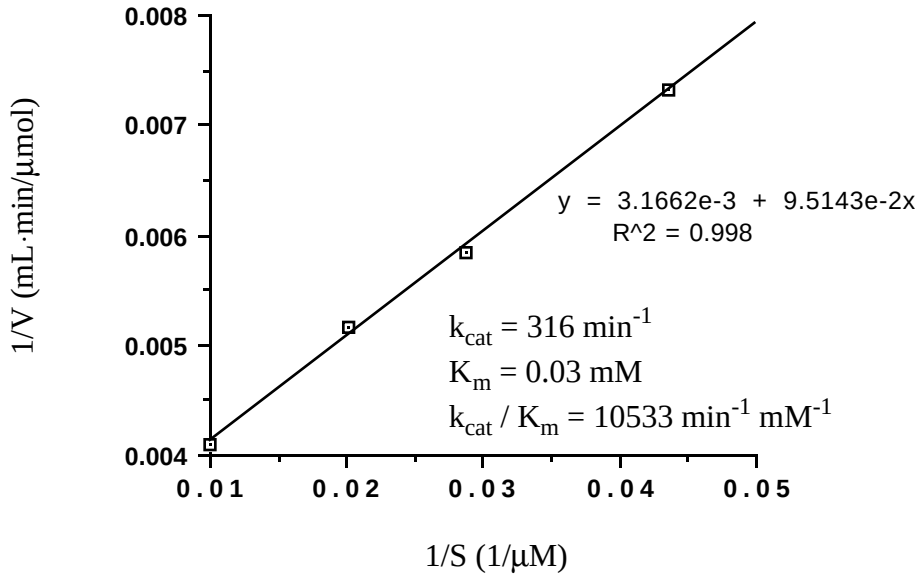

Figure 21. Lineweaver-Burke Plot for the MAO-B Catalyzed Oxidation of 1-Methyl-4-(1-ethylfuran-2-yl)-1,2,3,6-tetrahydropyridine **(104)**

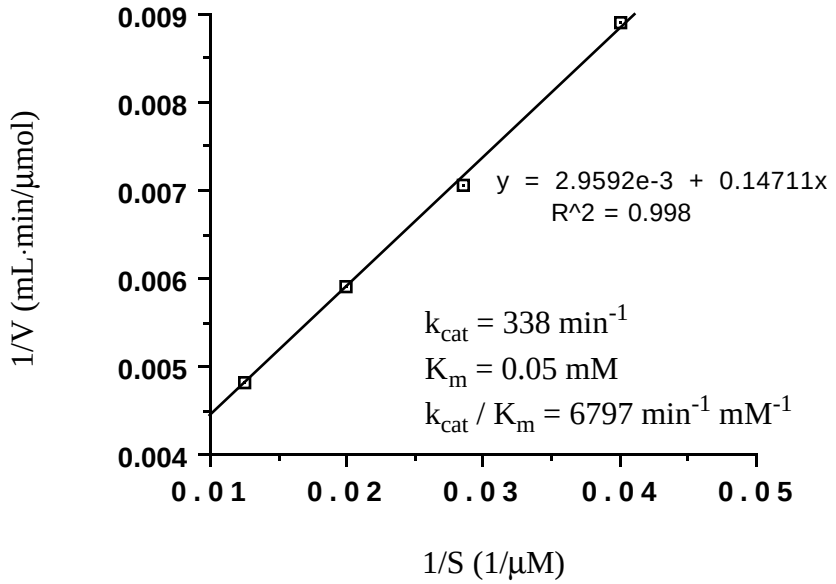

Figure 22. Lineweaver-Burke Plot for the MAO-B Catalyzed Oxidation of 1-Methyl-4-(1-methylthiophen-2-yl)-1,2,3,6-tetrahydropyridine **(105)**

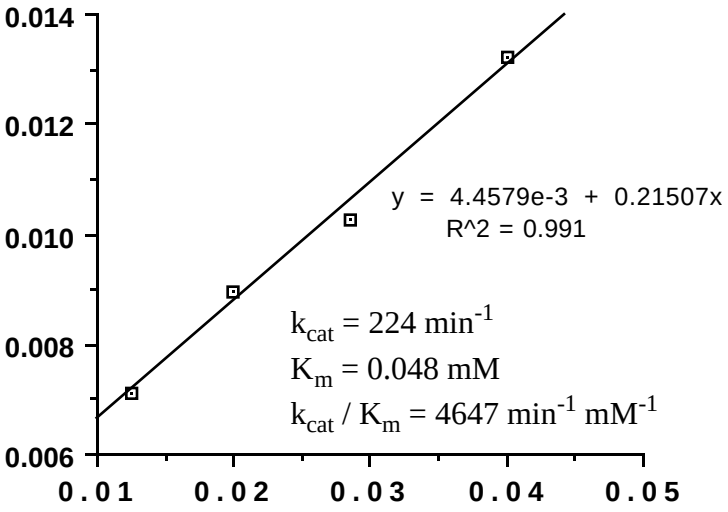

Figure 23. Lineweaver-Burke Plot for the MAO-B Catalyzed Oxidation of 1-Methyl-4-(1-ethylylthiophen-2-yl)-1,2,3,6-tetrahydropyridine **(106)**

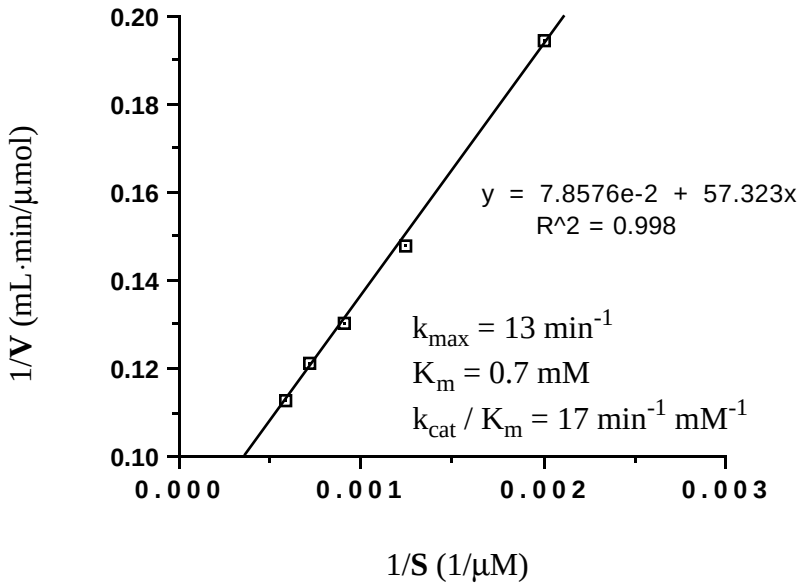

Figure 24. Lineweaver-Burke Plot for the MAO-B Catalyzed Oxidation of 1-Methyl-4-(1-methylimidazol-2-yl)-1,2,3,6-tetrahydropyridine **(107)**

Table 1. Kinetic Parameters for the MAO-B Catalyzed Oxidations of 1-Methyl-4-substituted-1,2,3,6-tetrahydropyridines and MPTP.

C-4 Substituent	λ_{max} (nm)[d]	k_{cat} $(min)^{-1}$	K_m (mM)	k_{cat}/K_m $(min^{-1}mM^{-1})$
C_6H_5 (**69**)[a]	343	270	0.2	1350 [91]
2-C_3H_2-1-CH_3(1,3)N (**107**)[b]	383	13	0.7	17
2-C_4H_4N (**83**)[b]	424	85	1.8	46[101]
2-C_4(1-CH_3)H_3N (**84**)[b]	420	360	0.2	1800[91]
2-C_4(1-CH_3CH_2)H_3N (**97**)[b]	420	360	0.16	2210
2-C_4(1-$CH_3CH_2CH_2$)H_3N (**98**)[b]	421	209	0.38	557
2-C_4(1-$CH_3(CH_2)_2$)H_3N (**99**)[b]	422	121	1.28	94
2-C_4(1-cyc-C_3H_5)H_3N (**100**)[b]	420	418	0.14	2878
1-C_4(3,4-CH_3)$_2H_2N$ (**96**)[b]	381	309	0.2	1510
2-C_4(3-CH_3)H_3N (**101**)[b]	432	640	0.92	690
2-C_4(1,3-CH_3)$_2H_2N$ (**102**)[b]	436	430	0.3	1436
2-C_4H_4O(**86**)[c]	384	31	0.2	155[91]
2-C_4(3-CH_3)H_2O (**103**)[c]	399	348	0.04	8620
2-C_4(3-CH_3CH_2)H_2O (**104**)[c]	399	336	0.03	11000
2-C_4H_4S(**85**)[d]	386	60	0.2	300[91]
2-C_4(3-CH_3)H_2S (**105**)[d]	400	337	0.05	6690
2-C_4(3-CH_3CH_2)H_2S (**106**)[d]	393	222	0.04	4892

[a]Estimated using ε=16,000 M^{-1}, the value for the perchlorate salt of the 1-methyl-4-phenyl-2,3-dihydropyridinium species[91]; [b]Estimated using ε=24,000 M^{-1}, the value for the perchlorate salt of the 1-methyl-4-(1-methylpyrrol-2-yl)-2,3-dihydropyridinium species [91]; [c]Estimated using ε=23,000 M^{-1}, the value for the perchlorate salt of the 1-methyl-4-(2-furanyl)-2,3-dihydropyridinium species; [d]Estimated ε=18,800 M^{-1}, the value for the perchlorate salt of the 1-methyl-4-(thiophen-2-yl)-2,3-dihydropyridinium species.[91]

2.4. Discussion

As observed earlier, electron donating heteroarene analogs are, in general, better substrates than analogs bearing the electron withdrawing heteroarene. For example, the N-methylpyrrolyl analog **84** is a much better substrate than the N-methylimidazoyl analog **107**. Comparisons of the substrate properties of analogs **86** vs **103** and **85** vs **105**, however, emphasize the importance of steric effects on the rates of the MAO-B catalyzed oxidations within this series of compounds. The introduction of the methyl group at C-3 of the thienyl and furanyl groups increases the k_{cat} values and decreases the K_m values so that the overall substrate properties, as measured by k_{cat}/K_m, increase by a factor of 22 for the thienyl compound and 55 for the furanyl compound. The slight bathochromic shifts in the λ_{max} values for the dihydropyridinium metabolites suggest increased electron delocalization of the heteroaryl electons into the 6-membered ring but it seems unlikely that such a nominal electronic effect could account for the dramatic increase in the substrate properties of the methylated analogs. Furthermore, comparison of the substrate properties of the NCH_3-2-pyrrolyl analog **84** and the NH-2-pyrrolyl analog **83** shows an analogous trend with the k_{cat}/K_m value for the methylated analog being 39 times greater than that of the NH compound. In this case the λ_{max} value for the NH compound is at a longer wavelength than that of the NCH_3 compound.

We have attempted to explore further the influence of steric and electronic effects of the pyrrolyl analogs with the aid of compounds **101** and **102**. It appears that factors other than steric and electronic may contribute to the interactions of these compounds with the enzyme. Note that, even though the k_{cat} values for these two analogs are similar, the presence of a hydrogen atom on the pyrrolyl nitrogen atom (compound **101**) appears to lead to unfavorable interactions with the active site since the K_m value increases by a factor of 3 relative to the NCH_3 analog. Alternatively, one could argue that the N-methyl group of **102** leads to favorable active site interations. This effect also is observed with analog **83** which has an exceptionally high K_m value (1.8 mM) compared to the structurally similar compounds **84**, **85**, **86** and **102** (K_m = 0.2, 0.2, 0.2, 0.3, respectively). In the case of **96**, the nitrogen atom is connected directly to the tetrahydropyridine. This compound, also lacking an NH group, exhibits the same substrate properties as those observed with analog **102**. These data lead us to speculate that, in addition to steric and electronic effects,

unfavorable polar interactions with the NH group may influence the substrate properties of compounds in this series.

The λ_{max} values of the putative dihydropyridinium species of all these compounds with different alkyl groups substituted on the ring of the N-pyrrolyl , furanyl and thienyl series displayed similar conjugations. It is reasonable to conclude therefore that the change of substrate properties is caused mostly by the steric feature of the substituted alkyl groups.

In the pyrrole system, when a methyl or ethyl or cyclopropyl group is substituted at 1′-position of the pyrrole ring, the k_{cat}/K_m values are much higher than that observed with the N′-H analog **83**. This is due both to an increase in k_{cat} and decrease in K_m. However, further lengthening of the side chain to three carbon atoms (**98**) leads to a decrease in k_{cat} and increase in K_m. In the case of N′-isopropyl analog **99**, interestingly, although the length of the side chain is not longer than ethyl group, the branched chain caused a dramatic drop in k_{cat}/K_m. Thus k_{cat}/K_m in this series follows the order 1'-cyclopropyl (**100**) > 1'-ethyl (**97**) > 1'-methyl (**84**) > 1'-propyl (**98**) > 1'-isopropyl (**99**) > 1′-hydrogen (**83**). These data suggest that the active site of the enzyme is very sensitive to the size and shape of the alkyl groups substituted at 1′-position of the pyrrole ring.

Both the furanyl and thienyl rings have a pentagon shape as with the pyrrole ring. We observed the same phenomenon with all these heteroarenes. A methyl or ethyl group substituted at the 3-position of the furan or thiophene ring leads to an increase in k_{cat} and decrease in K_m,. In fact, 1-methyl-4-(3-ethylfuran-2-yl)-1,2,3,6-tetrahydropyridine (**104**) is the most active MAO-B substrate we ever synthesized. In the furan series, the k_{cat}/K_m values follows the order 3′-ethyl (**104**) >3′-methyl (**103**) >3′-hydrogen (**86**). In the thiophene series, the k_{cat}/K_m follows the order 3′-methyl (**105**) > 3′-ethyl (**106**) > 3′-hydrogen (**85**).

These results indicate that steric factor plays an improtant role in determining of the substrate properties in this series. The methyl or ethyl group substituted at 1- or 3-position of the five-membered heteroarenes leads to a high substrate activity.

The results of these studies as well as those reported previously suggest that a variety of factors contribute to the MAO-B substrate properties of 4-substituted 1-methyl-1,2,3,6-tetrahydropyridinyl derivatives. Although, in general, electron donating substituents often improve the k_{cat}/K_m values, steric and, perhaps, polar factors appear to dominate the substrate interactions with the enzyme.

Chapter 3. Deuterium isotope effect studies on the MAO-catalyzed oxidation of MPTP analogs

3.1. Introduction

3.1.1. Kinetic isotope effects

A kinetic isotope effect is the expression of the ratio between the rate of reaction with an unlabelled molecule and the rate of reaction with a molecule containing a heavy isotope. Isotope effects have been used for many years to study the mechanisms of enzymatic and nonenzymatic reactions. Isotopic substitution has offen involved replacing protium by deuterium or tritium. Any C-H bond has characteristic vibrations which impart zero-point energy to the molecule in its normal state.[125] The energy associated with these vibrations is related to the mass of the vibrating atoms. The deuterium has greater mass than that of protium, therefore, the vibrations associated with a C-D bond contribute less to the zero-point energy than do those of the corresponding C-H bond. For this reason, substitution of protium by deuterium lowers the zero-point energy of a molecule (Figure 25).

For a reaction involving cleavage of a bond to hydrogen (or deuterium), a vibrational degree of freedom in the normal molecule is converted to a translational degree of freedom on passing through the translation state. The energy difference due to this vibration disappears at the transition state.[126] If the transition state is symmetrical, it has the same energy for the protonated and deuterated species. Since the deuterated molecule has the lower zero-point energy, it is necessary for it to have a higher activation energy to reach the same transition state. Therefore, the rate in the rate-determining step of the reaction for these two species are different (Figure 25).

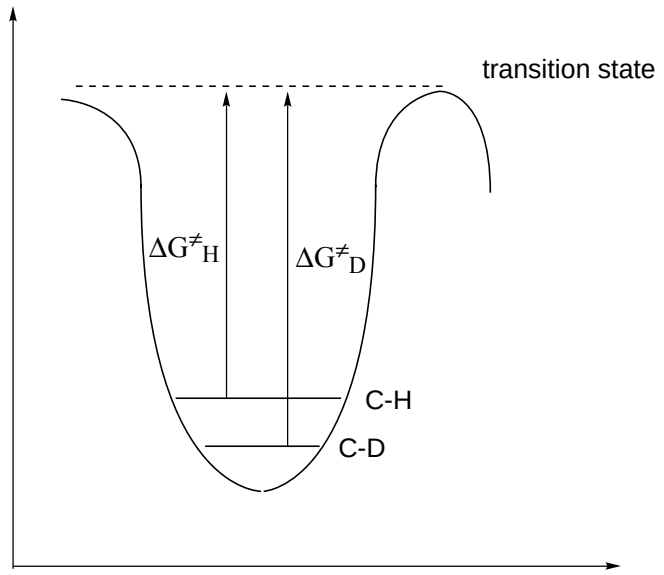

Figure 25. Differing Zero-Point Energies of Protium- and Deuterium- Substituted Molecules as the Cause of Primary Kinetic Isotope Effects When Their Transition State is Symmetrical

There are two kinds of kinetic isotope effects: primary and secondary kinetic isotope effects.

Primary kinetic isotope effects are those in which a bond to the isotopically substituted atom is broken or formed in the rate-determining step. Primary isotope effects provide two pieces of information about a reaction mechanisms. First, the existence of a substantial isotope effect ($k_H/k_D \geq 2$) is strong evidence that the bond to the isotopically substituted hydrogen atom is being broken or formed in the rate-determining step. Secondly, the magnitude of the isotope effect provides a qualitative indication of where the transition state lies with respect to product and reactant. A relatively low primary isotope effect implies that the bond to hydrogen is either only slightly or nearly completely broken at the transition state whereas the nearly maximum theoretical value is a good evidence that the transition state involves strong binding of the hydrogen to both its new and old bonding partner.[125-127]

Secondary isotope effects are those in which no bonds are made or broken to the isotopic atom during the reaction, but where the strength of bonding changes between

reactant and transition state. The strength of the bond may change because of a hybridization change or a change in the extent of hyperconjugation. For example, if an sp^3-hybridized carbon is converted to an sp^2 center as reaction occurs, a hydrogen bound to the carbon will experience decreased resistance to C-H bending. The freeing of the vibration for a C-H bond is greater than that for a C-D bond because the C-H bond is slightly longer and the vibration therefore has a larger amplitude. This will result in a normal isotope effect.

3.1.2. The application of isotope effects to enzyme-catalyzed reactions

A simplified enzyme-catalyzed reaction model[128] is given in Scheme 57.

$$E + S \underset{k_2}{\overset{k_1}{\rightleftharpoons}} ES \underset{k_4}{\overset{k_3}{\rightleftharpoons}} EP \underset{k_6}{\overset{k_5}{\rightleftharpoons}} E + P$$

Binding step Catalytic step Product releasing step

Scheme **57**. The Simplified Enzyme-Catalyzed Reaction Model

The first step is the binding of substrate to enzyme, governed by the rate constants k_1 and k_2. The second step is the transformation of the substrate to the product (catalytic step), governed by first-order rate constants k_3 and k_4. For irreversible catalysis, k_4 is set equal to zero. The third step is the dissociation of product from the enzyme, governed by the first-order rate constant k_5. Since initial velocity conditions are assumed, the concentration of product [P] is assumed to be zero and thus the rate of the reaction governed by k_6 is also zero. Steady-state kinetic analysis assumes that the concentration of the enzyme-substrate complex remains nearly constant. The rate equation for this reaction is given in eq. 3,[128] from which the kinetic expression for V_{max}, K_m and V_{max}/K_m may be derived (eq 4-6).[128]

$$v = \frac{k_1 k_3 k_5[S]}{k_5 (k_2 + k_3) + k_1 (k_3 + k_5)[S]} \qquad (3)$$

$$V = \frac{k_3 k_5}{k_3 + k_5} \qquad (4)$$

$$K_m = \frac{k_5 (k_2 + k_3)}{k_1 (k_3 + k_5)} \qquad (5)$$

$$V_{max}/K_m = \frac{k_1 k_3}{k_1 + k_3} \qquad (6)$$

Therefore, if the isotopic substitution exerts a specific effect on the binding step, we should observe the isotope effect in V_{max}/K_m but not V_{max}; substitution which alters the catalytic step will be expressed in both V_{max} and V_{max}/K_m; that which affects the product releasing step will be expressed in V_{max} but not V_{max}/K_m. The Michaelis constant K_m is related to the kinetic constants in all the three steps and thus is useless for interpretation of isotope effects.

3.1.3. The deuterium isotope effect studies on MPTP analogs

A. Regioselectivity of the MAO-catalyzed oxidation of MPTP analogs

It was initially proposed that the oxidation of MPTP (**67**) to the dihydropyridinium metabolite **68** could result from direct attack at C-6 or from initial attack at C-2[129] followed by rearrangement of the isomeric 2,5-dihydropyridinium intermediate **282** to **68** via the free base **283** (Scheme 58, a).

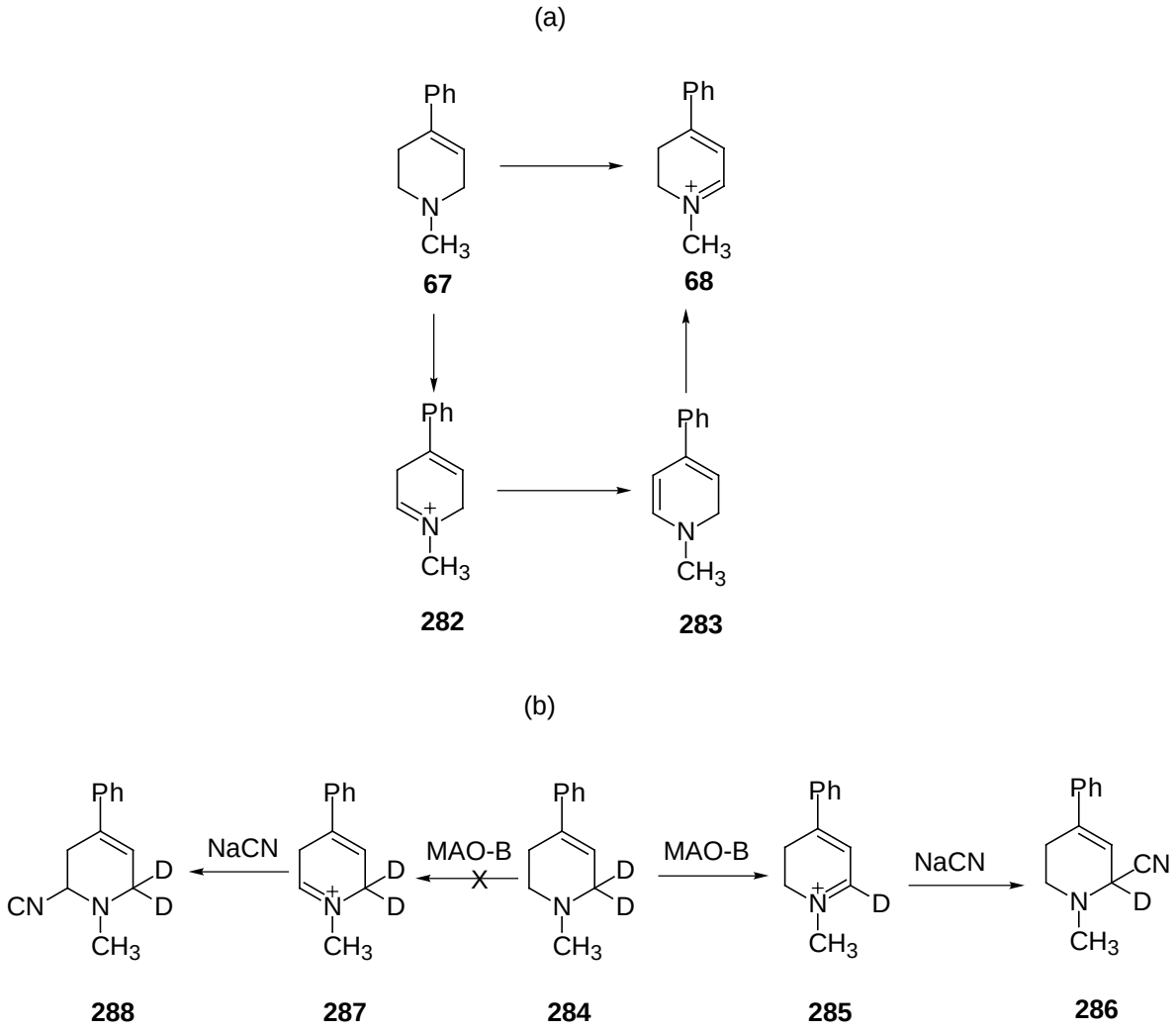

Scheme 58. The Regioselectivity of MAO-Catalyzed Oxidation of MPTP

Liquid secondary ion (LSI) mass spectral analysis of the α-cyano adduct **286**, derived from a 60-min MAO-B incubation mixture of MPTP-d_2 (**284**) which had been treated with NaCN, indicated that the formation of $MPDP^+$ occurs exclusively from oxidation of MPTP at C-6[129] (Scheme 58, b). Since no significant amount of **288** was found. Therefore, it was concluded that the isotope effect measurements will not be complicated by metabolic switching to the C-2 position.[129]

Our recent studies showed that the MPTP analogs bearing heteroaryl groups at the C-4 position exhibit different substrate activities. Sometimes, a small modification of the

structure may cause a dramatic change in substrate properties. For example, the 1-methyl-4-(3-methylfuran-yl)-1,2,3,6-tetrahydropyridine (**103**) is an excellent substrate. However, its structurally similar analog 1-methyl-4-(2-furanyl)-1-2-3-6-tetrahydropyridine(**86**) is a poor substrate.[91] When we use the values of k_{cat}/K_m to compare these substrate properties, we assume that the catalytic step of the enzyme-catalyzed reaction is rate-determining. The great change of the substrate property of these MPTP analogs have prompted us, however, to consider the possibility that the rate-determining step changes from one substrate to the other. When the substrates are oxidized to their dihydropyridinium metabolites, the products may exhibit different affinities to the enzyme. If the affinity is high enough, the product releasing step may become rate-determining. If this were true, we would lose the correct standard for the comparison of the substrate activities. Therefore, we synthesized the regioselectively deuterated analogs of both good and poor substrates and examined their isotope effects.

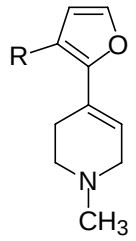

103 R=CH_3
86 R=H

B. Stereoselectivity of MAO-catalyzed oxidation of MPTP analogs

Researchers realized long ago that the MAO-catalyzed oxidation of some amines is stereoselective. It was found in the 1960s[130], that there was a significant difference in the enzyme-catalyzed (rat liver monoamine oxidase) oxidation of asymmetrically labelled tyramine. The ratio k_S/k_R was 2.3 clearly establishing that the prochiral hydrogen atoms in tyramine (**287**) are not equivalent for the enzyme.

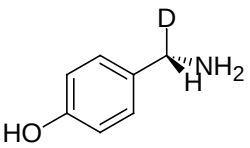

(*R*)-tyramine (**287**)

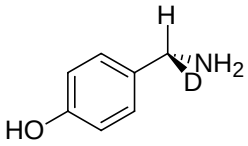

(*S*)-tyramine (**287**)

It was also observed that the absolute stereochemistry is involved in the elimination of *R*-hydrogen during dopamine oxidative deamination catalyzed by both MAO-A and MAO-B from different sources.[131]

It has been suggested that the MAO-B catalyzed α-carbon oxidation of MPTP may be stereoselective, since the C-6 position of MPTP is prochiral. CI mass spectral deuterium content analyses established that the d_1/d_0 product ratio of the incubation mixtures of (*R, S*)-MPTP-d_1 decreased from approximately 1.5 at 10 min to 1.1 at 60 min.[129] These data indicate that the enantiomeric composition of the substrate changes with time due to the stereoselective loss of one of the enantiotopic hydrogen/deuterium atoms. However, an accurate assessment of the stereoselectivity of MAO-catalyzed oxidation of MPTP analogs was unclear because synthetic difficulties prevented the preparation of highly stereoselectively deuterium labelled MPTP analogs.[132]

3.2. The regioselectivity studies of the MAO-catalyzed oxidation of MPTP analogs

3.2.1. The synthesis of the regioselectively deuterated MPTP analogs

The synthetic pathways for the deuterated analogs of **296**-**298** are given in Scheme 59.

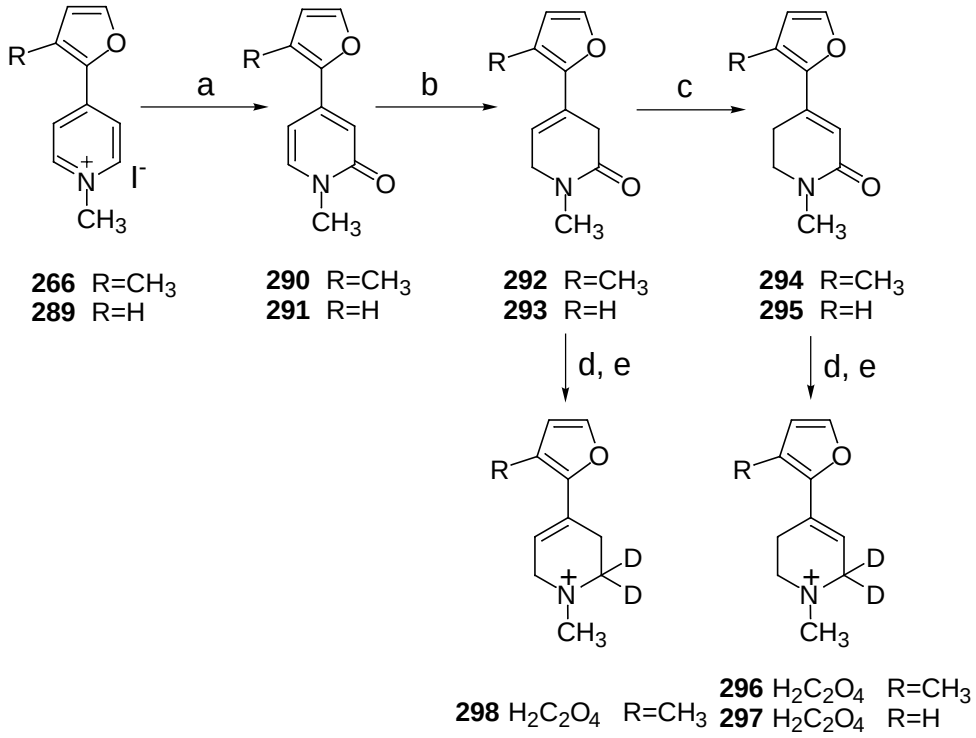

Conditions: a) NaOH, $K_3Fe(CN)_6$, 0 ^{0}C; b) LS-selectride, -78 ^{0}C; c) K(t-BuO); d) $LiAlD_4$, ether; e) $H_2C_2O_4$, ether.

Scheme 59. The Synthesis of Deuterated Analogs of 1-Methyl-4-(3-methylfuran-2-yl)-1,2,3,6-tetrahydropyridine and 1-Methyl-4-(2-furanyl)-1,2,3,6-tetrahydropyridine

Treatment of the 1-methyl-4-substituted pyridinium iodide (**266**) and (**289**) with the potassium ferricyanide (III) and potassium hydroxide at 0 °C in water[133-135] afforded the corresponding 1-methyl-4-substituted-2-pyridones (**290**) and (**291**) respectively, which upon reduction using LS-selectride at -78 ℃ produced the corresponding 1-methyl-4-substituted-3,6-dihydro-2-pyridones (**292**) and (**293**), respectively. These 3,6-dihydro-2-pyridones were converted into the corresponding 1-methyl-4-substituted-5,6-dihydro-2-pyridones (**294**) and (**295**) by the reaction with potassium *tert*-butoxide.

The reduction of the 1-methyl-4-(2-furanyl)-5,6-dihydro-2-pyridone (**295**) and 1-methyl-4-(3-methylfuran-2-yl)-5,6-dihydro-2-pyridone (**294**) using lithium aluminium deuteride yielded the 1-methyl-4-(2-furanyl)-1,2,3,6-tetrahydropyridine-6,6-d_2 (**297**) and

1-methyl-4-(3-methylfuran-2-yl)-1,2,3,6-tetrahydropyridine-6,6-d_2 (**296**), respectively, which were converted to their oxalates by the reaction with oxalic acid in ether. The reduction of the 1-methyl-4-(3-methylfuran-2-yl)-3,6-dihydro-2-pyridone (**292**) using lithium aluminium deuteride gave 1-methyl-4-(2-furanyl)-1,2,3,6-tetrahydropyridine-2,2-d_2 (**298**).

The 1-methyl-4-(2-furanyl)pyridinium species **289** was obtained by the methylation of 4-(2-furanyl)pyridine (**301**) with methyl iodide (Scheme 60). The pyridinyl derivative **301** was synthesized through a cross-coupling reaction between 2-furanyllithium (**300**) and 4-bromopyridine in the presence of $Pd(PPh_3)_4$.

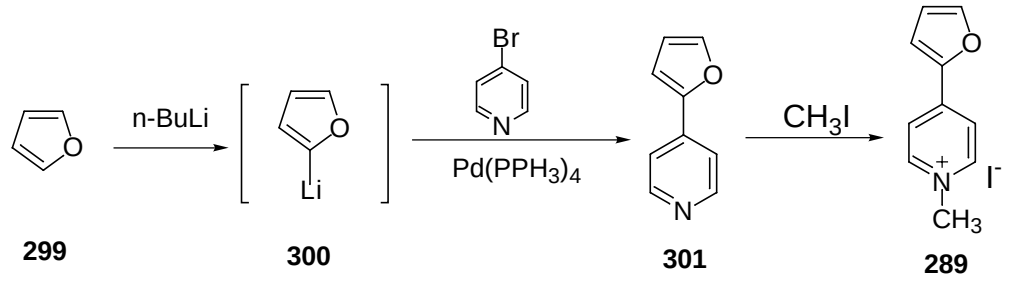

299 **300** **301** **289**

Scheme 60. The Synthesis of 1-Methyl-4-(2-furanyl)pyridinium iodide

The 1-methyl-4-(3-methylfuran-2-yl)-1,2,3,6-tetrahydropyridine-1,1,1-d_3 (**303**) was achieved by reduction of the 1-methyl-4-(3-methylfuran-2-yl)pyridinium-1,1,1-d_3 iodide (**302**) with $NaBH_4$ (Scheme 61). The pyridinium starting material **302** was obtained by the methylation of **301** using deuterated methyl iodide.

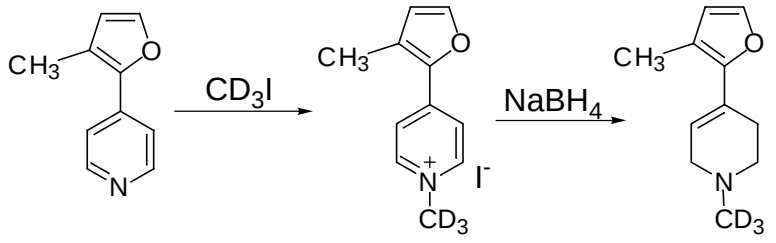

301 **302** **303**

Scheme 61. The Synthesis of Deuterated 1-Methyl-4-(3-methyl-furan-2-yl)-1,2,3,6-tetrahydropyridine-1,1,1-d_3

3.2.2. Enzymology results

Analysis of the kinetic isotope effects with their substrates was pursued to determine the rate determining step in these reactions. In these experiments, both tetrahydropyridines and their deuterated analogs were used as substrates of MAO-B. Linear initial velocities vs substrate concentration plots and linear double-reciprocal plots were obtained for all the compounds (Figure 26-30). The kinetic data are given in Table 2. The kinetic isotope effects are given in Table 3.

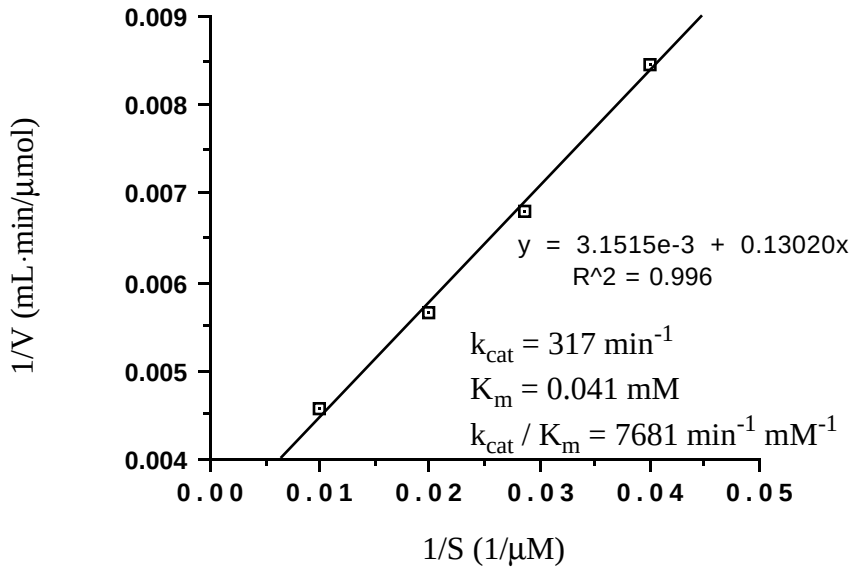

Figure 26. Lineweaver-Burke Plot for the MAO-B Catalyzed Oxidation of 1-Methyl-4-(3-methylfuran-2-yl)-1,2,3,6-tetrahydropyridine-2,2-d_2 (**298**)

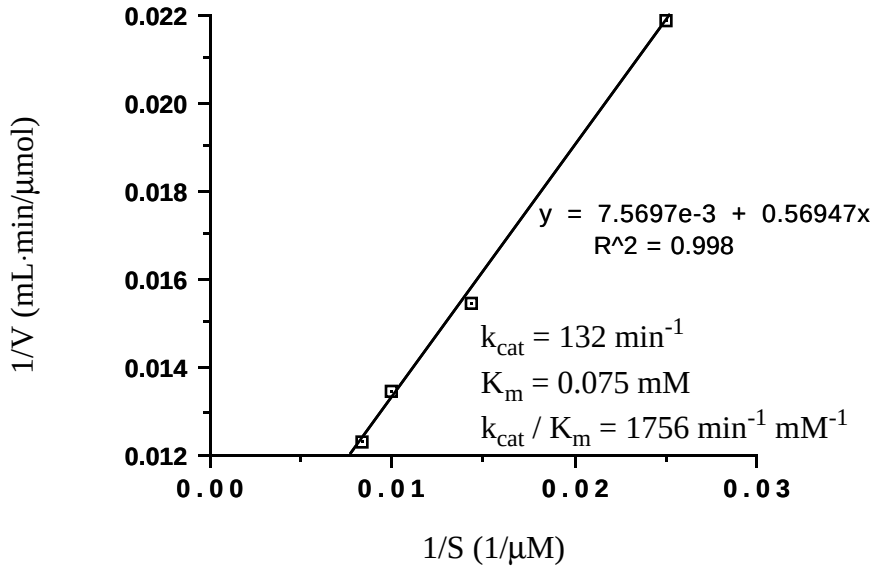

Figure 27. Lineweaver-Burke Plot for the MAO-B Catalyzed Oxidation of 1-Methyl-4-(3-methylfuran-2-yl)-1,2,3,6-tetrahydropyridine-6,6-d_2 (**296**)

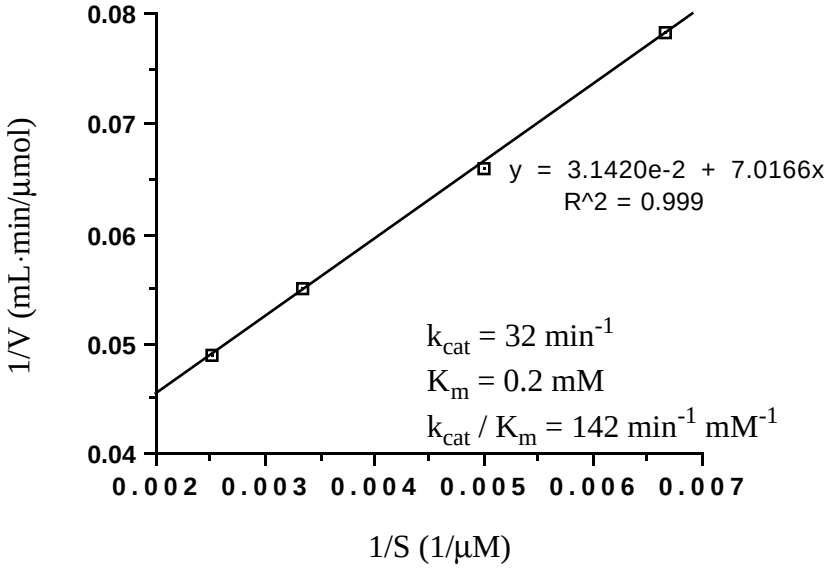

Figure 28. Lineweaver-Burke Plot for the MAO-B Catalyzed Oxidation of 1-Methyl-4-(2-furanyl)-1,2,3,6-tetrahydropyridine (**86**)

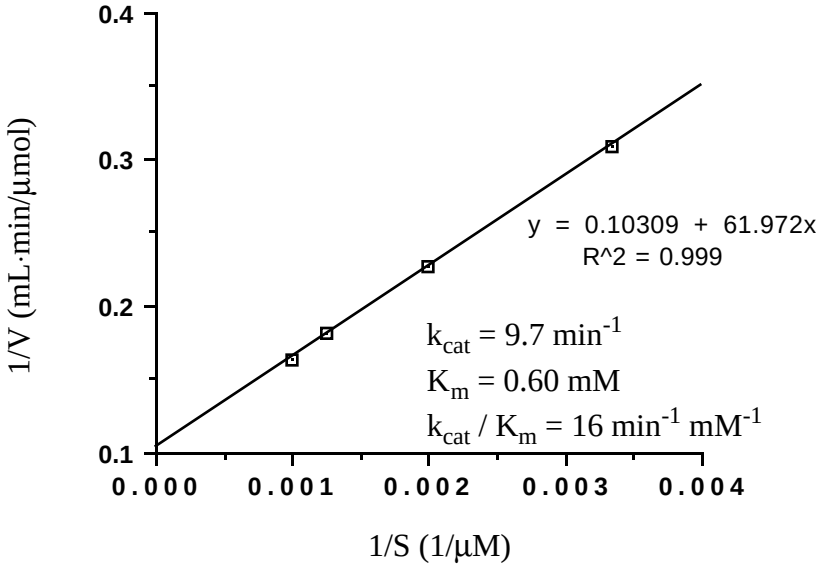

Figure 29. Lineweaver-Burke Plot for the MAO-B Catalyzed Oxidation of 1-Methyl-4-(2-furanyl)-1,2,3,6-tetrahydropyridine-6,6-d_2 (**297**)

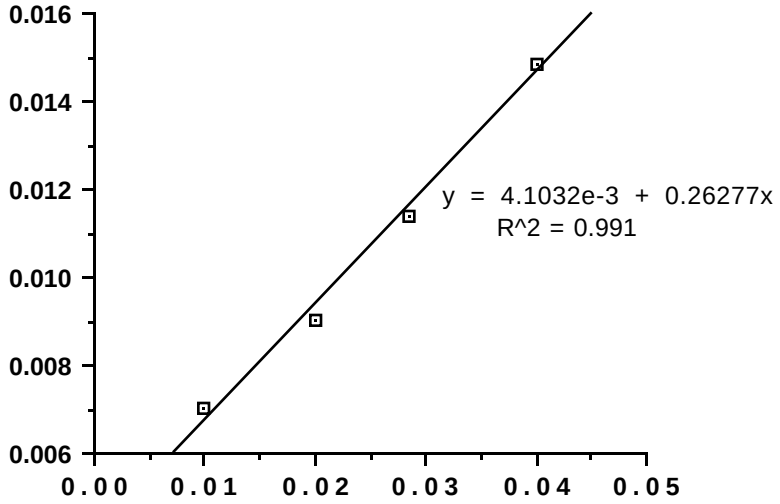

Figure 30. Lineweaver-Burke Plot for the MAO-B Catalyzed Oxidation of 1-Methyl-4-(3-methylfuran-2-yl)-1,2,3,6-tetrahydropyridine-1,1,1-d_3 (**303**)

Table 2. Kinetic Parameters for the MAO-B Catalyzed Oxidation of the MPTP Analogs

Deuterated analogs	k_{cat} $(min)^{-1}$	K_m (mM)	k_{cat}/K_m $(min^{-1}mM^{-1})$
103	349	0.042	8271
296	137	0.086	1604
298	326	0.043	7603
303	270	0.073	3737
86	26	0.24	110
297	10	0.62	16

Estimated using ε=23,000 M^{-1}, the value for the perchlorate salt of the 1-methyl-4-(2-furanyl)-2,3-dihydropyridinium species.[91]

Table 3. Deuterium Isotope Effects Observed with the 1-Methyl-4-substituted-1,2,3,6-tetrahydropyridines.

Deuterated analogous	$^{D}(k_{cat})$	$^{D}(K_m)$	$^{D}(k_{cat}/K_m)$
296	2.6	0.49	5.2
298	1.1	0.98	1.1
303	1.3	0.58	2.2
297	2.6	0.39	6.9

3.2.3. Discussion

High, normal isotope effects were observed in k_{cat} and k_{cat}/K_m with both tetrahydropyridine-6,6-d_2 compounds **296** and **297**. No significant isotope effects were observed with the tetrahydropyridine-2,2-d_2 compound (**298**). Substantial, normal isotope effects were observed in k_{cat} and k_{cat}/K_m with the compound **303**.

The substantial isotope effect observed with the compound with deuterated substitution at 1-methyl group (**303**) was unexpected. During the oxidation, the hybridization of the nitrogen atom changes from sp^3 to sp^2. This may cause the significant increase of the β-hyperconjugation of the deuterium atom with the p orbital of the nitrogen. Therefore, a secondary isotope effect should be observed. The reason that the experimental data are a little bit higher than the normal secondary isotope effect remains unclear. But this data clearly indicates the formation of the nitrogen cation during this transformation. Hydrogens at 2-position of the tetrahydropyridine may also lead to a secondary isotope effect. However, because of the ring strain, the hydrogen atoms can not rotate as freely as the hydrogens in methyl group. The smaller number of hydrogens at 2-position also will lower the contribution of stabilization through β-hyperconjugation. These may explain the small secondary isotope effect observed with **298**. The fact that the isoptope effect for the 2,2-d_2 compound is very small argues that the isotope effects observed with 6,6-d_2 compound are primary. It is, therefore, concluded that the cleavage of the C-H bond at 6-position of the 1,2,3,6-tetrahydropyrridine is rate determining for both good and poor substrates. This means that the rate determining step does not change from poor substrates to good substrates in this system.

3.3. The stereoselectivity of the MAO-catalyzed oxidation reaction of MPTP

Our experiments have indicated that the cleavage of this C-H bond at 6-position of the 1,2,3,6-tetrahydropyridine is rate-determining. The next question is if the enzyme removes the prochiral hydrogen stereoselectively? Although there are several methods available for the incorporation of deuterium at the 6-position of the MPTP type molecules, most of them lack stereoselectivity and some of them suffer from the incomplete incorporation of deuterium. Furthermore, traditional methods are not always effective for determining enantiomeric excesses (ee) of products which are chiral only by virtue of an isotope. Our synthetic strategy to obtain a high stereoselectively monodeuterated MPTP analog is based on the alkylation of heterocycles α to nitrogen. The analytic strategy employs a chiral liquid crystal matrix NMR technique.

3.3.1. Literature review

A. Synthetic strategies

1. The lithiation-substution sequences

Deprotonative lithiations are commonly used to generate enolates, ylides, and dipole-stablized, localized sp^2 or sp delocalized carbanions as reactive intermediates for diverse applications.[136] Beak proposed a sequence involving removal of a proton from **304** to give the formally sp^3 organolithium species **305**[137-138] (Scheme 62). In the prescence of chiral ligand, such as (-)-sparteine, or chiral auxiliaries, such as formamidines or oxazolines, after initial complexation a regioselective or diastereoselective deprotonation can occur. In an asymmetric deprotonation, the enantioenriched **306** or **306**•L* retains its configuration and reacts stereoselectively with electrophiles.[139] If **306** is produced in racemic form, two different diastereoselective pathways for asymmetric substitution are available.[136] The pathway which involves selective formation of one nonequilibrating complex is a dynamic thermodynamic resolution. If the diastereomeric complexes are in rapid equilibrium, a pathway of dynamic kinetic resolution is followed.

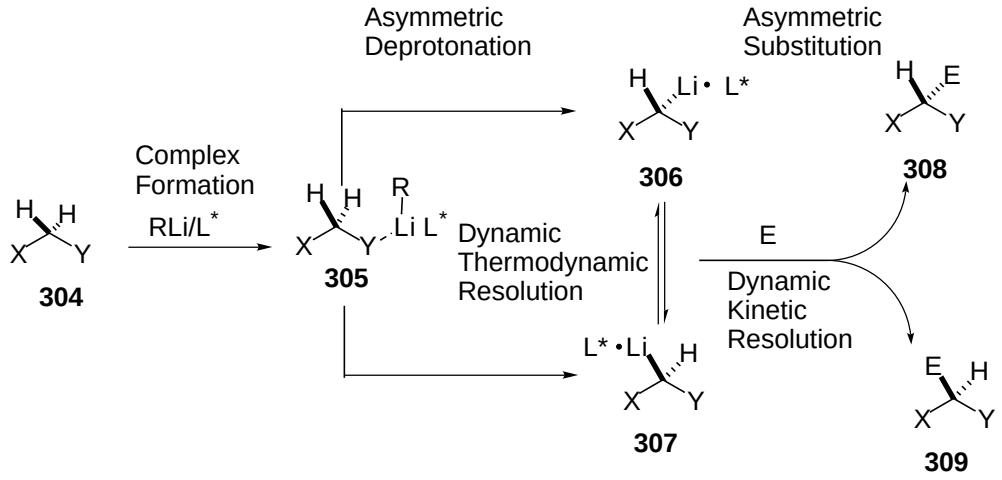

Scheme 62. The Lithiation-Substitution Sequences

The alkylation of heterocycles α to a nitrogen has been a focus of attention for synthetic chemists for over 20 years.[140-142] The strategy is to generate a carbanion adjacent

to nitrogen. The activation of the nitrogen with a suitable electron-withdrawing group would both increase the kinetic acidity of an α-proton and stabilize the configuration of the carbanion by chelation (Scheme 62). This concept of preparing anions has been termed by Beak as "dipole-stabilized" and has been the subject of considerable discussion.[141]

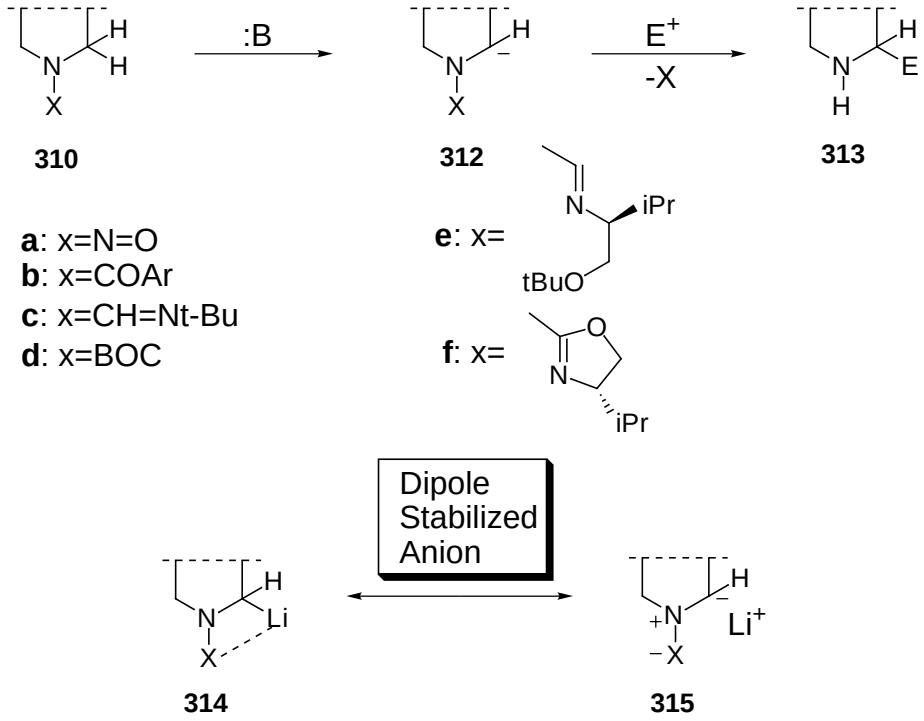

Scheme 63. Dipole Stabilized Carbanion α to Nitrogen

The electron-withdrawing groups may be nitroso (**a**)[143-144], amido (**b**)[145-146], formamidino (**c** and **e**)[147-150], urethyl (**d**)[151-153] and oxazolinyl (**f**).[154-156] Among these, the chiral formamidines (e.g **e**)[157] and chiral oxazolines (e.g **f**) have the most stereoselective synthetic potentials. They also exhibit different mechanisms.

2. The structures of α-aminocarbanions:

Although α-aminocarbanions have been known since 1965,[158-159] evidence that the carbanionic carbon of secondary α-aminoorganolithiums could be stereogenic (i.e., tetrahedral instead of trigonal) was not provided until Fraser[160] and Seebach[161] observed

fundamental differences between the chemical behavior of metalated nitrosamines and amides (Scheme 64).

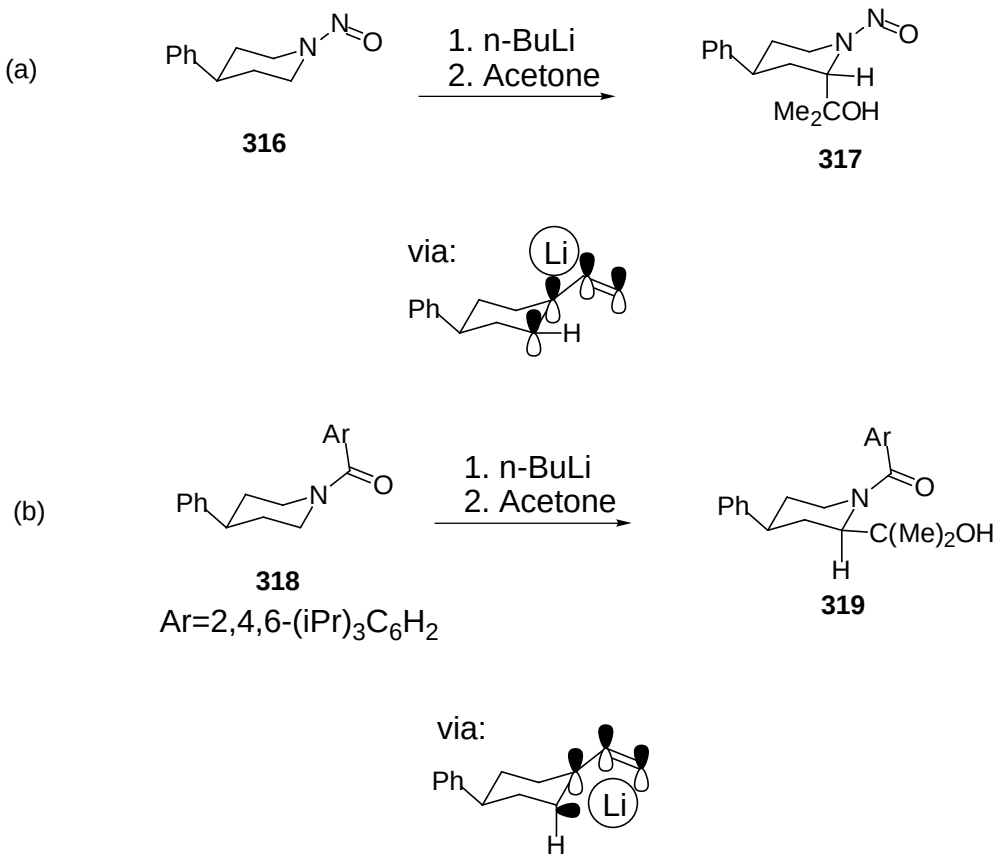

Scheme 64. The Chemical Behavior of Metalated Nitrosamines and Amides

Specifically, the alkylation of a conformationally locked piperidinyl nitrosamine (**316**) occured from the axial direction,[160-161] whereas a similar lithiated amide afforded the less stable,[162-163] equatorial substitution product **319**.[161,163] Since the equatorial isomer is the less stable product, it seems reasonable to assume that the carbanion is configurationally stable and that the Li-C-N-C=O atoms lie in an approximately equatorial plane.

Ab initio calculations also indicate that there is a strong stereoelectronic preference for the carbanion lone electron pair (10-20 kcal/mol, depending on geometry)[164] to remain in the nodal plane of the amide p-system, with the carbanionic carbon clearly pyramidal. When a lithium atom is included, metalated esters[163] and amides[165] show an additional

stablization when the lithium is chelated to the carbonyl oxygen (13 kcal/mol for esters and 28 kcal/mol for amides).

The single crystal structures of two α-aminoorganolithium: [α-(dimethylamino)benzyllithium-diethylether]$_2$ (**320**) and S-α-(methylpivaloylamino)-benzyllithium-sparteine (**321**) (Figure 31) have confirmed the pyramidalized carbanion structure.[166-167]

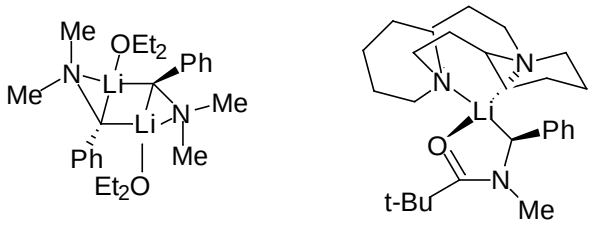

320 **321**

Figure 31. The Structures of [α-(Dimethylamino)benzyllithium-diethylether]$_2$ (**320**) and *S*-α-(Methylpivaloylamino)-benzyllithium-sparteine (**321**)

3. Chiral nitrogen activating groups:

In 1980, Meyers′ group reported[168] that the achiral formamidine moiety was yet another dipole stablized activating group that could be lead to the formation of α-aminocarbanions which could be elaborated to α-alkyl amines. However, it was soon recognized that the possibility existed to introduce a chiral element into these formamidines by simply affixing the appropriate group to the nitrogen. The opportunity may arise to not only alkylate a carbanion adjacent to nitrogen but to do so with attending absolute stereochemistry (Scheme 65). These formamidine chiral auxiliaries work very well when the metalated carbon is allylic or benzylic.

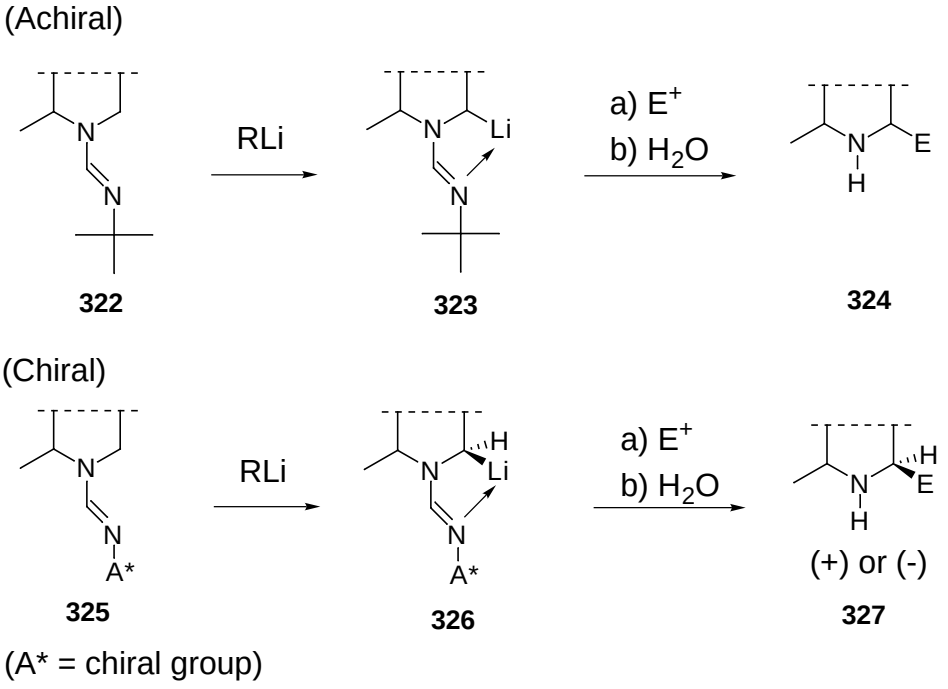

Scheme 65. The Lithiation-Substitution of Heterocyclic Formamidines

In 1981, Gawley introduced[156] a chiral oxazoline auxiliary whose performance is comparable to that of the formamidines in benzylically activated systems.[169] The oxazoline auxiliaries also mediates deprotonation at nonactivated positions.[154]

4. Mechanisms of stereoselective transformations

A considerable amount of effort has gone into sorting out the factors responsible for the high degree of stereoselectivity observed in these formamidine and oxazoline alkylations.

(1) Formamidine--bidentate complex:

Studies[170-174] showed that a) all deprotonations take place from the α-face, b) alkylation on the secondary carbanions occurs from the β-face with very high selectivity (>99%) and with net inversion of configuration of the C-Li bond, c), alkylation on tertiary carbanions occurs from the α-face with reasonably high selectivity (90-93%) with net retention of configuration (Scheme 66).

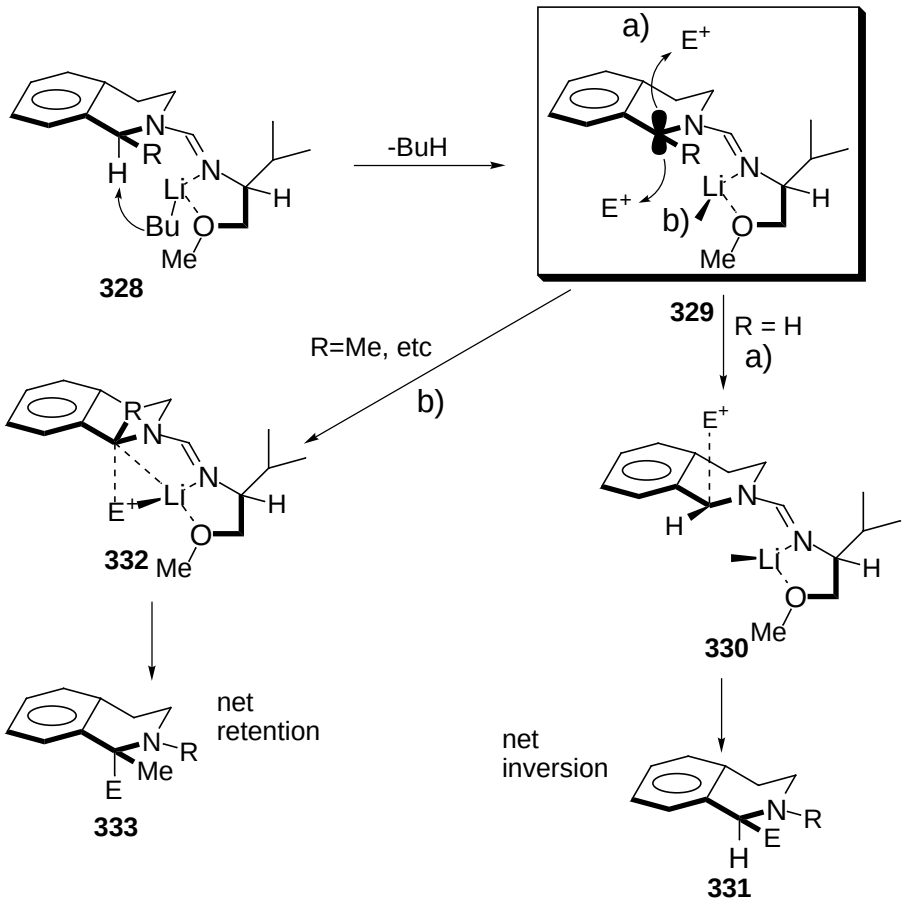

Scheme 66. The Mechanism of the Stereoselective Alkylation of Heterocyclic Chiral Formamidines

a. The depronation step:

It was shown that only the α-proton is removed when n-butyllithium is added to the chiral formamidine isoquinoline **334**[171-172] (Scheme 67).

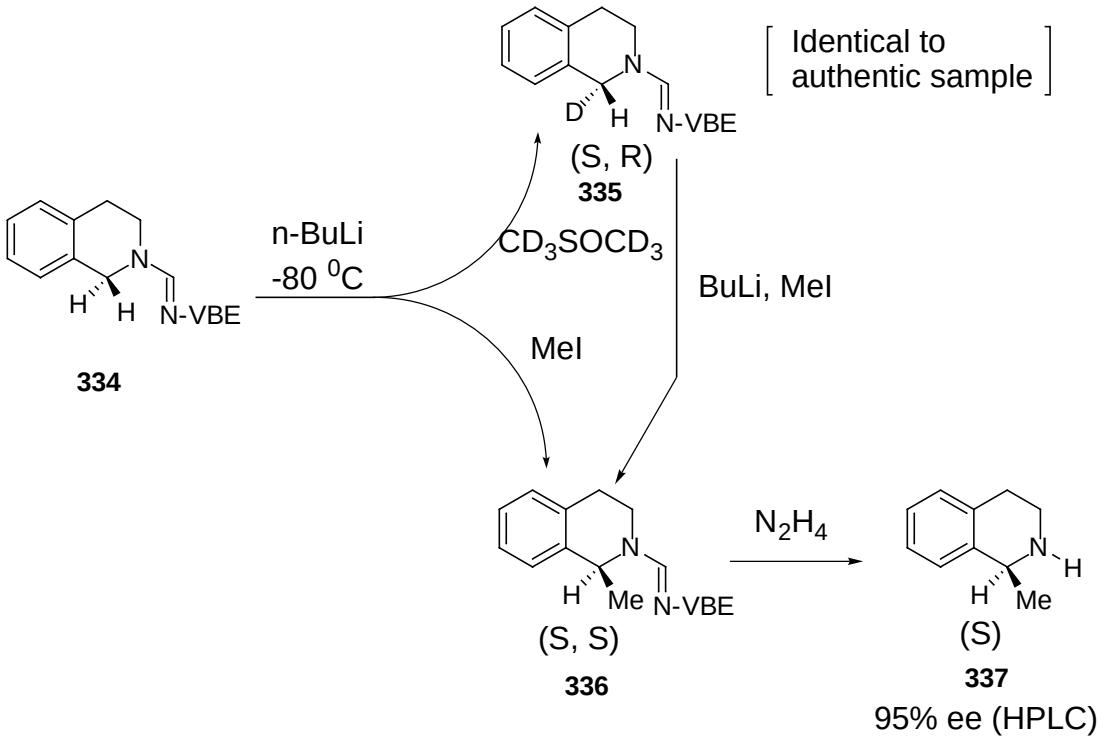

Scheme 67. The Asymmetric Deprotonation of the Chiral Formamidine Isoquinoline

This was explicitly shown when DMSO-d_6 was introduced into the lithiated formamidine and gave the α-D product which was identical to an authentic sample of (*R*)-1-D isoquinoline. However, when methyl iodide (or any other alkyl halide) was added to the lithio salt, the alkyl group entered from the β-face to afford the *S*-enantiomer.

Of further interest is the fact that the deuterium alone was cleanly removed when the mono-deutero isoquinoline was again treated with n-butyllithium-methyl iodide. Here the product was the *S*-enantiomer, devoid of any deuterium and the methylated isoquinoline produced in greater than 95% ee. The preference of the butyllithium mediated deprotonation indicates that only the atom on the α-face of the isoquinoline is removable regardless of whether it is proton or deuteron.

This interesting behavior led to another experiment designed to confirm whether or not an isotope effect was operating in the deprotonation step. A head-to-head competition study was performed using an equimolar mixture of the deutero and protio chiral formamidines and 0.5 equivalents of n-butyllithium (Scheme 68). After 15 min the

reaction mixture was quenched with excess methyl iodide and the mixture analyzed. The results indicated that 50% yield of the methylated product contained no deuterium and the recovered 50% of unreacted starting materials showed a 50-50 mixture of H and D isoquinoline. Thus, the base completely ignored the presence of the stronger C-D bond and deprotonated both compounds with equal facility. Since there was no measurable isotope effect in the deprotonation of the α-face, the rate determining step must be in the formation of the complex prior to deprotonation.

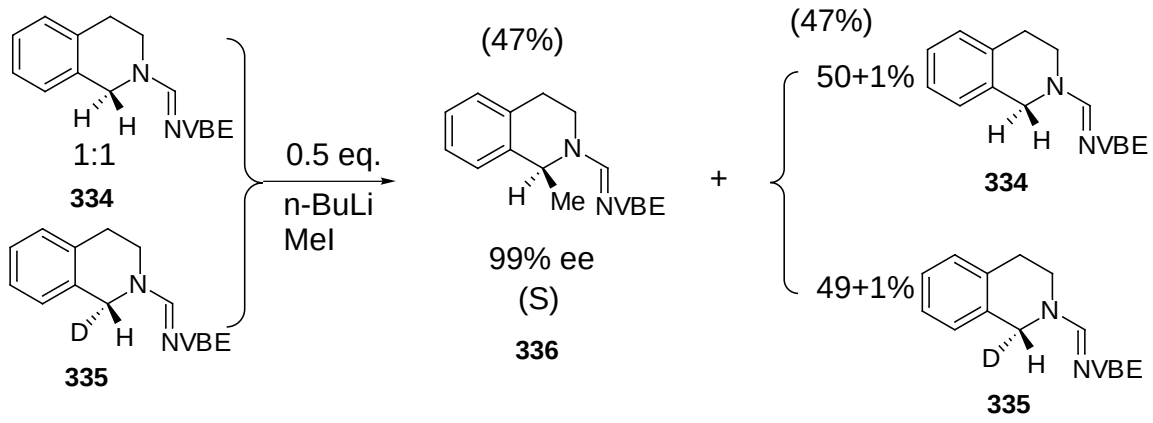

Scheme 68. The Rate-Determining Step *vs* . Deprotonation Step of Chiral Formamidines

b. The alkylation step

Even though deprotonation takes place from the α-face, alkylation occurs from the β-face. The major clue to the alkylation step came when it was shown that metalation of the *racemic* methoxy formamidine, derived from *tert*-leucinol with excess *sec*-butyllithium and followed by introduction of methyl iodide, gave the quaternary substituted isoquinoline **338** in 44% yield and with 85% diastereoselectivity[172-174] (Scheme 69). Also obtained was a 45% yield of the (*R*)-benzylisoquinoline **339** in greater than 98% ee. This showed unequivocally that a kinetic resolution had cleanly taken place and that only the enantiomer that possessed a proton on the α-face was both metalated and alkylated with respectable diastereoselectivity. It was the first example of a quaternary carbon being generated adjacent to nitrogen with attending stereocontrol.

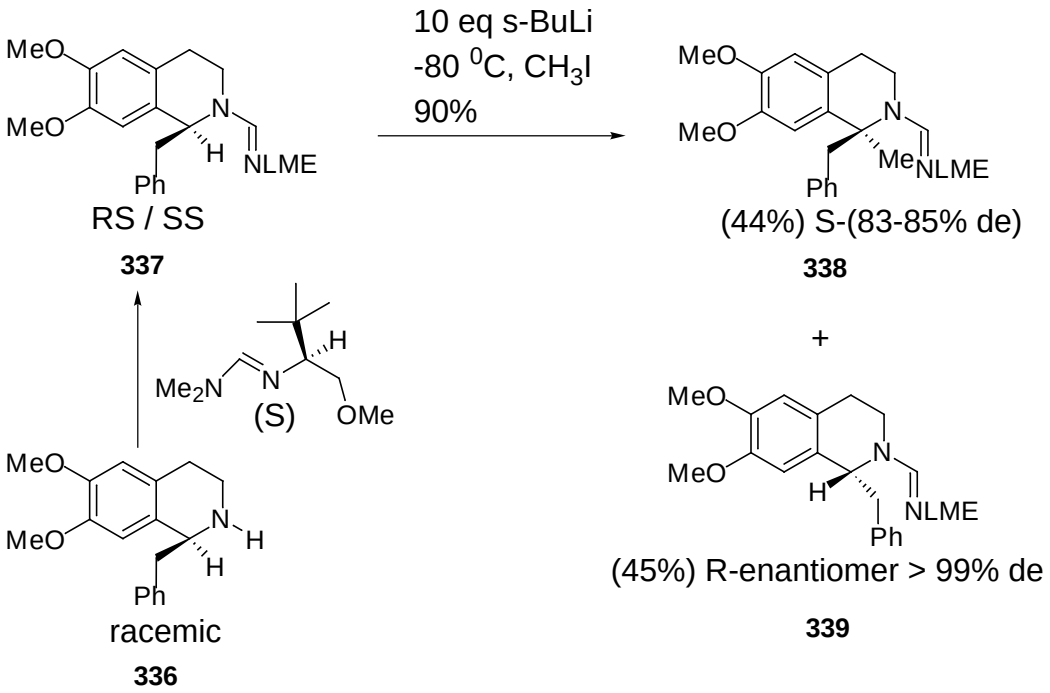

Scheme 69. The Alkylation of the Lithiated Chiral Formamidines

(2). The oxazolines--monodentate complex

Evidence[155,175-176] was provided that the β-proton at C-1 is indeed removed stereoselectively but that the resulting anion is equilibrated to a thermodynamic mixture of diastereomeric lithiated species and that the latter process accounts for the stereoselectivity observed in the overall process (Scheme 70).

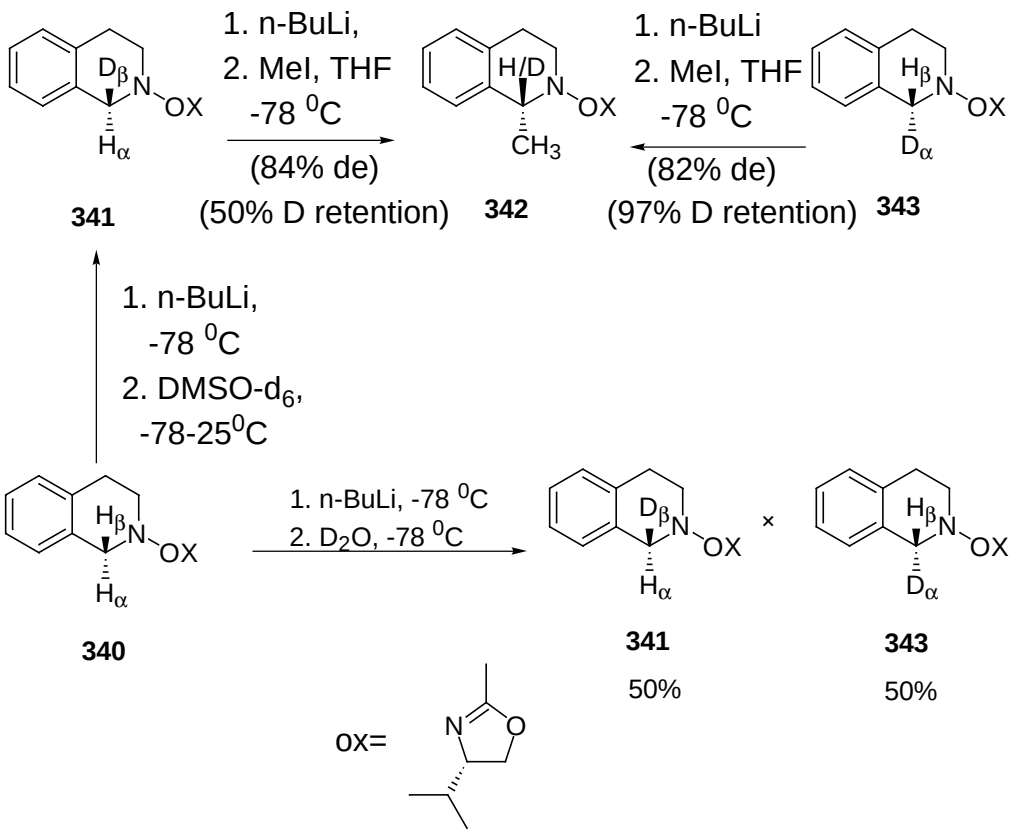

Scheme 70. The Mechanism of the Stereoselectivity of Chiral Oxazoline Isoquinoline

Quenching lithiated (S)-**340** with DMSO-d_6 at -78 ℃ and warming to room temperature afforded 96:4 mixture of the two 100% deuteriated epimers with major epimer **341** at C-1 being *S*. However, if the lithiated (*S*)-**340** was quenched with deuterium oxide, a 1:1 recemic mixture of **341** and **343** was obtained. When **341** was deprotonated at -78 °C and quenched with methyl iodide at the same temperature the methylated product **342** was obtained in 84% de but contained 50% deuterium.

Since the D/H ratio (1/1) is not the same as the diastereomer ratio (12/1), the stereoselectivity observed in the overall alkylation cannot be due to stereoselectivity in the deprotonation step. In contrast, deprotonation and methylation of **343** at -78 ◦C afforded about the same degree of asymmetric induction (82% ee) but the products contained 97% deuterium.

The selectivity of the deprotonation was explained by a conformational preference of the coordinated alkyllithium in which the butyl group is anti to the isopropyl (Figure 32).[175]

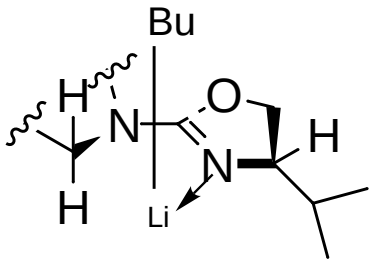

Figure 32. The Conformational Preference of the Coordination Compound Between Butyllithium and Chiral Oxazolines

The stereoselectivity in the deprotonation is determined quantitatively by the relative rates of abstraction of the two protons, Hα and Hβ. This quantity, as well as the isotope effect, can be calculated from the ratio of 6D/6H obtained from **341** and **343**. The calculations yield a relative rate of 5.8 and an isotope effect of 5.9.[175,177] Thus, when the deuterium is up (as in **341**), the stereoselectivity of the deprotonation (loss of Dβ favored) is opposed by the kinetic isotope effect, which directs the base to Hα. The results is deprotonation at both sites. In contrast, when the deuterium is down (as in **343**), both the stereoselectivity of the deprotonation and the isotope effect work in concert, directing the base to Hβ. Virtually complete retention of deuterium is observed.

The mechanism postulated to account for the observations[176] is shown in Scheme 71.

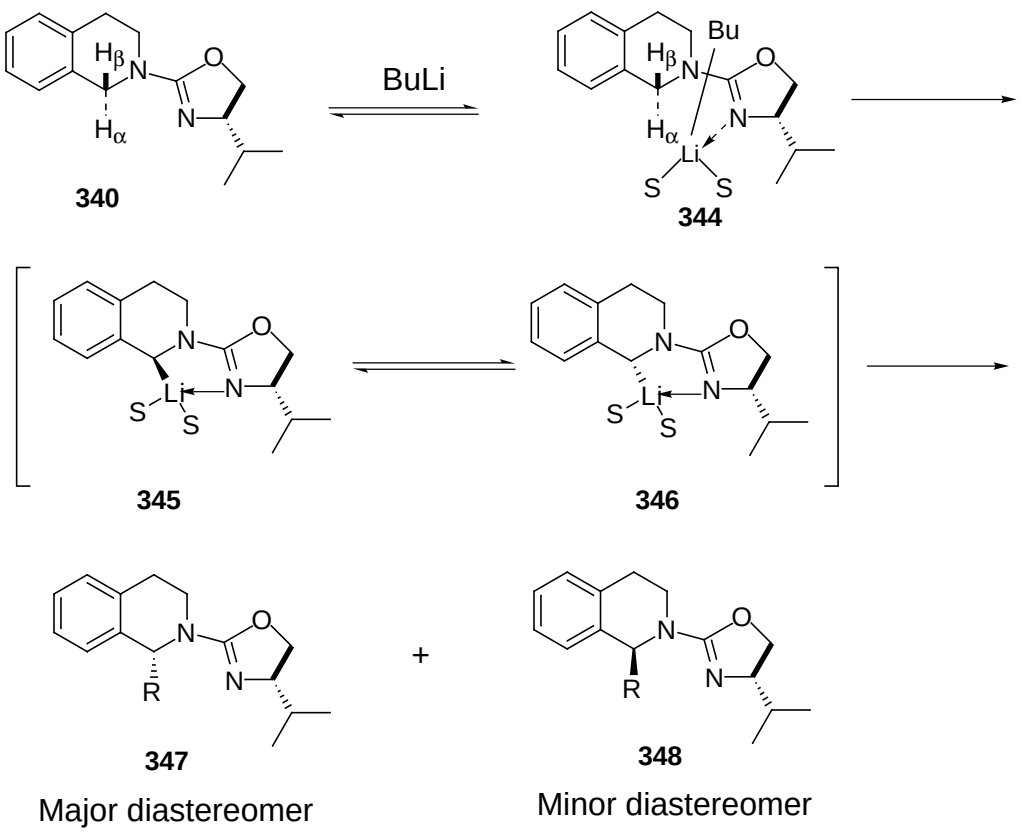

Scheme 71. The Lithiation-Substitution Sequence of Chiral Oxazoline Isoquinoline

The first step is the formation of a coordination complex. The butyl group is oriented anti to the substituent on the oxazoline and is positioned for selective removal of the Hβ proton. It is the configuration of this coordination complex that accounts for the stereoselectivity of the deprotonation. Proton loss then produces an equilibrating pair of organolithium diastereomers **345** and **346**, each of which is conformationally mobile.

Upon addition of an electrophile, **345** and **346** are converted to the mixture of product diastereomers **347** and **348,** respectively. The fact that all alkyl halides afford **347** as the major diastereomer whereas DMSO-d_6 affords **348** (R=D) suggests that one mode of electrophilic attack occurs with retention while the other occurs with inversion.

There was no data on the structure of organolithium species or on the mechanism for its reaction with electrophiles.

B. Analytic strategies

There are several methods to measure enantiomeric purity, such as optical rotation measurements, gas chromatographic methods, liquid chromatographic methods and nuclear magnetic resonance analysis. For compounds which are chiral only by virtue of an isotope, NMR methods play an important role. Several methods for enantiomeric analysis using the NMR technique have been developed.[178] In general, these methods are based on the association of chiral compounds with chiral reagents, producing new species which exhibit different NMR spectra for each enantiomer. These species may be diastereoisomers formed through chemical binding with an enantiopure compound or molecular complexes formed with lanthanide chiral shift reagents or chiral solvating agents. A different approach to enantiomeric analysis by NMR has been reported by Courtieu et al.[179-181] They found that dichloromethane solutions of poly(γ-benzyl L-glutamate) (PBLG) can be used as a chiral deuterium NMR solvent to distinguish enantiomers.

The proton-decoupled spectrum of deuterium in an isotropic solvent consists of a single line (Figure 32a). When the molecules are partially oriented in a nematic liquid crystal the average of the quadrupolar coupling becomes nonzero, which splits the line into two. The separation of the signal each doublet is the quadrupolar splitting $\Delta\nu_Q$. In the high-field approximation and assuming a negligible asymmetry parameter, this splitting is proportional to the order parameter of the principal component of the electric field gradient at the deuterium site with respect to the magnetic field.[182]

$$\Delta\nu_Q = \frac{3}{2}\frac{Q_D V_{CD}}{h}\left(\frac{1}{2} < 3\,COS^2\theta^Z_{CD} - 1 >\right)$$

where Q_D is the deuterium quadrupole moment, V_{CD} is the electric field gradient along the C-D bond and θ^z_{CD} is the angle between the electric field gradient and the external magnetic field. The < > brackts denotes the average value over the anisotropic molecular reorientations. If there is a difference in the molecular ordering between the *R* and *S* enantiomers four lines should be observed in a singly labeled molecule (Figure 32a).

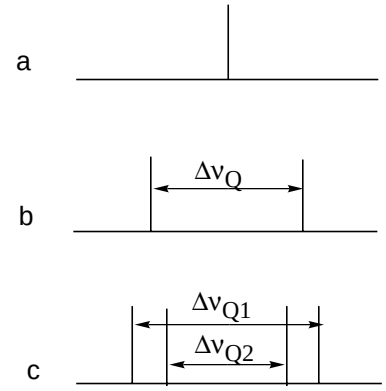

(a) Isotropic solvent
(b) Nonchiral nematic solvent
(c) Chiral nematic or cholesteric solvent where the *R* and *S* order parameters are different

Figure 32a. Schematic Proton Decoupled ^{2}H NMR Spectra of a Monodeuterated Racemic Molecule Dissolved in Various Solvents

The polypeptide chains exist in a helical conformation similar to that found with biopolymers such as DNA or polysaccharides. The side chains, which branch from the main helix, form a secondary molecular helical structure. The pitch of the rigid backbone is that of the α helical conformation, while the pitch of the secondary helix varies in a complex manner as a function of the solvent and the temperature.[183]

In isotropic solutions the anisotropy of the electronic shielding (chemical shift anisotropy), the dipolar and the quadrupolar interactions, of the different nuclei in the molecule, average to zero due to rapid isotropic molecular tumbling. Consequently the shifts or the splittings which arise in the NMR spectra due to these interactions cannot be observed.[183-184] On the other hand, solute molecules embedded in any liquid-crystalline system are partly ordered and consequently their NMR spectra exhibit all anisotropic interactions,[183] i.e., the anisotropy of the chemical shifts, the dipolar couplings and quadrupolar splittings for spins larger than 1/2. This behavor is based on the fact that the *R* and *S* enantiomers orient differently when dissolved in the PBLG/organic solvent liquid crystals, which implies that the chemical shift anisotropies, the dipolar interactions, or the quadrupolar interactions are different for each of them. The changes in orientation between the *R* and *S* enantiomers reflect the variance in their interactions with the chiral polymer.

3.3.2. The synthesis of stereoselectively monodeuterated MPTP analogs

A. Synthesis and attachment of the chiral oxazoline auxiliary

As previously reported,[154] the chiral auxiliaries utilized in these sequences have been almost always derived from amino acids which are reduced with various hydride agents to the amino alcohols. For example, the *R*-valine (**349**) can be reduced by lithium aluminium hydride (Scheme 72) in THF to give *R*-valinol (**350**) in good yield. This amino alcohol can be cyclized with diethyl carbonate to give the *R*-oxazolone **351**. The O-alkylation of this oxazolone with Meerwein's reagent affords the ethoxyoxazoline **352**. In our hands, condensation of *R*-**352** with 4-phenyl-1,2,3,6-tetrahydropyridine **353** afforded (*R*)-1-[4,5-dihydro-4-(1-methylethyl)-2-oxazolyl]-4-phenyl-1,2,3,6-tetrahydropyridine [(*R*)-**354**].

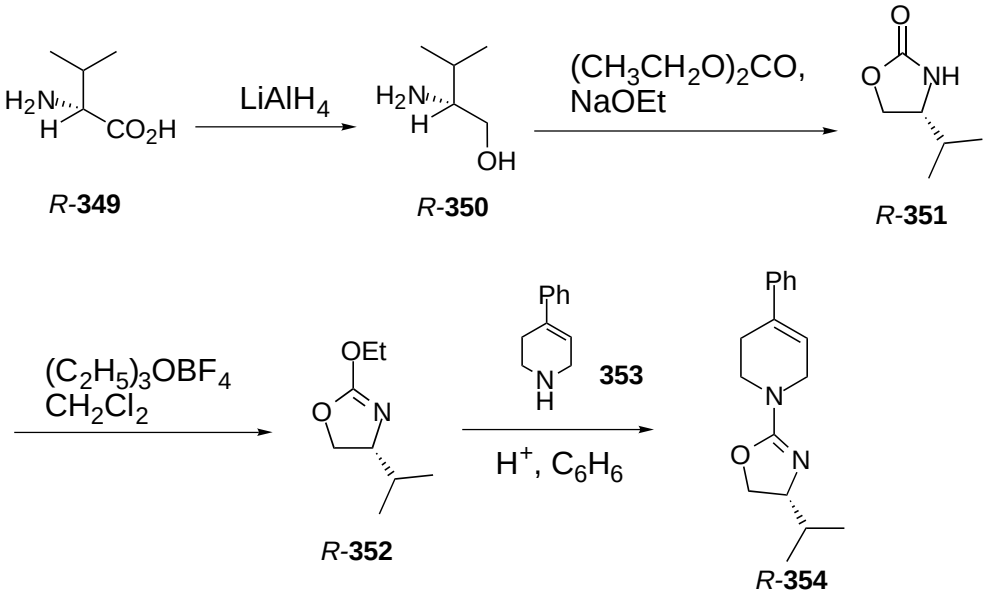

Scheme 72. The Synthesis and Attachment of the Chiral Auxiliary

The structure of (*R*)-**354** was determined by NMR and MS spectral analysis. The ^{1}H NMR spectrum (Figure 33) indicates that the proton signals of the benzene ring appear at δ = 7.25 to 7.30. These are followed by the C-5 olefinic proton at δ = 6.0. Because of the existence of a chiral center at C-4', the two methylene protons at C-5' in the oxazolyl ring and the two methyl groups in the isopropyl group are therefore diastereotopic,

consequently they both give separate resonances. Due to the coupling with 4'-H, we find the signals of 5'-H as two triplets centered at δ = 4.3 and δ = 4.0, respectively. Due to the coupling with 1'-H, we find the signals of 2"-H as two doublet at δ = 0.85 to 0.97 region. The signal of C-6 proton is observed at δ = 4.0 with twice the intensity of C-5 proton. The signal at δ = 3.8 in the spectrum orignated from the proton at the chiral center of C-4'. The multiplet at δ = 3.6 in the spectrum is assigned to the two C-2 protons. The signal of C-3 protons is found at δ = 2.5 and that of C-1" proton at δ = 1.7.

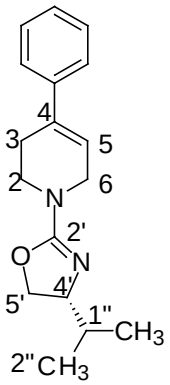

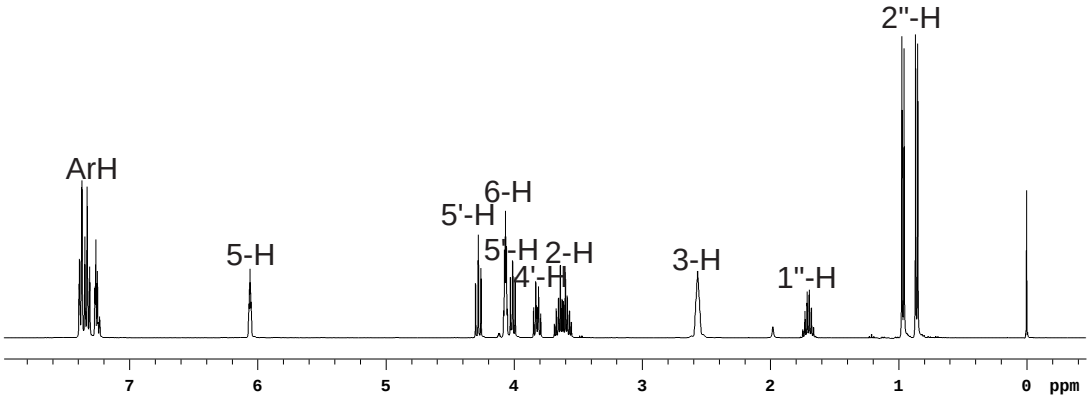

Figure 33. The ^{1}H NMR spectrum of (*R*)-1-[4,5-dihydro-4-(1-methylethyl)-2-oxazolyl]-4-phenyl-1,2,3,6-tetrahydropyridine [(*R*)-**354**] (in $CDCl_3$)

In the ^{13}C NMR spectrum (Figure 34), we find 15 singlets. The total carbon atom number in this molecule is 17. Among them, the 2, 6 and 3,5 carbon atoms in benzene are symmetrical. There are seven low field singlets, which correspond to the signals of the phenyl carbons and olefinic carbons (C-4, C-5, C-2'). The eight singlets at high field correspond to the alkyl carbons (C-2, C-3, C-6, C-4', C-5', C-1", C-2") in the molecule.

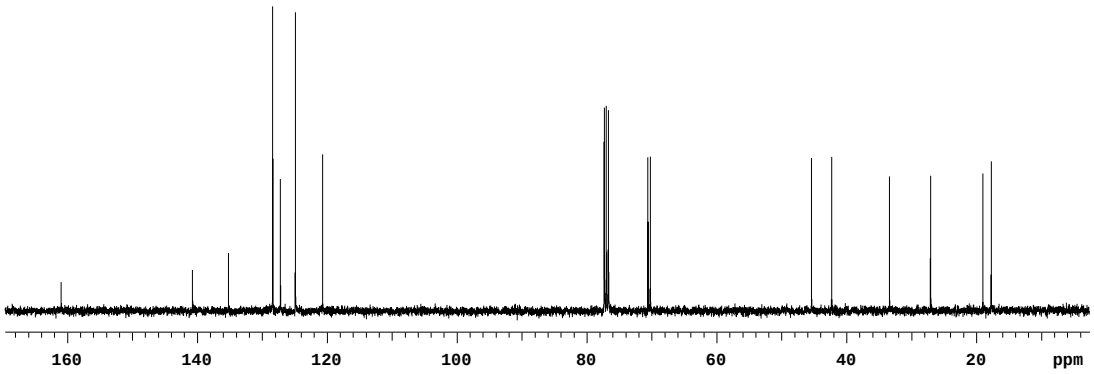

Figure 34. The ^{13}C NMR of (*R*)-1-[4,5-dihydro-4-(1-methylethyl)-2-oxazolyl]-4-phenyl-1,2,3,6-tetrahydropyridine [(*R*)-**354**] (in $CDCl_3$)

The above assignments are supported by the two-dimensional heteronuclear (H, C)-correlated NMR spectrum (Figure 35). The ^{13}C NMR spectrum obtained by projecting the peaks onto the F_2-axis is shown at the left-hand edge. We see here the 12 peaks belonging to all the carbon nuclei that have directly-bonded protons. Three tertiary carbons (C-4, C-2', C_1-phenyl) do not give correlation peaks. The normal one-dimensional 400 MHz ^1H NMR spectrum is shown at the top edge. The 2D spectrum contains peaks with the coordinates 6.0/121, 4.0/45, 3.8/70, 3.6/42, 2.5/42, 2.5/27, 1.6/33, which are consistent with a correlation between C-5 and 5-H, C-6 and 6-H, C-4' and 4'-H, C-2 and 2-H, C-3

and 3-H, C-1" and 1"-H, respectively. The peaks with the coordinates 4.3/70, 4.0/70 are consistent with a correlation between C-5' and 5'-H. The peaks with the coordinates 0.85/18, and 0.96/19 are consistent with a correlation between the protons and the carbons of the two methyl groups.

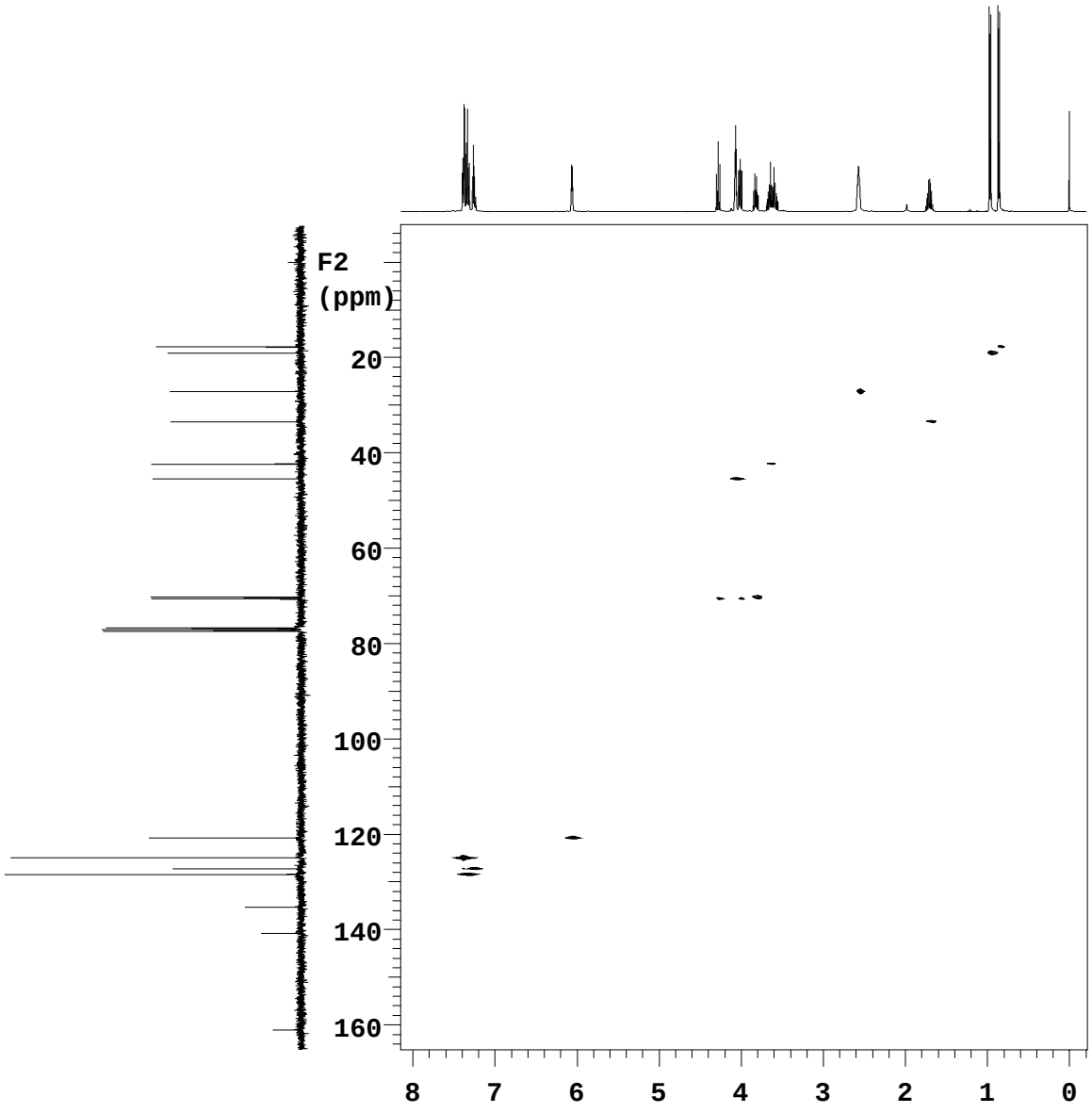

Figure 35. The two-dimensional heteronuclear (H, C)-correlated NMR spectrum of (*R*)-1-[4,5-dihydro-4-(1-methylethyl)-2-oxazolyl]-4-phenyl-1,2,3,6-tetrahydropyridine [(*R*)-**354**] (in $CDCl_3$)

EI-MS spectrum (Figure 36) indicates several important fragment ions. The parent peak $M^{\bullet+}$ is at 270. The ion at m/z = 227 corresponds to the fragment ion in which the molecule loses a propyl group [M-43] (Scheme 73). Also observed is the fragment ion at m/z = 158, which corresponds to the loss of N-substituent. [97] ion accounts for the base peak.

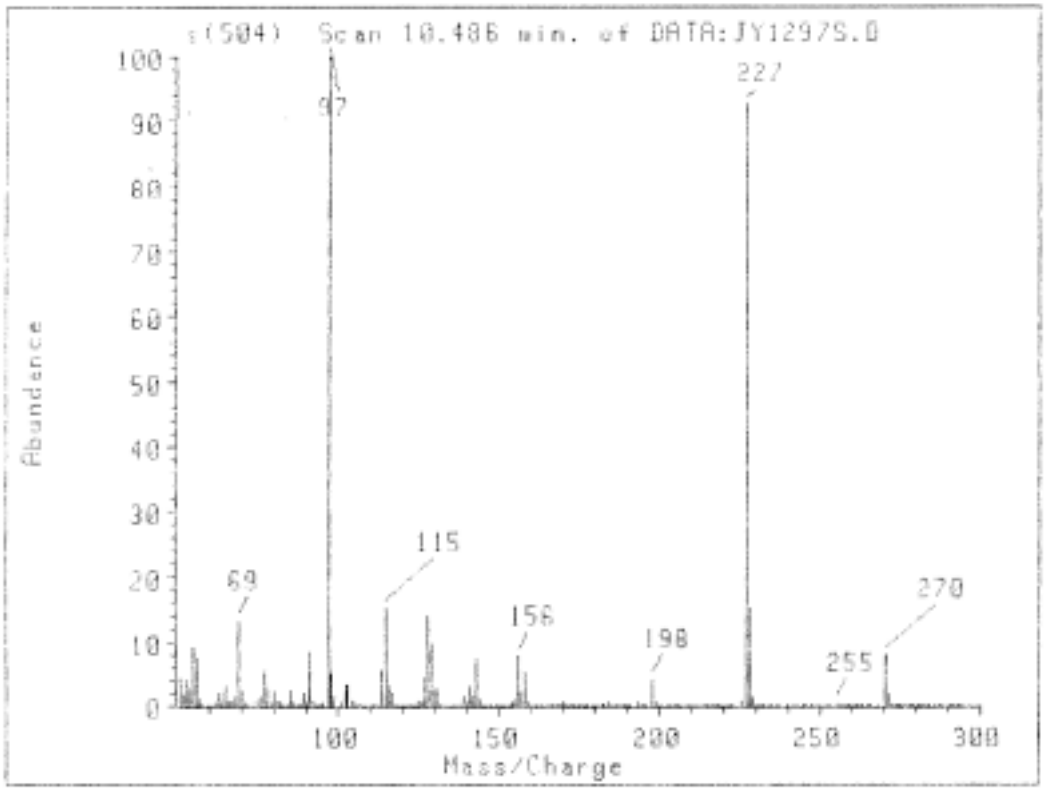

Figure 36. The MS spectrum of (*R*)-1-[4,5-dihydro-4-(1-methylethyl)-2-oxazolyl]-4-phenyl-1,2,3,6-tetrahydropyridine [(*R*)-**354**]

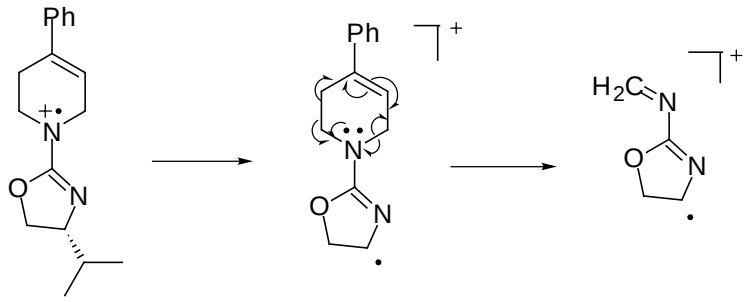

R-**354** **355** **356**

m/z = 270 m/z = 227 m/z = 97

Scheme 73. The Fragmentation of Compound **354**

B. Lithiation and deuterium incorporation

1. Quenching reaction with DMSO-d_6

The oxazoline (*S*)-**354** was lithiated with n-butyllithium at -78 °C in THF (Scheme 74). 20 min later, the reaction was quenched with DMSO-d_6 at -78 °C for 20 min and then the temperature was allowed to increase to room temperature. However, TLC indicated two close spots which could not be seperated well by column chromatography. NMR data indicated that the major product (> 98%) was the diasteromeric mixture of 1-[4,5-dihydro-4-(1-methylethyl)-2-oxazolyl]-4-phenyl-1,2,3,4-tetrahydropyridine-4-d_1 (**357**) with deuterium substituted at the 4-position of the tetrahydropyridinyl ring, and the double bond rearranged.

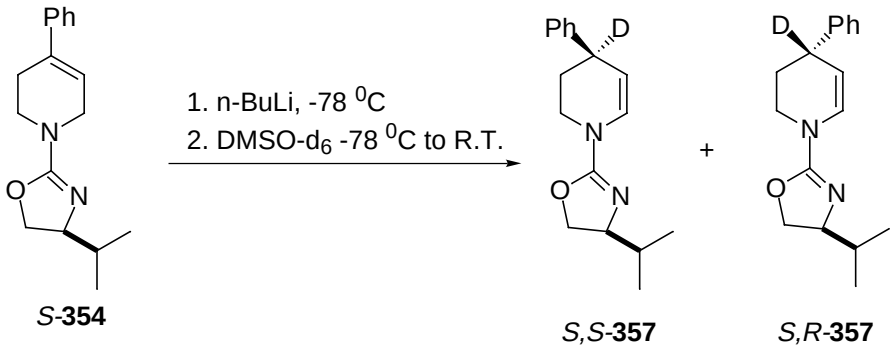

S-**354** *S,S*-**357** *S,R*-**357**

Scheme 74. The Lithiation and Quenching with DMSO-d_6

The structure of **357** was determined by the NMR and MS spectral analysis. The ^{1}H NMR spectrum (Figure 38) indicates that the three signals at δ = 6.0 (1H, C-5), 4.0 (2H, C-6), and 2.6 (2H, C-3) presenting the spectrum of **354** (Figure 33) have disappeared. There are four new signals at δ = 6.8, 4.8, 2.1, and 1.8 in the ^{1}H NMR spectrum of **357**, each integrating for one proton. This indicates structure changes in the tetrahydropyridinyl ring system.

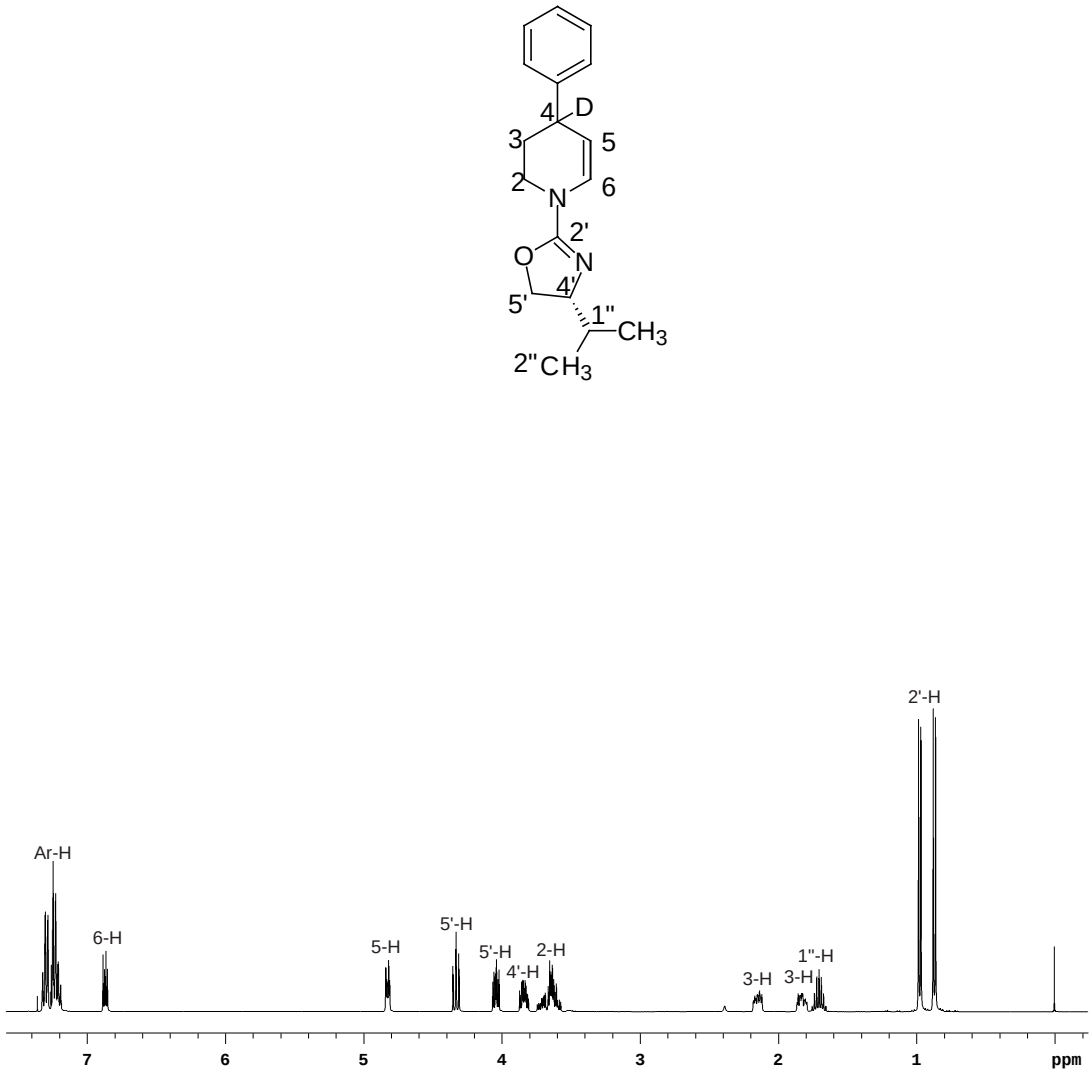

Figure 37. ^{1}H NMR spcctrum of 1-[4,5-dihydro-4-(1-methylethyl)-2-oxazolyl]-4-phenyl-1,2,3,4-tetrahydropyridine-4-d_1 (**357)** (in $CDCl_3$)

In the ^{13}C NMR spectrum of **357** (Figure 38), again we find 15 signals. But this time some of the peaks are doublets, indicating the compound is a mixture. Seven peaks (phenyl and olefinic carbon) are at low field. Eight peaks (alkyl carbons) are at high field.

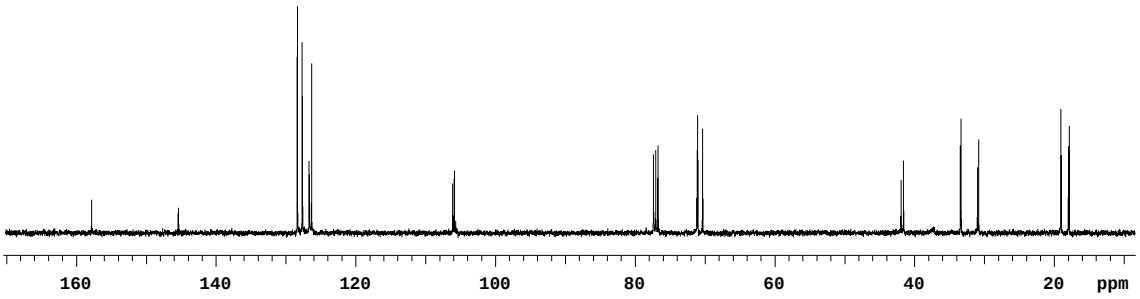

Figure 38. The ^{13}C NMR spectrum of 1-[4,5-dihydro-4-(1-methylethyl)-2-oxazolyl]-4-phenyl-1,2,3,4-tetrahydropyridine-4-d_1 (**357**) (in $CDCl_3$)

With the two-dimensional heteronuclear (H, C)-correlated NMR spectrum of **357** (Figure 39), the ^1H and ^{13}C spectra can be assigned on the basis of chemical shifts and multiplicities. This spectrum contains a peak with the coordinate 4.8/105, which is consistent with the correlation between a proton and an olefinic carbon. Although we can not determine which carbon with the signal at $\delta = 126$ is correlated with the proton with a δ of 6.8 because of overlaping, the 2D spectrum clearly indicates that this carbon signal is at low field which means it is an olefinic carbon. In this case, there are two protons which are connected with sp^2 carbons. The peaks with the coordinates of 2.1/30, 1.8/30 are consistent with a correlation between the two protons and the same carbon atoms, which means there is a methylene group. The splitting of the signal of the methylene protons in the ^1H NMR spectrum indicates these methylene protons are diastereotopic, which means this carbon is connected to a chiral center. The two-dimensional homonuclear (H, H)-correlated NMR spectrum (Figure 40) clearly indicates coupling between the proton with a signal at $\delta = 6.8$ and that with a signal at $\delta = 4.8$. It also indicates coupling between the proton with a signal at $\delta = 2.1$ and that with a signal at $\delta = 3.6$. In summary, these data indicates that there are two olefinic protons and a chiral center in the tetrahydropyridinyl ring. All of these data support the structure of **357**. The diastereomeric ratio of this product could not be determined by ^1H NMR.

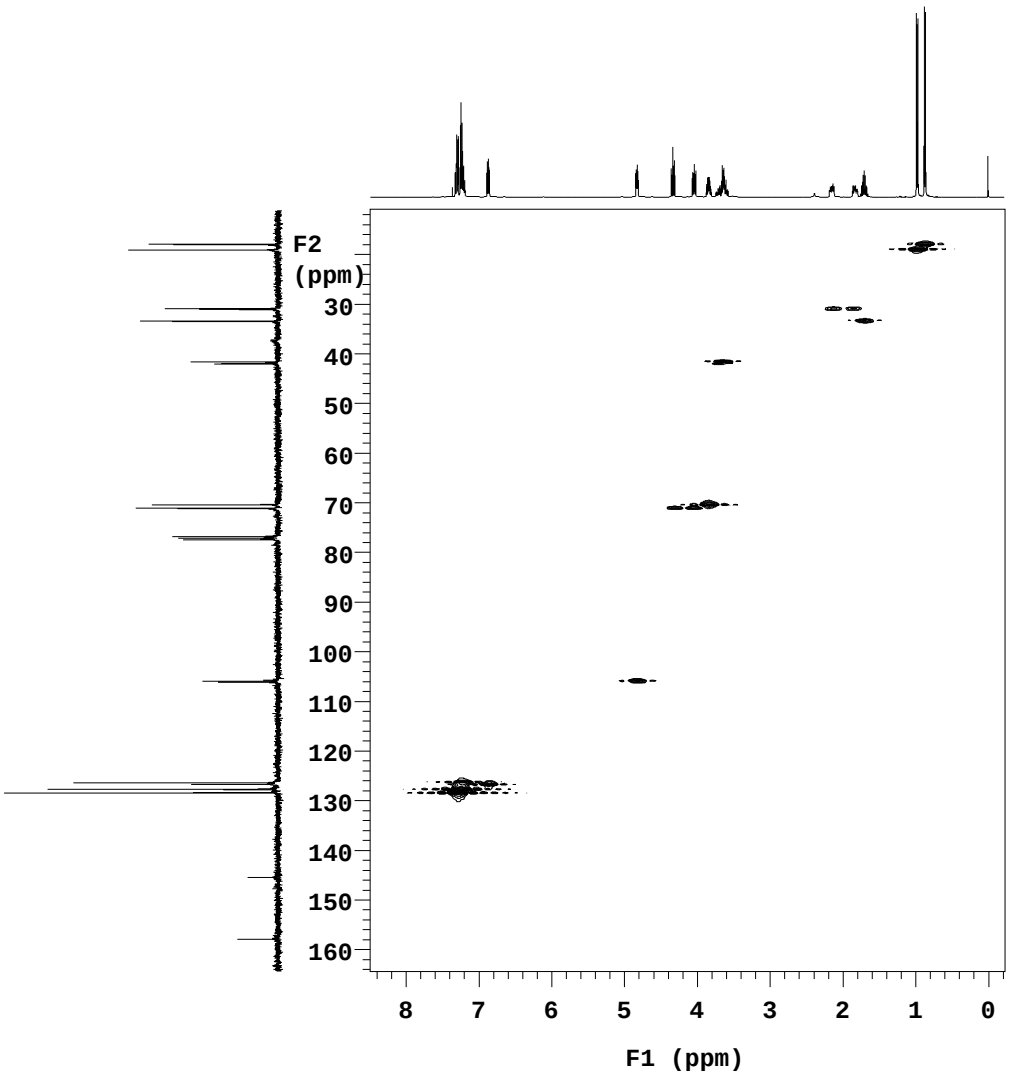

Figure 39. The two-dimensional heteronuclear (H, C)-correlated NMR spectrum of 1-[4,5-dihydro-4-(1-methylethyl)-2-oxazolyl]-4-phenyl-1,2,3,4-tetrahydropyridine-4-d_1 (**357**) (in $CDCl_3$)

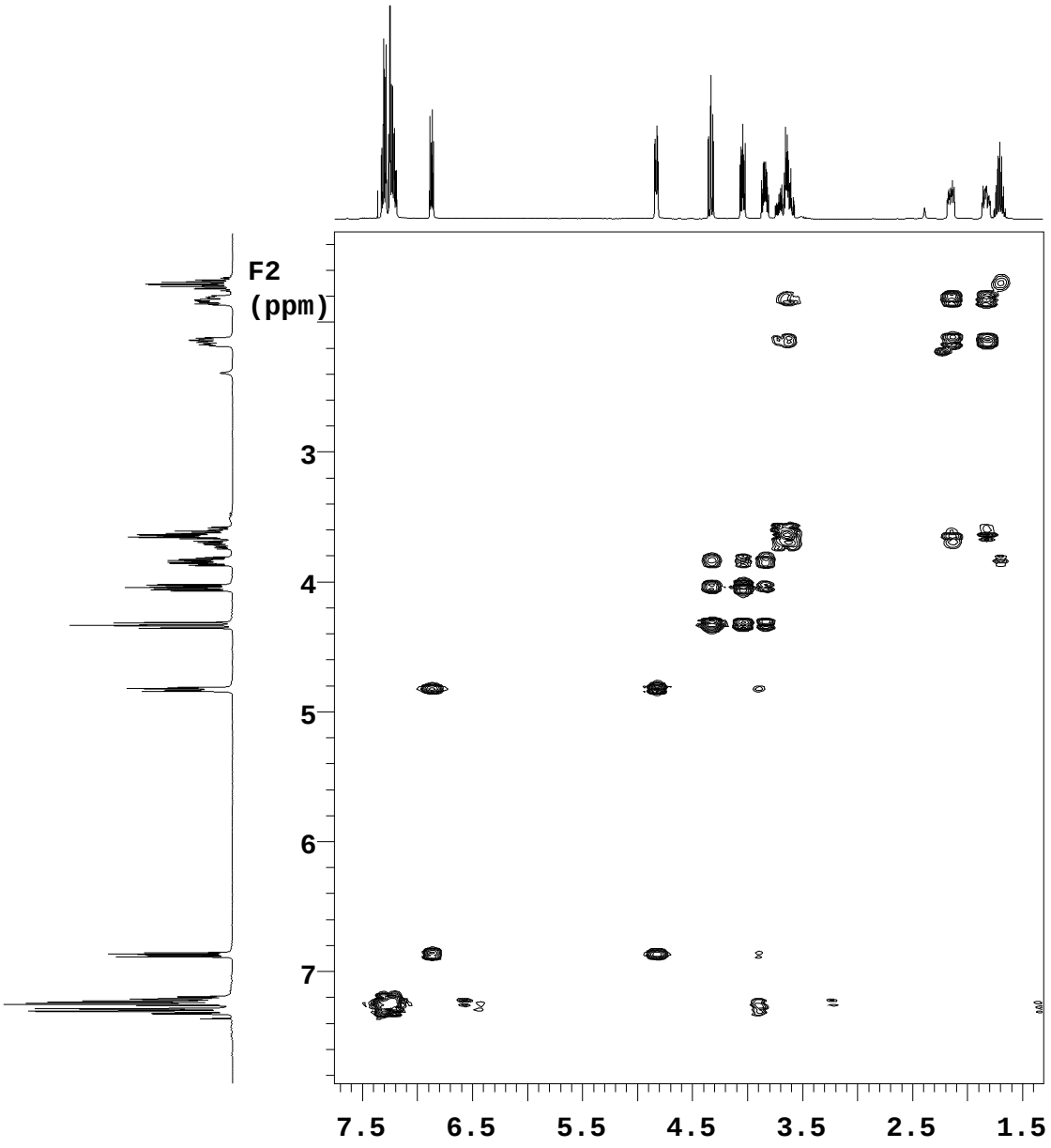

Figure 40. The two-dimensional homonuclear (H, H)-correlated NMR spectrum of 1-[4,5-dihydro-4-(1-methylethyl)-2-oxazolyl]-4-phenyl-1,2,3,4-tetrahydropyridine-4-d_1 (**357**) (in $CDCl_3$)

The EI-MS spectrum of **357** (Figure 41) shows the parent peak $M^{\bullet+}$ at m/z = 271 and a peak at m/z = 228, indicating the incorporation of one deuterium. The fragment ion

involving loss of a propyl group [M-43] (m/z = 228) accounts for the base peak. The absence of a peak at m/z = 227 is good evidence that the deuterium incorporation is 100%. The loss of the N-substitutent is also observed, leading to an ion at m/z = 159 ion. The peak at m/z = 97 found in the spectrum of **354** has disappeared.

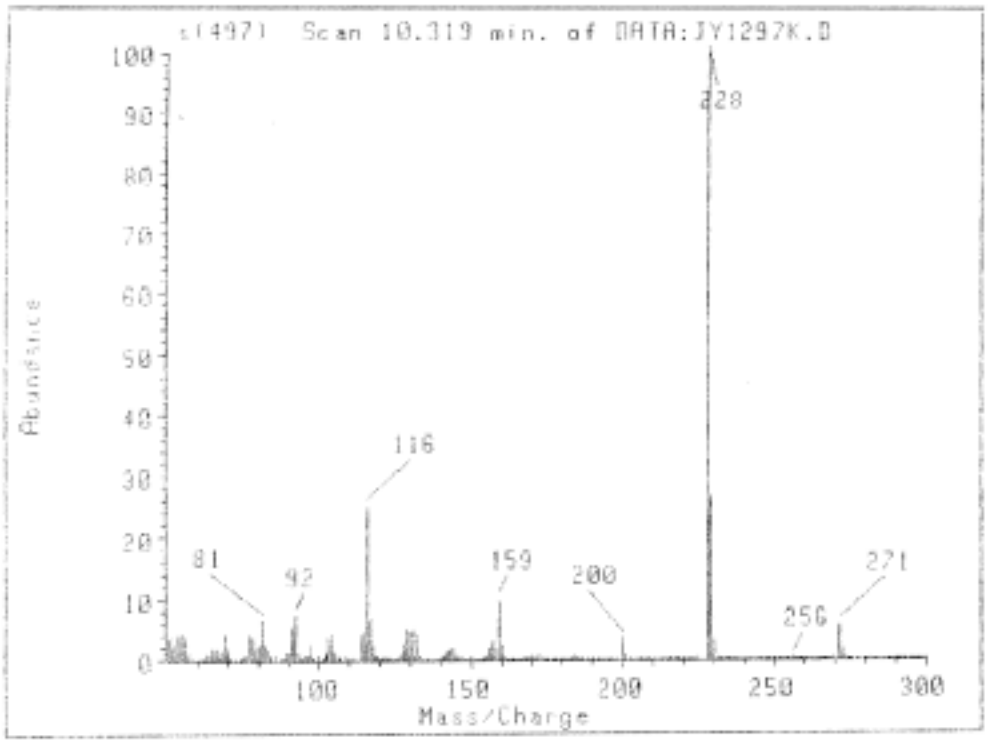

Figure 41. The MS spectrum of 1-[4,5-dihydro-4-(1-methylethyl)-2-oxazolyl]-4-phenyl-1,2,3,4-tetrahydropyridine-4-d_1 (**357**)

A similar result of this kind of double bond rearrangement was also observed by Gawley in the alkylation of the lithiated (3,4-dehydropiperidino)oxazoline (**358**) (Scheme 75).[176] In this case, about 40% of the product was found to be the 4-substituted piperidine **359**. HPLC analysis showed that the 2-substituted compound, **360**, was a single diastereomer.

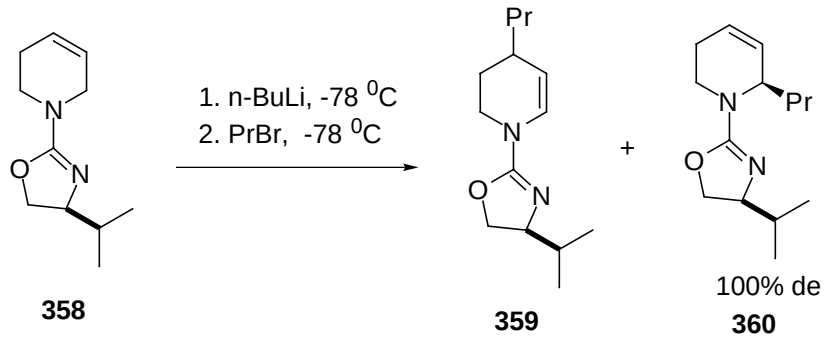

Scheme 75. The Alkylation of the (3,4-Dehydropiperidino)oxazoline

Many experiments, such as spectroscopic,[186-187] X-ray crystallographic[188] and computational studies[189-190] on the allylic lithium compounds support the delocalized structures (Figure 42). It is believed that this kind of compound undergoes a fast 1,3 lithium shift and form the contact ion pairs containing delocalized carbanions. It is this kind of character that leads to the double bond rearrangement and influences the stereochemistry of the reactions.[191]

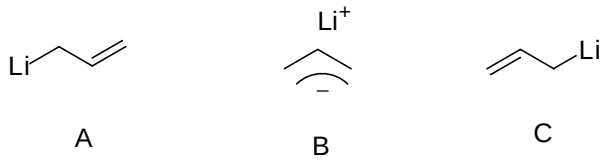

Figure 42. The 1,3 lithium Shift of the Allylic Lithium Compounds

In our case, because of this 1,3 lithium shift, the α-carbanion **361** would be expected to lose the sp3 geometry at C-6 and form the γ-carbanion **362** (Scheme 76). Because the charge in **362** can be delocalized efficiently by the phenyl ring, it is more stable and therefore **362** may be the dominant species under certain conditions. This leads to the incorporation of deuterium at 4-position.

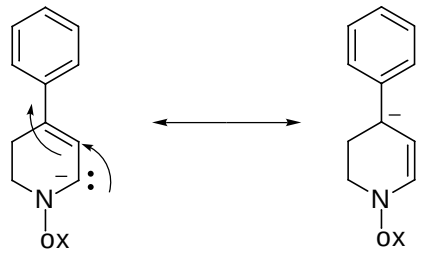

361 **362**

Scheme 76. The Structures of the α-Carbanion and γ-Carbanion

Temperature has big influence on this kind of rearrangement. When the reaction was quenched first with DMSO-d_6 at -78 °C and then mixed with water without increasing the temperature to room temperature, the amount of the double bond rearranged compound is small (about 30%, see below). However, MS spectra showed the existence of the ion at m/z = 227 and m/z = 97 fragment ions, indicating the incomplete incorporation of the deuterium (see below).

2. Quenching reaction with D_2O

According to previous reports, quenching of lithiated formamidines or oxazolines with CH_3OD or D_2O produces a mixture of deuterated diastereomers whereas quenching with DMSO-d_6 is usually highly stereoselective.[171,175] Our experiment has indicated that DMSO-d_6 is not a good choice. DMSO-d_6 is a very weak acid, the donation of a deuterium to the lithiated species must be carried out at higher temperature. However, at high temperature the double bond rearrangement becomes controlling. In order to accomplish the deuterium incorporation at the C-6 position at low temperature, we chose more acidic deuterium sources, such as D_2O. The oxazoline **354** was lithiated and quenched with D_2O under similar conditions (Scheme 77), and the product was seperated through a column. About 32% of the product was characterized as the diastereomeric mixture **357**. About 60% of the product was characterized as 1-[4,5-dihydro-4-(1-methylethyl)-2-oxazolyl]-4-phenyl-1,2,3,6-tetrahydropyridine-6-d_1 (**363**).

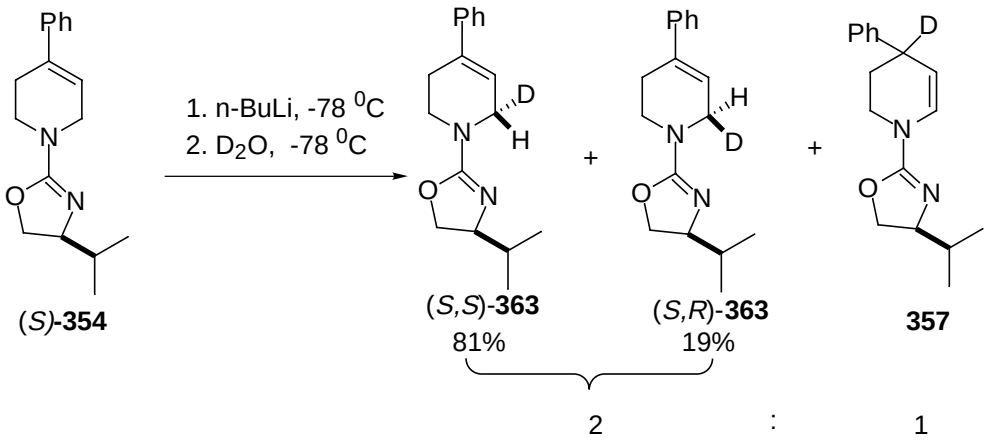

Scheme 77. The Lithiation and Quenching with D_2O

The structure of **363** was determined by NMR and MS spectral analysis. The ^1H NMR spectrum of **363** (Figure 43) is similar to that of the **354** (Figure 33) with the exception that the intensity of the signal at $\delta = 4.0$ has decreased. This indicates the incorporation of deuterium at the C-6 position. ^{13}C NMR (Figure 44) is the same as that of **354** (Figure 34).

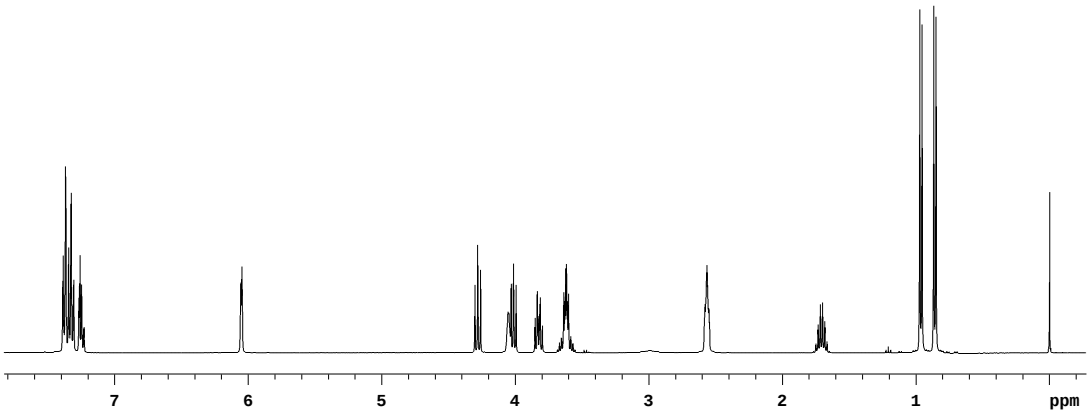

Figure 43. The ^{1}H NMR spectrum of 1-[4,5-dihydro-4-(1-methylethyl)-2-oxazolyl]-4-phenyl-1,2,3,6-tetrahydropyridine-6-d_1 (**363**) ($CDCl_3$)

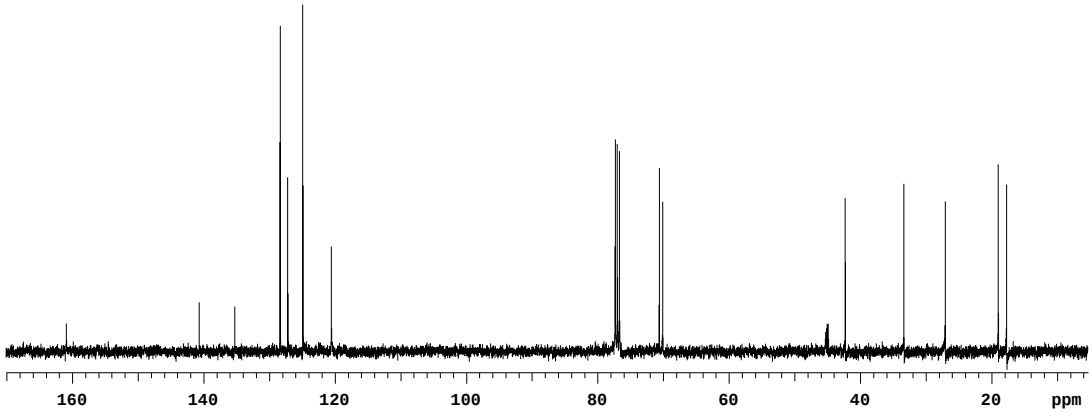

Figure 44. The ^{13}C NMR spectrum of 1-[4,5-dihydro-4-(1-methylethyl)-2-oxazolyl]-4-phenyl-1,2,3,6-tetrahydropyridine-6-d_1 (**363**) ($CDCl_3$)

The EI-MS spectrum (Figure 45) shows the same pattern as that of the **354**. The parent peak $M^{+\bullet}$ at m/z = 271 and the peak at m/z = 228, indicats the incorporation of one deuterium. The fragment ion in which the molecule loses a propyl group [M-43] (m/z = 228) accounts for the base peak. The absence of an ion at m/z = 227 ion is good evidence that the deuterium incorporation is 100%. The loss of N-substituent is also observed, leading to a m/z=159 ion. The ion at m/z = 97 ion is significant.

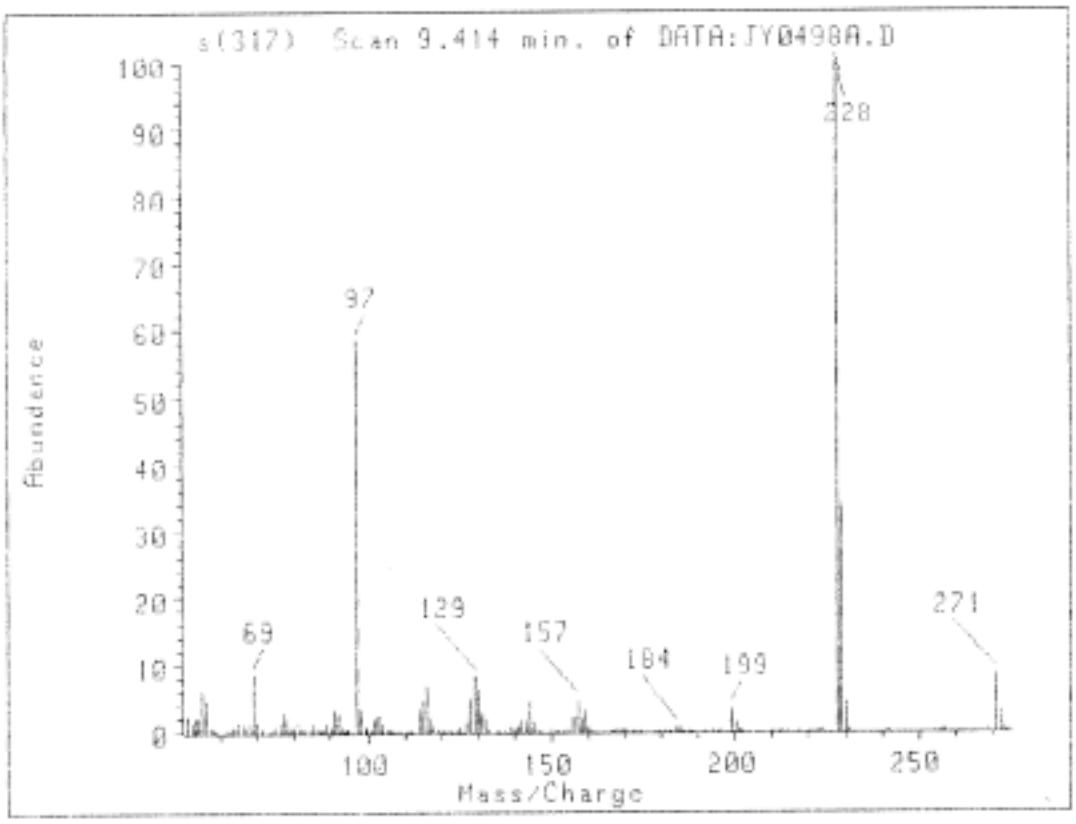

Figure 45. The MS spectrum of 1-[4,5-dihydro-4-(1-methylethyl)-2-oxazolyl]-4-phenyl-1,2,3,6-tetrahydropyridine-6-d_1 (**363**)

The compounds (*S*,*S*)-**363** and (*S*,*R*)-**363** are diastereomers. Theoretically, the signal differences can be detected by ^{1}H NMR or ^{2}H NMR. Unfortunately, in our case, the important signal of 6-proton is partially overlaped with the signal of 5'-proton (Figure 43) and because of the coupling with 5-proton, the signal of the C-6 proton becomes broadened. The broad-band proton decoupling ^{2}H NMR spectrum of the compound **363** (Figure 46) indicates only one unsplit peak.

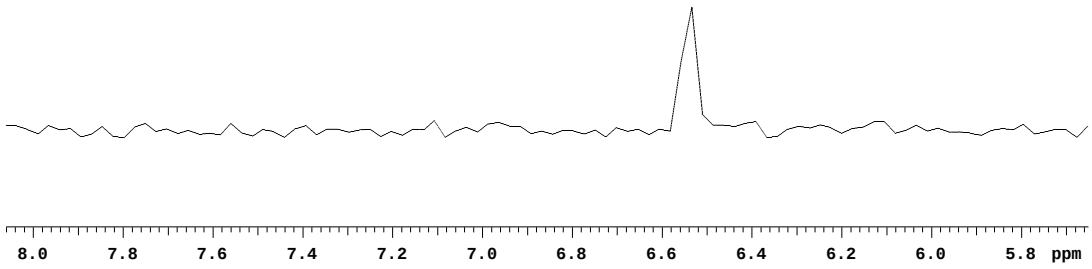

Figure 46. The broad-band proton decoupling ^{2}H NMR spectrum of 1-[4,5-dihydro-4-(1-methylethyl)-2-oxazolyl]-4-phenyl-1,2,3,6-tetrahydropyridine-6-d_1 (**363**) (in CH_2Cl_2)

Finally we employed the technique of deuterium NMR in PBLG liquid crystal system. The liquid crystal ^{2}H NMR spectrum indicates that compound **363** is a mixture of diastereomers (Figure 46, a). Starting from (*S*)-**354**, the ^{2}H NMR spectrum of the product exhibits four peaks with the major peak at the inner side (Figure 47,a). If the (*R*)-**354** is used as starting material, under the same conditions, the major peak appears outside (Figure 47, b). Integration indicates that the ratio of each of the two diastereomers is about 81:19. This result suggests that the reaction under this condition does exhibit stereoselectivity.

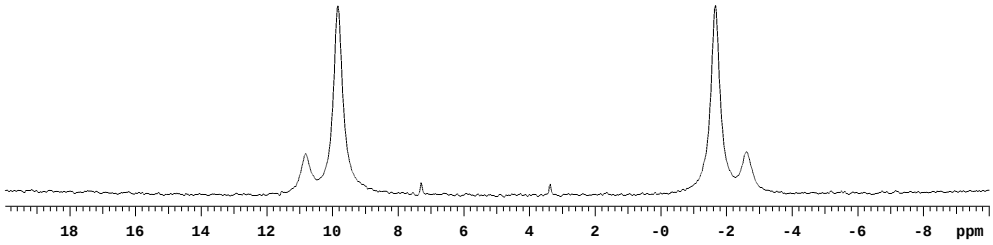

(a) (*S*,*S*)-**363** and (*S*,*R*)-**363** (81:19)

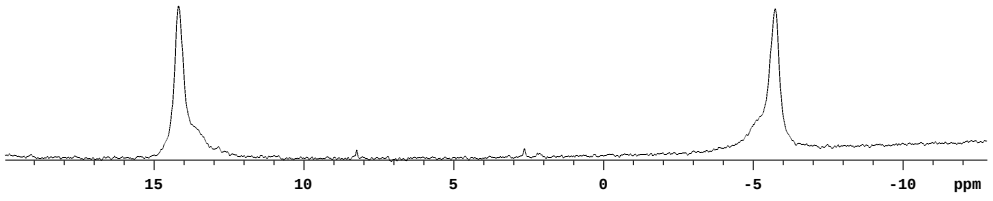

(b) (*R*,*R*)-**363** and (*R*,*S*)-**363** (80:20)

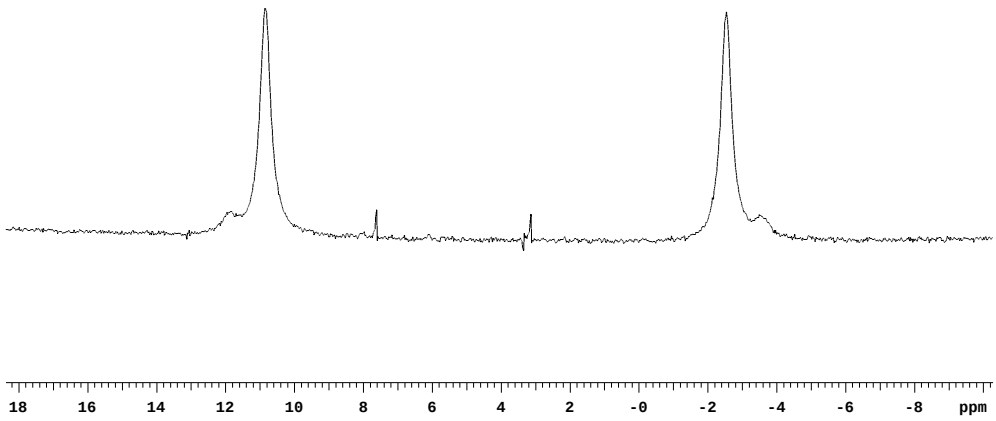

(c) (*S*,*S*)- and (*S*,*R*)-**363** (89:11)

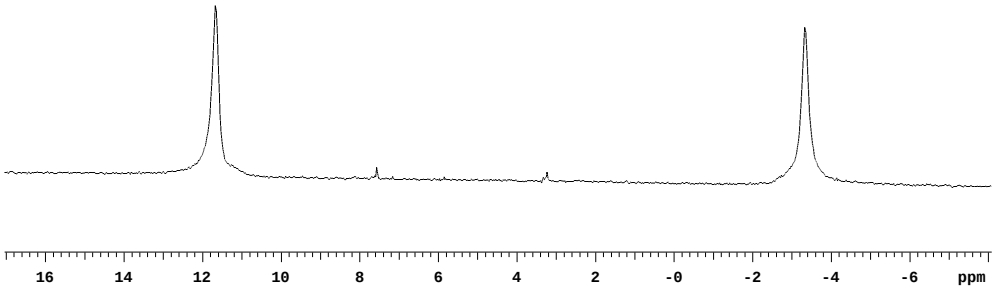

(d) (*R*,*R*)- and (*R*,*S*)-**363**

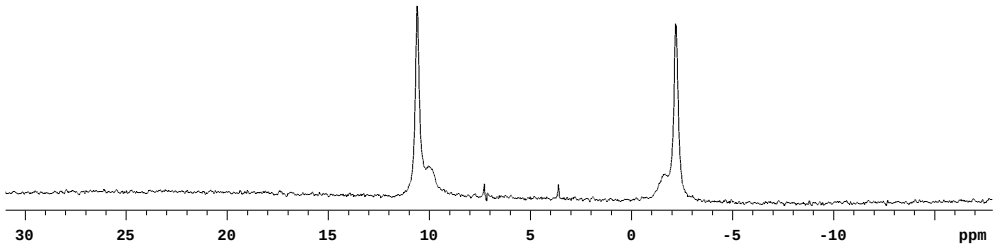

(e) (*R*,*R*)- and (*R*, *S*)-**363** (85:15)

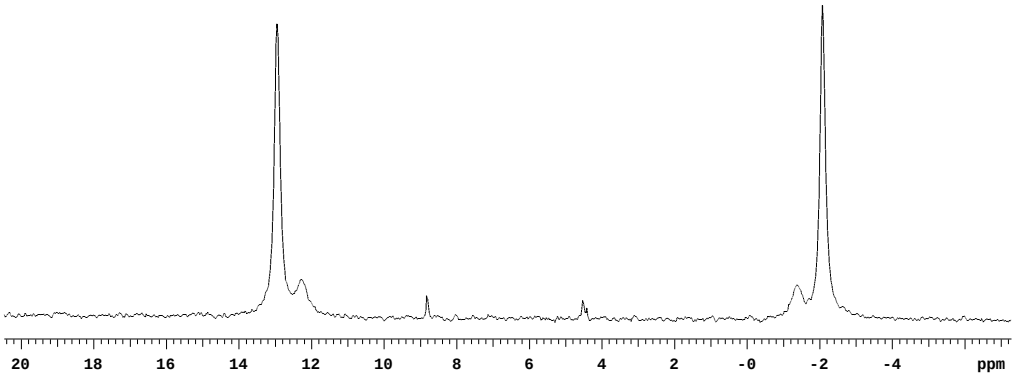

(f) (*R*, *R*)- and (*R*, *S*)-**363** (85:15)

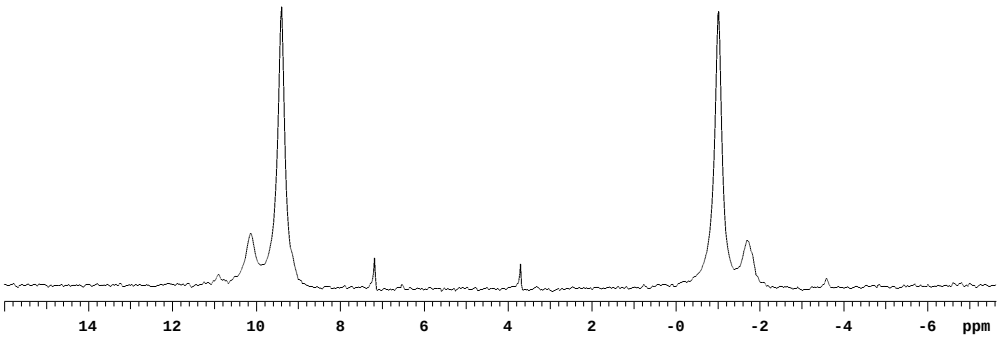

(g) (*S*,*S*)- and (*S*,*R*)-**363** (85:15)

Figure 47. The ^{2}H NMR spectrum of **363** (in PBLG/CH_2Cl_2)

It is believed that the isotope effect for removal of the C-6 proton is high. If the deprotonation is rate determining, when a portion of butyllithium is added to the above 2-substituted diastereomeric mixture **363**, the reactivity of the α proton or deuteron will be different. From the aspect of deprotonation, because of the existence of the chiral auxiliary, D_α in (*S*,*S*)-**363** or H_α in (*S*,*R*)-**363** will be removed preferentially. From the aspect of isotope effect, proton other than deuteron should be attacked by the base preferentially. If these two factors are combined, it is obvious that the H_α in (*S*,*R*)-**363** would be prefered to be removed in the reaction. Therefore, if we start with the diastereomeric mixture of (*S*,*S*)- and (*S*,*R*)-**363** (81:19), the expected result is that, when 0.2 equivalent of butyllithium is added, the (*S*, *R*)-**363** will be completely consumed.

We carried out this experiment. However, when up to 0.4 equivalent of butyllithium is added to the above 2-substituted diasteromeric mixture **363** and quenched with DMSO-d_6 (Scheme 78), the % de was found to be increased only to 89:11 (Figure

47,c and d), not as high as expected. This result prompted us to analyze for the double bond rearranged component in the product.

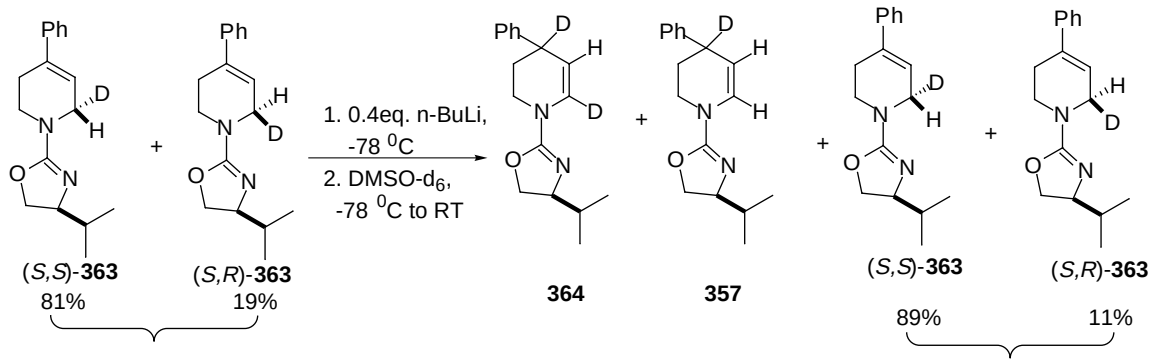

Scheme 78. Isotope Effect *vs.* Asymmetric Deprotonation

The EI-MS spectrum of the double bond rearranged componunt (Figure 48) shows the ions of m/z = 272 and m/z = 229, indicating the formation of compound **364**. The ions at m/z=228 and 271 ions indicate the formation of **357**. This is also confirmed by the ^{1}H NMR spectrum of the double bond rearranged (Figure 49) mixture which indicating the existence of C-6 proton at $\delta = 6.8$ furthermore the intensity of the 6-H signal at $\delta = 4.8$ is stronger than that of the signal at $\delta = 6.8$. It is not clear why an ion at m/z = 227 is present.

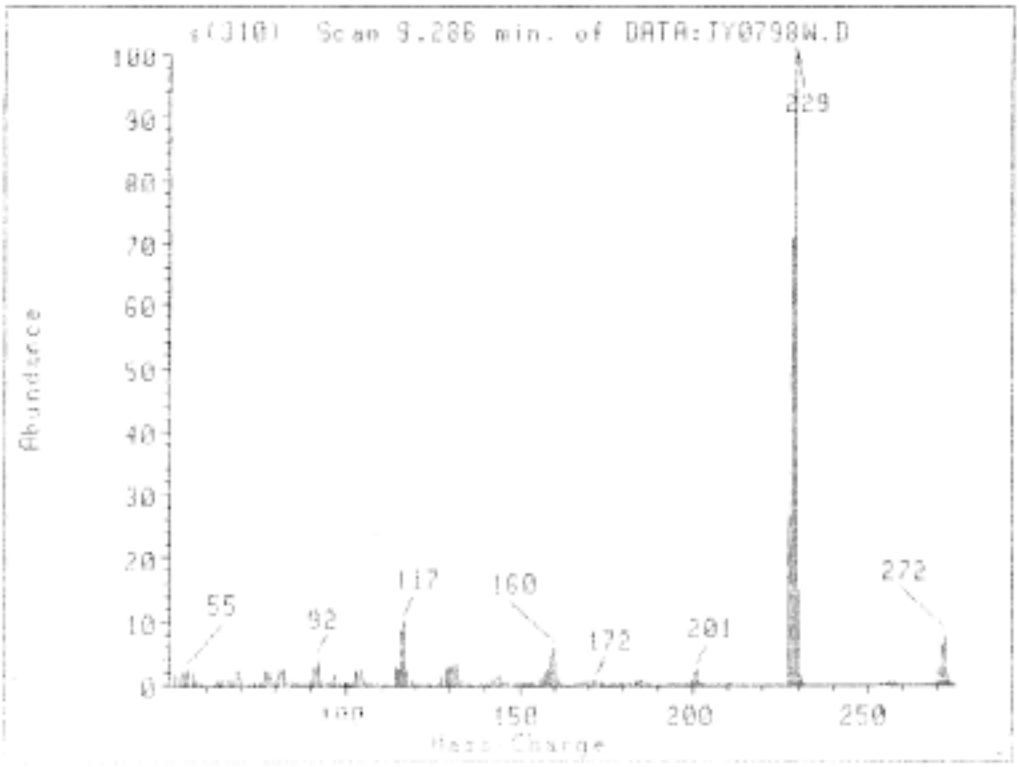

Figure 48. The MS spectrum of the double bond rearranged mixture

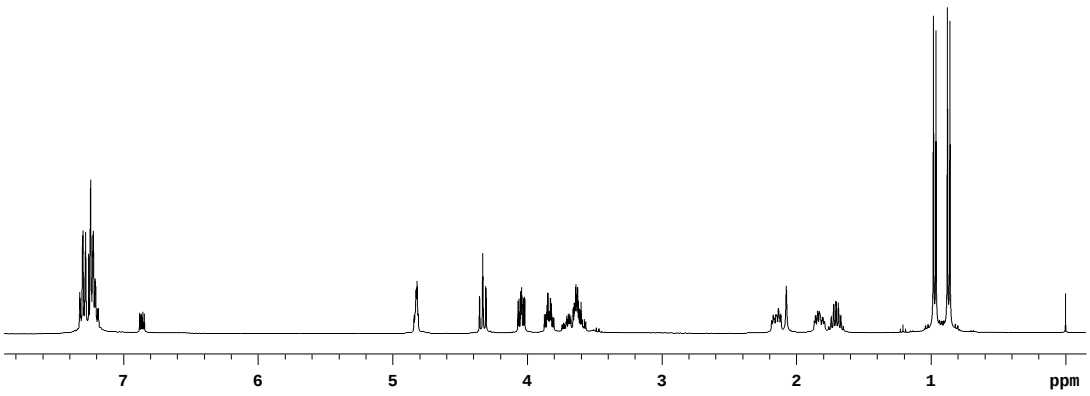

Figure 49. The ^{1}H NMR spectrum of the double bond rearranged mixture ($CDCl_3$)

The presence of **357** in the product indicates that the isotope effect may not be completely rate-determining. Since during the reaction, the deuteron was removed. It appears that the rate-determining step is in the formation of the complex prior to deprotonation [see 3.3.1. 4 (1)] and that the butyllithium consumes both (*S,S*)-**363** and (*S,R*)-**363** equally. The fact that %de ratio is not significantly increased is consistent with this argument. When 0.6 equivalent of butylithium was used in the reaction, the ratio of the product **363** is approximately 85:15 (Figure 47, e). This result again supports the assumption that the isotope effect may not be completely rate-determining. Because 0.6 equivalent of butyllithium is enough to remove all the H_α in (*S,R*)-**363** and leave the (*S,S*)-**363** as the pure component if the isotope effect is operating in the rate-determining step. The similar % de of the 2-substituted component in this case also suggests that the formation of lithium complex prior to the deprotonation is rate-determining. The formation of the lithium complex will not be affected by the substitution of protium with a deuterium.

3. Quenching reaction with CF_3COOD

The fact that quenching oxazolines with DMSO-d_6 is highly stereoselective compared with D_2O or CH_3OD in some examples[171,175] requires some explanation. The deuterium on the α carbon of DMSO-d_6 is a weak acid. During the reaction, we assumed that the DMSO may form some kind of five-membered coordination compound because the oxygen atom is a good ligand atom for lithium. Trifluroacetic acid- d_1 is a much stronger acid than D_2O and its carboxylic group also has the possibility to form a coordination compound with lithium (Figure 50). So we used trifluroacetic acid- d_1 to quench the reaction under the same conditions and found a % de ratio of 85:15 (Figure 47, f). The deuterium incoporation is complete. The double bond rearranged component **357** is about 40%. The % de ratio indicates that the formation of the complex between the deuterium source and lithium may not be important in this case. The minor part of the 2-substituted component may be caused by the 1,3 lithium shift.

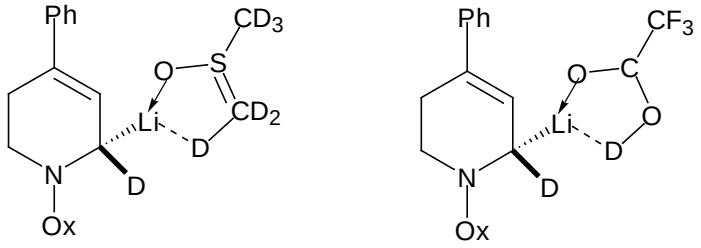

Figure 50. The Coordination of DMSO-d_6 and Trifluroacetic acid with Lithiated Intermediate

4. The use of BuLi/(-)-sparteine system

Beak *et al*. reported the effectiveness of (-)-sparteine as an external chiral ligand in asymmetric deprotonation-substitution reactions.[186] Rimoldi[132] synthesized the N-Boc-MPTP and used it to react with n-BuLi/(-)-sparteine in THF. It was found that the deuterium incorporation is high but the % de was estimated to be only about 33%.

The BuLi/(-)-sparteine method was also employed in our experiments (Scheme 79). This time we used toluene as a solvent.

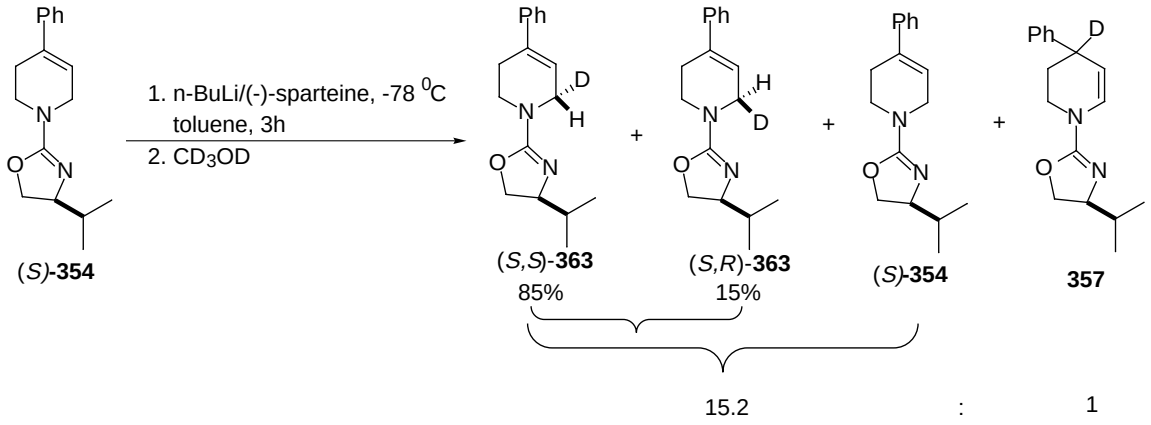

Scheme 79. Lithiation using BuLi/(-)-sparteine method

n-Butyllithium first was mixed with (-)-sparteine in toluene at -78 °C for 30 min, then transfered to the (*S*)-**354** solution in toluene at -78 °C. Three hours later, the reaction mixture was quenched with CD_3OD at -78 °C. GC and NMR analysis indicated that the amount of double bond rearranged compound **357** is only 6%. Deuterium NMR in the liquid crystal indicated the % de is 85:15 (Figure 47, g). However, MS also indicated that there exist significant amount of m/z = 227 ion which means the deuterium incorporation is not complete under these conditions. When n-BuLi was substituted by *sec*-BuLi, the deuterium incorporation is still not complete. When the above reaction was quenched by DMSO-d_6 at -78 °C first followed by increased to room temperature, the double bond rearranged compound **357** is about 40%. Still the deuterium incorporation is not complete. The fact that the % de does not change at low temperature for a long time indicated that the formation of the lithium complex is thermadynamically rather than kinetically controlled. The formation of a relatively low yield of the double bond rearranged compound in this reaction indicated that the solvent may affect the 1,3 lithium shift.

C. The detachment of the chiral auxiliary

There are several ways to detach the chiral auxiliary, such as hydrazinolysis with hydrazine or reduction with lithium aluminum hydride.[155,185] In our case, both of these two

pathways consume the starting material but they also destroy the formed 4-phenyl-1,2,3,6-tetrahydropyridine-6-d_1,(**365**) leading to a very low yield (Scheme 80).

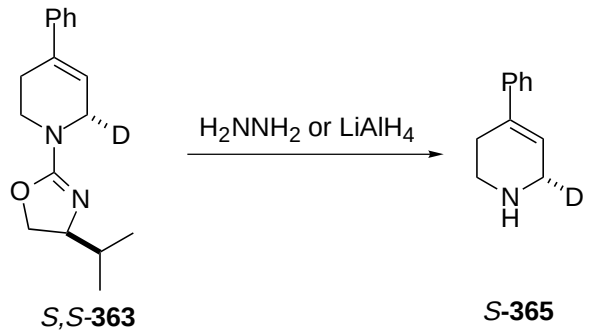

S,S-**363** *S*-**365**

Scheme 80. The Detachment of Oxazoline Auxiliary (1)

We noticed that acetic formic anhydride converts some of the oxazolines, such as **366** (Scheme 81), to a ring opened N,O-diformyl compound **367**,[155] which then can be reduced to the N-methyl compound **368** without changing the %ee.

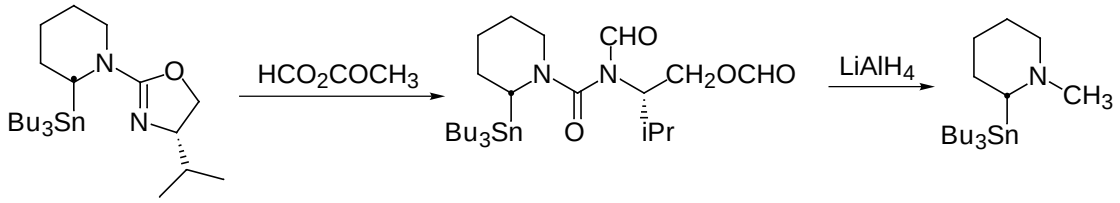

366 **367** **368**

Scheme 81. The Detachment of Oxazoline Auxiliary (2)

Starting with the 2-substituted diastereomer mixture (81:19) **363**, similar treatment with acetic formic anhydride (Scheme 82) afforded the unstable ring opened compound, which was then reduced immediately by lithium aluminium hydride to 1-methyl-4-phenyl-1,2,3,6-tetrahydropyridine-6-d_1 (**369**).

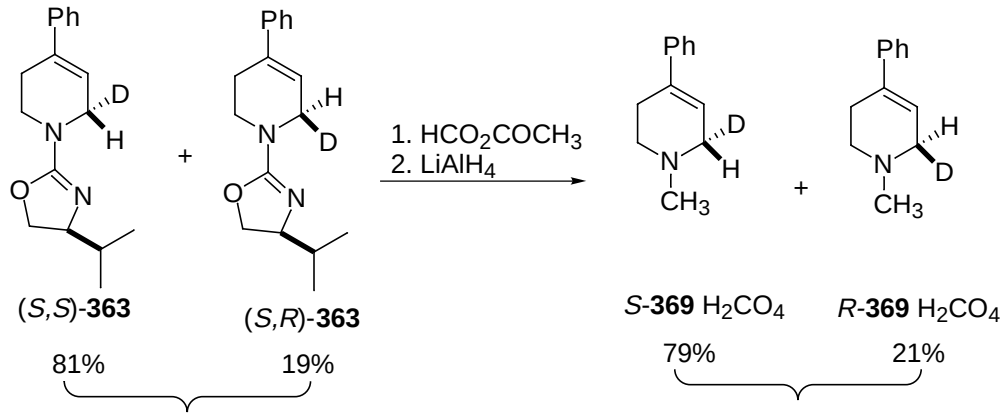

Scheme 82. The Synthesis of the Final Product

The liquid crystal ^{2}H NMR spectrum (Figure 51) indicated a similar % ee ratio (79:21) to the starting material which confirmed that there was little or no racemization in the detachment of the chiral auxiliary.

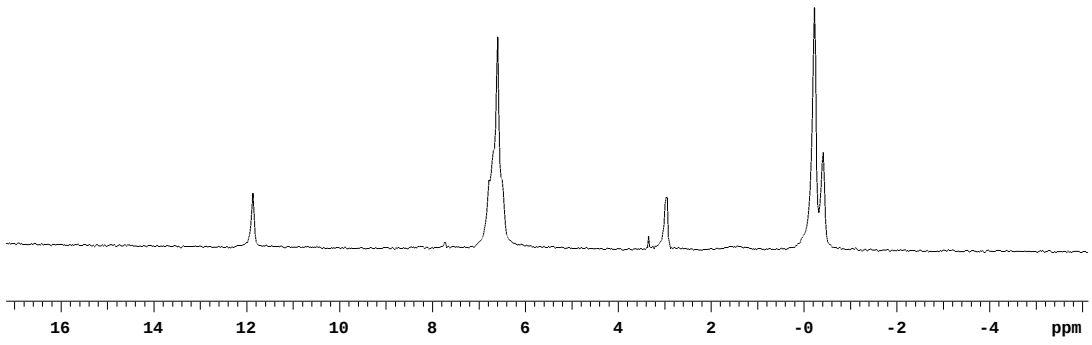

(a) (*S*)-enriched MPTP

(Because of the instrument conditions, only one side of the signal was detected correctly)

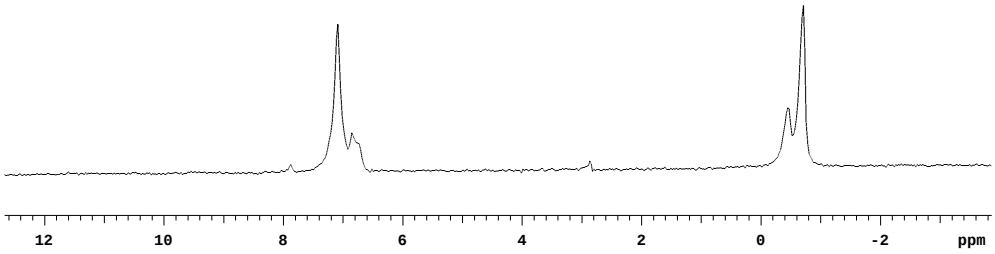

(b) (*R*)-enriched MPTP

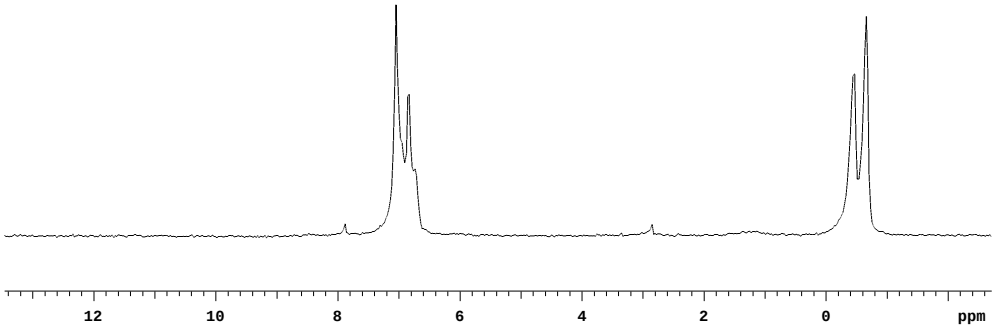

(c) The mixture of (*R*)-and (*S*)-MPTP

Figure 51. The ^{2}H NMR spectrum of the (*R)*-and (*S)*-enriched MPTP (**369**) (PBLG/CH_2Cl_2)

The above experiments indicate that the reaction does exhibit relatively high stereoselectivity. This stereoselectivity may be caused by the formation of the lithium complex prior to deprotonation. The temperature and the solvents may affect the 1,3 lithium shift in our case. The detachment of the chiral auxiliary does not destroy the %ee.

3.3.3. Enzymology results

The MAO-B substrate properties of the synthesized labelled and unlabelled compounds were examined. Linear initial velocities vs substrate concentrations plots and linear double-reciprocal plots were obtained for all the compounds (Figure 51-52). The kinetic data and their ratios are given in Table 4.

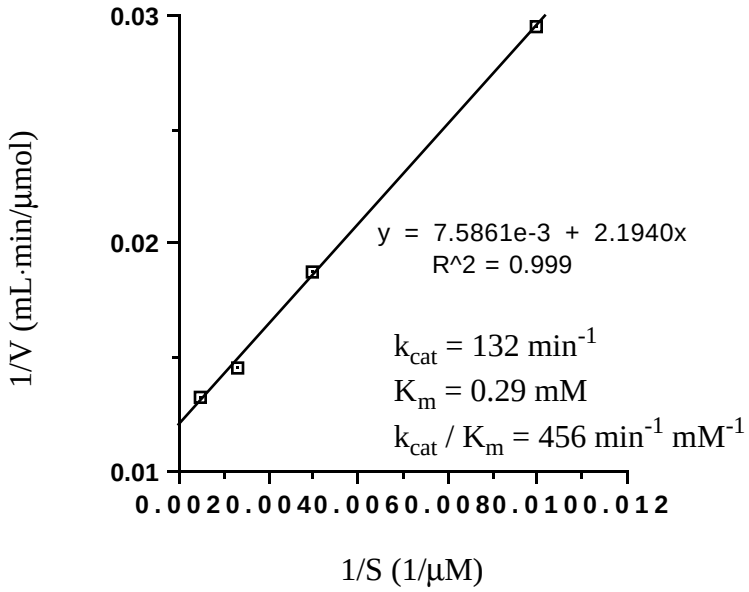

Figure 52. Lineweaver-Burke Plot for the MAO-B Catalyzed Oxidation of (*S*)-enriched Monodeuterated MPTP (**369**)

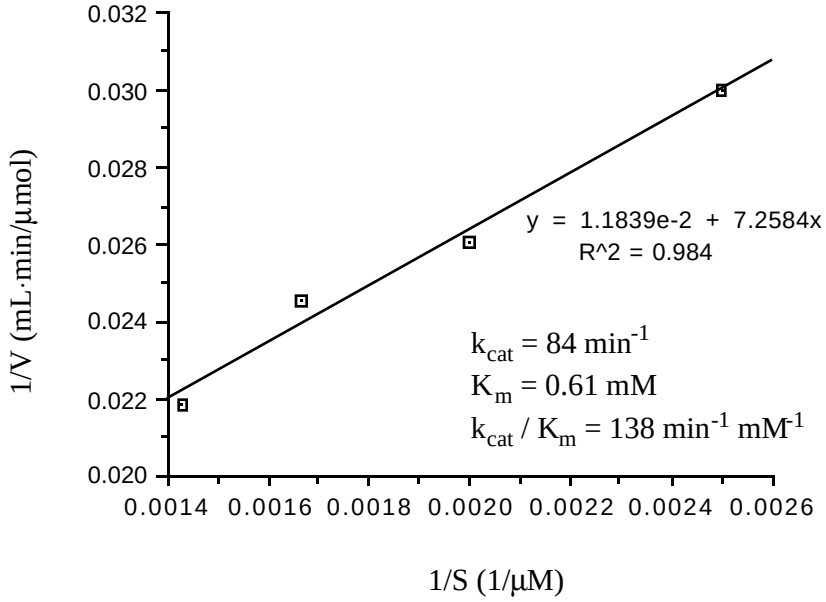

Figure 53. Lineweaver-Burke Plot for the MAO-B Catalyzed Oxidation of (*R*)-enriched Monodeuterated MPTP (**369**)

Table 4. Kinetic Parameters for the MAO-B Catalyzed Oxidation of the *R* and *S*-Enriched Monodeuterated MPTP Analogs

Deuterated analogs	k_{cat} $(min)^{-1}$	K_m (mM)	k_{cat}/K_m $(min^{-1}mM^{-1})$
***R*-enriched-(369)**	80	0.55	147
***S*-enriched-(369)**	132	0.30	446
Selectivity (*S*/*R*)	1.6	0.54	3.0

Estimated using e=16,000 M^{-1}, the value for the perchlorate salt of the 1-methyl-4-phenyl-2,3-dihydropyridinium species.[91]

3.3.4. Discussion

Primary isotope effect studies indicate that MAO-B catalyzed oxidation of MPTP does exhibit stereoselectivity. The two α-hydrogens are not equivalent for the enzyme. The enzyme prefers to remove the *S*-hydrogen during the oxidation reaction.

Chapter 4. The study on the MAO-catalyzed oxidation of 1-cyclopropyl-4-substituted-1,2,3,6-tetrahydropyridines

As was pointed out in Chapter 1, when the N-1 position of MPTP analogs is substituted by a cyclopropyl group, the compound is expected to behave as a mechanism-based inhibitor. Based on the SAR studies, we have designed and synthesized some 1-cyclopropyl-4-substituted-1,2,3,6-tetrahydropyridines.

4.1. The synthesis of 1-cyclopropyl-4-substituted-1,2,3,6-tetrahydropyridines

The 1-cyclopropyl-4-substituted-1,2,3,6-tetrahydropyridines have been synthesized in several steps (Scheme 82). The 4-substituted pyridines A upon reaction with 1-chloro-2,4-dinitrobenzene (**139**) gave the 4-substituted-1-(2,4-dinitrophenyl)pyridinium chloride products **370**-**375**, which, upon reaction with cyclopropylamine, gave the N-cyclopropylpyridinium chloride intermediates **376**-**381**. Subsequent reduction of **376**-**381** with $NaBH_4$ gave the 1-cyclopropyl-4-substituted-1,2,3,6-tetrahydropyridines **382**-**387**.

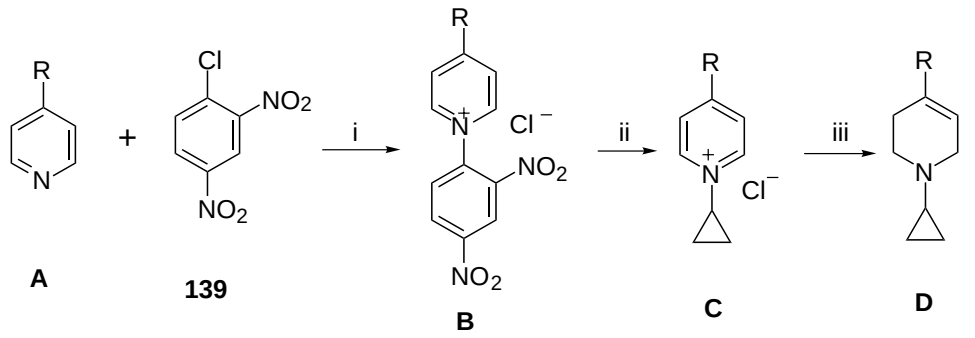

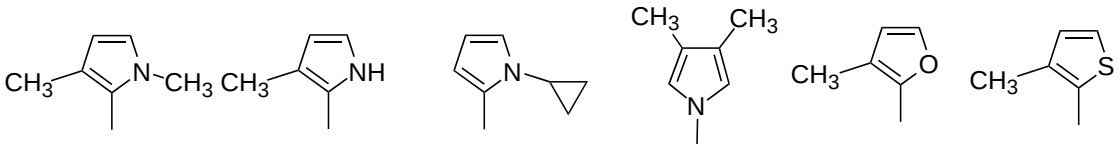

A	**256**	**255**	**254**	**235**	**265**	**275**
B	**370**	**371**	**372**	**373**	**374**	**375**
C	**376**	**377**	**378**	**379**	**380**	**381**
D	**382**	**383**	**384**	**385**	**386**	**387**

Reaction conditions: i) Acetone, reflux; ii) cyclopropylamine, 1-butanol, reflux;
iii) $NaBH_4$, methanol, 0 ^0C

Scheme 83. The Synthesis of 1-Cyclopropyl-4-substituted-1,2,3,6-tetrahydropyridines

Chapter 5 Conclusions

1. A series of 1,4-disubstituted-1,2,3,6-tetrahydropyridines and their corresponding intermediates have been synthesized and characterized. Their enzyme substrate properties are examined with the MAO-B preparations isolated from beef liver.

2. SAR studies indicate that steric factors play an important role in determining of the substrate properties in this series. The binding site of the enzyme can accommodate a methyl or ethyl group substituted at the 1- or 3-position of the 5-membered heteroarenes. Alkyl groups substituted at the 3-position (which is connected with the carbon) of these five-membered heteroarenes extend the conjugation. Electron withdrawing heteroarene group substituted at the 4-position of the 1,2,3,6-tetrahydrpyridine ring decreases its substrate activity. In addition to steric and electronic effects, unfavorable polar interactions with the NH group may affect the substrate properties of compounds in this series.

3. Deuterium isotope effect studies establish that of C-H bond cleavage at C-6 of the tetrahydropyridine is rate-determining for both good and poor substrates and, therefore, there is no change in the rate-determining step of this oxidation reaction. The substantial secondary isotope effect observed with 1-CD_3 in analog **303** indicates the formation of nitrogen cation. Primary isotope effect studies also indicate that MAO-B catalyzed oxidation of MPTP are stereoselective. The enzyme prefers to remove the *S*-hydrogen during the oxidation reaction.

4. The incorporation of deuterium at 6-position of the 1-[4,5-dihydro-4-(1-methylethyl)-2-oxazolyl]-4-phenyl-1,2,3,6-tetrahydropyridine exhibits high stereoselectivity. The stereoselectivity may be caused by the formation of the lithium complex prior to deprotonation.

Chapter 6 Experimental

Chemistry

All reagents were obtained from commercial sources and were used directly. Synthetic reactions were carried out under a nitrogen atmosphere. Tetrahydrofuran (THF) and diethyl ether were distilled from sodium benzophenone ketyl. Acetone was distilled from potassium carbonate. Dichloroform and toluene were distilled from calcium hydride. Melting points were determined using a Thoms-Hoover melting point apparatus and are uncorrected. UV-Vis spectra were recorded on a Beckman DU 7400 spectrophotometer. Proton NMR spectra were recorded on a Bruker WP 360-MHz or a 270-MHz or a 200 MHz spectrometer. Chemical shifts (δ) are reported in parts per million (ppm) relative to tetramethylsilane as an internal standard. The conventional symbols are used to describe spin multiplicities. Gas chromatography-electron ionization mass spectrometry (GC-EIMS) was performed on a Hewlett Packard 5890 GC fitted with an HP-1 capillary column (15 m × 0.2 mm i.d., 0.33 mm film thickness) which was coupled to a Hewlett Packard 5870 mass-selective detector. Data were acquired using an HP 5970 ChemStation. Normalized peak heights are reported as a percentage of the base peak. High resolution-electron ionization mass spectrometry (HR-EIMS) and high resolution-chemical ionization mass spectrometry (HR-CIMS) were performed on a VG 7070 HF instrument. Elemental analyses were performed by Atlantic Microlab, Inc., Norcross, GA.

4-(1-Methylimidazol-2-yl)-4-piperidinol (281). To a solution of 1-methylimidazole **279** (4.1 mL, 50 mmol) in dry THF (50 mL) was added n-butyllithium (20 mL, 50 mmol) dropwise at room temperature under nitrogen. The solution was stirred at 40 °C for 3h. The temperature was then decreased to -78 °C and 1-methyl-4-piperidone **125** (5.7 g, 50 mmol) was added. This mixture was allowed to warm to room temperature slowly and stirred at this temperature for 6h and for an additional 3h at 40 °C. The reaction was quenched with water (30 mL). The aqueous layer was extracted with ethyl acetate (4 × 40 mL). The combined organic extracts were dried over $MgSO_4$ and the solvent was removed in vacuo. The residue was purified by recrystallization from diethyl ether/methanol affording pure **281** (8.279 g, 84.8%): mp 151.5-152 °C; GC (t_R=7.98 min)-EIMS m/z (%) 195 (4, $M^{+\bullet}$), 177 (61), 125 (100), 83 (98), 72 (70); ^{1}H NMR ($CDCl_3$, 270 MHz) δ 6.82 (s, 1H, ArH), 6.78 (s, 1H, ArH), 3.84 (s, 3H, N'CH_3), 3.57

(s, 1H, OH), 2.63-2.68 (m, 2H, $NCHH_{eq}$), 2.42-2.50 (dt, 2H, $NCHH_{ax}$), 2.29 (s, 3H, NCH_3), 2.04-2.24 (m, 2H, NCH_2CHH_{eq}), 1.84-1.89 (d, 2H, NCH_2CHH_{ax}); ^{13}C NMR ($CDCl_3$, 360 MHz) δ 151.64, 125.44, 122.62, 67.79, 51.26, 46.14, 35.76, 34.65; Anal Calcd for $C_{10}H_{17}N_3O$: C, 61.51; H, 8.78; N, 21.53. Found: C, 61.63; H, 8.77; N, 21.49.

1-Methyl-4-(1-methylimidazol-2-yl)-1,2,3,6-tetrahydropyridine dihydrochloride (107•2HCl). To **281** (1.757 g, 9 mmol) was added aqueous H_3PO_4 solution (85% H_3PO_4 : H_2O = 4:1). This mixture was stirred and heated at 100 °C for 12h. The solution was then cooled and neutralized with Na_2CO_3 saturated solution until pH=9. The aqueous layer was extracted with ethyl acetate (4 × 40 mL). The extracts were dried over $MgSO_4$ and the solvent was removed in vacuo. To the residue in dry diethyl ether (50 mL), was introduced dry HCl while stirring. After stirring for 3h, the white solid was filtrated and recrystallized from methanol/diethyl ether affording pure **107•2HCl** (2.07 g, 92%): mp 256 °C (decomposed); GC (t_R=7.84 min)-EIMS m/z (%) 177 (100, $M^{+\bullet}$), 162 (87), 133 (72), 120 (30), 107 (20), 94 (37); ^1H NMR (CD_3OD, 270 MHz) δ 7.56-7.59 (dd, 2H, ArH), 6.53 (m, 1H, C-5), 4.16 (m, 2H, C-6), 3.91 (s, 3H, NCH_3), 3.71 (m, 2H, C-2), 3.00 (s, 3H, $N'CH_3$), 2.86 (m, 2H, C-3); ^{13}C NMR (CD_3OD, 360 MHz) δ 144.12, 132.11, 126.28, 122.03, 120.31, 52.76, 51.01, 43.22, 36.78, 25.71; UV (phosphate buffer, pH 7.4) λ_{max} 253 nm (ε = 8,666 M^{-1}); Anal Calcd for $C_{10}H_{17}Cl_2N_3$: C, 48.01; H, 6.85; N, 16.80. Found: C, 48.24; H, 6.82; N, 16.63.

Oxalate salt of 4-(3-methylfuran-2-yl)pyridine (265•$H_2C_2O_4$). Method 1: 4-bromopyridine (3.16 g, 20 mmol) was dissolved in 50 mL of anhydrous diethyl ether at -78 °C under nitrogen. A hexane solution of n-butyllithium (8 mL, 20 mmol) was added dropwise at this temperature under nitrogen. A yellow precipitate was formed. 30 min later, 3-methyl-2 (5H)-furanone **263** (1.95 mL, 20 mmol) was added. The mixture was stirred for four hours at -78 °C. Then the temperature was allowed to rise to room temperature following which the reaction mixture was stirred for 24h. The temperature was decreased again to -78 °C, a dilute H_2SO_4 solution in THF was added until pH=2. The reaction mixture was allowed to slowly work up to room temperature. 50 ml of water was added. The aqueous layer was adjusted to pH=8 and extracted with ditheyl ether (4 × 50 mL). The extracts was dried over $MgSO_4$ and the solvent was removed in vacuo. The obtained brown oil was chromatographed (silica gel, 10:1 ethyl acetate-hexane) to give **265** in 87% yield. Method 2: The same procedures are used, except the reaction was quenched

by a solution of NaOH in water at -78 °C and the aqueous layer was extracted by ethyl acetate. After recrystallization from methanol/acetone/diethyl ether, **267** was obtained as a white solid in 78% yield. mp 152.5-153 °C; GC (t_R=7.14 min)-EIMS m/z (%) 177 (2, $M^{+\bullet}$), 159 (6), 133 (13), 117 (7), 99(100), 79 (56); ^{1}H NMR ($CDCl_3$, 200 MHz) δ 8.57-8.59 (dd, 2H, C-2 and C-6), 7.40-7.42 (dd, 2H, C-3 and C-5), 5.82 (m, 1H, C=CH), 4.71-4.87 (m, 2H, CH_2), 3.71 (s, 1H, OH), 1.62-1.65 (m, 3H, CH_3); ^{13}C NMR (DMSO-d_6, 360 MHz) δ 151.58, 149.30, 137.98, 123.35, 120.88, 109.26, 72.59, 11.00;. Anal calcd for $C_{10}H_{11}NO_2$: C, 67.78; H, 6.26; N, 7.90. Found: C, 67.69; H, 6.26; N, 7.82. To **267** (30 mmol) in 30 mL THF and 10 mL H_2O, 1 mL concentrated H_2SO_4 was added slowly. The solution was stirred overnight at room temperature. THF was removed in vacuo. The Na_2CO_3 solution was added until pH=9. The mixture was extracted by diethyl ether. The extracts were dried over $MgSO_4$ and the solvent was removed in vacuo. The residue was chromatographed to give **265** in 99% yield. This brown oil in anhydrous diethyl ether (50 mL) was treated with oxalic acid (2.16 g, 24 mmol) in 10 mL of anhydrous diethyl ether. The precipitate was recrystallized from methanol/diethyl ether to afford a white crystalline solid **265•$H_2C_2O_4$** in 90% yield. mp 165 °C; GC (t_R=10.74 min)-EIMS m/z (%) 159 (100, $M^{+\bullet}$), 130 (100), 103 (22), 77 (50); ^{1}H NMR (DMSO-D_6, 270 MHz) δ 8.60-8.62 (d, 2H, C-2 and C-6), 7.79-7.80 (d, 1H, C'-5), 7.58-7.61 (dd, 1H, C-3 and C-5), 6.57-6.58 (d, 1H, C'-4), 2.3 (s, 3H, CH_3); ^{13}C NMR (DMSO-d_6, 360 MHz) δ 161.24, 149.08, 145.00, 143.79, 137.43, 122.33, 118.67, 116.35, 11.76; Anal Calcd for $C_{12}H_{11}NO_5$•$0.51H_2C_2O_4$: C, 52.97; H, 4.10; N, 4.74. Found: C, 53.17; H, 4.08; N, 4.73.

Oxalate salt of 4-(3-methylthiophen-2-yl)pyridine (275•$H_2C_2O_4$). To the 2-bromo-3-methylthiophene **273** (5 g, 97%, 27.4 mmol) in dry THF (25 mL) at -78 °C under nitrogen, was added n-butyllithium in hexane (12 mL, 30 mmol) dropwise. The mixture was stirred at -78 °C for 1.5h and then transfered to a solution of dry $ZnCl_2$ (30 mmol) in THF (15 mL). After stirring for 3h at room temperature, the new mixture was transfered again to the mixture of 4-bromopyridine (4.725 g, 30 mmol) and tetrakis(triphenylphosphine)palladium (1 g, 3 mmol%) in THF (20 mL) at 0 °C. After the mixture was stirred at 45 °C for 2 days, water was added. The water layer was adjusted to pH=8 and extracted with ethyl acetate (4 × 100 mL). The extracts were dried over $MgSO_4$ and the solvent was removed in vacuo. Column chromatography (silica gel, ethyl acetate)

of the residue afforded **37** as a yellow oil. Treatment of this oil in dry diethyl ether with oxalic acid afforded a yellow precipatate which was recrystallized in methanol/diethyl ether to give a yellow solid **37•$H_2C_2O_4$** (4.45 g, 93%). mp 138-140 °C; GC (t_R=7.06 min)-EIMS m/z (%) 175 (100, $M^{+\bullet}$), 147 (24), 130 (13), 103 (5), 97 (39); ^{1}H NMR (DMSO-d_6, 200 MHz) δ 8.60-8.65 (d, 2H, C-2 and C-6), 7.63-7.65 (d, 1H, C'-5), 7.50-7.57 (dd, 2H, C-3 and C-5), 7.04-7.09 (d, 1H, C'-4), 2.38 (s, 3H, CH_3); ^{13}C NMR (DMSO-d_6, 360 MHz) δ 161.19, 149.36, 142.22, 136.18, 133.67, 132.33, 126.60, 122.56, 15.13; Anal Calcd for $C_{12}H_{11}NO_4S \cdot 0.23\ H_2C_2O_4$: C, 52.34; H,4.04; N, 4.90. Found: C, 52.36; H, 4.14; N, 4.78.

4-(3,4-Dimethylpyrrol-2-yl)pyridine (235). A hexane solution of n-butyllithium (6 mL, 15 mmol) was added to a stirred solution of 3,4-dimethylpyrrole **232** (1.43 g, 15 mmol) in 10 mL THF at room temperature under nitrogen. The mixture was stirred for 1h and then was transfered to a stirred solution of dry zinc chloride (2.72 g, 20 mmol) in 10 mL THF at room temperature. The mixture was stirred for 1.5h. After that, the 3,4-dimethyl-1-pyrrolyl zinc chloride solution was transfered to a mixture of 4-bromopyridine (2.36 g, 15 mmol) and tetrakis(triphenylphosphine)palladium (0.75 g, 4.3 mol%) in dry THF (25 mL) at 0 °C. The reaction mixture was allowed to raise to 65 °C and stirred for 3 days. After the mixture was cooled, 50 mL of water was added. The aqueous layer was saturated with NaCl and extracted with ethyl acetate (4 × 50 mL). The extracts were dried over $MgSO_4$ and the solvent was removed in vacuo. The residue was recrystallized in diethyl ether affording a white solid **235** (1.03 g, 40%). mp 125-126 °C; GC (t_R=13.43 min)-EIMS m/z (%) 172 (76, $M^{+\bullet}$), 171 (100), 157 (76), 130 (6), 94 (6); ^{1}H NMR ($CDCl_3$, 200 MHz) δ 8.51-8.53 (dd, 2H, C-2 and C-6), 7.17-7.19 (dd, 2H, C-3 and C-5), 6.94 (s, 2H, C'-2 and C'-5), 2.06 (s, 6H, CH_3); ^{13}C NMR ($CDCl_3$, 200 MHz) δ 150.99, 146.00, 123.00, 115.80, 112.05, 10.33; Anal Calcd for $C_{11}H_{12}N_2$: C, 76.71; H, 7.02; N, 16.26. Found: C, 76.76; H, 7.07; N, 16.33.

4-(3-Methylpyrrol-2-yl)pyridine (255). A solution of 4-pyridinecarboxaldehyde (5.85 g, 0.05 mol) in anhydrous DMF (25 mL) was added dropwise to a mixture of potassium cyanide (0.26g, 0.004 mol) and anhydrous DMF (25 mL) at 0 °C under nitrogen. 30 min later, the crotonaldehyde (3.54 g, 0.05 mol) in 10 mL of anhydrous DMF was added dropwise. The mixture was stirred for 2 hours at 0 °C and then acetic acid (2.5 mL) was added. The mixture was stirred for 10 min. After that, ice

water was added to the mixture. The water layer was adjusted to pH=9 and extracted with ethyl acetate (4 × 150 mL) and the organic solution was washed with dilute $NaHCO_3$ aqueous solution and dried over $MgSO_4$ and the solvent was removed in vacuo. The residue was chromatographed (silica gel, 10:2 ethyl acetate :hexane) to give **244** in 40% yield. GC(t_R=6.59 min)-EIMS m/z (%) 177 (1, $M^{+\bullet}$), 149 (3), 135 (54), 106 (100), 78 (90), 51 (72); ^{1}H NMR ($CDCl_3$, 360 MHz) δ 9.76 (s, 1H, CHO), 8.76-8.81 (dd, 2H, C-2 and C-6), 7.74-7.79 (dd, 2H, C-3 and C-5), 3.85-3.94 (m, 1H, C<u>H</u>CH_3), 3.16-3.24 (dd, 1H, C<u>H_1</u>H_2), 2.64-2.70 (dd, 1H, CH_1<u>H_2</u>), 1.20-1.27 (d, 3H, CH_3); ^{13}C NMR ($CDCl_3$, 360 MHz) δ 202.20, 200.05, 150.96, 142.21, 121.56, 47.18, 35.50, 17.44; HR-CIMS. Calcd for $C_{10}H_{11}NO_2H^+$: 178.0868038. Found: 178.087585.

A solution of ammonium hydroxide (6.8 g, 30%, 0.12 mol) was added to the solution of **244** (10 mmol) in ethanol (75 mL). The mixture was heated and stirred for 3 hours at 80 °C. The solvent was removed in vacuo. An aqueous solution (50 mL) containing the residue was extracted with ethyl acetate (4 × 50 mL). The extracts were washed with 150 mL 5% $NaHCO_3$ solution and dried over $MgSO_4$ and the solvent was removed in vacuo. The residue was chromatographed (silica gel, 10:1 ethyl acetate: methanol) to give a white solid **45** (1.03 g, 65%). mp 137.5-138.5 °C; GC (t_R=7.68 min)-EIMS m/z (%) 158 (93, $M^{+\bullet}$), 157 (100), 130 (28), 103 (86), 80 (20); ^{1}H NMR ($CDCl_3$, 200 MHz) δ 8.52-8.55 (dd, 2H, C-2 and C-6), 7.33-7.34 (dd, 2H, C-3 and C-5), 6.86-6.88 (t, 1H, C'-5), 6.18 (t, 1H, C'-4), 2.35 (s, 3H, CH_3); ^{13}C NMR ($CDCl_3$, 360 MHz) δ 150.07, 145.08, 140.77, 125.16, 120.45, 119.72, 113.41, 13.30; Anal Calcd for $C_{10}H_{10}N_2 \cdot 0.16\ H_2O$: C, 75.01; H, 6.46; N, 17.38. Found: C, 75.01; H, 6.41; N, 17.39.

4-(1,3-Dimethylpyrrol-2-yl)pyridine (256). To the solution of **244** (10 mmol) in methanol (20 mL), was added a solution of methylamine (20 mmol) in methanol. This solution was stirred at room temperature for 24h. The solvent was removed in vacuo. An aqueous solution (20 mL) containing the residue was extracted with diethyl ether (4 × 30 mL). The extracts were dried over $MgSO_4$ and the solvent was removed in vacuo. The residue was chromatographed (silic gel, 10:1 ethyl acetate:methanol) to give **256** as a yellow oil (1.211 g, 70%). GC (t_R=7.20 min)-EIMS m/z (%) 172 (93, $M^{+\bullet}$), 171 (100), 156 (20), 130 (15), 103 (8), 94 (41); ^{1}H NMR ($CDCl_3$, 200 MHz) δ 8.62-8.66 (dd, 2H, C-2 and C-6), 7.18-7.22 (dd, 2H, C-3 and C-5), 6.68-6.69 (d, 1H, C'-5), 6.09-6.10 (d, 1H, C'-4), 3.58 (s, 3H, N-CH_3), 2.13 (s, 3H, CH_3); ^{13}C NMR ($CDCl_3$, 360 MHz) δ

149.76, 140.71, 128.57, 124.44, 124.02, 110.17, 35.38, 12.50; HR-EIMS Calcd for $C_{11}H_{12}N_2$: 172.1000485. Found: 172.100327.

4-Oxo-4-(4-pyridyl-)-1-butanol (248) To the 4-bromopyridine (3.95 g, 25 mol) in anhydrous diethyl ether (50 mL) at -78 °C, was added n-butyllithium (25 mmol) in hexane dropwise. The mixture was stirred at -78 °C for 1h. g-butyrolactone (2.2 g, 25 mmol) was added dropwise to the mixture at -78 °C. The mixture was stirred at this temperature for 4h and then was raised to room temperature and stirred for another 6h. The reaction mixture was quenched with dilute Na_2CO_3 aqueous solution (30 mL). The aqueous layer was extracted by ethyl acetate (40 mL × 4). The extracts were dried over MgSO4 and the solvent was removed in vacuo. The residue was purified by column (silica gel, ethyl acetate) to afford **248** in 94.5% yield. ^{1}H NMR and ^{13}C NMR indicate the mixture of the isomers. GC(t_R=6.65 min)-EIMS m/z (%) 165 (10, $M^{+\bullet}$), 147 (3), 134 (5), 121 (100), 106 (100), 87 (10), 78 (98), 51 (72); HR-CIMS Calcd for $C_9H_{11}NO_2H^+$: 166.0868038. Found: 166.086151.

3-Ethyl-4-oxo-4-(4-pyridyl)-1-butanol (269) was prepared with 4-bromopyridine and a-ethyl-γ- butyrolactone using the same method. The crude product was recrystallized in methylene chloride/ diethyl ether in 53.5% yield. ^{1}H NMR and ^{13}C NMR indicate the mixture of the isomers. GC (t_R=7.63 min)-EIMS m/z (%) 192 (4, $M^{+\bullet}$), 160 (3), 149 (66), 124 (28), 106 (100), 78 (86), 51 (92); Anal. Calcd for $C_{11}H_{15}NO_2$: C, 68.37; H, 7.82; N, 7.25. Found: C, 68.27; H, 7.84; N, 7.16.

4-Oxo-4-(4-pyridyl)butanal (250) To the stirred solution of pyridine (20 g, 240 mmol) in anhydrous methylene chloride (300 mL) at room temperature, was added chromium trioxide (12.0 g, 120 mmol) in portions. The deep burgandy solution was stirred for 30 min. A solution of **248** (20 mmole) in a 20 mL of methylene chloride was added in one portion. The mixture was stirred for 12h at room temperature. The solution was decanted from the residue and the residue was washed with methylene chloride (2 × 200 mL). The solvent was removed in vacuo and the residue was purified by column (silica gel, ethyl acetate). **250** was obtained in 65% yield. GC(t_R=6.25 min)-EIMS m/z (%) 163 (1, $M^{+\bullet}$), 135 (44), 121 (34), 106 (76), 78 (100), 51 (80); ^{1}H NMR ($CDCl_3$, 360 MHz) δ 9.89 (s, 1H, CHO), 8.81-8.83 (dd, 2H, C-2 and C-6), 7.75-7.77 (dd, 2H, C-3 and C-5), 3.29-3.32 (t, 2H, 3-CH_2), 2.96-3.00 (t, 2H, 2-CH_2); ^{13}C NMR ($CDCl_3$, 360

MHz) δ 200.00, 197.56, 151.12, 142.36, 121.11, 37.46, 31.30; HR-CIMS Calcd for $C_9H_9NO_2H^+$: 164.0711537. Found: 164.071381.

3-Ethyl-4-oxo-4-(4-pyridyl)butanal (270) was prepared using the same methods as **250** in 59.7% yield. GC (t_R=7.26 min)-EIMS m/z (%) 191 (1, $M^{+\bullet}$), 163 (2), 149 (34), 134 (12), 106 (100), 78 (74), 51 (67); ^{1}H NMR ($CDCl_3$, 360 MHz) δ 9.78 (s, 1H, CHO), 8.81-8.82 (dd, 2H, C-2 and C-6), 7.76-7.77 (dd, 2H, C-3 and C-5), 3.78-3.86 (m, 1H, CH), 3.18-3.26 (dd, 1H, 2-C<u>H</u>H), 2.70-2.76 (dd, 1H, 2-CH<u>H</u>), 1.68-1.78 (m, 1H, 1'-C<u>H</u>H), 1.50-1.60 (m, 1H, 1'-CH<u>H</u>), 0.84-0.92 (t, 3H, CH_3); ^{13}C NMR ($CDCl_3$, 360 MHz) δ 202.23, 200.30, 151.00, 142.89, 121.45, 45.08, 41.67, 25.02, 11.42; HR-EIMS Calcd for $C_{11}H_{13}NO_2H^+$: 192.1024538. Found: 192.102249.

General procedures for the synthesis of the oxalate salts of 4-(1-alkylpyrrol-2-yl)pyridine: To 4-oxo-4-pyridylbutanal (20 mmol) in 40 mL methanol, was added the corresponding primary amines (4eq.). The mixture was stirred at room temperature for 1 day. The solvent was removed in vacuo. After chromatography (silica gel, ethyl acetate), a yellow oil of 4-(1-alkylpyrrol-2-yl)pyridine was obtained. To this yellow oil (5 mmol) in dry diethyl ether (15 mL) was added the oxalic acid (6 mmol) in 5 mL diethyl ether. The mixture was stirred for 4h and the precipitate was filtrated and recrystallized in methanol/diethyl ether.

Oxalate salt of 4-(1-ethylpyrrol-2-yl)pyridine (251•$H_2C_2O_4$) was obtained in 93% yield. mp 142.5-143 °C; GC (t_R=7.10 min)-EIMS m/z (%) 172 (100, $M^{+\bullet}$), 157 (39), 144 (22), 130 (22), 117 (22), 104 (9), 89 (35); ^{1}H NMR (DMSO-d_6, 270 MHz) δ 8.56-8.59 (dd, 2H, C-6 and C-2), 7.47-7.50 (dd, 2H, C-3 and C-5), 7.08-7.10 (dd, 1H, C'-5), 6.47-6.50 (dd, 1H, C'-4), 6.16-6.19 (dd, 1H, C'-3), 4.06-4.17 (q, 2H, CH_2), 1.10-1.29 (t, 3H, CH_3); ^{13}C NMR (DMSO-d_6, 360 MHz) δ 162.03, 147.63, 141.87, 129.40, 126.32, 121.59, 112.60,108.78, 42.19, 16.43; Anal. Calcd for $C_{13}H_{14}N_2O_4$•0.58 $H_2C_2O_4$: C, 54.06; H, 4.86; N, 8.90. Found: C, 54.01; H, 5.03; N, 8.90.

Oxalate salt of 4-(1-propylpyrrol-2-yl)pyridine (252•$H_2C_2O_4$) was obtained in 90% yield. mp 115-117 °C; GC(t_R=7.45 min)-EIMS m/z (%) 186 (72, $M^{+\bullet}$), 157 (100), 144 (30), 130 (22), 117 (20), 104 (11), 89 (28); ^{1}H NMR (DMSO-d_6, 270 MHz) δ 8.55-8.58 (dd, 2H, C-2 and C-6), 7.47-7.50 (dd, 2H, C-3 and C-5), 7.06-7.08 (dd, 1H, C'-5), 6.47-6.49 (dd, 1H, C'-4), 6.14-6.18 (dd, 1H, C'-3), 4.02-4.10 (t, 2H,

CH_2N), 1.53-1.64 (m, 2H, CH_2), 0.70-0.77 (t, 3H, CH_3); ^{13}C NMR (DMSO-d_6, 360 MHz) δ 162.03, 147.82, 141.90, 129.66, 127.10, 121.59, 112.61, 108.49, 48.96, 24.02, 10.70; Anal. Calcd for $C_{14}H_{16}N_2O_4 \bullet 0.58\ H_2C_2O_4$: C, 55.40; H,5.26; N, 8.52. Found: C, 55.37; H, 5.46; N, 8.62.

4-(1-Isopropylpyrrrol-2-yl)pyridine (253) was obtained in 87% yield. GC (t_R=6.78 min)-EIMS m/z (%) 186 (56, $M^{+\bullet}$), 171 (10), 144 (100), 117 (21), 89 (18); ^1H NMR ($CDCl_3$, 360 MHz) δ 8.59-8.61 (dd, 2H, C-2 and C-6), 7.26-7.27 (dd, 2H, C-3 and C-5), 6.98 (dd, 1H, C'-5), 6.28 (m, 2H, C'-3 and C'-4), 4.52-4.59 (m, 1H, CH), 1.43-1.44 (d, 6H, CH_3); ^{13}C NMR ($CDCl_3$, 360 MHz) δ 150.13, 141.32, 131.34, 123.13, 119.88, 110.59, 109.20, 47.78, 24.31; HR-EIMS Calcd for $C_{12}H_{14}N_2$: 186.1156986. Found: 186.115219.

Oxalate salt of 4-(1-cyclopropylpyrrol-2-yl)pyridine (254•$H_2C_2O_4$) was obtained in 97% yield. mp 150.5-151.5 °C; GC (t_R=7.87 min)-EIMS m/z (%) 184 (100, $M^{+\bullet}$), 169 (29), 156 (22), 142 (11), 130 (13), 116 (23), 106 (33), 89 (39); ^1H NMR (DMSO-d_6, 360MHz) δ 8.55-8.57 (dd, 2H, C-2 and C-6), 7.74-7.77 (dd, 2H, C-3 and C-5), 7.07 (dd, 1H, C'-5), 6.61-6.63 (dd, 1H, C'-4), 6.11-6.14 (dd, 1H, C'-3), 3.73-3.74 (m, 1H, NCH), 0.95-1.0 (m, 2H, CH_2), 0.81-0.85 (m, 2H, CH_2); ^{13}C NMR (DMSO-d_6, 360 MHz) δ 162.03, 146.99, 141.82, 130.48, 127.20, 121.10, 112.80, 108.37, 30.04, 8.41; Anal. Calcd for $C_{14}H_{14}N_2O_4 \bullet 0.38\ H_2O$: C, 59.83; H, 5.29; N, 9.97. Found: C, 59.85; H, 5.15; N, 9.73.

Oxalate salt of 4-(3-ethylfuran-2-yl)pyridine (271•$H_2C_2O_4$). To the 3-ethyl-4-oxo-4-(4-pyridyl)butanal **270** (1.00g, 5.23 mmol) in 20 mL THF and 10 mL H_2O, was added 5 mL H_2SO_4 dropwise. The mixture was stirred for 15h at 55 °C. THF was evaporated in vacuo. The remaining solution was basified and extracted with diethyl ether (4×40 mL). The extracts were dried over $MgSO_4$ and the solvent was removed in vacuo. The crude product was chromatographed (silica gel, 10:1.5 ethyl acetate-hexane) to give **271** (0.875 g, 96.6%). Treatment of **271** in dry diethyl ether with oxalic acid (1.2 eq.) afforded a precipatate which was recrystallized in methanol/diethyl ether to give a yellow solid **271**$\cdot$ •$H_2C_2O_4$in 97% yield. mp 170-171 °C (decomposed); GC(t_R=6.85 min)-EIMS m/z (%) 173 (100, $M^{+\bullet}$), 158 (87), 144 (11), 130 (93), 115 (13), 103 (26), 89 (11); ^1H NMR (DMSO-d_6, 200 MHz) δ 8.61-8.63 (dd, 2H, C-2 and C-6), 7.82 (d, 1H, C'-5), 7.57-7.60 (dd, 2H, C-3 and C-5), 6.65 (d, 1H, C'-4), 2.69-2.81 (q, 2H, CH_2), 1.18-

1.26 (t, 3H, CH_3); ^{13}C NMR (DMSO-d_6, 360 MHz) δ 161.40, 148.56, 144.21, 143.96, 138.70, 128.86, 118.76, 114.24, 18.67, 13.75; Anal. Calcd for $C_{13}H_{13}O_5N \bullet 0.45$ $H_2C_2O_4$: C, 54.93; H, 4.61; N, 4.59. Found: C, 54.95; H, 4.76; N, 4.58.

1-Methyl-4-(3-ethylthien-2-yl)pyridine (277). To the 3-ethyl-4-oxo-4-(4-pyridyl)butanal **270** (0.955 g, 5 mmole) in dry toluene (20 mL), was added powdered phosphorus pentasulfide (5.5 g, 25 mmole). The mixture was stirred for 2h at 100 °C under N_2. The mixture was cooled and treated with water (25 mL) and the aqueous layer was adjusted to PH=8. The aqueous layer was extracted with ether (3 × 40 mL). The combined organic layer was washed with dilute Na_2CO_3 solution, dried over $MgSO_4$ and evaporated. The residue was separated through column (silica gel, ethyl acetate:hexane, 10:2). 0.284 g yellow oil was obtained in 30 % yield. GC (t_R=6.98 min)-EIMS m/z (%) 189 (71, $M^{+\bullet}$), 174 (100), 147 (20), 130 (15), 115 (6), 102 (7); ^1H NMR ($CDCl_3$, 360 MHz) δ 8.58-8.62 (dd, 2H, C-3 and C-5), 7.34-7.36 (m, 3H, C-2, C-6 and C'-5), 7.03-7.04 (d, 1H,), 2,72-2.78 (q, 2H, CH_2), 1.24-1.30 (t, 3H, CH_3); ^{13}C NMR (CDCL3, 360 Mhz) δ 150.00, 142.50, 142.07, 134.30, 129.85, 125.66, 123.34, 22. 169, 15.28; HR-EIMS Anal. Calcd for $C_{11}H_{11}NS$: 189.0612212. Found: 189.061310.

General procedure for the synthesis of the N-methyl-4-substituted pyridinium iodide: a mixture of iodomethane (8 mmol) and 4-substituted pyridine (2 mmol) in anhydrous acetone (10 mL) was stirred at room temperature overnight. After filtration, the precipitate was recrystallized from the appropriate solvent.

1-Methyl-4-(3-methylfuran-2-yl)pyridinium iodide (266) was recrystallized from methanol in yield 97%; mp 203-203.5 °C; ^1H NMR (DMSO-d_6, 200 MHz) δ 8.82-8.87 (d, 2H, C-2 and C-6), 8.11-8.15 (d, 2H, C-3 and C-5) 8.08-8.10 (d, 1H, C'-5), 6.79-6.80 (d, 1H, C'-4), 4.27 (s, 3H, NCH_3), 2.46 (s, 3H, CH_3); ^{13}C NMR (DMSO-d_6, 360 MHz) δ 147.86, 145.56, 143.70, 143.50, 130.20, 120.68, 118.47, 47.50, 12.95; Anal. calcd for $C_{11}H_{12}INO$: C, 43.88; H, 4.02; N, 4.65. Found: C, 43.71; H, 3.97; N, 4.53.

1-Methyl-4-(3-methylthiophen-2-yl)pyridium iodide (276) was recrystallized from methanol/diethyl ether in 67% yield. mp 194 °C (decomposed); ^1H NMR (DMSO-d_6, 200 MHz) δ 8.87-8.91 (d, 2H, C-2 and C-6), 8.16-8.20 (d, 2H, C-3 and C-5), 7.93-7.98 (d, 1H, C'-5), 7.21-7.22 (d, 1H, C'-4), 4.30 (s, 3H, NCH_3), 2.52 (s, 3H, CH_3); ^{13}C NMR (DMSO-d_6, 360 MHz) δ 148.77, 145.64, 145.19, 141.39,

133.62, 131.20, 124.35, 46.92, 15.93; Anal calcd $C_{11}H_{12}INS \bullet 0.7\ H_2O$: C, 40.06; H, 4.09; N, 4.25. Found: C, 40.02; H, 3.72; N, 4.29.

4-(3,4-Dimethylpyrrol-1-yl)-1-methylpyridinium iodide (236) was recrystallized from methanol in 90% yield. mp 239-239.5 °C; ^{1}H NMR (DMSO-d_6, 200 MHz) δ 8.79-8.81 (d, 2H, C-2 and C-6), 8.10-8.12 (d, 2H, C-3 and C-5), 7.58 (s, 2H, C'-2 and C'-5), 4.14 (s, 3H, NCH_3), 2.01 (s, 6H, CH_3); ^{13}C NMR (DMSO-d_6, 360 MHz) δ 149.60, 146.13, 125.81, 117.12, 112.92, 45.88, 9.92; Anal Calcd for $C_{12}H_{15}IN_2$: C, 45.88; H, 4.81; N,8.92. Found: C, 45.72; H, 4.86; N, 8.81.

1-Methyl-4-(3-methylpyrrol-2-yl)pyridinium iodide (261) was recrystallized from methanol and acetone in 84% yield. mp 244-245 °C; ^{1}H NMR (DMSO-d_6, 200 MHz) δ 8.64-8.67 (dd, 2H, C-2 and C-6), 7.91-7.94 (dd, 2H, C-3 and C-5), 7.25-7.28 (t, 1H, C'-5), 6.25 (t, 1H, C'-4), 4.14 (s, 3H, NCH_3), 2.40 (s, 3H, CH_3); ^{13}C NMR (DMSO-d_6, 360 MHz) δ 145.43, 144.18, 127.73, 126.07, 122.56, 119.09, 115.02, 45.99, 14.44; Anal Calcd $C_{11}H_{13}IN_2$: C, 44.02; H, 4.36; N, 9.33. Found: C, 43.93; H, 4.38; N, 9.26.

4-(1,3-Dimethylpyrrol-2-yl)-1-methylpyridinium iodide (262) was recrystallized from methanol in 96% yield. mp 274 °C (decomposed); ^{1}H NMR (DMSO-d_6, 200 MHz) δ 8.79-8.82 (d, 2H, C-2 and C-6), 7.95-7.99 (d, 2H, C-3 and C-5), 7.14-7.15 (d, 1H, C'-5), 6.14-6.16 (d, 1H, C'-4), 4.26 (s, 3H, NCH_3), 3.74 (s, 3H, $N'CH_3$), 2.21 (s, 3H, CH_3); ^{13}C NMR (DMSO-d_6, 360 MHz) δ 146.12, 144.23, 129.71, 125.60, 125.22, 124.43, 111.53, 46.54, 35.85, 13.03; Anal calcd for $C_{12}H_{15}IN_2$: C, 45.88; H, 4.81; N, 8.92. Found: C, 45.77; H, 4.86; N, 8.81.

1-Methyl-4-(3-ethylfuran-2-yl)pyridinium iodide (272). To the 4-(3-ethylfuran-2-yl)pyridine (0.484 g, 2.8 mmol) in 5 mL dry acetone, was added methyl iodide (5 eq.). The solution was stirred overnight. After filtration, the crude product was recrystallized from methanol/diethyl ether to afford a yellow solid **272** (0.37 g, 42%). mp 162.5-163.5 °C; ^{1}H NMR (DMSO-d_6, 200 MHz) δ 8.82-8.85 (dd, 2H, C-2 and C-6), 8.11-8.14 (m, 3H, C-3, C-5 and C'-5), 6.85 (d, 1H, C'-4), 4.28 (s, 3H, NCH_3), 2.82-2.94 (q, 2H, CH_2), 1.21-1.29 (t, 3H, CH_3); ^{13}C NMR (DMSO-d_6, 360 MHz) δ 147.61, 145.28, 143.03, 142.80, 135.77, 120.30, 115.66, 46.84, 19.13, 13.41; Anal. Calcd for $C_{12}H_{14}INO$: C, 45.73; H, 4.48; N, 4.44. Found: C, 45.56; H, 4.54; N, 4.36.

1-Methyl-4-(3-ethylthien-2-yl)pyridinium iodide (278). To the 4-(3-

ethylthien-2-yl)pyridine (0.19 g, 1 mmole) in 5 mL dry acetone, was added methyl iodide (5 eq.). The solution was stirred overnight. After filtration, the crude product was recrystallized from methanol/diethyl ether to afford a yellow solid **278** in 45% yield. mp 164-165 °C; ^{1}H NMR (DMSO-d_6, 360 MHz) δ 8.89-8.90 (dd, 2H, C-2 and C-6), 8.13-8.15 (dd, 2H, C-3 and C-5), 7.97-7.98 (d, 1H, C'-5), 7.30 (d, 1H, C'-4), 4.31 (s, 3H, NCH_3), 2.84-2.88 (q, 2H, CH_2), 1.22-1.27 (t, 3H, CH_3); ^{13}C NMR (DMSO-d_6, 360 MHz) δ 148.86, 147.12, 145.30, 131.56, 131.36, 130.65, 124.90, 46.98, 22.17, 14.55; Anal. Calcd for $C_{12}H_{14}INS$: C, 43.52 ; H, 4.26 ; N, 4.23 . Found: C, 43.55; H, 4.31; N, 4.17 .

General procedures for the synthesis of the oxalate salts of N-methyl-4-substituted-1,2,3,6-tetrahydropyridine: sodium borohydride (4 mmol) was added in portions to a stirred solution of the appropriate N-methyl-4-substituted pyridinium iodide (2 mmol) in 30-150 ml of methanol at 0 °C. The mixture was stirred for an additional 1h at room temperature and the solvent was subsequently removed in vacuo. The residue was taken up in 15 ml of water and the aqueous solution was extracted with diethyl ether (4 × 30 mL). The combined organic layers were dried over $MgSO_4$, filtered, and concentrated to 15% of the original volume. Treatment with oxalic acid (2.4 mmol) in 10 mL of diethyl ether precipitated the crude oxalate salt which was recrystallized from the appropriate solvent.

1-Methyl-4-(3-methylfuran-2-yl)-1,2,3,6-tetrahydropyridine oxalate (103•$H_2C_2O_4$) was recrystallized from ethanol in 66% yield; mp 157-157.5 °C; GC (t_R=11.31 min)-EIMS m/z (%) 177 (100, $M^{+\bullet}$), 176 (76), 162 (13), 148 (22), 134 (20), 119 (28), 105 (20), 95 (30), 83 (41); ^{1}H NMR (DMSO-d_6, 270 MHz) δ 7.53 (d, 1H, C'-5), 6.37-6.38 (d, 1H, C'-4), 5.92 (b, 1H, C-5), 3.73 (d, 2H, C-6), 3.24-3.28 (t, 2H, C-2), 2.77 (s, 3H, NCH_3), 2.70 (m, 2H, C-3), 2.1 (s, 3H, CH_3); ^{13}C NMR (DMSO-d_6, 360 MHz) δ 164.67, 147.04, 140.98, 126.13, 116.73, 115.35, 115.29, 50.94, 49.19, 41.82, 22.98, 11.49; UV (phosphate buffer, pH 7.4) λ_{max} 264 nm (ε=13,204 M^{-1}). Anal Calcd for $C_{13}H_{17}NO_5 \cdot 0.083\ H_2C_2O_4$: C, 57.56; H, 6.30; N, 5.10. Found: C, 57.60; H, 6.35; N, 5.17.

1-Methyl-4-(3-methylthiophen-2-yl)-1,2,3,6-tetrahydropyridine oxalate (105•$H_2C_2O_4$) was recrystallized from methanol/diethyl ether in 98% yield. mp 139-140 °C; GC (t_R=7.57 min)-EIMS m/z (%) 193 (100, $M^{+\bullet}$), 192 (72), 178 (13), 164 (13), 150

(13), 135 (24), 111 (22), 94 (20); ^{1}H NMR (DMSO-d_6, 200 MHz) δ 7.38-7.40 (d, 1H, C'-5), 6.90-6.92 (d, 1H, C'-4). 5.83 (b, 1H, C-5), 3.75-3.77 (d, 1H, C-6), 3.28-3.32 (t, 2H, C-2), 2.79 (s, 3H, NCH_3), 2.67 (b, 2H, C-3), 2.24 (s, 3H, CH_3); ^{13}C NMR (DMSO-d_6, 360 MHz) δ 164.11, 136.35, 133.39, 131.48, 129.10, 123.23, 119.42, 51.36, 49.65, 41.97, 27.17, 15.30; UV (phosphate buffer, pH 7.4) λ_{max} 264 nm (ε=14,211 M^{-1}). Anal Calcd for $C_{13}H_{17}NO_4S$: C, 55.11; H, 6.05; N, 4.94. Found: C, 54.84; H, 6.04; N, 5.00.

4-(3,4-Dimethylpyrrol-1-yl)-1-methyl-1,2,3,6-tetrahydropyridine oxalate (96•$H_2C_2O_4$) was recrystallized from ethanol in 69% yield. mp 152-153 °C; GC (t_R=13.87 min)-EIMS m/z (%) 190 (30, $M^{+\bullet}$), 189 (26), 175 (2), 146 (22), 132 (15), 108 (11), 96 (100); ^{1}H NMR (DMSO-d_6, 270 MHz) δ 6.82 (s, 2H, C'-2 and C'-5), 5.60 (b, 1H, C-5), 3.65 (s, 2H, C-6), 3.26-3.30 (t, 2H, C-2), 2.7 (s, 3H, NCH_3), 1.90 (s, 6H, CH_3); ^{13}C NMR (DMSO-d_6, 360 MHz) δ 164.58, 132.89, 119.16, 115.30, 100.44, 50.14, 49.17, 41.65, 23.22, 9.90; Anal Calcd for $C_{14}H_{20}N_2O_4$: C, 59.98; H, 7.19; N, 9.99. Found: C, 60.04; H, 7.23; N, 10.07.

1-Methyl-4-(3-methylpyrrol-2-yl)-1,2,3,6-tetrahydropyridine oxalate (101•$H_2C_2O_4$) was recrystallized from methanol/diethyl ether in 56% yield. mp 170 °C (decomposed); GC (t_R=7.60 min)-EIMS m/z (%) 176 (91, $M^{+\bullet}$), 175 (67), 161 (41), 132 (46), 118 (78), 94 (100); ^{1}H NMR (DMSO-d_6, 200 MHz) δ 6.61-6.63 (t, 1H, C'-5), 5.89 (b, 1H, C'-4), 5.68 (b, 1H, C-5), 3.74 (s, 2H, C-6), 3.27-3.30 (t, 2H, C-2), 2.79 (s, 3H, NCH_3), 2.69 (m, 2H, C-3), 2.11 (s, 3H, CH_3); ^{13}C NMR (DMSO-d_6, 360 MHz) δ 164.64, 127.86, 126.10, 117.03, 115.54, 112.07, 111.37, 51.15, 49.45, 41.77, 24.24, 13.49; Anal Calcd for $C_{13}H_{18}N_2O_4$: C, 58.63; H, 6.81; N, 10.52. Found: C, 58.46; H, 6.86; N, 10.43.

4-(1,3-Dimethylpyrrol-2-yl)-1-methyl-1,2,3,6-tetrahydropyridine oxalate (102•$H_2C_2O_4$) was recrystallized from methanol/diethyl ether in yield 62%. mp 144 °C (decomposed); GC (t_R=7.10 min)-EIMS m/z (%) 190 (91, $M^{+\bullet}$), 175 (35), 161 (33), 147 (59), 132 (100), 108 (80), 94 (80), 70 (69); ^{1}H NMR (DMSO-d_6, 200 MHz) δ 6.57-6.58 (d, 1H, C'-5), 5.8 (d, 1H, C'-4), 5.60 (s, 1H, C-5), 3.76 (d, 2H, C-6), 3.59 (s, 3H, NCH_3), 3.28-3.34 (t, 2H, C-2), 2.81 (s, 3H, N'CH_3), 1.94 (s, 3H, CH_3); ^{13}C NMR (DMSO-d_6, 360 mHz) δ 164.58, 132.89, 119.16, 115.30, 100.44, 50.14, 49.17, 41.65, 23.22, 9.90; Anal Calcd for $C_{14}H_{20}N_2O_4$: C, 59.98; H, 7.19; N, 9.99. Found: C, 59.88; H, 7.23; N, 9.97.

Oxalate salt of 1-methyl-4-(1-ethylpyrrol-2-yl)-1,2,3,6-tetrahydropyridine (97•$H_2C_2O_4$) was obtained in 80% yield. mp 146.5-147.7 °C; GC (t_R=7.15 min)-EIMS m/z (%). 190 (100, $M^{+\bullet}$), 176 (16), 161 (63), 146 (29), 132 (83), 117 (43), 108 (55), 94 (96); ^{1}H NMR (DMSO-d_6, 200 MHz) δ 6.82 (dd, 1H, C'-5), 6.06 (m, 1H, C'-3), 5.98-6.01 (m, 1H, C'-4), 5.65 (b, 1H, C-5), 3.90-4.0 (q, 2H, N'-CH_2), 3.75 (d, 2H, C-6), 3.26-3.32 (t, 2H, C-2), 2.80 (s, 3H, NCH_3), 2.60 (b, 2H, C-3), 1.22-1.29 (t, 3H, CH_3); ^{13}C NMR (DMSO-d_6, 360 mHz) δ 164.39, 131.22, 127.31, 122.89, 116.13, 108.18, 107.13, 51.19, 49.67, 41.76, 41.66, 26.18, 16.61; Anal. Calcd for $C_{14}H_{20}N_2O_4$•0.15 $H_2C_2O_4$: C, 58.46; H,6.96; N, 9.54. Found: C, 58.49; H, 7.03; N, 9.65.

Oxalate salt of 1-methyl-4-(1-propylpyrrol-2-yl)-1,2,3,6-tetrahydropyridine (98•$H_2C_2O_4$) was obtained in 76% yield . mp 177.5-178 °C; GC (t_R=7.49 min)-EIMS m/z (%) 204 (89, $M^{+\bullet}$), 189 (13), 175 (41), 161 (27), 146 (35), 132 (50), 117 (46), 104 (28), 94 (100); ^{1}H NMR (DMSO-d_6, 200 MHz) δ 6.80-6.82 (dd, 1H, C'-5), 6.06-6.09 (m, 1H, C'-3), 5.98-6.01 (m, 1H, C'-4), 5.65 (b, 1H, C-5), 3.85-3.91 (t, 2H, N'CH_2), 3.75 (d, 2H, C-6), 3.28-3.32 (t, 2H, C-2), 2.80 (s, 3H, NCH_3), 2.60 (b, 2H, C-3), 1.55-1.72 (m, 2H, N'$CHCH_2$), 0.72-0.82 (t, 3H, CH_3); ^{13}C NMR (DMSO-d_6, 360 mHz) δ 164.39, 131.51, 127.45, 123.66, 116.38, 108.22, 106.89, 51.23, 49.71, 48.51, 41.83, 26.35, 24.08, 10.84; Anal. calcd for $C_{15}H_{22}N_2O_4$: C, 61.21; H, 7.53; N, 9.52. Found: C, 61.12; H, 7.49; N, 9.55.

Oxalate salt of 1-methyl-4-(1-isopropylpyrrol-2-yl)-1,2,3,6-tetrahydropyridine (99•$H_2C_2O_4$) was obtained in 91% yield. mp 180-180.5 °C; GC (t_R=7.38 min)-EIMS m/z (%) 204 (100, $M^{+\bullet}$), 189 (20), 175 (24), 161 (39), 146 (46), 133 (17), 118 (30), 104 (14); ^{1}H NMR (DMSO-d_6, 270 MHz) δ 6.94 (s, 1H, C'-5), 6.02-6.03 (m, 1H, C'-4), 6.98 (m, 1H, C'-3), 5.60 (b, 1H, C-5), 4.43-4.48 (m, 1H, N'CH), 3.75 (d, 2H, C-6), 3.30 (t, 2H, C-2), 2.80 (s, 3H, NCH_3), 2.58 (b, 2H, C-3), 1.31-1.34 (d, 6H, CH_3); ^{13}C NMR (DMSO-d_6, 360 mHz) δ 164.39, 132.03, 127.85, 118.41, 118.01, 107.53, 107.17, 51.26, 49.76, 46.71, 41.84, 26.99, 23.87; Anal. Calcd for $C_{15}H_{22}N_2O_4$•0.07 $H_2C_2O_4$: C, 60.50; H,7.42; N, 9.32. Found: C, 60.50; H, 7.44; N, 9.25.

Oxalate salt of 1-methyl-4-(1-cyclopropylpyrrol-2-yl)-1,2,3,6-tetrahydropyridine (100•$H_2C_2O_4$) was obtained in 71% yield. mp 183-183.5 °C; GC (t_R=8.05 min)-EIMS m/z (%) 202 (100, $M^{+\bullet}$), 187 (11), 173 (42), 159 (30), 144 (41), 130

(36), 118 (41), 94 (55); ^{1}H NMR (DMSO-d_6, 270 MHz) δ 6.80 (d, 1H, C'-5), 6.08 (m, 2H, C'-3 and C'-4), 5.93-5.95 (m, 1H, C-5), 3.77 (s, 2H, C-6), 3.38 (m, 1H, N'CH), 3.28-3.32 (t, 2H, C-2), 2.80 (s, 3H, NCH_3), 2.68 (b, 2H, C-3), 0.94-0.98 (m, 2H, CH_2CH_2), 0.86 (m, 2H, CH_2CH_2); ^{13}C NMR (DMSO-d_6, 360 MHz) δ 164.39, 132.70, 126.76, 123.72, 115.25, 108.43, 106.63, 51.28, 49.68, 41.80, 29.96, 25.24, 8.25; Anal. Calcd for $C_{15}H_{20}N_2O_4$: C, 61.63; H, 6.90; N, 9.58. Found: C, 61.53; H, 6.88; N, 9.66.

Oxalate salt of 1-methyl-4-(3-ethylfuran-2-yl)-1,2,3,6-tetrahydropyridine (104•$H_2C_2O_4$) was obtained in 86% yield. mp 148.5-149 °C; GC (t_R=6.96 min)-EIMS m/z (%) 191 (26, $M^{+\bullet}$), 176 (6.5), 162 (6.5), 148 (3.3), 133 (15), 105 (20), 91 (14), 83 (45), 70 (100); ^{1}H NMR (DMSO-d_6, 200 MHz) δ 7.57 (d, 1H, C'-5), 6.47-6.48 (d, 1H, C'-4), 5.92 (b, 1H, C-5), 3.76 (d, 2H, C-6), 3.26-3.29 (t, 2H, C-2), 2.79 (s, 3H, NCH_3), 2.71 (b, 2H, C-3), 2.50-2.51 (m, 2H, CH_2), 1.10-1.17 (t, 3H, CH_3); ^{13}C NMR (DMSO-d_6, 360 MHz) δ 164.32, 146.40, 141.24, 126.36, xx, 115.76, 113.11, 51.01, 49.25, 41.85, 23.09, 18.38, 14.34; Anal. Calcd for $C_{14}H_{19}NO_5$•0.22 H_2O: C, 58.94; H, 6.87; N, 4.91. Found: C, 58.89; H, 6.78; N, 4.91.

Oxalate salt of 1-methyl-4-(3-ethylthiophen-2-yl)-1,2,3,6-tetrahydropyridine (106•$H_2C_2O_4$) was obtained in 90% yield. mp: 162-162.5 °C, GC (t_R=7.13 min)-EIMS m/z (%) 207 (41, $M^{+\bullet}$), 192 (13), 178 (13), 164 (6), 149 (41), 134 (25), 115 (11), 94 (21), 83 (51), 70 (100); ^{1}H NMR (DMSO-d_6, 360 MHz) δ 7.41-7.40 (d, 1H, C'-5), 6.99-6.98 (d, 1H, C'-4), 5.80 (b, 1H, C-5), 3.73 (d, 2H, C-6), 3.28 (b, 2H, C-2), 2.78 (s, 3H, NCH_3), 2.57-2.59 (m, 4H, CH_2 and C-3), 1.13-1.17 9t, 3H, CH_3); ^{13}C NMR (DMSO-d_6, 360 MHz) δ 164.13, 140.07, 136.20, 129.67, 129.07, 123.93, 120.07, 51.60, 49.93, 28.00, 21.87, 15.47; Anal. Calcd for $C_{14}H_{19}NO_4S$: C, 56.55; H, 6.44; N, 4.71. Found: C,56.42; H, 6.45; N, 4.63.

1-methyl-4-(3-methylfuran-2-yl)-2-pyridone (290). To the mixture of 1-methyl-4-(3-ethylfuran-2-yl)pyridinium iodide **266** (1.505 g, 5 mmol) with water (15 mL) at 0 °C, was added the solution of potassium ferricyanide (III) (6 g, 18 mmol 25 mL in water). To this well-stirred mixture was added dropwise a solution of potasium hydroxide (4 g, 7 mmol) in water (7.5 mL) at 0 °C over a period of 1h. Benzene was then added and the reaction mixture was stirred at room temperature for 15h. The two layers were separated and the aqueous layer was extracted with benzene (10 mL × 4). The extracts

were dried over $MgSO_4$ and the solvent was removed in vacuo. The residue was recrystallized in benzene/ether, 0.528 g of white solid was obtained (55%). mp: 137-138 °C; GC (t_R=8.77 min)-EIMS m/z (%) 189 (100, $M^{+\bullet}$), 161 (56), 160 (58), 146 (11), 132 (63), 117 (26), 91 (24), 77 (13); ^{1}H NMR ($CDCl_3$, 200 MHz) δ 7.41-7.42 (d, 1H, C'-5), 7.26-7.30 (d, 1H, C-6), 6.74-6.75 (d, 1H, C-3), 6.53-6.57 (dd, 1H, C-5), 6.35 (d, 1H, C'-4), 3.55 (s, 3H, NCH_3), 2.30 (s, 3H, CH_3); ^{13}C NMR ($CDCl_3$, 360 MHz) δ 163.42, 145.42, 142.77, 141.91, 138.14, 122.19, 116.17, 113.75, 103.43, 37.51, 12.62; Anal. Calcd for $C_{11}H_{11}NO_2$: C, 69.83; H, 5.86; N, 7.40. Found: C, 69.66; H, 5.96; N, 7.33.

4-(2-furanyl)pyridine (301). To furan (3.7 mL. 50 mmol) in 10 mL dry THF, was add *sec*-butyllithium (30 mL, 40 mmol) dropwise at 0 °C. The mixture was stirred at room temperature for 1.5h and was transfered to the solution of $ZnCl_2$ (5.5 g, 40 mmol) in THF (20 mL). The mixture was stirred at room temperature for 2h and transfered to the mixture of tetrakis(triphenylphosphine)palladinium (0) (1.2 g) and 4-bromopyridine (30 mmol) in THF (15 mL). The mixture was stirred at 40 °C under nitrogen for 16h and quenched with water. The water layer was adjusted to pH = 8 and extracted with ethyl acetate (4 × 30 mL). The extracts were dried over MaSO4 and the solvent was removed in vacuo. Column chromatography (silca gel, ethyl acetate) of the residue afforded **301** as a white solid (64%). mp: 71 °C; GC (t_R=6.10 min)-EIMS m/z (%) 145 (100, $M^{+\bullet}$), 116 (47), 90 (40), 89 (42), 63 (42); ^{1}H NMR ($CDCl_3$, 200 MHz) δ 8.57-8.60 (dd, 2H, C-2 and C-6), 7.49-7.52 (dd, 2H, C-3 and C-5), 7.53-7.54 (m, 1H, C'-5), 6.86-6.88 (d, 1H, C'-3), 6.50-6.53 (dd, 1H, C'-4).

1-Methyl-4-(2-furanyl)-2-pyridone (291). The 1-methyl-4-(2-furanyl)pyridinium iodide **289** reacted with potassium hydroxide and potasium ferricyanide (III) using the same method as the synthesis of **290** with a yield of 64%. mp: 171.5-172 °C; GC (t_R=8.18 min)-EIMS m/z (%) 175 (100, $M^{+\bullet}$), 147 (37), 146 (33), 118 (53), 104 (13), 91 (11), 77 (11); ^{1}H NMR ($CDCl_3$, 200 MHz) δ 7.54-7.55 (d, 1H, C'-5), 7.27-7.30 (d, 1H, C-6), 6.85-6.86 (d, 1H, C-3), 6.79-6.81 (d, 1H, C'-3), 6.50-6.53 (dd, 1H, C'-4), 6.43-6.48 (dd, 1H, C-5), 3.55 (s, 3H, CH_3); ^{13}C NMR ($CDCl_3$, 360 MHz) δ 163.41, 150.72, 140.65, 138.48, 112.75, 112.36, 111.70, 110.04, 102.42, 37.55;

1-Methyl-4-(3-methylfuran-2-yl)-3,6-dihydro-2-pyridone (292). To the stirred solution of **290** (0.64 g, 3.38 mmol) in dry THF (15 mL) at -78 °C, was added dropwise LS-Selectride (8 mmol) in THF. The temperature was raised to room temperature slowly and the solution was stirred for 12h. The temperature was droped

again to -78 °C, a saturated NaCl solution (5 mL) was added. After the temperature was raised to 0 °C, an aqueous solution of 30% hydrogen peroxide (10 mL) was added slowly followed by 3M NaOH (5 mL). The aqueous layer was extracted with ethyl ether (30 mL × 3) and the combined organic layer was washed with saturated NaCl solution, dried over $MgSO_4$. The solvent was removed in vacuo to give the purified white solid in 100% yield. mp 100.5-101 °C; GC (t_R=8.31 min)-EIMS m/z (%) 191 (100, $M^{+\bullet}$), 176 (11), 162 (74), 148 (34), 134 (54), 120 (36), 91(43), 77 (35); ^{1}H NMR ($CDCl_3$, 200 MHz) δ 7.26 (b, 1H, C'-5), 6.24-6.23 (d, 1H, C'-4), 5.97 (m, 1H, C-5), 4.13-4.06 (d, 2H, C-3), 3.32-3.38 (dt, 2H, C-6), 3.04 (s, 3H, NCH_3), 2.17 (s, 3H, CH_3); ^{13}C NMR ($CDCl_3$, 360 MHz) δ 167.14, 147.14, 140.73, 125.71, 118.00, 115.28, 114.74, 51.11, 34.08, 32.82, 12.00; Anal. Calcd for $C_{11}H_{13}NO_2$: C, 69.09; H, 6.85; N, 7.32. Found: C, 68.99, H, 6.88, N, 7.33.

1-Methyl-4-(3-methylfuran-2-yl)-5,6-dihydro-2-pyridone (294). To a stirred solution of **292** (0.382 g, 2 mmol) in tert-butanol (10 mL), was added potassium *tert*-butoxide (0.672 g, 6 mmol). After the mixture was stirred for 1 day at room temperature, hydrochloric acid (600 ml, 37%) was added followed by water (15 mL). The aqueous layer was extracted by ethyl acetate (20 mL × 4). The extracts were washed with saturated NaCl solution and Na_2CO_3 solution, dried over $MgSO_4$ and the solvent was removed in vacuo to give 0.39 g of **294** (99%). mp: 113-114 °C; GC (t_R= min)-EIMS m/z (%) 191 (100, M), 163 (13), 148 (36), 134 (9), 120 (49), 91 (51), 77 (11); ^{1}H NMR ($CDCl_3$, 360MHz) δ 7.34-7.35 (d, 1H, C'-5), 6.29-6.30 (m, 1H, C'-4), 6.09 (s, 1H, C-5), 3.43-3.48 9t, 2H, C-2), 3.00 (s, 3H, NCH_3), 2.78-2.82 (dt, 2H, C-3), 2.21 (s, 3H, CH_3); ^{13}C NMR ($CDCl_3$, 360 MHz) δ 165.97, 146.39, 142.29, 139.92, 122.16, 116.79, 115.97, 47.30, 34.48, 24.74, 12.65.

The general method for the synthesis of the oxalate salt of deuteride 1-methyl-4-substituted-1,2,3,6-tetrahydropyridine. To the stirred solution of 2-pyridone (1 mmol) in diethyl ether (25 mL), was added the $LiAlD_4$ (2 mmol). The mixture was stirred and heated to reflux for 1.5h. The mixture was then cooled with ice water. 25 mL of ice water was added to the mixture slowly. The water layer was extracted with diethyl ether (30 mL × 3). The extracts were dried over $MgSO_4$ and the solvent was removed in vacuo. To the residue in diethyl ether (15 mL), was added a solution of oxalic acid (1.5 eq.) in ether (10 mL) while stirring. The precipitate was filtered and recrystallized in methanol/ether.

Oxalate salt of 1-methyl-4-(3-methylfuran-2-yl)-1,2,3,6-tetrahydropyridine-6,6-d2 (296•$H_2C_2O_4$), was obtained in 98% yield. mp 156.5-157 °C; GC (t_R=6.52 min)-EIMS m/z (%) 179 (100, $M^{\bullet+}$), 164 (9), 150 (26), 136 (22), 121 (37), 107 (28), 93 (43), 84 (43), 83 (39), 77 (36); ^{1}H NMR (DMSO-d_6, 200 MHz) δ 7.54-7.55 (d, 1H, C'-5), 6.39-6.40 (d, 1H, C'-4), 5.92 (b, 1H, C-5), 3.25-3.31 (t, 2H, C-2), 2.78 (s, 3H, NCH3), 2.68-2.74 (t, 2H, C-5), 2.12 (s, 3H, CH3); Anal. Calcd for $C_{13}D_2H_{15}NO_5$: C, 57.98; H+D, 7.11; N, 5.20. Found: C, 58.10; H+D, 6.40; N, 5.14.

Oxalate salt of 1-methyl-4-(2-furanyl)-1,2,3,6-tetrahydropyridine-6,6-d2 (297•$H_2C_2O_4$), was obtained in 96% yield. mp: °C; GC (t_R=5.98 min)-EIMS; 165 (100, $M^{+\bullet}$), 146 (4), 136 (30), 122 (25), 96 (16), 93 (50), 83 (30); ^{1}H NMR (DMSO-d_6, 270 MHz) δ 7.68 (s, 1H, C'-5), 6.53 (s, 2H, C'-4 and C'-3), 6.09 (s, 1H, C-5), 3.29-3.34 (t, 2H, C-2), 2.80 (s, 3H, NCH_3), 2.61-2.65 (m, 2H, C-3); Anal. Calcd for $C_{10}D_2H_{11}NO$: C, ; H+D, ; N, . Found: C, ; H, ; N, .

Oxalate salt of 1-methyl-4-(3-methylfuran-2-yl)-1,2,3,6-tetrahydropyridine-2,2-d2 (298•$H_2C_2O_4$), was obtained in 96% yield. mp 158-159 °C; GC (t_R=6.54 min)-EIMS m/z (%) 179 (100, $M^{\bullet+}$), 164 (11), 150 (17), 134 (16), 119 (28), 105 (23), 95 (28), 91 (37), 85 (41), 77 (14), 72 (39); ^{1}H NMR (DMSO-d_6, 200 MHz) δ 7.53-7.54 (d, 1H, C'-5), 6.38-6.39 (d, 1H, C'-4), 5.94 (b, 1H, C-5), 3.75 (b, 2H, C-6), 2.78 (s, 3H, NCH_3), 2.70 (b, 2H, C-3), 2.12 (s, 3H, CH_3); Anal. Calcd for $C_{13}H_{15}D_2NO_5$: C, 57.98; H, 7.11; N, 5.20. Found: C, 57.89; H, 6.35; N, 5.23.

1-Methyl-4-(3-methylfuran-2-yl)pyridinium iodide-1,1,1-d3 (289). To the 1-methyl-4-(3-methylfuran-2-yl)pyridine **301** (1 mmol) in acetone, was added iodomethane-d3 (4 mmol). This mixture was stirred overnight at room temperature. The precipitate was filtered and recrystallized in methanol/ether with yield 84%. mp 204-204.5 °C; ^{1}H NMR (DMSO-d_6, 200 MHz) δ 8.82-8.87 (dd, 2H, C-2 and C-6), 8.11-8.15 (d, 2H, C-3 and C-5), 8.08-8.09 (d, 1H, C'-5), 6.78-6.79 (d, 1H, C'-4), 2.50 (s, 3H, CH_3); Anal. Calcd for $C_{11}H_9D_3INO$: C, 43.44; H+D, 4.97; N, 4.60. Found: C, 43.39; H+D, 3.93; N, 4.65.

Oxalate salt of 1-Methyl-4-(3-methylfuran-2-yl)-1,2,3,6-tetrahydropyridine-1,1,1-d_3 (303). To 24 (0.5 mmol) in methanol (15 mL) at 0 °C, was added the sodium borohydride (1.0 mmol) in protions. The mixture was stirred at 0°C for 1h and then for another 1h at room temperature. The solvent was removed in vacuo.

The residue was taken up in 15 mL of water and the aqueous solution was extracted with diethyl ether (4 × 20 mL). The extracts were dried over $MgSO_4$, filtered and concentrated to 15 mL. Treatment with oxalic acid (0.5 mmol) in 10 mL of diethyl ether precipitated the oxalate salt which was recrystallized from methanol/ether to give **303** in 97% yield. mp: 158-158.5 °C; GC (t_R=6.5 min)-EIMS m/z (%) 180 (100, $M^{+\bullet}$), 165 (13), 151 (27), 137 (15), 119 (28), 105 (26), 97 (28), 95 (26), 91 (45), 86 (45), 77 (28), 73 (42); ^{1}H NMR (DMSO-d_6, 200 MHz) δ 7.54 (d, 1H, C'-5), 6.40 (d, 1H, C'-4), 5.94 (b, 1H, C-5), 3.79 (b, 2H, C-6), 3.27-3.33 (t, 2H, C-2), 2.72 (b, 2H, C-3), 2.11 (s, 3H, CH_3); Anal. Calcd for $C_{13}D_3H_{14}NO_5$: C, 57.77; H +D, 7.46; N, 5.18. Found: C, 57.85; H +D, 6.30, N, 5.11

(*S*)-1-[4,5-dihydro-4-(1-methylethyl)-2-oxazolyl]-4-phenyl-1,2,3,6-tetrahydropyridine (354). To a solution of 4-phenyl-1,2,3,6-tetrahydropyridine (3.0 g, 18.7 mmol) in benzene (50 mL), was added (*S*)-2-ethoxy-4,5-dihydro-4-(1-methylethyl)oxazole (3.1 g, 19.7 mmol) and 0.05 g p-toluenesulfonic acid. The mixture was stirred at 50 °C overnight. The solvent was removed in vacuo. The residue was dissolved in diethyl ether. The organic solution was washed with saturated sodium bicarbonate solution and dried over $MgSO_4$ and the solvent was removed in vacuo. The solid was recrystallized in cold ether. 4.85 g white solid was obtained in 96% yield. mp: 65-65.5 °C; GC (t_R=9.78 min)-EIMS m/z (%) 270 (9, $M^{+\bullet}$), 227 (100), 198 (4), 156 (6), 115 (13), 97 (58); ^{1}H NMR ($CDCl_3$, 360 MHz) δ 7.26-7.37 (m, 5H, ArH), 6.02-6.06 (m, 1H, C-5), 4.25-4.30 (t, 1H, C'-5), 4.05-4.08 (m, 1H, C-6), 3.98-4.00 (t, 1H, C'-5), 3.77-3.85 (m, 1H, C'-4), 3.54-3.68 (m, 2H, C-2), 2.54-2.58 (m, 2H, C-3), 1.66-1.77 (m, 1H, C'-6), 0.85-0.97 (dd, 6H, CH_3); ^{13}C NMR ($CDCl_3$, 360 MHz) δ 161.16, 140.94, 135.41, 128.57, 127.40, 125.11, 120.91, 70.80, 70.45, 45.61, 42.50, 33.61, 27.28, 19.22, 17.95. Anal. Calcd for $C_{17}H_{22}N_2O$: C, 75.52; H, 8.20; N, 10.36. Found: C, 75.40; H, 8.25; N, 10.37.

(*R*)-1-[4,5-dihydro-4-(1-methylethyl)-2-oxazolyl]-4-phenyl-1,2,3,6-tetrahydropyridine (354). The solid was recrystallized in cold ether. 4.85 g white solid was obtained in 96% yield. mp: 65-65.5 °C; GC (t_R=9.78 min)-EIMS m/z (%) 270 (9, $M^{+\bullet}$), 227 (100), 198 (4), 156 (6), 115 (13), 97 (58); ^{1}H NMR ($CDCl_3$, 360 MHz) δ 7.21-7.37 (m, 5H, ArH), 6.02-6.05 (m, 1H, C-5), 4.23-4.28 (t, 1H, C'-5), 4.03-4.06

(m, 1H, C-6), 3.97-4.00 (t, 1H, C'-5), 3.77-3.83 (m, 1H, C'-4), 3.54-3.67 (m, 2H, C-2), 2.54-2.56 (m, 2H, C-3), 1.64-1.73 (m, 1H, C'-6), 0.83-0.95 (dd, 6H, CH_3); ^{13}C NMR ($CDCl_3$, 360 MHz) δ 161.16, 140.94, 135.42, 128.59, 127.40, 125.11, 120.91, 70.80, 70.45, 45.61, 42.50, 33.61, 27.28, 19.22, 17.93. Anal. Calcd for $C_{17}H_{22}N_2O$: C, 75.52; H, 8.20; N, 10.36. Found: C, 75.64; H, 8.20; N, 10.38.

Diastereomeric mixture of 1-[4,5-dihydro-4-(1-methylethyl)-2-oxazolyl]-4-phenyl-1,2,3,4-tetrahydropyridine-4-d_1 (357). To the (*S*)-**354** (2.16 g, 8 mmol) in 50 mL dry THF at -78 °C, was added n-butyllthium (3.6 mL, 8.8 mmol) dropwise. The mixture was stirred at this temperature for 20 min. DMSO-d_6 (99.9%, 2 g) was added. The mixture was stirred at -78 °C for 20 min and then warmed to room temperature and diluted with brine. The aqueous layer was extracted with diethyl ether (30 mL × 3). The extracts were dried over $MgSO_4$ and the solvent was removed in vacuo. The residue was purified through column (chloroform:methanol=10:1). A yellow oil was obtained in 98% yield. GC (t_R=10.30 min) m/z (%) 271 (6, $M^{+\bullet}$), 228 (100), 200 (3), 159 (11), 116 (24), 92 (8); ^1H NMR ($CDCl_3$, 360 MHz) δ 7.19-7.39 (m, 5H, ArH), 6.85-6.88 (dd, 1H, C-6), 4.81-4.84 (dd, 1H, C-5), 4.31-4.36 (t, 1H, C'-5), 4.02-4.07 (dt, 1H, C'-5), 3.80-3.87 (m, 1H, C'-4), 3.58-3.75 (m, 2H, C-2), 2.12-2.17 (m, 1H, C-3), 1.80-1.86 (m, 1H, C-3), 1.67-1.76 (m, 1H, C'-6), 0.86-0.98 (dd, 6H, CH_3); ^{13}C NMR ($CDCl_3$, 360 MHz) δ 158.06, 145.65, 128.60, 127.91, 127.84, 126.91, 126.89, 125.14, 106.35, 106.11, 71.36, 71.25, 70.56, 42.17, 41.81, 33.65, 33.55, 31.21, 31.03, 19.25, 19.21, 18.18, 18.08.

***(S,S)*-enriched 1-[4,5-dihydro-4-(1-methylethyl)-2-oxazolyl]-4-phenyl-1,2,3,6-tetrahydropyridine-6-d_1 (363).** To the (*S*)-1-[4,5-dihydro-4-(1-methylethyl)-2-oxazolyl]-4-phenyl-1,2,3,6-tetrahydropyridine (2.16 g, 8 mmol) in 50 mL dry THF at -78 °C, was added n-butyllithium (3.6 mL, 8.8 mmol) dropwise. The mixture was stirred at this temperature for 20 min. D_2O (100%, 2 g) was added. The mixture was stirred at this temperature for 30 min and warmed to room temperature and brine was added. The aqueous layer was extracted with diethyl ether (30 mL× 3). The extracts were dried over $MgSO_4$ and the solvent was removed in vacuo. The residue was separated by column (silica gel, chloroform:methanol:triethylamine=100:5:5). A white solid was obtained in 60% yield. GC (t_R=9.48)-EIMS m/z (%) 271 (9, $M^{+\bullet}$), 228 (100), 199 (4),

144 (6), 129 (8), 97 (60); ^{1}H NMR ($CDCl_3$, 360 MHz) δ 7.24-7.35 (m, 5H, ArH), 6.03-6.04 (m, 1H, C-5), 4.24-4.31 (t, 1H, C'-5), 3.97-4.03 (m, 2H, C-6 and C'-5), 3.77-3.83 (m, 1H, C'-4), 3.53-3.65 (m, 2H, C-2), 2.55-2.56 (b, 2H, C-3), 1.64-1.73 (m, 1H, C'-6), 0.83-0.95 (dd, 6H, CH_3); ^{13}C NMR ($CDCl_3$, 360 MHz) δ 161.19, 140.95, 135.51, 128.60, 127.43, 125.14, 120.84, 70.82, 70.40, 42.52, 33.61, 27.28, 19.22, 17.94.

Oxalate salt of the *R*- or *S*-enriched 1-methyl-4-phenyl-1,2,3,6-tetrahydropyridine-6-d$_1$ (369•$H_2C_2O_4$). (*R, R*)- or (*S, S*)-enriched 1-[4,5-dihydro-4-(1-methylethyl)-2-oxazolyl]-4-phenyl-1,2,3,6-tetrahydropyridine-6-d_6 (0.54 g, 2 mmol) was dissolved in THF (5 mL) with 0.5 g of anhydrous Na_2CO_3. Acetic formic anhydride (15 eq.) was added to the solution slowly. The reaction mixture was stirred at room temperature overnight. After concentrated in vacuo, the residue was dissolved in ether, washed with saturated sodium bicarbonate solution. The ether solution was dried with $MgSO_4$ and the solvent was removed in vacuo. The residue in 1 mL THF was added to the mixture of $LiAlH_4$ in THF (10 mL). The solution was stirred at room temperature for 4h. After cooling to 0 °C, the reaction was quenched with water (0.5 mL), 20% NaOH (0.5 mL), and water (1 mL). After filteration, the cake was washed with ether (3 × 10 mL). The ether solution was dried with MgSO4 and the solvent was removed. The residue was purified through column (chloroform : triethylamine=100:5). A white solid was obtained. To this solid in dry diethyl ether (5 mL), was added oxalic acid (1 eq.) solution in diethyl ether. The precipitate was filtered and recrystallized in methanol/ether. A white solid was obtained in 45% yield. mp: 161 °C; ^{1}H NMR (DMSO-d_6, 360 MHz) δ 7.28-7.52 (m, 5H, ArH), 6.18 (s, 1H, C-5), 3.75 (s, 1H, C-6), 3.31-3.67 (t, 2H, C-2), 2.81 (s, 3H, CH_3), 2.75-2.77 (b, 2H, C-3).

The general methods for the synthesis of the oxalate salts of 1-cyclopropyl-4-substituted-1,2,3,6-tetrahydropyridines. To a solution of the 1-chloro-2,4-dinitrobenzene (0.40 g, 2 mmol) in dry acetone (10 mL) was added the 4-substituted pyridine (2 mmol). The mixture was stirred under reflux overnight. The solid was filtered and washed with cold acetone. This solid was dissolved in 1-butanol (20-50 mL). Cyclopropylamine was added dropwise at room temperature. The mixture was stirred at room temperature for 1h and refluxed overnight. The solvent was removed in vacuo. An aqueous solution (30 mL) containing the residue was washed with ethyl acetone. The water was removed in vacuo. The residue was dissolved in methanol (15

mL). To this solution at 0 °C, was added $NaBH_4$ (5 eq.) in portions. The solution was stirred at 0 °C for 1h and at room temperature for 3h. The solvent was removed in vacuo. The residue was dissolved in water (15 mL). The aqueous solution was extracted with diethyl ether (30 mL × 3). The extracts were dried over $MgSO_4$ and the solvent was removed in vacuo. The residue was purified through column (silica gel, ethyl acetate) and a yellow oil was obtained. To this yellow oil in diethyl ether (5 mL), was added the solution of oxalic acid (1 eq.) in dithyl ether. The precipitate was filtered and recrystallized in methanol/ether. A solid was obtained.

Oxalate salt of 1-cyclopropyl-4-(3-methylfuran-2-yl)-1,2,3,6-tetrahydropyridine (386•$H_2C_2O_4$) was obtained in 42%. mp: 156.5-157 °C; GC(t_R=7.58 min)-EIMS m/z (%) 203 (49, $M^{+\bullet}$), 188 (100), 160 (7), 146 (16), 119 (16), 105 (18), 91 (40), 77 (27); ^{1}H NMR (DMSO-d_6, 200Mhz) δ 7.48-7.49 (d, 1H, C'-5), 6.34-6.35 (d, 1H, C'-4), 5.92 (b, 1H, C-5), 3.58 (d, 2H, C-6), 3.08-3.15 (t, 2H, C-2), 2.58 (b, 2H, C-3), 2.32 (m, 1H, NCH), 2.09 (s, 3H, CH_3), 0.62-0.65 (m, 4H, $NCHCH_2$); Anal. Calcd for $C_{15}H_{19}NO_5$: C, 61.42; H, 6.53; N, 4.78. Found: C, 61.36; H, 6.52; N, 4.84.

Oxalate salt of 1-cyclopropyl-4-(3-methylthien-2-yl)-1,2,3,6-tetrahydropyridine (387•$H_2C_2O_4$) was obtained in 51% yield. mp: 152°C; GC (t_R=7.96 min)-EIMS m/z (%) 219 (53, $M^{\bullet+}$), 204 (100), 190 (3), 162 (11), 149 (19), 135 929), 111 913), 91 (18); ^{1}H NMR (DMSO-d_6, 360 MHz) δ 7.68-7.69 (d, 1H, C'-5), 7.33-7.34 (d, 1H, C'-4), 5.83 (b, 1H, C-5), 3.60-3.64 (b, 2H, C-6), 3.19 (b, 2H, C-2), 2.56 (b, 2H, C-3), 2.28 (b, 1H, NCH), 2.22 (s, 3H, CH_3), 0.65-0.74 (m, 4H, $NCHCH_2$); ^{13}C NMR (DMSO-d_6, 360 MHz) δ 163.13, 136.00, 132.11, 131.47, 129.21, 124.07, 122.90, 121.32, 51.26, 49.38, 37.76, 28.48, 15.35, 4.43.

Oxalate salt of 1-cyclopropyl-4-(1-cyclopropylpyrrol-2-yl)-1,2,3,6-tetrahydropyridine (384•$H_2C_2O_4$) was obtained in 70%. mp: 144.5-145.5 °C; GC (t_R=8.68 min)-EIMS m/z (%) 228 (56, $M^{+\bullet}$), 213 (100), 199 (4), 170 (20), 144 (36), 130 (470, 117 (44), 106 (24), 91 (30), 77 (40); ^{1}H NMR (DMSO-d_6, 200 MHz) δ 6.76 (m, 1H, C'-5), 6.02 (m, 2H, C'-4 and C'-5), 5.91-5.93 (m, 1H, C'-3), 3.64 (b, 2H, C-6), 3.31-3.42 (m, 1H, N'CH), 3.17 (t, 2H, C-2), 2.56 (b, 2H, C-3), 2.32-2.45 (m, 1H,

NCH), 0.86-0.98 (m, 4H, N'CHCH$_2$), 0.68 (m, 4H, NCHCH$_2$); Anal. Calcd for $C_{17}H_{22}N_2O_4$: C, 64.13; H, 6.96; N, 8.80; Found: C, 64.05; H, 6.94; N, 8.74.

Oxalate salt of 1-cyclopropyl-4-(3-methylpyrrol-2-yl)-1,2,3,6-tetrahydropyridine (383•$H_2C_2O_4$) was obtained in 64% yield. mp: 165 °C (decomposed); GC (t_R=8.41 min)-EIMS m/z (%) 202 (60, $M^{+\bullet}$), 187 (100), 159 (7), 150 (27), 130 (28), 118 (40), 106 (13), 94 (24), 80 (18); ^{1}H NMR (DMSO-d6, 270 MHz) δ 10.52 (s, 1H, N'H), 6.60 (m, 1H, C'-5), 5.85 (s, 1H, C'-4), 5.67 (b, 1H, C-5), 3.65 (b, 2H, C-6), 3.20 (m, 2H, C-2), 2.59 (b, 2H, C-3), 2.49 (b, 1H, NCH), 0.66-0.74 (m, 4H, NCHCH$_2$); Anal. Calcd for $C_{15}H_{20}N_2O_4$: C, 61.63; H, 6.90; N, 9.58. Found: C, 61.55; H, 6.93; N, 9.48.

Oxalate salt of 1-cyclopropyl-4-(3,4-dimethylpyrrol-1-yl)-1,2,3,6-tetrahydropyridine (385•$H_2C_2O_4$) was obtained in 70% yield. mp: 157-157.5 °C; GC (t_R=8.56 min)-EIMS m/z (%) 216 (58, $M^{+\bullet}$), 201 (100), 180 (4), 160 (31), 146 (38), 132 (29), 122 (22), 108 (22), 94 (36), 80 (20); ^{1}H NMR (DMSO-d6, 270 MHz) δ 6.77 (s, 2H, C'-2 and C'-5), 5.58 (s, 1H, C-5), 3.43 (b, 2H, C-6), 3.07 (t, 2H, C-2), 2.57 (b, 2H, C-3), 2.15-2.22 (m, 1H, NCH), 0.57-0.59 (d, 4H, NCHCH$_2$); Anal. Calcd for $C_{16}H_{22}N_2O_4$: C, 62.73; H, 7.24; N, 9.14. Found: C, 62.47; H, 7.25; N, 9.04.

Oxalate salt of 1-cyclopropyl-4-(1,3-dimethylpyrrol-2-yl)-1,2,3,6-tetrahydropyridine (382•$H_2C_2O_4$) was obtained in 59% yield. mp: 161°C; GC (t_R=7.93 min)-EIMS m/z (%) 216 (67, $M^{+\bullet}$), 201 (100), 187 (2), 160 (22), 146 (24), 132 (47), 108 (53), 91 (18); ^{1}H NMR (DMSO-d_6, 270 MHz) δ 6.55-6.56 (d, 1H, C'-5), 5.78 (d, 1H, C'-4), 5.58 (b, 1H, C-5), 3.69 (s, 2H, C-6), 3.42 (s, 3H, NCH3), 3.21-3.26 (t, 2H, C-2), 2.41 (b, 2H, C-3), 1.93 (s, 3H, CH3), 0.68-0,82 (m, 4H, NCHCH$_2$); Anal. Cacld for $C_{16}H_{22}N_2O_4$: C, 62.73; H, 7.24; N, 9.14. Found: C, 62.47; H, 7.19; N, 9.01.

Enzyme studies

MAO-B was isolated from bovine liver mitochondria according to the method of Salach and Weyler.[192] The activity was determined spectrophotometrically at 30 °C on a Beckman 7400 series spectrophotometer using 5 mM MPTP as a substrate and recording initial rates (120s) of formation of the dihydropyridinium metabolite (λ_{max}=343 nm, e=16,000 M^{-1}) as described previously.[193] The final enzyme concentration was calculated

to be 9 nmol/mL.

All enzyme assays were performed at 37 °C on a Beckman DU 7400 spectrophotometer. The substrate properties of each test compound (50 μM-1000 μM) were first examined by recording repeated scans (300 to 500 nm) in the presence of MAO-B. For kinetic studies, initial rates of oxidation of the tetrahydropyridinyl analogs were determined at four substrate concentrations. Solutions (ranging from 25 to 1400 mM) of the substrates were prepared in 100 mM sodium phosphate buffer (pH=7.4). A 480-495 mL aliquot of each solution was added to the sample cuvette which was placed in the spectrophotometer and maintained at 37 °C. After a 3 min equilibration period, 5 mL of the MAO-B enzyme preparation was added (final MAO-B concentration was 0.09 mM). For compound **107** and **297**, 20 mL MAO-B enzyme-B preparation was added (final MAO-B enzyme concentration was 0.36 mM). The rates of oxidation of each substrate were estimated by monitoring the absorbance of the corresponding dihydropyridium metabolite every 5 sec for 2 min (for compound **107** and **297**, the time is 5 min). The K_m and k_{cat} values were calculated from Lineweaver-Burk double-reciprocal plots.

The preparation of ^{2}H NMR samples

A total of 100 mg of [(poly(γ-benzyl L-glutamate)] (PBLG, DP 1352, MW 296, 000 from Sigma) was weighed directly into a 5 mm NMR tube. A solution of 15-20 mg of the compound dissolved in 600-650 mg of CH_2Cl_2 was added. The NMR tube was plugged and centrifuged back and forth until an optically homogeneous mixture was obtained. After a few minutes in the field a deuterium spectrum was measured with proton broad-band decoupling. The measureing temperature was 39 °C.

Chapter 7 References

(1) Zubay, G. L. In *Biochemistry*; 4Ed, Worthington, R., Ed.:McGraw-Hill Companies, Inc.: Dubuque,**1998**.

(2) Dugas, H. In *Bioorganic Chemistry*; Cantor, C. R., Ed.; Springer: New Youk, **1996**.

(3) Gaál, J.; Hermecz, I. In *Inhibitors of Monoamine Oxidase B: Pharmaclogy and Clinical Use in Neurodegenerative Disorders*; Szelenyi, I., Ed.: Birkhauser: Boston; Berlin, **1993**.

(4) Silverman, R. B. *Methods in Enzymol*., **1995**, *249*, 240.

(5) Silverman, R. B. *Acc. Chem. Res*., **1995**, *28*, 335.

(6) Silverman, R. B. In *The Organic Chemistry of Drug Design and Drug Action*; Academic press: London, **1992**.

(7) Bach, A. W. J.; Lan, N. C.; Johnson, D. L.; Abell, C. W.; Bembenek, M. E.; Kwan, S. W.; Seeburg, P. H.; Shih, J. C. *Proc. Natl. Acad. Sci*. U.S.A., **1988**, *85*, 4934.

(8) Grimsby, J.; Chen, K.; Wang, L. J.; Lan, N. C.; Shih, J. C. *Proc. Natl. Acad. Sci*., U.S.A., **1991**, *88*, 3637.

(9) Knoll, *J. Med. Res. Rev*. **1992**, *12*, 505.

(10) Ives, J. L.; Heym, *J. Annu. Rep. Med. Chem*. **1989**, *24*, 21.

(11) Rinne, U. K. *J. Neural transm*. **1987**, *25* (suppl.), 149.

(12) Tetrud, V. W.; Langston, J. W. *Science* **1989**, *245*, 519.

(13) Kearney, E. B.; Salach, J. I.; Walker, W. H.; Seng, R. L.; Kenney, W.; Zeszotek, R.; Singer, T. P. *Eur. J. Biochem*. **1971**, *24*, 321.

(14) Yu, P. H. *Can. J. Biochem*., **1981**, *59*, 30.

(15) Wu, H. F.; Chen, K.; Shih, J. C. *Mol. Pharmacol*. **1993**, *43*, 888.

(16) Tan, A.; Glantz, M. D.; Piette, L. H.; Yasunobu, K. T. *Biochem. Biophys. Res. Commun*., **1983**, *117*, 517.

(17) Husain, M.; Edmondson, D. E.; Singer, T. P. *Biochemistry*, **1982**, *21*, 595.

(18) Simpson, J. T.; Krantz, A.; Lewis, F. D.; Kokel, B. *J. Am. Chem. Soc*., **1982**, *104*, 7155.

(19) Krantz, A.; Kokel, B.; Sachdevu, Y.P.; Salach, J.; Detmer, K.; Claesson, A.; Sahlberg, C. In *Monoanine Oxidase: Structure, Function, and Altered Functions*; Singer, T. P.; Von Korff, R. W.; Murphy, D. L.; eds.; Academic Press: New York, **1979**; p51.

(20) Maeda, Y.; Ingold, K. U. *J. Am. Chem. Soc*., **1980**, *102*, 328.

(21) Silverman, R. B.; Hoffman, S. J. *J. Am. Chem. Soc*., **1980**, *102*, 884.

(22) Silverman, R. B.; Hoffman, S. J. *Biochem. Biophys. Res. Commun*., **1981**, *101*, 1396.

(23) Silverman, R. B.; Yamasaki, R. B. *Biochemistry*, **1984**, *23*, 1322.

(24) Silverman, R. B.; Zieske, P. A. *Biochemistry*, **1985**, *24*, 2128.

(25) Yamasaki, R. B.; Silverman, R. B. *Biochemistry*, **1985**, *24*, 6543.

(26) Silverman, R. B.; Zieske, P. A. *Biochem. Biophys. Res. Commun*., **1986**, *135*, 154.

(27) Silverman, R. B.; Cesarone, J. M.; Lu, X. *J. Am. Chem. Soc*. **1993**, *115*, 4955.

(28) Pettit, G. R.; Van Tamelen, E. E. *Org. React*. (N. Y.) **1962**, *12*, 356.

(29) Danenberg, P. V.; Heidelberg, C. *Biochemistry* **1976**, *15*, 1331.

(30) Zhong, B. Y.; Silverman, R. B. *J. Am. Chem. Soc*. **1997**, *119*, 6690.

(31) Silverman, R. B.; Zieske, P. A. *Biochemistry*, **1986**, *25*, 341.

(32) Wilt, J. W.; Maravetz, L. L.; Zawadzki, J. F. *J. Org. Chem*. **1966**, *31*, 3018.

(33) Menapace, L. W.; Kuivila, H. G. *J. Am. Chem. Soc*. **1964**, *86*, 3047.

(34) Tanner, D. D.; Rahimi, R. M. *J. Org. Chem*. **1979**, *44*, 1674.

(35) Yelekci, K.; Lu, X.; Silverman, R. B. *J. Am. Chem. Soc*. **1989**, *111*, 1138.

(36) Zelechonok, Y.; Silverman, R. B. *J. Org. Chem*. **1992**, *57*, 5787.

(37) Newcomb, M.; Johnson, C. C.; Manek, M. B.; Varick, T. R. *J. Am. Chem. Soc*. **1992**, *114*, 10915.

(38) Silverman, R. B.; Zhou, T. P.; Eaton, P. E. *J. Am. Chem. Soc*. **1993**, *115*, 8841.

(39) Choi, S. Y.; Eaton, P. E.; Newcomb, M.; Yip, Y. C. *J. Am. Chem. Soc*. **1992**, *114*, 6326.

(40) Cole, T. W. Jr. Ph.D. Dissertation, University of Chicago, Chicago, IL, **1966**

(41) Luh, T. Y. Ph.D. Dissertation, University of Chicago, Chicago, IL, **1974**

(42) Mak, T. C. W.; Yip, Y. C.; Luh, T. Y. *Tetrahydron* **1986**, *42*, 1981.

(43) Klunder, A. J. H.; Zwanenburg, B. *Tetrahydron* **1975**, *31*, 1419.

(44) Ashby, E. C.; Park, B.; Patil, G. S.; Gadru, K.; Gurumurthy, R. *J. Org. Chem*. **1993**, *58*, 424.

(45) Silverman, R. B.; Lu, X.; Zhou, J. J. P.; Swihart, A. *J. Am. Chem. Soc*. **1994**, *116*, 11590.

(46) Gates, K. S.; Silverman, R. B. *J. Am. Chem. Soc*. **1990**, *112*, 9364.

(47) Miller, J. R.; Edmondson, D. E.; Grissom, C. B. *J. Am. Chem. Soc*., **1995**, *117*, 7830.

(48) Walker, M. C.; Edmondson, D. E. *Biochemistry*, **1994**, *33*, 7088.

(49) Dinnocenzo, J. P.; Karki, S. B.; Jones, J. P. *J. Am. Chem. Soc*., **1993**, *115*, 7111.

(**50**) (a) Castagnoli, Jr. N.; Rimodi, J. M.; Bloomquist, J.; Castagnoli, K. P. *Chem. Res. Toxicol*. **1997**, *10*, 924. (b)

(51) Hamilton, G. A. In *Prog. Bioorg. Chem*. **1971**, *1*, 83.

(52) Kim, J. M.; Bogdan, M. A.; Mariano, P. S. J. Am. Chem. Soc. **1993**, *115*, 10591.

(53) Kim, J. M.; Hoegy, S. E.; Mariano, P. S. *J. Am. Chem. Soc*. **1995**, *117*, 100.

(54) Youngster, S. K.; McKeown, K. A.; Jin, Y.-Z.; Ramsay, R. R.; Heikkila, R. E.; Singer, T. P. *J. Neurochem*., **1989**, *53*, 1837.

(55) Langston, J. W.; Ballard, P.; Tetrud, J. W.; Irwin, I. *Science*, **1983**, *219*, 979.

(56) Langston, J. W. MPTP induced Parkinsonism: How good a model is it? In *Recent Developments in Parkinson's Disease*, **1983**, (Eds: Fahn, S.; Marsden, C. D.; Jenner, P.; Teychenne, P.), Raven Press, New York, pp 119.

(57) Burns, R. C.; Chieuh, C. C.; Markey, S. P.; Ebert, M. H. E.; Jacobwitz, D. M.; Kopin, I, J. *Proc. Natl. Acad. Sci*. U.S.A., **1984**, *80*, 4546.

(58) Langston, J. W.; Forno, L. S.; Rebert, C. S.; Irwin, I. *Brain Res*., **1984**, 292, 390.

(59) "Parkinson's disease: Hope through research", NIH publication, 1998.

(60) Chiba, K.; Trevor, A. J.; Castagnoli, N., Jr. *Biochem. Biophys. Res. Commun*., **1984**, *120*, 574.

(61) Chiba, K.; Peterson, L. A.; Castagnoli, K.; Trevor, A. J.; Castagnoli, N., Jr. *Drug Metab. Dispos*., **1985**, *13*, 342.

(62) Trevor, A. J.; Castagnoli, N., Jr.; Singer, T. P. *Toxicology*, **1988**, *49*, 513.

(63) Peterson, L. A.; Caldera, P. S.; Trevor, A. J.; Chiba, K.; Castagnoli, N., Jr. *J. Med. Chem*., **1985**, *28*, 1432.

(64) Langston, J. W.; Irwin, I.; Langston, E. B.; Forno, L. S. *Neurosci. Lett*., **1984**, *48*, 87.

(65) Castagnoli, N., Jr.; Chiba, K.; Trevor, A. J. *Life Sci*., **1985**, *36*, 225.

(66) Trevor, A. J.; Castagnoli, N., Jr.; Caldera, P. S.; Ramsay, R. R.; Singer, T. P. *Life Sci*., **1987**, *40*, 713.

(67) Javitch, J. A.; D'Amata, R. J.; Strittmatter, S. M.; Snyder, S. H. *Proc. Natl. Acad. Sci*. U.S.A., **1985**, *82*, 2173.

(68) Chiba, K,; Trevor, A. J.; Castagnoli, N., Jr. *Biochem. Biophys. Res. Commun*., **1985**, *128*, 1228.

(69) Nicklas, W. J.; Vyas, I.; Heikkila, R. E. *Life Sci*., **1985**, *36*, 2503.

(70) Vyas, I.; Heikkila, R. E.; Nicklas, W. J. *J. Neurochem*., **1986**, *46*, 1501.

(71) Ramsay, R. R.; Salach, J. I.; Singer, T. P. *Biochem. Biophys. Res. Commun*., **1986**, *134*, 743.

(72) Heikkila, R. E.; Manzino, L.; Cabbat, R. S.; Duvoisin, R. C. *Nature*, **1984**, *311*, 467.

(73) Langston, J. W.; Irwin, I.; Langston, E. B.; Forno, L. S. *Science*, **1984**, *225*, 1480.

(74) Shen, R. S.; Abell, C. N. Gessner, W. and Brossi, A. Hypothalamic uptake of (3H)-MPTP and strial uptake of (3H)-MPP+ in rat brain synaptosomes. In MPTP: A Neurotoxin Producing a Parkinsonian Syndrome, ed. by S. P. Markey, N. Castagnoli, Jr., A. J. Trevor, and I. J. Kopin, pp. 563-567, Academic Press, Inc., London, **1986**.

(75) Mayer, R. A.; Kindt, M. V. and Heikkila, R. E. *J. Neurochem*. **1986**, *47*, 1073.

(76) Mizuno, Y.; Sone, N.; Suzuki, K. and SaitoH, T. *J. Neurol. Sci*. **1988**, *86*, 97.

(77) Singer, T. P.; Salach, J. I.; Crabtree, D. *Biochem. Biophys. Res. Commun*., **1985**, *127*, 707.

(78) Singer, T. P.; Salach, J. I.; Castagnoli, N., Jr.; Trevor, A. J. *Biochem. J*., **1986**, *235*, 785.

(79) Krueger, M. J.; McKeown, K.; Ramsay, R. R.; Youngster, S.; Singer, T. P. *Biochem. J*., **1990**, *268*, 219.

(80) Langston, J. W.; Irwin, I.; Langston, E. B.; Forno, L. S. *Neurosci. Lett*., **1984**, *50*, 289.

(81) Maret, G.; Testa, B.; Jenner, P.; El Tayar, N.; Carrupt, P. A. *Drug Metab. Rev*., **1990**, *22*, 291.

(82) Youngster, S. K.; Sonsalla, P. K.; Heikkila, R. E. *J. Neurochem*., **1987**, *48*, 929.

(83) Finnegan, K. T.; Irwin, I.; DeLanney, L. E.; Ricaurte, G. A.; Langston, J. W. *J. Pharmacol. Exp. Ther*., **1987**, *242*, 1144.

(84) Kalgutkar, A. S.; Castagnoli, K.; Hall, A.; Castagnoli, N., Jr. *J. Med. Chem*., **1994**, *37*, 944.

(85) Zhao, Z.; Dalvie, D.; Naiman, N.; Castagnoli, K.; Castagnoli, N., Jr. *J. Med. Chem*., **1992**, *35*, 4473.

(86) Altomare, C.; Carrupt, P.-A.; Gaillard, P.; Tayar, N. E.; Testa, B.; Carotti, A. *Chem. Res. Toxicol*., **1992**, 5, 366.

(87) Youngster, S. K.; Duvoisin, R. C.; Hess, A.; Sonsalla, P. K.; Kindt, M. V.; Heikkila, R. E. *Eur. J. Pharmacol*., **1986**, *122*, 283.

(**88**) Younger, S. K.; Nicklas, W. J.; Heikkila, R. E. *J. Pharmacol. Exp. Ther*. **1989**, *249*, 820.

(89) Younger, S. K.; Nicklas, W. J.; Heikkila, R. E. *J. Pharmacol. Exp. Ther*. **1989**, *249*, 829.

(90) Heikkila, R. E.; Youngster, S. K.; Panek, D. U.; Giovanni, A.; Sonsalla, P. K. *Toxicology*, **1988**, *49*, 493.

(91) Nimkar, S. K.; Anderson, H. A.; Rimoldi, J. M.; Stanton, M.; Castagnoli, K. P.; Mabic, S.; Wang, Y.-X.; Castagnoli, N. Jr. *Chem. Res. Toxicol*. **1996**, *9*, 1013.

(92) Mabic, S.; Castagnoli, N., Jr. *J. Med. Chem*., **1996**, *39*, 3694.

(93) Hall, L.; Murray, S.; Castagnoli, K.; Castagnoli, N., Jr. *Chem. Res. Toxicol*., **1992**, *5*, 625.

(94) Anderson, A. H.; Kuttab, S.; Castagnoli, N. Jr. *Biochemistry* **1996**, *35*, 3335.

(95) Eicher, T.; Hauptmann, S. The chemistry of heterocycles, Georg Thiene verlag, Stuttart:New York, 1995.

(96) Gronowitz, S. Ed.; Thiophene and its deterivatives, part four, Ed.; John Wiley &Sons, Inc:New York, 1991.

(97) Jones, R.A. Pyrroles part one: The synthesis and physical and chemical aspects of the pyrrole ring, John Wiley & Sons, Inc.:New York, **1990**, Vol. 48

(98) Katritzky, A. R.; Rees, C. W.; Scriven, E. V. In *Comprehensive Hetereocyclic Chemistry*, Pergamon Press:New York, **1996**, Vol. 2

(99) Katritzky, A. R.; Rees, C. W.; Potts, K. T. In *Comprehensive Hetereocyclic Chemistry*, Pergamon Press: Oxford, **1984**, Vol 6.

(**100**) Youngster, S. K.; Sonsalla, P. K.; Sieber, B.-A.; Heikkila, R. E. *J. pharmacol. Exp. Ther*. **1989**, *249*, 820.

(101) Anderson, A. H. Ph. D. Dissertation, Virginia Polytechnic Institute and State University, **1997**, page 86.

(102) Kalgutkar A. S.; Castagnoli, N. Jr. *J. Med. Chem*. **1992**, *35*, 4165.

(103) Schmidle, C. J.; Mansfield, R. C. *J. Am. Chem. Soc*. **1956**, *78*, 1702.

(104) Schmidle, C. J.; Mansfield, R. C. *J. Am. Chem. Soc*. **1956**, 78, 425.

(105) Genisson, Y.; Marazano, C.; Mehmandoust, M.; Gnecco, D.; Das, B. C. *Synlett*, **1992**, 431.

(106) Vander Schyf, C. J.; Castagnoli, K.; Usuki, E.; Fouda, H. G.; Rimoldi, J. M. *Chem. Res. Toxicol*, **1994**, *7*, 281.

(107) Efange, S. M. N.; Michelson, R. H.; Remmel, R. P.; Boudreau, R. J.; Dutta, A. K.; Freshler, A. *J. Med. Chem*., **1990**, *33*, 3133.

(108) Stille, J. K. *Angew. Chem., Int. Ed. Engl*., **1986** *25*, 508.

(109) Ichimura, K.; Ichikawa, S.; Imamura, K. *Bull. Chem. Soc. Jpn*. **1976**, *49*, 1157.

(110) Rio, G.; Lecas-Nawrocka, A.; *Bull. Soc. Chim. Fr.*, **1976**, 317.

(111) Mussatto, M. C.; Savoia, D.; Trombini, C.; Umani-Ronchi, A. *J. Org. Chem*. **1980**, *45*, 4004.

(112) Maying, L.; Severin, T.; *Chem. Ber.;* **1981**, *114*, 3863.

(113) Rosini, G.; Ballini, R.; Sorrenti, P. *Tetrahedron*, **1983**, *39*, 4127.

(114) Naki, T.; Wada, E.; Okawara, M. *Tetrahydron Lett*.; **1975**, *19* 1531.

(115) KulinLovich, O. G.; Tischenko, I. G.; Sorokin, V. L. *Synthesis*, **1985**, 1058.

(116) Meyers, A. I.; Nazarenko, N. *J. Org. Chem*., **1973**, *38*, 175.

(117) Seyferth, D.; Hui, R. C. *J. Am. Chem. Soc*., **1985**, *107*, 4551.

(118) Rosini, G.; Ballini, R.; Petrini, M.; Sorrenti, P. *Tetrahydron* **1984**, *40*, 3809.

(119) Kruse, C. G.; Bouw, J. P.; van Hes, R.; Vande kuilen, A.; den hartog, J. A. J. *Heterocycles* **1987**, *26*, 3141.

(120) Stetter, H.; Krasselt, J. *Heterocyclic Chem*. **1977**, *14*, 573.

(121) Ratcliffe, R.; Rodehorst, R. *J. Org. Chem*., **1970**, *35*, 4000.

(122) Kondo, K.; Matsumoto, M. *Chemistry Letters* **1974**, *XX*, 701.

(123) Herrmann, J. L.; Schlessinger, R. H. *J. C. S. Chem. Comm*. **1973**, 711.

(124) Hirano, S.; Hiyama, T.; Fujita, S.; Kawaguti, T.; Hayashi, Y.; Nozaki, H. *Tetrahedron* **1974**, *30*, 263.

(125) Carey, F. A.; Sundberg, R. J. In Adced organic chemistry, Part A, Plenum Publishing Corporation:New York, 1990, pp216-221.

(126) "Enzyme mechanism from isotope effects", Cook, P. F., Ed.; CRS Press:Boca Raton, 1991.

(127) Cleland, W.W. In *Methods in Enzymol.*, **1995**, *249*. pp 341.

(128) Northrop, D. B. *Biochemistry*, **1975**, *14*, 2644.

(129) Ottoboni, S.; Caldera, P.; Trevor, A.; Castagnoli, N., Jr. *J. Biol. Chem*., **1989**, *264*, 13684.

(130) Belleau, B.; Fang, M.; Burga, J.; Moran, J. *J. Am. Chem. Soc.*, **1960**, *82*, 5752.

(131) Yu, P. H.; Bailey, B. A.; Durden, D. A.; Boulton, A. A. *Biochem. Pharmacol.*, **1986**, *35*, 1027.

(132) Rimoldi, J. M.; Castagnoli, N. Jr. **1994**, unpublished results.

(133) Mabic, S.; Castagnoli, N. Jr. *J. Org. Chem*. **1996**, *61*, 309.

(134) Mabic, S.; Castagnoli, N. Jr. *J. Labelled Comp. Radiopharm*. **1995**, Vol. *XXXVIII*, 255.

(135) Fujii, T.; Yoshifuji, S. *Tetrahydron* **1970**, *26*, 5953.

(136) Gray, M.; Tinkl, M.; Snieckus, V.; In Comprehensive organometallic chemistry; Abel, E. W., Stone, F. G. A., Wilkinson, G., Eds.; Elsevier Science Ltd.:New York, **1995**; Vol. 11, Chapter 1.

(137) Beak, P.; Basu, A.; Gallagher, D. J.; Park, Y. S.; Thayumanavan, S. *Acc. Chem. Res*. **1996**, *29*, 552.

(138) Beak, P.; Meyers, A. I. *Acc. Chem. Res*. **1986**, *19*, 356.

(139) Houk, K. N.; Rondan, N. G.; Beak, P.; Zajdel, W. J.; Schleyer, P. V. R.; Chandrashekhar, J. *J. Org. Chem*. **1981**, *46*, 4108.

(140) Beak, P.; Reitz, D. B. *Chem. Rev*. **1978**, *78*, 275.

(141) Beak, P.; Zajdel, W. J.; Reitz, D. B. *Chem. Rev*. **1984**, *84*, 471.

(142) Gawley, R. E.; Rein, K. S. In *Comprehensive Organic Synthesis*; Trost, B. M., Fleming, I., Eds.; Pergamon: Oxford, **1991**; Vol. 3, Chapter 1.2.

(143) Keefer, L. K.; Fodor, C. H.; *J. Am. Chem. Soc*. **1970**, *92*, 5747.

(144) Seebach, D.; Enders, D. *Angen. Chem., Int. Ed. Engl*. **1972**, *11*, 30.

(145) Fraser, R. R.; Boussard, G.; Postescu, D.; Whiting, J. J.; Wigfield, Y. Y. *Can. J. Chem*. **1973**, *51*, 1109

(146) Beak, P.; Farney, R. *J. Am. Chem. Soc*. **1973**, *95*, 4771.

(147) Meyers, A. I.; Santiago, B. *Tetrahedron Lett*. **1995**, *36*, 5877.

(148) Meyers, A. I.; Edwards, P. D.; Reiker, W. F.; Bailey, T. R. *J. Am. Chem. Soc*. **1984**, *106*, 3270.

(149) Shawe, T. T.; Meyers, A. I. *J. Org. Chem*. **1991**, *56*, 2751.

(150) Meyers, A. I.; Milot, G. *J. Am. Chem. Soc*. **1993**, *115*, 6652.

(151) Beak, P.; Lee, W.-K. *Tetrahedron Lett*. **1989**, *30*, 1197.

(152) Beak, P.; Lee, W. K. *J. Org. Chem*. **1990**, *55*, 2578.

(153) Beak, P.; Lee, W. K. *J. Org. Chem*. **1993**, *58*, 1109.

(154) Gawley, R. E.; Hart, G. C.; Bartolotti, L. J. *J. Org. Chem*. **1989**, *54*, 175.

(155) Gawley, R. E.; Zhang, Q. *Tetrahedron* **1994**, *50*, 6077.

(156) Gawley, R. E.; Hart, G.; Goicoechea-pappas, M.; Smith, A. L. *J. Org. Chem*. **1986**, *51*, 3076.

(157) Meyers, A.I. *Tetrahydron* **1992**, *48*, 2589.

(158) Peterson, D. J.; Hays, H. R. *J. Org. Chem*. **1965**, *30*, 1939.

(159) Peterson, D. J.; *J. Organometall. Chem.* **1970**, *21*, p63-64.

(160) Fraser, R. R.; Grindley, T. B.; Passannanti, S. *Can. J. Chem.* **1975**, *53*, 2473.

(161) Seebach, D.; Wykpiel, W.; Lubosch, W.; kalinowski, H. O. *Helv. Chim. Acta* **1978**, *61*, 3100.

(162) Fraser, R. R.; Grindley, T. B. *Can. J. Chem*. **1975**, *53*, 2465.

(163) Rondan, N. G.; Houk, K. N.; Beak, P.; Zajdel, W. J.; Chandrasekhar, J.; Schleyer, P. V. R. *J. Org. Chem.* **1981**, *46*, 4108.

(164) Bach, R. D.; Braden, M. L.; Wolber, G. J. *J. Org. Chem*. **1983**, *48*, 1509.

(165) Bartolott, L. J.; Gawley, R. E. *J. Org. Chem*. **1989**, *54*, 2980.

(166) Seebach, D.; Hansen, J.; Seiler, P.; Gromek, J. M. *J. Organometall. Chem.* **1985**, *285*, 1.

(167) Boche, G.; Marsch, M.; Harbach, J.; Harms, K.; Ledig, B.; Schubert, F.; Lohrenz, J. C. W.; Ahlbrecht, H. *Chem. Ber*. **1993**, *126*, 1887.

(168) Mayers, A. I.; ten Hoeve, W. *J. Am. Chem. Soc.* **1980**, *102*, 7125.

(169) Gawley, R. E.; Smith, G. A. *Tetrahedron Lett.* **1988**, *29*, 301.

(170) Meyers, A.I.; Warmus, J. S.; Gonzalez, M. A.; Guiles, J.; Akahane, A. *Tetrahedron Lett.* **1991**, *32*, 5509.

(171) Meyers, A. I.; Dickman, D. A. *J. Am. Chem. Soc*. **1987**, *109*, 1263.

(172) Loewe, M. F.; Boes, M.; Meyers, A. I. *Tetradron Lett.* **1985**, *26*, 3295.

(173) Meyers, A. I.; Gonzalez, M. A.; Struzka, V.; Akahane, A.; Guiles, J.; Warmus, J. S. *Tetrahedron Lett*. **1991**, *32*, 5501.

(174) Meyers, A. I.; Guiles, J.; Warmus, J. S.; Gonzalez, M. A. *Tetrahedron Lett.* **1991**, *32*, 5505.

(175) Gawley, R. E. *J. Am. Chem. Soc*. **1987**, *109*, 1265.

(176) Rein, K.; Goicocechea-Pappas, M.; Anklekar, T. V.; Hart, G. C.; Smith, G. A.; Gawley, R. E. *J. Am. Chem. Soc.* **1989**, *111*, 2211.

(177) Eliel, E. L.; Hartmann, A. A.; Abatjoglou, A. G. *J. Am. Chem. Soc*. **1974**, *96*, 1807.

(178) Parker, D. *Chem. Rev*. **1991**, 1441.

(179) Lafontaine, E.; Bayle, J. P.; Courtieu, J. *J. Am. Chem. Soc*. **1989**, *111*, 8294.

(180) Lafontaine, E.; Péchiné, J. M.; Mayne, C. L.; Courtieu, *J. Liq. Cryst*. **1990**, *7*, 293.

(181) Canet, I.; Løvschall, J.; Courtieu, *J. Liq. Cryst*. **1994**, *16*, 405.

(182) Emsley, J. W.; Lindon, J. C. NMR spectroscopy using liquid crystal solvents. Pergamon Press: Oxford **1975**, pp 221-257.

(183) Canet, I.; Courtieu, I.; Loewenstein, A.; Meddour, A.; Péchiné, J. M. *J. Am. Chem. Soc*. **1995**, *117*, 6520.

(184) Meddour, A.; Canet, I.; Loewenstein, A.; Péchiné, J. M.; Courtieu, I. *J. Am. Chem. Soc*. **1994**, *116*, 9652.

(185) Gawley, R. E.; Zhang, P.; *J. Org. Chem*. **1996**, *61*, 8103.

(186) (a) West, P.; Purmort, J. I.; Mckinley, S. V. *J. Am. Chem. Soc*. **1968**, *90*, 797. (b) O'Brian, D. H.; Hart, A. J.; Russell, C. R. *J. Am. Chem. Soc*. **1975**, *97*, 4410. (c) Benn, R.; Rufinska, A. *J. Organomet. Chem*. **1982**, *239*, C19. (d) Fraenkel, G.; Winchester, W. R. *J. Am. Chem. Soc*. **1989**, *111*, 3794.

(187) (a) Bates, R. B.; Beavers, W. A. J. Am. Chem. Soc. **1974**, *96*, 5001. (b)Thompson, T. B.; Ford, W. T. *J. Am. Chem. Soc*. **1979**, *101*, 5459.

(188) (a) Boche, G.; Fraenkel, G.; Cabral, J.; Harms, K.; van Eikema-Hommes, N. J. P.; Lorenz, J.; Marsch, M.; Schleyer, P. V. R. *J. Am. Chem. Soc*. **1992**, *114*, 1562. (b) Boche, G.; Etzrodt, H.; Marsh, M.; Massa, H.; Baum, G.; Dietrich, H.; Mahdi, W. *Angew. Chem*. **1986**, *98*, 84.

(189) (a) Bushby, R. J.; Tytho, M. P. *J. Organomet. Chem*. **1984**, *270*, 265. (b) Pratt, L. M.; Khan, I. M. *J. Comput. Chem*. **1995**, *16*, 1070.

(190) van Eikema-Hommes, N. J. R.; Buhl, M.; Schleyer, P. v. R. *J. Organomet. Chem*. **1991**, *409*, 307.

(191) Fraenkel, G.; Qiu, F. *J. Am. Chem. Soc*. **1997**, *119*, 3571.

(192) Salach, J. I.; Weyler, W. *Methods Enzymol*. **1987**, *142*, 627.

(193) Tipton, K. F.; Singer, TP. *J. Neurochem*. **1993**, *61*, 1191

VITA

Jian Yu

Jian Yu was born on April 9, 1964 in Chengdu, Sichuan province in People's Republic of China. She received her Bachelor of Science degree in Chemistry from Beijing Normal University in June 1985 and her Master of Science degree in Inorganic Chemistry from the same University in 1988. She joined the graduate program in the Department of Chemistry at Virginia Polytechnic Institute and State University in the Fall of 1994 under the direction of Professor Neal Castagnoli, Jr. Her research was sponsored by the Harvey W. Peters Research Center for the study of Parkinson's Disease and Disorders of the Central Nervous System and NIH. She received the Doctor of Philosophy degree in Chemistry from Virginia Polytechnic Institute and State University in August 1998.